

GROUNDWATER RESOURCE ASSESSMENT OF THE WATERBERG COAL RESERVES

By

MICHAEL BESTER

Submitted in fulfilment of the requirements of the degree

Magister Scientiae

In the Faculty of Natural and Agricultural Sciences

Institute for Groundwater Studies

University of the Free State

November 2009

Study Leader: Dr P.D. Vermeulen

DECLARATION

I hereby declare that this dissertation, submitted for the degree Masters in the Faculty of Natural and Agricultural Sciences, Department of Geohydrology, University of the Free State, Bloemfontein, South Africa, is my own work and has not been submitted to any other institution of higher education. I further declare that all sources cited or quoted are indicated and acknowledged by means of a list of references.

M. Bester

16 November 2009

ACKNOWLEDGEMENTS

This project was made possible by the co-operation of many individuals and institutions. I wish to record my sincere thanks to the following:

- The Water Research Commission for funding and support of the project.
- Dr Jo Burges at the WRC for her support of the project and her leadership.
- Dr Vermeulen in particular for his continuous assistance.
- Mr Claris Dreyer for his invaluable information and assistance with the project.
- Prof G. Van Tonder for his assistance and time.
- Mr E. Lukas for his help and technical advice.
- The Doctors Dennis for their help and advice.
- Mrs Lore-Marie Cruywagen for assistance with the acid-base analyses.
- Exxaro Ltd. for provision of data.
- Sasol mining, and in particular Mr Bertie Botha and Mr Gawie vd Merwe for the provision of data.
- Mr Reinhard Weideman and VSA Leboa consulting.
- Mr Stoffel Fourie of the CSIR for the provision of data.
- The personnel and fellow students at the Institute for Groundwater Studies.
- Mrs Catherine Bitzer for help with language preparation.
- Special thanks to my parents and brothers for their prayers and support during my studies.
- My wife Alida for motivation and love.
- Dumpies, Rambo and Angus Bester for your support through difficult times.

And finally to my Lord and Saviour Jesus Christ for carrying me through the good and the bad times.

Table of Contents

CHAPTER 1: INTRODUCTION.....	1
1.1. OBJECTIVES	1
1.2. METHODS OF INVESTIGATION	2
1.3. STRUCTURE OF THE THESIS.....	4
CHAPTER 2: COAL AND IT'S PLACE IN THE WORLD.....	5
2.1. INTRODUCTION	5
2.2. COAL AS FUEL	6
2.3. ENVIRONMENTAL EFFECTS OF COAL BURNING AND MINING	7
2.3.1. <i>Effects from Coal Burning</i>	7
2.3.2. <i>Effects from Coal Mining</i>	7
2.4. WORLD COAL RESERVES	8
2.5. MAJOR COAL PRODUCERS	10
2.6. COAL IN SOUTH AFRICA	12
2.7. SOUTH AFRICAN GOVERNMENT ENERGY POLICY.....	13
2.7.1. <i>Existing Coal-Fired Power Stations</i>	14
2.7.2. <i>Currently Mothballed Coal-fired Stations Being Re-Commissioned</i>	15
2.7.3. <i>New Coal-Fired Power Stations</i>	15
2.8. THE WATERBERG COALFIELDS.....	16
CHAPTER 3: MINING METHODS	17
3.1. INTRODUCTION	17
3.2. HISTORY OF COAL MINING IN SOUTH AFRICA	18
3.3. METHODS OF COAL EXTRACTION	18
3.3.1. <i>Modern Surface Mining</i>	20
3.3.2. <i>Sub-Surface Mining Methods</i>	22
3.4. COAL PRODUCTION.....	25
3.4.1. <i>Effects of Modern Mining on Production</i>	26
3.5. ENVIRONMENTAL EFFECTS OF COAL MINING	26
3.6. MINING METHODS IN THE WATERBERG COALFIELD.....	27
3.7. PROPOSED MINING PLANS AND METHODS.....	29
3.8. CONCLUSION	29
CHAPTER 4: STUDY AREA LOCATION	30
4.1. INTRODUCTION	30
4.1.1. <i>Mining and Minerals</i>	31
4.1.2. <i>The Waterberg Region</i>	31
4.2. THE STUDY AREA	31
4.3. CLIMATE.....	33
4.4. SURFACE HYDROLOGY & TOPOGRAPHY.....	35
4.5. SOIL DEPTHS, SOIL TYPES AND LAND COVER.....	40

CHAPTER 5: METHODOLOGY	43
5.1. INTRODUCTION	43
5.2. SAMPLING.....	43
5.2.1. <i>Groundwater Samples</i>	44
5.2.2. <i>Geological Samples</i>	44
5.3. WATER QUALITY	45
5.4. ACID-BASE ACCOUNTING	46
5.4.1. <i>The Primary Advantages of ABA</i>	47
5.4.2. <i>The Primary Disadvantages of ABA</i>	47
5.4.3. <i>Prediction Methods</i>	47
5.4.4. <i>Static Methods (Acid-Base Accounting)</i>	48
5.4.5. <i>Peroxide Methods</i>	48
5.5. AQUIFER PARAMETERS	50
5.5.1. <i>Slug Tests</i>	50
5.5.2. <i>Pump Testing</i>	51
5.6. RECHARGE.....	53
5.6.1. <i>The Chloride Mass Balance Method</i>	54
5.6.2. <i>The E.A.R.T.H. Model</i>	54
5.7. NUMERICAL GROUNDWATER MODELS	55
5.7.1. <i>Collection and Interpretation of Field Data</i>	56
5.7.2. <i>Conceptualizing the Natural System</i>	56
5.7.3. <i>Calibration & Validation</i>	57
5.7.4. <i>Modelling Scenarios</i>	57
5.7.5. <i>Assumptions and Limitations of Numerical Modelling</i>	58
5.7.6. <i>Generation of a Finite Difference Network</i>	59
CHAPTER 6: GEOLOGY OF THE WATERBERG COALFIELDS.....	63
6.1. INTRODUCTION	63
6.2. COAL-BEARING SUCCESSIONS IN THE COALFIELD	65
6.3. CONCLUSION	68
CHAPTER 7: ACID-BASE ACCOUNTING.....	69
7.1. INTRODUCTION	69
7.1.1. <i>The Primary Advantages of the ABA Methods are:</i>	70
7.1.2. <i>The Principal Disadvantages of Acid-Base Accounting are:</i>	70
7.1.3. <i>Static Tests Used in this Study</i>	71
7.2. OVERVIEW OF ABA DATA TYPES OBTAINED	72
7.2.1. <i>In an Open System</i>	73
7.2.2. <i>In a Closed System</i>	73
7.3. CALCULATED PARAMETERS FROM ABA.....	74
7.4. INTERPRETATION OF RESULTS	74
7.4.1. <i>Screening Criteria</i>	74
7.5. RESULTS FOR THE WATERBERG SAMPLES	77

7.5.1.	<i>Acid-Base Accounting</i>	77
7.5.2.	<i>Mineralogy</i>	78
7.5.3.	<i>Weathering Zones</i>	78
7.6.	FULL SUCCESSION AREAS (GREEN AREAS)	78
7.6.1.	<i>North western Samples</i>	78
7.6.2.	<i>South Eastern Samples</i>	81
7.7.	MIDDLE ECCA WEATHERING (YELLOW AREA)	84
7.8.	SANDSTONE SAMPLES	87
7.9.	DISCARD SAMPLES	89
7.10.	DISCUSSION OF RESULTS	91
7.10.1.	<i>The North Western Samples</i>	91
7.10.2.	<i>The Northern and South Eastern Samples</i>	91
7.11.	COMPARISON OF ABA RESULTS TO WEATHERING DEPTH	92
7.11.1.	<i>The Green Areas (N/W & S/E Sampling Locations)</i>	92
7.11.2.	<i>The Yellow Areas (Northern Sampling Locations)</i>	95
7.11.3.	<i>The Red Areas (South Eastern Sampling Location)</i>	97
7.12.	CONCLUSION	98
7.12.1.	<i>The North Western Samples</i>	98
7.12.2.	<i>Northern and South Eastern Samples:</i>	98
7.12.3.	<i>ABA Compared to Weathering</i>	98
CHAPTER 8: PRE-MINING WATER QUALITY OF THE WATERBERG COALFIELDS		99
8.1.	INTRODUCTION	99
8.2.	SAMPLING	99
8.2.1.	<i>Water Samples</i>	99
8.3.	WATER-QUALITY DETERMINATION	99
8.4.	DISCUSSION OF RESULTS	100
8.4.1.	<i>pH</i>	100
8.4.2.	<i>Electrical Conductivity (EC)</i>	102
8.5.	CONCLUSION	113
8.5.1.	<i>Power Generation and its Effect on Groundwater Quality</i>	113
8.5.2.	<i>Coal Mining and its Effect on Groundwater Quality</i>	114
CHAPTER 9: GEOHYDROLOGY		116
9.1.	INTRODUCTION	116
9.2.	AQUIFERS	117
9.2.1.	<i>The Weathered Groundwater System</i>	118
9.2.2.	<i>The Fractured Groundwater System</i>	119
9.3.	WATER LEVELS	119
9.3.1.	<i>Water Level Contouring</i>	121
9.3.2.	<i>Water Level Elevation Contouring</i>	123
9.3.3.	<i>Bayesian Interpolated Water Level Contouring</i>	123
9.4.	AQUIFER PARAMETERS	126
9.4.1.	<i>Slug Testing</i>	126

9.4.2.	<i>Pumping Tests</i>	129
9.4.3.	<i>Discussion of Aquifer-Parameter Testing Results</i>	136
9.5.	RECHARGE	138
9.5.1.	<i>Chloride in the Study Area</i>	138
9.6.	RECHARGE DETERMINATIONS	142
9.6.1.	<i>The Chloride Mass Balance Method for Determining Recharge</i>	142
9.6.2.	<i>The E.A.R.T.H. Method for Determining Recharge</i>	146
9.7.	CONCLUSION	149
9.7.1.	<i>Aquifer Parameters</i>	149
9.7.2.	<i>Recharge</i>	150
CHAPTER 10: MODELLING		151
10.1.	INTRODUCTION	151
10.2.	NUMERICAL MODELLING.....	151
10.2.1.	<i>Parameters for the Model</i>	152
10.2.2.	<i>Model Scenarios</i>	155
10.2.3.	<i>Dewatering for Scenario 1</i>	155
10.2.4.	<i>Decant Model for Scenario 1</i>	164
10.2.5.	<i>Dewatering for Scenario 2: Mine Intersecting a Fault</i>	165
10.2.6.	<i>Decant Model for Scenario 2</i>	168
10.2.7.	<i>Dewatering Models for Scenario 3: Three Pits & Active Faults</i>	169
10.2.8.	<i>Decant Model for Scenario 3</i>	174
10.3.	DISCUSSION OF MODEL RESULTS	175
10.3.1.	<i>Inflow of Water</i>	175
10.3.2.	<i>Drawdown Cones</i>	176
10.4.	CONCLUSION	177
10.4.1.	<i>Dewatering</i>	177
10.4.2.	<i>Decant</i>	177
CHAPTER 11: GROUNDWATER MANAGEMENT IN THE WATERBERG COALFIELDS		178
11.1.	INTRODUCTION	178
11.2.	WATER QUALITY MANAGEMENT.....	179
11.3.	POTENTIAL REHABILITATION METHODS FOR AMD.....	181
11.3.1.	<i>Preventative measures</i>	181
11.3.2.	<i>Containment measures</i>	181
11.3.3.	<i>Additional Options for the Treatment of Acidic Waters</i>	182
11.4.	CONCLUSION	183
CHAPTER 12: CONCLUSIONS		184
12.1.	INTRODUCTION	184
12.1.1.	<i>Climate</i>	184
12.1.2.	<i>Geology</i>	184
12.1.3.	<i>The Mine Workings</i>	184
12.1.4.	<i>Measured Parameters and Modelling Results</i>	185

12.1.5. Acid-Base Results.....	185
12.1.6. Water Quality.....	185
12.2. RECOMMENDATIONS.....	187
CHAPTER 13: REFERENCES.....	188
APPENDIX A.....	191
RESULTS FOR THE ACID-BASE ACCOUNTING ANALYSES.....	191
APPENDIX B.....	201
SLUG TEST RESULTS.....	201
APPENDIX D.....	202
CL VALUES AND RECHARGE.....	202
APPENDIX D.....	203
RECHARGE DETERMINATION RESULTS FOR THE E.A.R.T.H. MODEL.....	203

List of Figures

<i>Figure 1: Geological map of the Waterberg Coalfield after Vermeulen (2006).....</i>	<i>16</i>
<i>Figure 2: Dragline mining in an opencast pit (from Snyman, 1998, Optimum Colliery).....</i>	<i>17</i>
<i>Figure 3: Open-pit mining (www.numahammers.com).....</i>	<i>20</i>
<i>Figure 4: Area mining, Courtesy of Dr Vermeulen.....</i>	<i>21</i>
<i>Figure 5: Mountaintop removal mining (www.coal-is-dirty.com).....</i>	<i>22</i>
<i>Figure 6: Example of board-and-pillar mining in a modern underground colliery taken from Grobbelaar , (2001).</i>	<i>23</i>
<i>Figure 7: Example of stooped areas at Usutu Colliery taken from Grobbelaar, (2001).....</i>	<i>24</i>
<i>Figure 8: A longwall mining operation taken form Grobbelaar, (2001).....</i>	<i>25</i>
<i>Figure 9: Opencast mine in the study area curtsey of the Grootegeluk mine.....</i>	<i>27</i>
<i>Figure 10: The opencast at the Grootegeluk mine curtsey of the Grootegeluk mine.</i>	<i>28</i>
<i>Figure 11: Location of the Limpopo province.....</i>	<i>30</i>
<i>Figure 12: Location of the study area (regional), (http://www.deat.gov.za/Maps).....</i>	<i>32</i>
<i>Figure 13: Location of the study area (Local).....</i>	<i>33</i>
<i>Figure 14: Rainfall in the study area (regional) (http://www.deat.gov.za/Maps).....</i>	<i>34</i>
<i>Figure 15: Saturated soil with water pooling in the surface during the rainy season.....</i>	<i>34</i>
<i>Figure 16: Rainfall figures for the study area (1973 - 2007).</i>	<i>35</i>
<i>Figure 17: Location of the study area in the Limpopo catchment (http://www.deat.gov.za/Maps).....</i>	<i>36</i>
<i>Figure 18: Location of the study area in the quaternary catchments A41E and A42J (http://www.deat.gov.za/Maps).....</i>	<i>36</i>
<i>Figure 19: Topographic contour map generated for the study area.</i>	<i>37</i>
<i>Figure 20: Topographic contour map of the study area showing flow vectors and the Daarby fault.</i>	<i>38</i>
<i>Figure 21: Exaggerated 3D view of the study area topography.....</i>	<i>39</i>
<i>Figure 22: Exaggerated 3D view of the study area topography (Side view).....</i>	<i>40</i>
<i>Figure 23: Soil depths in the study area (regional) (http://www.deat.gov.za/Maps/).....</i>	<i>41</i>
<i>Figure 24: Soil types in the study area (regional) (http://www.deat.gov.za/Maps/).....</i>	<i>41</i>

Figure 25: Photo of the land cover of the study area.....	42
Figure 26: Groundwater sampling in the study area.....	44
Figure 27: Core sample from exploration borehole near the Grootegeluk mine (from the left Mr Claris Dreyer and Dr Danie Vermeulen).....	45
Figure 28: To the left Core samples, to the right Chip samples.....	45
Figure 29: Slug test yield determinations.....	51
Figure 30: Process involved in pump testing after Van Tonder et al., 2002.....	53
Figure 31: Illustration of the E.A.R.T.H model.....	55
Figure 32: Simplified geological map of the Waterberg Coalfield after Snyman (1998).....	63
Figure 33: Phase magnetics map of the study area indicating the dominant structures, courtesy of the CSIR. ..	64
Figure 34: Generalized stratigraphic column of the coal-bearing interval in the Waterberg coalfield (Snyman, 1998).....	65
Figure 35: Exaggerated 3D side view of the topography and Coal Zone 2 (legend).....	66
Figure 36: Plan view of Coal Zone 2.....	66
Figure 37: North/south and west/east cross-sections of the study area.....	67
Figure 38: The weathered zones and major faults in the study area.....	68
Figure 39: NNP vs. pH (initial and final) (closed system).....	72
Figure 40: NP vs. AP graph, indicating areas of likely and unlikely acid generation.....	76
Figure 41: %S vs. NPR.....	76
Figure 42: NNP vs. pH for all samples tested.....	77
Figure 43: AP vs. NP for all samples tested.....	77
Figure 44: Borehole position of the north western sample.....	79
Figure 45: Net neutralizing potential (closed) vs. pH for north/western core.....	79
Figure 46: %S vs. NPR for the north/western core.....	80
Figure 47: NP vs. NA (NPR) for the north/western samples.....	80
Figure 48: Borehole positions of the south eastern boreholes.....	82
Figure 49: NNP (closed) vs. pH for south/eastern core.....	82
Figure 50: % S vs. NPR for the south/eastern core samples.....	83
Figure 51: NP vs. NA (NPR) for the south/eastern samples.....	83
Figure 52: Positions of the chip sampling points.....	85
Figure 53: NNP (closed) vs. pH for northern chips samples.....	85
Figure 54: %S vs. NPR for the northern chip samples.....	86
Figure 55: NP vs. NA (NPR) for the northern samples.....	86
Figure 56: NNP (closed) vs. pH for Sandstone.....	87
Figure 57: %S vs. NPR for the sandstone samples.....	88
Figure 58: NP vs. NA (NPR) for the sandstone samples.....	88
Figure 59: Net neutralizing potential (closed) vs. pH values for discard samples.....	89
Figure 60: %S vs. NPR for the discard samples.....	90
Figure 61: NP vs. NA (NPR) for the discard samples.....	90
Figure 62: Location of the sample localities with regards to weathering.....	93
Figure 63: Sample GGS 2 Taken 52 m below the surface in the south eastern area.....	93
Figure 64: Samples SS5 & SS6 Taken 54 m & 66 m respectively below the surface in the north western area. .	94
Figure 65: Sample SS6 showing the presence of pyrite.....	94

Figure 66: Samples GT1.1 & GT7.5, respectively, with no acid potential.....	95
Figure 67: Samples GT1.9 & GT7.1, respectively, with acid potential.....	95
Figure 68: Sample GT2.12 with no acid potential.	96
Figure 69: Sample GT3.2 (on the left) with acid potential and sample GT3.3 (on the right) with no acid potential.....	96
Figure 70: Sample GGVZ1, collected 1 m below the surface with acid potential.	97
Figure 71: Sample GGSVZ1.4 4 m below the surface with acid potential.	97
Figure 72: Groundwater pH levels in the study area.	101
Figure 73: pH contour map of the study area.	101
Figure 74: Distribution of elevated EC values found in the study area.	102
Figure 75: Location of the 6 borehole pairs at the Medupi power station.	104
Figure 76: Graph of the EC for the deep (D) and shallow (S) boreholes drilled at the Medupi power station.	105
Figure 77: Graph of electrical conductivity at the ash dump boreholes (taken from Vermeulen and Dennis 2007).....	106
Figure 78: Contour map of the EC values encountered in the study area.....	107
Figure 79: Location of the eastern boreholes with the high EC values.....	108
Figure 80: Time series data for the eastern boreholes.....	108
Figure 81: Size distribution for EC values of boreholes and evaporation ponds at the Grootegeluk mine.	109
Figure 82: EC values for the boreholes drilled on the Grootegeluk mine site.	110
Figure 83: SO ₄ values for boreholes drilled on the Grootegeluk mine.....	110
Figure 84: EC map of the study area showing the areas that have not been affected by activities such as mining or power generation (outline in black).	111
Figure 85: Time graph for EC values in areas that have not been affected by activities.....	111
Figure 86: Time graph for Cl values of groundwater unaffected by activities.....	112
Figure 87: Time graph of SO ₄ values for areas that have not been affected by activities.	113
Figure 88: The groundwater compartments numbered 1 – 4, formed by the faults in the study area.	117
Figure 89: Rocks from the weathered aquifer zones of the study area.....	118
Figure 90: Rocks from the fractured aquifer zone, showing a bedding plane fracture outlined in red.....	119
Figure 91: Boreholes in the study area for which water level data is available.	120
Figure 92: Map showing boreholes with proportional distribution of water level data.	120
Figure 93: Contour map of the depth of water levels found in the study area (m below surface).....	122
Figure 94: Topography and water level contour maps.	122
Figure 95: Water level elevation contour map for the study area.....	123
Figure 96: Correlation between Topography and water level data used for Bayesian interpolation.	124
Figure 97: Bayesian interpolated water levels for the study area.....	124
Figure 98: Bayesian interpolated water level contour map with flow vectors, indicating flow away from the central parts of the study area.	125
Figure 99: Sections through the study area, with the top section running through the Grootegeluk mine.	126
Figure 100: Location of the slug tested boreholes.	127
Figure 101: Location of the pump tested boreholes.	129
Figure 102: Log vs. Log plot of the analysed pump test data.....	131
Figure 103: A Cooper-Jacob graph of the drawdown at Borehole 1 (Slpmt1).	131
Figure 104: Log vs. log plot of borehole Slpmt 2.	133

Figure 105: A Cooper-Jacob graph of the drawdown for Borehole 2 (Slpmt2).....	133
Figure 106: A Log-Log graph of the drawdown observed at Slpmt3, the red line indicating a possible fracture.	135
Figure 107: A Cooper-Jacob graph of the drawdown at Slpmt3.....	135
Figure 108: The Big Hole located in the city of Kimberley in the Northern Cape province of South Africa.	137
Figure 109: Distribution of the samples boreholes in the study area.....	138
Figure 110: Value distribution for the measured Cl in the study area.	139
Figure 111: Contour map for Cl values in the study area.....	140
Figure 112: Boreholes located between the faults.	141
Figure 113: Close-up look at the boreholes located between the faults.....	141
Figure 114: % Recharge for individual boreholes.....	142
Figure 115: Cl values for each individual borehole.....	143
Figure 116: % Recharge v Cl in mg/l.....	143
Figure 117: Water Level elevation, % Recharge and Cl plotted against one another.	144
Figure 118: Recharge contour map of the study area.	145
Figure 119: Recharge contour map of the study area outlining northern high recharge zones.....	146
Figure 120: Distribution of the boreholes used for the E.A.R.T.H. model.	147
Figure 121: The E.A.R.T.H model for borehole 1.	148
Figure 122: Dewatering of Layer 2 with a transmissivity of $0.4 \text{ m}^2/\text{d}$ showing the drawdown cone.	156
Figure 123: Layer 2 at a transmissivity of $0.4 \text{ m}^2/\text{d}$ with Layer 3 being dewatered.....	156
Figure 124: Layer 3 at a transmissivity of $0.4 \text{ m}^2/\text{d}$ with Layer 3 being dewatered.	156
Figure 125: Dewatering of Layer 4 showing the drawdown cone for layer 2.....	157
Figure 126: Dewatering of layer 4, showing layer 3's drawdown cone.....	157
Figure 127: Showing the drawdown cone for layer 4 with layer 4 being dewatered.....	157
Figure 128: Showing the drawdown cone for layer 2 with layer 2 being dewatered at a transmissivity of $0.28 \text{ m}^2/\text{d}$	158
Figure 129: Drawdown cone for layer 2 with layer 3 being dewatered.....	159
Figure 130: Drawdown cone for layer 3 with layer 3 being dewatered.....	159
Figure 131: Drawdown cone for layer 2 with layer 4 being dewatered.....	159
Figure 132: The drawdown cone for layer 3 with layer 4 being dewatered.....	160
Figure 133: The dewatering of layer 4 showing the drawdown cone for layer 4.....	160
Figure 134: Dewatering of layer 2, showing drawdown cone of layer 2.	161
Figure 135: Drawdown cone for layer 2 with layer 3 being dewatered.....	161
Figure 136: Drawdown cone for layer 3 with layer 3 being dewatered.....	161
Figure 137: Showing drawdown cone for layer 2with layer 4 being dewatered.....	162
Figure 138: Drawdown cone for layer 3 with layer 4 being dewatered.....	162
Figure 139: Showing the drawdown cone for layer 4 with layer 4 being dewatered.	162
Figure 140: Showing the drawdown cone for layer 4, 50 years after mining has stopped.....	164
Figure 141: Head-Time graph of the first decant scenario, showing the initial fall in water level and the later rise of the water in the pit.....	164
Figure 142: Draw down cone for Layer 2, dewatering of layer 4, after 10 years.....	165
Figure 143: Drawdown cone for layer 2, dewatering layer 4, after 50 years.	166
Figure 144: Drawdown cone for layer 3 after 10 years.	166

<i>Figure 145: Drawdown cone for layer 3 after 50 years.</i>	166
<i>Figure 146: Drawdown cone for layer 4 after 10 years.</i>	167
<i>Figure 147: Drawdown cone for layer 4 after 50 years.</i>	167
<i>Figure 148: Decant model for Scenario 2.</i>	169
<i>Figure 149: The Head-Time graph for the second scenario.</i>	169
<i>Figure 150: Drawdown cone for layer 2, 10 years after dewatering.</i>	170
<i>Figure 151: Drawdown cone for layer 2, 50 years after dewatering.</i>	170
<i>Figure 152: Drawdown cone for layer 3 after 10 years of dewatering.</i>	170
<i>Figure 153: Drawdown cones for layer 3 after 50 years of dewatering.</i>	171
<i>Figure 154: Drawdown cones for layer 4, 10 years after dewatering.</i>	171
<i>Figure 155: Drawdown cones for layer 4 after 50 years of dewatering.</i>	171
<i>Figure 156: Decant model for the third scenario.</i>	175
<i>Figure 157: A graph for the decant model of the third scenario.</i>	175
<i>Figure 158: Surface runoff and groundwater inflow concentrated in a single location in the mine workings, courtesy of the Grootegeluk mine.</i>	178
<i>Figure 159: An obsolete sump being backfilled, courtesy of the Grootegeluk mine.</i>	179
<i>Figure 160: Conceptual model for the Waterberg coalfield, showing a single pit backfilled in the manner as is being done at the Grootegeluk mine. Additionally the model provides a summary of the water quality for the various localities of the study area along with aquifer parameters such as recharge. This model is not to scale.</i>	186
<i>Figure 162: The fitted curve for borehole 2.</i>	203
<i>Figure 163: E.A.R.T.H model results for borehole 3.</i>	203
<i>Figure 164: The fitted graph for borehole 4.</i>	204
<i>Figure 165: Results for borehole 5.</i>	204
<i>Figure 166: The graphic results for borehole 6.</i>	205
<i>Figure 167: The E.A.R.T.H model results for borehole 7.</i>	205
<i>Figure 168: The fitted graph for borehole 8.</i>	206

List of Tables

<i>Table 1: World coal reserves taken from the BP statistical review of world energy (2009).</i>	9
<i>Table 2: World coal production from 1988 - 2008, taken from the BP Statistical Review of World Energy.</i>	11
<i>Table 3: Elements analysed for during chemical analysis.</i>	45
<i>Table 4: Most commonly used static ABA methods after Usher et al., (2002).</i>	48
<i>Table 5: Interpretation of final NAG test pH (Usher et al., 2002).</i>	49
<i>Table 6: Initial and Final pH and Interpretation</i>	72
<i>Table 7: Calculated parameters from ABA</i>	74
<i>Table 8: Guidelines for ABA screening criteria (from Price et al., 1997b).</i>	75
<i>Table 9: Interpretation of each sample according to NNP criteria.</i>	75
<i>Table 10: Interpretation of each sample according to NPR criteria.</i>	75
<i>Table 11: XRD classification table.</i>	78
<i>Table 12: XRD results for the north western samples.</i>	81

<i>Table 13: XRD results for the south/eastern core samples.....</i>	<i>84</i>
<i>Table 14: XRD results for the northern samples.</i>	<i>87</i>
<i>Table 15: Summary of slug test results for the study area.....</i>	<i>127</i>
<i>Table 16: Slug test results for Slpmt1.....</i>	<i>128</i>
<i>Table 17: Summary of pumping test results for the boreholes in the study area.....</i>	<i>130</i>
<i>Table 18: Sustainable yield for Slpmt1.....</i>	<i>130</i>
<i>Table 19: Pumping test result summary for Slpmt1.....</i>	<i>132</i>
<i>Table 21: Sustainable yield for Slpmt2.....</i>	<i>132</i>
<i>Table 22: Pumping test result summary for borehole Slpmt2.</i>	<i>134</i>
<i>Table 23: Sustainable yield for Slpmt4.....</i>	<i>134</i>
<i>Table 24: Pumping test result summary for Slpmt4.....</i>	<i>136</i>
<i>Table 25: Results for borehole 1.</i>	<i>147</i>
<i>Table 26: A summary of the predicted water influxes and drawdown cones.....</i>	<i>163</i>
<i>Table 27: A summary of the inflow and drawdown cones for the dewatering of scenario 2.</i>	<i>168</i>
<i>Table 28: A Summary of the drawdown cones and expected inflow in the northern pit for scenario 3.....</i>	<i>173</i>
<i>Table 29: A summary of the expected inflow and drawdown cones for the central pit.</i>	<i>173</i>
<i>Table 30: A Summary of the drawdown cones and the expected inflow for the south eastern pit.....</i>	<i>174</i>
<i>Table 31: Interpretation of ABA pH results.....</i>	<i>191</i>
<i>Table 32: Interpretation of ABA Net Neutralizing Potential results.....</i>	<i>192</i>
<i>Table 33: Interpretation and NP/AP ratios for the north/western core samples.....</i>	<i>192</i>
<i>Table 34: Initial and final pH values for south eastern samples.</i>	<i>193</i>
<i>Table 35: Interpretation of ABA Net Neutralizing Potential results.....</i>	<i>193</i>
<i>Table 36: Interpretation and NP/AP ratios for Exxaro core samples.</i>	<i>194</i>
<i>Table 37: Interpretation of ABA pH results.....</i>	<i>194</i>
<i>Table 38: Interpretation of ABA Net Neutralizing Potential results.....</i>	<i>196</i>
<i>Table 39: Interpretation and NP/AP ratios for northern samples.....</i>	<i>197</i>
<i>Table 40: Interpretation of ABA pH results.....</i>	<i>199</i>
<i>Table 41: Interpretation of ABA Net Neutralizing Potential results.....</i>	<i>199</i>
<i>Table 42: Interpretation and NP/AP ratios for the sandstone samples.</i>	<i>199</i>
<i>Table 43: Interpretation of ABA pH results.....</i>	<i>199</i>
<i>Table 44: Interpretation of ABA Net Neutralizing Potential results.....</i>	<i>200</i>
<i>Table 45: Interpretation and NP/AP ratios for Exxaro core samples.</i>	<i>200</i>
<i>Table 46: Slug test results for Slpmt2.....</i>	<i>201</i>
<i>Table 47: Slug test results for Slpmt3.....</i>	<i>201</i>
<i>Table 48: Slug test results for Slpmt4.....</i>	<i>201</i>
<i>Table 49: Results for borehole 2.</i>	<i>203</i>
<i>Table 50: Results for borehole 3.</i>	<i>203</i>
<i>Table 51: The results for boreholes 4, 5, 6 and 7.....</i>	<i>204</i>
<i>Table 52: Results for borehole 8.</i>	<i>206</i>

CHAPTER 1: Introduction

Local and international experience in the field of coal mining has yielded the generally known fact that coal mining has a pronounced impact on surface and groundwater quality and quantity. The influx of water may be as low as 1% of rainfall for deep board and pillar mines with no subsidence, to as much as 20% for some opencast mines (Hodgson *et al.*, 2007). Such differences have significant impacts on the quantity and quality of surface and groundwater resources on the local scale and further a field. The Waterberg coal reserves represent the only large area with proven coal resources remaining in South Africa. These resources have been targeted for large-scale mining in the foreseeable future.

The application of lessons from other mining areas is appropriate here. The fact that new extraction options such as *in-situ* coal gasification are considered in addition to more traditional mining options brings additional uncertainties to the fore. Although several factors, over and above the effect on water resources should be considered when selecting a mining method, the long-term effect on water quality calls for a careful consideration of alternatives. It is desirable that both developers and regulators be aware of the long-term liabilities and costs associated with different mining methods. The Waterberg coal resources are situated in a relatively dry area. In view of the low rainfall and limited surface-water resources, the necessary level of safeguard measures to ensure the quantity and quality of existing water resources remains unclear. Experience gleaned from other areas cannot necessarily be extrapolated directly as the area is unique in terms of the setting and local conditions for a South African coal field.

1.1. Objectives

A scoping level study was performed to consolidate the existing information on

- The different aquifers in the study area and their geohydrological parameters.
- Pre-mining water quantity and quality of water resources associated with the Waterberg coal field.
- The acid generating potential of the geology found in the study area.
- Detect potential problem lithologies with regards to higher acid generation potential.
- Predicting the impact of additional mines in the area.
- Determining whether the mines would ever reach decant level.
- Providing recommendations on management methods that are applicable to the study area and that are relevant to the study area.

1.2. Methods of Investigation

In order to obtain the necessary information for the completion of the study, many different methods needed to be employed. The project was conducted in several stages to accommodate the different types of information required. Accordingly the initial stages of the project consisted of two hydrocensus, the aim of which was to locate as many boreholes in the study area as possible.

The information recorded during this initial field work included parameters such as water levels, borehole depths, location (X, Y, Z), and preliminary EC and pH measurements. As adjuncts to these parameters, groundwater samples were collected from boreholes in the study area to be used for quality determinations.

The samples were collected by means of through flow bailers, which were cleaned with deionised water prior to sampling. In addition to the hydrocensus, other sources were approached, namely: the geologists at the Grootegeluk mine, Sasol mining, and Eskom to name but a few, for the purpose of gathering additional information on the study area. Geological samples were obtained from the Grootegeluk mine and Sasol, for the purpose of determining the acid potential of the rocks in the study area.

Once sufficient information had been gathered, it was compiled into a single database. This database was used for other determinations, such as for example, the construction of contour maps, the determination of recharge and so forth. Following the initial hydrocensus and information gathering expeditions, numerous tests were conducted in the field to determine the aquifer parameters of the different aquifers present in the study area.

These parameters were necessary for the determination of, for example, yields of the different aquifers and for further use during numerical groundwater flow modelling. These tests comprised pumping test and slug tests, and were performed where possible and according to the requirements of the project.

To account for the influx of water to the study area, the recharge for the study area was calculated by means of the Chloride mass balance method and the E.A.R.T.H. recharge-calculation model. These calculations indicated a low recharge for the study area in accordance with maps constructed by Vegter (1995), which indicated a recharge of between 1.5% and 1.9%.

All these parameters would later be used during the modelling process. For the purpose of determining the acid potential, acid-base accounting was performed on the collected samples by using the peroxide static- test method.

This method is only a screening mechanism to determine if certain rocks would become acidic. It cannot, unfortunately, provide any indication of the amount of acid that will be generated or the length of time it will take for the acid to be generated.

The ABA test indicated that most of the samples collected would become acidic upon oxidation. To form a more rounded conclusion of the potential impact of mining of the coal field, samples were collected from the beneficiation plants at the Grootegeluk mine.

These samples were also analysed for acid potential, and the results indicated that the samples would become acidic upon oxidation. The sampling for the ABA was done according to the weathering depth of the geology in the study area. This information was provided by Dreyer (pers. comm. 2009) who indicated that, due to the difference in the level of weathering, it might also be possible that different areas in the study area would have different acid potentials based on this weathering pattern.

Accordingly the study area was divided into three zones, according to the level of weathering. The results from the tests indicated that some areas were more prone to acid generation, and in certain areas the rocks located at certain depths even more so.

In order to determine the impact the mines would have on both the groundwater and the flow directions of the groundwater, numerical modelling was done using the Visual MODFLOW and PMWIN. Several different scenarios were simulated using the parameters collected during the field work.

The scenarios were constructed in such a manner as to simulate the conditions for both the dewatering and decant potential of the mine pits. The dewatering models indicated that there was very little water available in the study area, with small volumes of water predicted to flow into the mines. The decant models indicated that there was no possibility of the pits ever reaching decant levels with the highest recorded rise being seven meters 50 years after mining had stopped.

Given all the results obtained from the various tests, the relevant literature, and people from the mining industry were consulted with a view to establishing appropriate water-management options for the study area. It was concluded that the most effective way to preserve the water quality and protect the groundwater quality from further deterioration, was to keep all acid-generating material dry as it would not be possible to flood this material once the mine closed, due to the small volumes of water in the study area.

1.3. Structure of the Thesis

This thesis comprises 11 chapters.

- Chapter 1 serves as an introduction, focussing on the reasons for doing the project and the types of investigations performed.
- Chapter 2 contains a discussion and background information on the importance of coal and the impacts which its mining, and its use as a fuel, have on the environment.
- In Chapter 3, the most commonly used methods for mining coal are discussed.
- Chapter 4 is a discussion on the study area.
- Chapter 5 is a discussion on the methods used during testing and analysis, and the parameters used and discussed in the project.
- Chapter 6 is a brief over view of the geology of the Waterberg coalfields.
- Chapters 7 and 8 comprise discussions on acid-base accounting and a discussion of the water quality of the study area respectively,
- Chapter 9, involves a discussion on the analysis and testing of aquifer parameters
- Chapter 10 is a discussion on the numerical modelling and the results for the study area
- Chapter 11 comprises a discussion of possible water management strategies to be employed in the study area.
- This is followed by Chapter 12, which presents a conclusion and recommendations.
- Chapter 13 contains a list of appropriate references.

A list of appendices follows in Chapter 13.

CHAPTER 2: Coal and it's Place in the World

2.1. Introduction

As the primary objective of the project is to determine what the impact of coal mining in the Waterberg coal fields will be on the groundwater resources, it is prudent to first examine the importance of coal and the role it plays in energy production. This, together with the energy policies of the South African government, plays a vital role in determining the extent to which the Waterberg coal resources will be mined and for what length of time these resources may be exploited. Of additional importance, are the different methods used for the extraction of coal, the reason being that different extraction methods have different impacts on the environment. Early on in the project it was determined that, at present, only one form of extraction is used in the Waterberg coal fields, namely, bulk mining. According to Dreyer (pers. comm. 2009) it is the only form of surface mining planned for the study area. The surface mining will be conducted to the west of the Daarby fault, as this marks the transition from shallow coal to the west to deeper coal to the east of the fault. Sub-surface mining of the coal field located to the west of the Daarby fault is possible but will only be implemented once all the coal which is extracted through surface mining methods has been removed. In addition, Coal Bed Methane (CBM) extraction is being tested east of the Daarby fault, in the deeper coal beds, as a potential mining method for the deeper coal fields. The methane has been found suitable for use in power generation.

According to Snyman (1998) coal is a readily combustible sedimentary rock that contains more than 50%, in mass, and more than 70%, in volume, carbonaceous material (petrified plants) and is formed by the accumulation, compaction and induration of variously altered plant remains in an anoxic environment. Coal is generally classified as a sedimentary rock, but the harder forms such as anthracite, can be regarded as a metamorphic rock, due to its later exposure to elevated temperatures and pressure. It is primarily composed of carbon and hydrogen along with small quantities of other elements; notably sulphur.

Coal is extracted from the ground by coal mining; either by underground or surface methods. Coal is the primary source of fuel used for the generation of electricity and also one of the main contributors to carbon dioxide emissions around the world. According to Vermeulen (2006) 68% of South Africa's produced energy was coal dependent in 1997. Coal is classified according to grade, rank and typed into six different types of coal, which are formed when geological processes apply pressure to dead biotic matter over time. Under suitable conditions, the material is slowly transformed successively into; Peat, Lignite, Sub-bituminous coal, Bituminous coal, Anthracite and Graphite.

2.2. Coal as Fuel

Coal as a mineral has a wide variety of uses, some of which are:

- As a fuel source,
- For coke burning used in metallurgical process,
- Gasification for the production of syngas
- And liquefaction (coal to liquids) which is presently being done by Sasol.
- Coal is also used as a trade commodity and it has some cultural uses.

This study, however, will focus on coal as a fuel source. The primary use of coal is as a solid fuel, used for the production of electricity and heat through combustion. According to the British Petroleum Statistical Review of World Energy, the world coal consumption was around 3303 Mtoe (million tonnes oil equivalent) in 2008. China consumed roughly 1406 Mtoe, while producing 2782 Mt in 2008 (www.bp.com). India consumed roughly 231 Mtoe and produced 512 Mt in 2008 (www.bp.com). Accordingly, the USA consumed 565 Mtoe in 2008 with a country wide production of 1062 Mt for the same year of which 49% was used for the generation of electricity (www.eia.doe.gov).

When coal is used as fuel for the generation of electricity, it is pulverised and then burned in a furnace with a boiler. The furnace heat converts the boiler water to steam, which is used to spin the turbines attached to the system. These turn generators that create (generate) electricity.

Currently the most advanced steam turbines have reached 35% thermodynamic efficiency for the entire process, which indicates that 65% of the energy is wasted in the form of heat that is released into the surrounding environment (www.worldcoal.org). Older coal power plants are significantly less efficient and produce even higher levels of waste heat. Roughly 40% of the world's electricity is generated with coal as primary fuel source, with approximately 49% of electricity generated in the United States being generated with coal (www.eia.doe.gov).

From the above mentioned it is clear that there is a very high demand all over the world for coal as a cheap and effective fuel for the generation of electricity. Coal is, however a limited and non-renewable resource which is dwindling fast. The world's hunger for a cheap and effective energy source will lead to the consumption of all such resources with the environment being left to pick up the bill. At present South Africa's primary source of fuel for the production of electricity is coal, with coal accounting for 94% of all electricity generated in South Africa (www.worldcoal.org).

2.3. Environmental Effects of Coal Burning and Mining

Coal mining and coal burning result in a number of adverse environmental effects. These effects are in many cases especially visible in and around power stations and coal mines.

2.3.1. Effects from Coal Burning

The environmental impacts associated with the burning of coal are numerous. Some of the more common problems are briefly discussed. The burning of coal releases carbon dioxide a greenhouse gases that cause climate change and global warming (www.sourcewatch.org). Additionally, the burning of coal generates hundreds of millions of tons in waste products, including fly ash, bottom ash, flue gas, desulphurisation sludge, which contains mercury, uranium, thorium, arsenic and other heavy metals. The release of SO₂ into the atmosphere can lead to the generation of acid rain. This is however a more localized phenomenon but is still a cause for concern. The SO₂ forms particles in the atmosphere that can cause lung damage and heart disease (www.sourcewatch.org).

Coal-fired power plants without effective fly ash capture are one of the largest sources of human-caused background radiation exposure. The sheer volume of fly-ash produced by a single power station and the area needed for dumping the ash poses its own problems. The ash heaps are unsightly and take up a very large area that increases with the age of the power station. There are no known beneficial uses of the fly-ash except for use in the management of acid mine drainage, but this also has some drawbacks associated with it. An example of the drawbacks associated with the use of fly-ash for acid neutralization was discussed by Hodgson and Krantz (1995) who pointed out that, if all the acid is not initially neutralized, the low pH values present in the effluent could mobilize the heavy metals in the fly-ash. This would lead to more dangerous effluents than those initially present. All of the above mentioned environmental impacts can be extremely dangerous if not properly monitored and it should be the power generator or coal burner's first priority to minimise these impacts to as large a degree as possible.

2.3.2. Effects from Coal Mining

The excavation of open pits and excavations for sub-surface mining leads to disturbances in the water table. These disturbances are not only felt locally within the mine, but can be felt further afield by groundwater users near the mines. The mining may lead to a decrease in water levels and might alter the groundwater flow direction in severe cases. Coal mining may have impacts on water use and river flows and subsequent impact on other land uses. Other impacts that stem from coal mining are, for example, acid-mine-drainage.

Acid mine drainage can find its way into the groundwater system or, it can decant from abandoned mine workings into surface water bodies where it decreases the pH of the water and releases all the pollutants that were held in solution. The transport of the coal in the mine and from the mine to the beneficiation plants and the manner in which an open cast mine is excavated, leads to the generation of vast quantities of dust. In most cases efforts are made to suppress dust, but inevitably dust is generated and cannot be confined to the perimeter of the mine. Besides being a nuisance, the dust can lead to respiratory disease, reduced visibility in severe cases and in extreme cases may even halt the production of the mine. The tunnelling from sub-surface mining can lead to subsidence above the tunnels which can cause damage to infrastructure (Grobbelaar, 2001).

The subsidence can in severe cases lead to a total collapse of the mined out areas which can render a piece of land completely useless. This will depend on the use of the land and the size of the collapse (Grobbelaar, 2001). Open-cast mining can also alter the land on which it and its dumps are located making it unfit for other uses. This is due to contamination of the soil, or the scarring left by the open pit (www.sourcewatch.org). Subsurface mines can reduce the integrity of the surrounding rock to such a degree that the rock will not support large structures on the surface. Another serious problem associated with open-cast mining is noise pollution. The noise from the blasting and the excavation can be very disturbing to both humans and animals. Therefore, the environmental impacts of coal and its attributed mining and burning are far reaching and can be devastating. It is recommended that the impacts of the mining of coal be considered thoroughly by the mining houses involved in the development of the mines, before mining starts.

2.4. World Coal Reserves

It is estimated that by the end of 2006, the recoverable global coal reserves amounted to around 800 or 900 gigatons (International Energy Annual 2005). The United States Energy Information Administration estimates the world reserves as 998 billion short tons (equal to 905 gigatons), and it is estimated that approximately half of this is hard coal (International Energy Annual 2005, and www.eia.doe.gov). According to www.eia.doe.gov, "At the current global consumption rate, these resources will last 164 years". According to British Petroleum (www.bp.com), the total recoverable reserves of coal from around the world were 826001 Mt at the end of 2008 (Table 1). This gives a reserve-to-production ration (the ration of remaining reserves to the amount of reserves being removed) of 122 years for the world as a whole. For South Africa the estimated reserves are placed at 30408 Mt and 121 years of reserves if the reserve-to-production ratio is taken into account. Only reserves classified as "proven" are included in these estimates as exploration drilling programmes by mining companies, particularly in under-explored areas, are continually uncovering new reserves.

Companies are however often aware of coal deposits that have not been sufficiently drilled to qualify as "proven". Some nations also do not update their information and assume that reserves remain at the same levels even after much of the resources have been removed. According to British Petroleum (www.bp.com), the world coal consumption was 4954.5 Mt (3303 Mtoe) at the end of 2008. At current consumption levels (4954.5 Mt/a for 2008) there are sufficient coal reserves to supply the world's demand for coal for 166 years. It can be concluded from the differing levels of estimated remaining coal reserves, that there is a level of uncertainty with regards to just how much coal is still available for exploitation. Coal has the most widely distributed reserves of the three fossil fuels and is mined in over 100 countries and all continents, except Antarctica. The largest reserves are located in the USA, Russia, Australia, China, India and South Africa (www.bp.com)

Table 1: World coal reserves taken from the BP statistical review of world energy (2009).

Coal: Proved Reserves at end 2008					
Million tonnes	Anthracite and bituminous	Sub-bituminous and lignite	Total	Share of Total	R/P ratio
US	108950	129358	238308	28.9%	224
Canada	3471	3107	6578	0.8%	97
Mexico	860	351	1211	0.1%	106
Total North America	113281	132816	246097	29.8%	216
Brazil	-	7059	7059	0.9%	*
Colombia	6434	380	6814	0.8%	93
Venezuela	479	-	479	0.1%	74
Other S. & Cent. America	51	603	654	0.1%	*
Total S. & Cent. America	6964	8042	15006	1.8%	172
Bulgaria	5	1991	1996	0.2%	70
Czech Republic	1673	2828	4501	0.5%	75
Germany	152	6556	6708	0.8%	35
Greece	-	3900	3900	0.5%	58
Hungary	199	3103	3302	0.4%	351
Kazakhstan	28170	3130	31300	3.8%	273
Poland	6012	1490	7502	0.9%	52
Romania	12	410	422	0.1%	12
Russian Federation	49088	107922	157010	19.0%	481
Spain	200	330	530	0.1%	32
Turkey	-	1814	1814	0.2%	21
Ukraine	15351	18522	33873	4.1%	438
United Kingdom	155	-	155	-	9
Other Europe & Eurasia	1025	18208	19233	2.3%	268
Total Europe & Eurasia	102042	170204	272246	33.0%	218
South Africa	30408	-	30408	3.7%	121
Zimbabwe	502	-	502	0.1%	287
Other Africa	929	174	1103	0.1%	*
Middle East	1386	-	1386	0.2%	*
Total Middle East & Africa	33225	174	33399	4.0%	131
Australia	36800	39400	76200	9.2%	190
China	62200	52300	114500	13.9%	41
India	54000	4600	58600	7.1%	114
Indonesia	1721	2607	4328	0.5%	19
Japan	355	-	355	-	289
New Zealand	33	538	571	0.1%	111
North Korea	300	300	600	0.1%	17
Pakistan	1	2069	2070	0.3%	496
South Korea	133	-	133	-	48
Thailand	-	1354	1354	0.2%	75
Vietnam	150	-	150	-	4
Other Asia Pacific	115	276	391	-	26
Total Asia Pacific	155809	103444	259253	31.4%	64
Total World	411321	414680	826001	100.0%	122
of which: European Union	8427	21143	29570	3.6%	51
OECD	159012	193083	352095	42.6%	164
Former Soviet Union	93609	132386	225995	27.4%	433
Other EMEs	158700	89211	247911	30.0%	60

2.5. Major Coal Producers

Coal is commercially mined in over 50 countries worldwide (www.bp.com). According to the British Petroleum (www.bp.com), 6780 Mt of coal was produced in 2008 (Table 2). From these statistics one can conclude that there is a very large demand for coal. It is likely that this demand will increase as more African and Asian nations develop and expand. The expansion in these countries goes hand in hand with the production of electricity for which coal is still one of the cheapest fuel sources.

Generally most of the coal produced in a country is used in the country of origin mainly for power generation, or in the process of making steel. Some coal is however exported. Table 2 shows that there has been a sharp increase in the production of coal over the past 20 years. This is likely due to large scale development of many African and Asian countries, with Asia showing the biggest increase in the tonnes of coal produced over the past 20 years.

The largest producers of coal are also the countries that have the largest reserves, namely the USA, Russia, Australia, China, India and South Africa.

The production figures for these areas are listed below:

- China produced 2782 Mt
- USA, 1062 Mt
- India, 512 Mt
- Australia, 401 Mt
- Russia, 326 Mt,
- South Africa having produced 250 Mt in 2008 (www.bp.com).

This places South Africa as the sixth biggest producer of coal in the world, with China being the biggest. These production trends are likely to continue in the future as countries continue to expand, and the need for cheap and efficient fuels is ever present.

Table 2: World coal production from 1988 - 2008, BP Statistical Review of World Energy.

Coal: Production *																					Change	2008	
Million tonnes	1988	1989	1990	1991	1992	1993	1994	1995	1996	1997	1998	1999	2000	2001	2002	2003	2004	2005	2006	2007	2008	2007	of total
US	862.1	889.7	933.6	903.5	905.0	857.7	937.6	937.1	965.1	988.8	1013.8	998.3	974.0	1023.0	992.7	972.3	1008.9	1026.5	1054.8	1040.2	1062.8	1.3%	18.0%
Canada	70.7	70.5	68.4	71.1	65.3	69.1	72.8	75.0	75.8	78.7	75.4	72.5	69.2	70.4	66.6	62.1	66.3	67.6	66.0	69.4	67.7	-2.6%	1.1%
Mexico	5.6	6.0	6.9	6.5	6.1	6.6	8.9	9.3	10.3	10.4	11.2	10.3	11.3	11.3	11.1	9.6	9.9	10.8	11.5	12.5	11.5	-8.6%	0.2%
Total North America	938.3	966.2	1008.9	981.1	976.4	933.3	1019.3	1021.4	1051.2	1077.8	1100.4	1081.1	1054.5	1104.7	1070.4	1044.0	1085.1	1104.8	1132.3	1122.1	1142.0	1.0%	19.2%
Brazil	7.3	6.7	4.6	5.2	4.7	4.6	5.1	5.2	4.8	5.7	5.5	5.7	6.8	5.7	5.1	4.7	5.4	6.3	5.9	6.0	6.4	7.6%	0.1%
Colombia	15.8	19.9	20.5	21.2	23.5	21.7	22.7	25.7	30.1	32.3	33.8	32.8	38.2	43.9	39.5	50.0	53.7	59.1	65.6	69.9	73.5	4.9%	1.4%
Venezuela	1.1	2.1	2.2	2.4	2.5	4.0	4.4	4.4	4.2	5.3	6.5	6.6	7.9	7.7	8.1	7.0	8.1	7.2	7.5	8.0	6.4	-20.2%	0.1%
Other S. & Cent. America	2.6	2.6	2.5	2.6	1.9	1.6	1.5	1.4	1.3	1.3	1.2	0.8	0.6	0.8	0.5	0.7	0.3	0.5	0.9	0.7	0.9	36.3%	
Total S. & Cent. America	26.8	31.3	29.8	31.3	32.6	31.9	33.8	36.7	40.4	44.6	47.0	45.8	53.6	58.0	53.3	62.4	67.5	73.0	79.9	84.6	87.3	2.5%	1.7%
Bulgaria	34.2	34.3	31.7	28.5	30.3	29.0	28.8	30.8	31.3	29.7	30.1	25.3	26.4	26.6	26.1	27.3	26.6	24.6	25.3	28.2	28.4	1.3%	0.1%
Czech Republic	119.8	114.1	102.8	96.2	86.6	85.2	77.0	74.3	73.9	73.5	67.5	59.1	65.2	66.1	63.4	63.9	62.0	62.0	62.4	62.2	60.3	-3.0%	0.7%
France	15.2	14.5	13.6	12.9	11.8	11.0	9.5	8.9	8.6	7.3	6.1	5.7	4.1	2.8	2.0	2.2	0.9	0.6	0.5	0.4	0.2	-50.1%	
Germany	497.9	482.3	426.7	345.9	307.3	279.7	259.5	245.9	235.1	223.3	207.0	200.8	201.0	202.5	208.2	204.9	207.8	202.8	197.1	201.9	192.4	-7.7%	1.4%
Greece	48.3	51.9	51.9	52.7	55.1	54.8	56.7	57.7	59.8	58.8	60.9	62.1	63.9	66.3	70.5	71.0	71.6	70.6	64.8	67.4	67.8	0.3%	0.3%
Hungary	20.9	20.0	17.6	17.0	15.8	12.6	13.9	12.2	15.1	15.6	14.5	14.6	14.0	13.9	13.0	13.3	11.5	9.6	10.0	9.8	9.4	-4.5%	0.1%
Kazakhstan	143.1	138.4	131.4	130.0	126.5	111.9	104.6	83.4	76.8	72.6	69.8	58.4	74.9	79.1	73.7	84.9	86.9	86.6	96.2	97.8	114.7	17.1%	1.8%
Poland	266.5	249.5	215.3	209.8	198.4	198.6	200.7	200.7	201.7	200.9	178.6	172.7	162.8	163.5	161.9	163.8	162.4	159.5	156.1	145.9	143.9	-3.3%	1.8%
Romania	58.8	61.3	38.2	32.4	38.4	39.8	40.6	41.1	41.9	33.8	26.2	22.9	29.3	33.3	30.4	33.1	31.8	31.2	34.9	35.8	34.7	-3.2%	0.2%
Russian Federation	425.5	409.8	395.3	353.3	337.3	305.9	272.0	262.8	256.5	245.0	231.9	249.5	258.3	269.6	255.8	276.7	281.7	298.3	309.9	314.2	326.5	2.8%	4.6%
Spain	31.9	36.5	36.0	33.9	33.3	31.8	29.5	28.5	27.4	26.5	26.1	24.3	23.5	22.7	22.0	20.5	20.5	19.4	19.2	18.2	16.6	-9.1%	0.2%
Turkey	39.2	52.2	47.4	46.1	51.4	48.6	54.4	55.1	56.4	59.9	67.4	67.0	66.6	67.7	54.4	49.3	49.9	61.7	64.9	76.6	86.2	12.6%	0.5%
Ukraine	191.7	180.2	164.9	135.6	133.6	115.7	94.4	83.8	70.5	76.9	77.2	81.7	81.0	83.9	82.5	80.2	81.3	78.7	80.4	76.8	77.3	0.4%	1.2%
United Kingdom	104.1	99.8	92.8	94.2	84.5	68.2	49.0	53.0	50.2	48.5	41.2	37.1	31.2	31.9	30.0	28.3	25.1	20.5	18.5	17.0	17.9	5.0%	0.3%
Other Europe & Eurasia	98.0	99.8	101.7	87.9	82.3	75.0	60.4	62.2	59.4	69.5	73.8	58.4	62.9	62.2	65.1	66.6	65.4	64.0	67.0	68.3	71.7	2.0%	0.5%
Total Europe & Eurasia	2095.0	2044.5	1867.2	1676.4	1592.6	1467.7	1350.9	1300.5	1264.4	1242.0	1178.2	1139.5	1165.0	1192.2	1158.9	1186.1	1185.3	1190.1	1207.3	1220.3	1248.1	1.8%	13.7%
Total Middle East	1.3	1.2	1.3	1.0	1.0	1.0	1.3	1.1	1.2	0.9	1.0	1.1	1.0	0.8	0.6	1.0	1.1	1.1	0.8	0.8	0.8	-0.3%	
South Africa	181.4	176.3	174.8	178.4	174.4	182.3	195.8	206.2	206.3	219.9	224.8	222.3	224.1	223.7	220.2	237.9	243.4	244.4	244.8	247.7	250.4	0.8%	4.2%
Zimbabwe	5.1	5.1	5.5	5.6	5.6	5.3	5.5	5.5	5.2	5.3	5.5	5.0	4.4	4.5	3.9	2.8	3.8	2.9	2.1	2.1	1.7	-17.2%	
Other Africa	2.4	2.2	2.3	2.4	2.4	2.2	2.3	2.3	2.1	2.0	2.3	2.2	2.0	2.0	2.1	2.6	2.1	1.9	2.0	1.8	1.8	-0.3%	
Total Africa	188.8	183.6	182.6	186.4	182.3	189.8	203.6	214.1	213.6	227.2	232.6	229.5	230.6	230.2	226.3	243.3	249.3	249.2	248.8	251.6	254.0	0.6%	4.3%
Australia	187.5	201.9	210.4	218.4	229.1	228.7	233.6	245.3	256.1	279.7	288.0	303.0	310.9	333.2	342.0	351.5	366.1	378.8	385.3	399.0	401.5	0.3%	6.6%
China	979.9	1054.2	1079.9	1087.4	1116.4	1150.7	1239.9	1360.7	1396.7	1372.8	1250.0	1280.0	1299.2	1381.5	1454.6	1722.0	1992.3	2205.7	2373.0	2526.0	2782.0	10.0%	42.5%
India	197.0	215.3	223.3	239.9	253.8	263.2	270.9	289.0	311.0	319.4	320.9	314.4	334.8	341.9	358.1	375.4	407.7	428.4	449.2	478.4	512.3	7.0%	5.8%
Indonesia	4.5	8.7	10.7	13.8	22.4	27.6	32.9	41.8	50.4	54.8	62.2	73.7	77.0	91.9	103.4	114.3	132.4	152.7	193.8	217.4	229.5	5.3%	4.2%
Japan	11.2	10.2	8.3	8.1	7.6	7.2	6.9	6.3	6.5	4.3	3.7	3.9	3.1	3.2	1.4	1.3	1.3	1.1	1.4	1.4	1.2	-14.0%	
New Zealand	2.4	2.7	2.6	2.7	3.0	3.1	3.0	3.5	3.6	3.4	3.3	3.5	3.6	3.9	4.5	5.2	5.2	5.3	5.8	4.8	5.1	5.5%	0.1%
Pakistan	2.7	2.7	2.8	2.8	3.0	3.2	3.0	3.2	3.5	3.1	3.3	3.3	3.2	3.3	3.5	3.3	3.3	3.5	3.9	3.6	4.2	14.8%	0.1%
South Korea	24.3	20.8	17.2	15.1	12.0	9.4	7.4	5.7	5.0	4.5	4.4	4.2	4.2	3.8	3.3	3.3	3.2	2.8	2.8	2.9	2.8	-4.0%	
Thailand	7.3	8.9	12.4	14.7	15.4	15.6	17.1	18.4	21.5	23.4	20.2	18.3	17.7	19.6	19.6	18.8	20.1	20.9	19.0	18.2	18.1	-1.3%	0.2%
Vietnam	6.1	5.1	5.1	5.2	5.2	6.5	6.0	6.9	8.8	11.3	11.4	8.8	11.6	13.4	16.4	19.3	26.3	32.6	38.9	41.2	42.2	2.1%	0.7%
Other Asia Pacific	61.2	60.0	56.2	54.4	47.4	43.7	40.5	38.0	34.2	33.5	30.9	34.3	36.7	37.6	36.8	38.2	41.9	46.2	47.0	48.8	50.2	1.6%	0.8%
Total Asia Pacific	1484.1	1590.4	1628.9	1662.5	1715.2	1758.8	1861.3	2018.8	2097.1	2110.2	1998.2	2047.4	2102.0	2233.4	2343.5	2652.6	2999.7	3278.1	3520.1	3741.8	4049.1	8.0%	61.1%
Total World	4734.2	4817.2	4718.6	4538.7	4500.1	4382.4	4470.1	4592.6	4667.9	4702.8	4557.5	4544.4	4606.6	4819.3	4852.9	5189.4	5587.8	5896.2	6189.1	6421.2	6781.2	5.3%	100.0%
of which: European Union #	1209.0	1174.7	1036.0	936.7	873.6	821.7	773.3	761.9	753.3	728.1	668.1	633.9	630.9	638.6	637.2	638.0	628.4	608.0	595.5	593.4	578.7	-3.9%	5.2%
OECD	2319.3	2333.3	2261.2	2142.4	2079.1	1978.5	2024.1	2022.5	2054.3	2089.6	2074.3	2044.3	2014.1	2093.0	2054.1	2030.4	2078.8	2103.5	2125.7	2135.8	2153.2	0.1%	31.4%
Former Soviet Union	771.9	740.3	703.8	629.6	604.8	539.5	476.0	433.6	407.1	398.1	382.2	393.0	417.1	435.8	4								

2.6. Coal in South Africa

The Karoo Supergroup host all the coal resources in South Africa. Coal seams are found to be virtually horizontal throughout the main Karoo basin. The only significant disturbances to this trend is produced by sills, dykes and / or faulting, which does not merely displace the seams, but which also leads to devolatilisation of the coal. According to Cadle *et al.*, (1993) the primary control on the distribution, lateral extent, maceral content and thickness of the coal seams, derives from basin tectonics and differential subsidence. Pre-Karoo and Dwyka glacial topographic features along with sedimentological factors (depositional environment, palaeoclimates, timing of marine transgressions and fluvial clastic influences) also playing a role in coal distribution. The wide range of depositional settings within which peats can accumulate, combined with variations in climate and plant communities, as well as Jurassic dolerite intrusions, impart significant differences in the grade and the type of the coal found in the Karoo basin. For example the peats of the Vryheid Formation accumulated in swamps in a cool temperate climate regime.

The lower and upper delta-plains, back-barriers and fluvial environments, are generally associated with peat formation, with thick, laterally extensive coal seams preferentially accumulating in fluvial environments. The coals from the Karoo basin are generally, inertinite-rich with high ash content. However, it has been found by Johnson *et al.*, (2006) that there is an increase in vitrinite content and a decrease in ash content within seams moving from west to east across the coalfields of South Africa. The Molteno coal seams, dating from the Triassic, accumulated within restricted swamps in fluvial environments under a warm temperate climatic regime (Snyman, 1998). Work done by Johnson *et al.*, (2006) indicated that rapid subsidence coinciding with high sedimentation rates, resulted in coals that are “thin, laterally impersistent, vitrinite rich and shaly”. According to studies done by Snyman (1998) a generally accepted setting for the formation of peat in the Lephalale area is a floodplain setting with meandering rivers. The repeated flooding together with the creation of crevasse splays contributed to the rapid alteration of mudstone and coal in the Grootegeluk formation. The Grootegeluk formation being present in the study area and being the predominant formation from which coal is mined.

Similar depositional environments may be postulated for the Tuli and Springbok Flats sub-basins. According to the results of a study done by Bredell (1987) the total recoverable coal reserves of the Karoo Supergroup is estimated to be 55333 Mt (in situ resources of 121218 Mt), with 37625 Mt present in the Main Karoo basin . According to Snyman (1998) the total beneficiated reserves located within the Karoo basin are in the order of 29000 Mt, a large component (77%) of which is low-grade (<25.5 MJ/kg) bituminous coal. Johnson *et al.*, (2006) further indicates that high-grade (non-coking) bituminous reserves (12%) contribute the bulk of the 59.7Mt of coal exported in 1995.

From information collected by Johnson *et al.*, (2006) it is estimated that of the approximately 206 Mt coal produced during 1995, 94% was non-coking bituminous coal constituted, with coking coal and anthracite accounting for approximately 4% and 1.5% of saleable (beneficiated) reserves respectively. According to Source Watch, it was estimated that in 2005, coal-fired power stations accounted for approximately 93% of South Africa's electricity production, with Eskom being the dominant domestic coal consumer. Approximately one-third of the coal which is domestically consumed is used by Sasol as the source for synthetic fuel and chemical production. South Africa has become a major player in the global coal trade, exporting an estimated 69 million tonnes of coal in 2006, the bulk of which is exported to Germany, Spain and Japan. According to Eskom, 53% of domestic consumption is used for electricity generation, with a further "12% for metallurgical industries and 2% for domestic heating and cooking". According to Source Watch, Eskom confines its considerations to major centralised power station options of gas, hydro and nuclear power. The energy provider argues "that domestic gas and hydro resources are limited; importing hydro power from the Zaire River basin could be unreliable due to political instability". The as yet unproven pebble-bed nuclear reactor is projected in a somewhat more positive light in terms of its future potential as a power source. Its implementation is, however, still only a distant possibility. From information provided by Source Watch, Eskom is not considering any other options for power generation, and places its faith in "clean coal" technologies. According to its spokespersons: "There are many existing and emerging clean coal technologies that will enable the production, processing, conveyance and utilisation of coal in a more environmentally compatible manner".

2.7. South African Government Energy Policy

After years of substantial overcapacity, the recent rapid economic growth of South Africa and power generation constraints, led to the proposal by the South African government of a massive expansion of the country's electricity generation system. According to Source Watch instead of relying solely on the publicly owned electricity utility (Eskom) the government directed that 30% of the new capacity should be provided by independent power producers. In 2004 this led to the approval of a five-year R93 billion expansion plan being approved by the South African Cabinet, of which Eskom would be funding R84 billion. In response to this, Eskom increased its projected electricity demand forecast from 2.3% per annum, to 4% in 2004 and is now set to spend R150 billion in the five-year period to be concluded in the financial year 2011-2012. To meet these deadlines Eskom has taken the following steps: "As of November 2007, there are currently 11,941 megawatts of plants in the 'project execution phase". Of this, Eskom reported that 1577 megawatts have already been commissioned. Other 'in execution' generation projects comprise the construction of six new coal-fired 6-900 megawatt units (for between 3,600 megawatts and 5,400 megawatts

capacity); the re-commissioning of previously mothballed power stations providing 3,600 megawatts; the construction of the Ingula Pumped Storage Scheme hydro scheme, with four 333 megawatt turbines (for 1332 megawatts of installed capacity) to provide increased peaking capacity; the construction of fourteen 150 megawatt open cycle gas units for a total of 2,100 megawatts installed capacity; and a 100 megawatt wind farm” (www.sourcewatch.org). This ambitious expansion project can be witnessed firsthand in the study area in the form of the Medupi Power Station Construction Project. The re-commissioning and up-keep of older and mothballed power stations has led to widespread blackouts, termed "load shedding" by the Department of Minerals and Energy (www.sourcewatch.org). According to Source Watch this “load shedding” emphasised the need for urgent measures to increase the ability of the electricity system in South Africa to cater for peak demand and to allow sufficient time for necessary maintenance. To help fund the cost of the massive construction programme, Eskom was initially granted permission by the South African Government to increase its electricity tariff by 27.5% in the 2008 / 2009 financial year. Recently however, the government has granted Eskom permission to increase its tariff by 31% (www.sourcewatch.org).

2.7.1.Existing Coal-Fired Power Stations

The following data was derived from Source Watch (www.sourcewatch.org) to demonstrate the current lack of capacity and the attempts to alleviate the problem:

- Arnot Power Station: 2,140 MW installed capacity comprising 4 X 350 MW units and 2 X 370 MW units. The power station is located in Middelburg, Mpumalanga; Eskom plans to commission 60 megawatts upgrades in 2008, a further 60 megawatts in each of 2009 and a further 30 megawatts in 2010.
- Duvha Power Station: 3,600 MW installed capacity comprising 6 X 600 MW units. The power station is located in Witbank, Mpumalanga.
- Hendrina Power Station: 2,000 MW installed capacity comprising 10 X 200 MW units. The power station is located in Hendrina, Mpumalanga.
- Kendal Power Station: 4,116 MW installed capacity comprising 6 X 686 MW units. The power station is located in Witbank, Mpumalanga.
- Kriel Power Station: 3,000 MW installed capacity comprising 6 X 500 MW units. The power station is located in Kriel, Mpumalanga.
- Lethabo Power Station: 3,708 MW installed capacity comprising 6 X 618 MW units. The power station is located in Sasolburg, Free State.
- Majuba Power Station: 4,110 MW installed capacity comprising 3 X 657 MW units and 3 X 713 MW units. The power station is located in Volksrust, Mpumalanga.

- Matimba Power Station: 3,990 MW installed capacity comprising 6 X 665 MW units. The power station is located in Lephalale, Limpopo Province.
- Matla Power Station: 3,600 MW installed capacity comprising 6 X 600 MW units. The power station is located in Kriel, Mpumalanga.
- Tutuka Power Station: 3,654 MW installed capacity comprising 6 X 609 MW units. The power station is located in Standerton, Mpumalanga.

2.7.2. Currently Mothballed Coal-fired Stations Being Re-Commissioned

The following coal-fired power stations were mothballed in 1990, but are currently in the process of being re-commissioned - the process having begun in 2005:

- Camden Power Station: 1,580 MW installed capacity comprising 6 X 200 MW units and 2 X 190 MW units. The power station is located in Ermelo, Mpumalanga. In 2007 Eskom re-commissioned 390 megawatts. Plans are to re-commission a further 390 megawatts in 2008.
- Grootvlei Power Station: 1 200 MW installed capacity comprising 6 X 200 MW units. The power station is located in Balfour, Mpumalanga. Eskom plans to re-commission 585 megawatts in 2008 and 2009 respectively.
- Komati Power Station: 1 000 MW installed capacity comprising 5 X 100 MW units and 4 X 125 MW units. The power station is located in Middelburg, Mpumalanga. Eskom plans to re-commission 120 megawatts in 2008, 240 megawatts in 2009, 320 megawatts in 2010 and 285 megawatts in 2011.

2.7.3. New Coal-Fired Power Stations

As part of its "new build" expansion plan, Eskom plans to build two new coal-fired power stations (www.sourcewatch.org). They are:

- The 4,788 megawatt Medupi Power Station, proposed to be progressively commissioned from 2013. 803 megawatts in 2012, 1,596 megawatts in 2013, 798 megawatts in 2014, and a further 1,596 in 2015.
- The 3,212 megawatt Kusile Power Station, proposed to be progressively commissioned from 2012 (798 megawatts in 2013, 1,606 megawatts in 2014, and a further 803 megawatts in 2015).

This ambitious expansion project has attracted new investors to South Africa. According to Source Watch "the Perth-based energy company, the Aviva Corporation, announced its interest in developing the national Mmamantswe Coal Project as a major coal mine with an associated power station".

2.8. The Waterberg Coalfields

The importance of the Waterberg Coalfields resides in the fact that the coalfields have, to a large extent, not been exploited with only one colliery currently active in the study area (Figure 1). Therefore, with the projected expansion of energy resources and the accompanying increase in the demand for coal, the future expansion of these coalfields is necessary in order to contend with the ever-growing need for coal in South Africa.

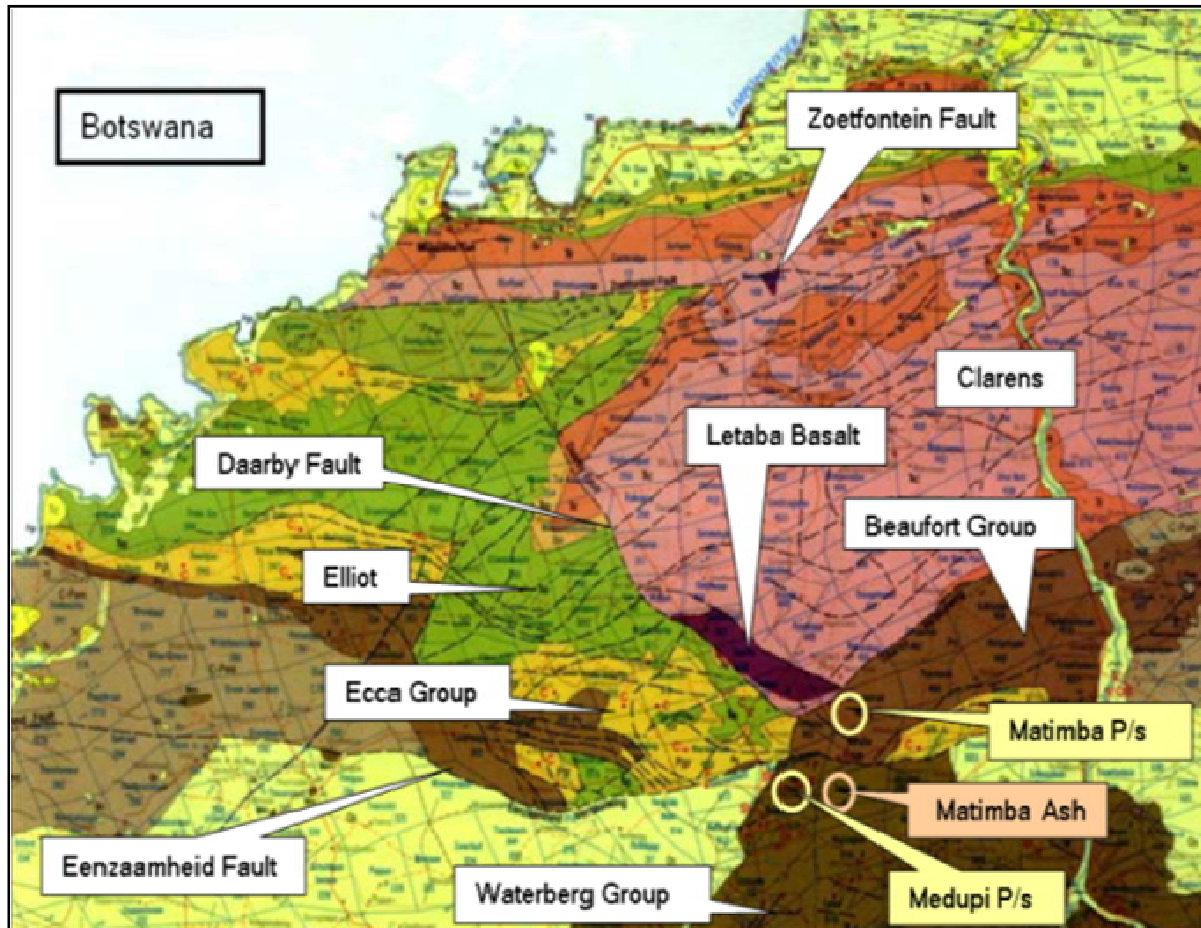


Figure 1: Geological map of the Waterberg Coalfield after Vermeulen (2006).

These coal resources are currently being actively prospected and will be mined extensively in the near future (pers. comm. Dreyer 2009). The opening of several new mines, power stations and petro-chemical plants in the area will have far-reaching and lasting impact on the area and the region. According to Dreyer (pers. comm. 2009) the Waterberg coal fields account for nearly 50% of the remaining coal resources of South Africa.

CHAPTER 3: Mining Methods

3.1. Introduction

As stated in the previous chapter, coal mining has a significant impact on the environment. This impact is often not merely confined to the immediate area of the mine. The effects are often far reaching and enduring, An example would be the collapse of the tunnels of a sub-surface mine, which would render the land unfit for agriculture or development through construction.

Accordingly it was felt that, for the purposes of this study, it was necessary to examine some of the different coal mining methods, as well as the potential impacts of these methods on the environment. Coal mining involves the economical extraction or removal of coal from the earth by means of different mining methods. Coal that is used for fuel in power generation is referred to as steaming or thermal coal (Figure 2).



Figure 2: Dragline mining in an opencast pit (from Snyman, 1998, Optimum Colliery).

3.2. History of Coal Mining in South Africa

The discovery of coal in the Kwazulu-Natal, Mpumalanga and Eastern Cape provinces was first documented between 1838 and 1859. The first commercial exploitation of coal on a reasonable scale took place in 1870 in the now dormant Molteno coal field of the Eastern Cape. This coal was transported to the newly opened diamond fields of Kimberly in the Northern Cape. The East Rand coal fields (Springs, Boksburg, Steenkoolspruit) were brought into production shortly after the discovery of the Witwatersrand gold fields in 1886. According to Snyman (1998) the commercial exploitation of the Free State, Mpumalanga and Kwazulu Natal coalfields commenced between 1881 and 1895.

The accelerated industrialisation of South Africa after World War II as reflected by the development of the Far West-Rand, Free State, Evander and Klerksdorp gold fields, the establishment of steel plants at Vanderbijlpark and Newcastle, and the establishment of Sasol I, II and III etc, created an increased demand for electricity, which led to the erection of many coal-fired power stations by Eskom. These power stations were in the main supplied by dedicated collieries. In the 1980's however the demand for electricity fell below the expected levels and as a result some of the older coal-fired power stations were moth-balled, resulting in the temporary closure of the relevant dedicated collieries. From this period onwards, Eskom pursued the policy of interlinking power stations and possible coal suppliers to ensure a greater mobility of coal, and to alleviate the dependence on a single colliery for coal provision to the power stations.

The 1973 world oil crisis stimulated overseas interests in South African coal and enabled South Africa to penetrate the world coal market with coal exports, which at present play a big part in the economy of South Africa (Snyman, 1998). Thus there has always been a great demand for South African coal both locally and abroad and this is not likely to change anytime soon. The extraction of coal in South Africa will continue well into the future, and it is thus important to be familiar with the methods by which coal extraction takes place at present.

3.3. Methods of Coal Extraction

The most economic method for the extraction of coal depends on the depth and quality of the seams, and factors such as the geology and environmental factors of the area being mined. Coal mining processes are differentiated in terms of the location of the mine - either beneath the surface, or on the surface. This distinction is important as the methods that are employed to remove the coal vary according to the spatial location of the mine (on or below the surface). Coal is only mined where technically feasible and economically justifiable or in cases where the necessity for the coal outweighs the economic implications.

Evaluation of the technical and economic feasibility of a potential coal mine requires the consideration of many factors, some of these being the following:

- The regional geologic conditions, such as faulting, folding, intrusions and the successions in which the coal is located, are important as these will affect the placement and size of the mine.
- The overburden (e.g. rock and soil removed during mining) characteristics such as thickness, type, location and strength (for sub-surface mines) are important. Another factor to be taken into account with regard to the overburden is its potential to generate acid. Many coal mines have a problem with acid generation and if the potential of the overburden to produce acid can be determined beforehand much money can be saved in the long run.
- The coal seam continuity, thickness, structure, quality, depth, thickness of partings between the seams, variations in the elevation of the seam floor, in-seam partings and coal washouts.
- The strength of materials above and below the seam for roof and floor conditions which can influence the location of supports or the ease of mining which are important for sub-surface mining.
- The topography can have a serious effect on the type of mining that will take place at a specific location (for example the presence of mountains will impact the decision on what type of mining will be used, surface or sub-surface).
- The climate, in an open-pit environment, due to much precipitation, can slow or stop production and for example extraction of coal in very cold climates can also reduce the efficiency of the mining process.
- The surface drainage patterns in a potential mining area are important as the presence of rivers and streams will have an impact on the placement of the mining infrastructure and will also influence the decision making with regards to water quality monitoring programs (surface and / or groundwater).
- The groundwater conditions in the immediate mining area as well as the surrounding area are generally heavily impacted by the mining activity, the level of impact depending on the type of mining operation taking place and the size of the mine. It is very important that this aspect be taken into account when planning a mine.
- The availability of labour, materials and infrastructure.
- As with any type of mining, a large capital investment is required to get the mining operation off the ground.

The choice about which mining method should be implemented depends on the depth and thickness of the coal seam, the location of the planned mine and the above-mentioned factors.

3.3.1. Modern Surface Mining

Coal seams located near enough to the surface, are usually extracted by opencast (also referred to as open-cut or open-pit) mining methods. In most cases involving near- surface coal, some form of strip mining is typically used (Figure 3).



Figure 3: Open-pit mining (www.numahammers.com)

Strip mining works by exposing the coal through the advancement of an open-pit or strip by removal of the overburden. A strip of overburden next to the previously mined strip is usually drilled and filled with explosives for blasting. The overburden loosened by the blasting, is removed using large earthmoving equipment such as draglines, shovel and trucks, excavators and trucks, or bucket-wheels and conveyors. The overburden is then transferred to the previously mined (and now empty) strip where it is used for rehabilitation and backfill.

When all the overburden has been removed, the underlying coal seam is exposed as a strip. Depending on the hardness of the coal it may be drilled and blasted (if the coal is hard) or (if the coal is soft) loaded onto trucks or conveyors for transport to the coal beneficiation plant. This process is repeated until all the coal that can be extracted in this fashion has been removed. Surface coal mining recovers a greater proportion of the coal deposit than sub-surface methods, as more of the coal seams in the strata may be exploited and nothing needs to be left behind. This contrasts with sub-surface mines, where pillars of coal are left as roof supports. Surface coal mines can vary greatly in size, from only a few hectares to many square kilometres.

3.3.1.1. Area Mining

During area mining, overburden is removed in long cuts to expose the coal beneath it. The removed spoil from the first cut is deposited in an area outside the planned mining area and is later used as backfill in the previous cut (Figure 4).



Figure 4: Area mining, Courtesy of Dr Vermeulen.

A large number of separate operations are involved in this type of surface mining, and a wide range of equipment is used to remove the coal and overburden, such as draglines, truck and shovel, front-end loader, and bucket wheel excavators. The suitability of the equipment used is generally governed by geological conditions.

3.3.1.2. Contour Mining

Contour mining consists of removing the overburden from the seam in a manner following the contours along a ridge or around a hillside. This method is most commonly practised in areas with a rolling to steep topography.

3.3.1.3. Mountaintop Removal

Mountaintop-removal coal mining is a surface-mining method that involves the removal of mountaintops to expose coal seams, and the disposal of associated mining overburden in adjacent valleys (Figure 5).

These valley fills occur in steep areas that have limited disposal alternatives. Mountaintop removal is a combination of both contour mining and area mining. In areas with a rolling or steep topography, with the coal seams being present near the top of a ridge or hill, the entire top is removed in a series of parallel cuts. The overburden is deposited in nearby valleys and hollows. This method usually leaves ridges and hill tops as flattened plateaus. Spoil is placed at the head of a narrow, steep-sided valley or hollow usually located very near the mine.

In preparation for filling of this area, the vegetation and soil are removed and a rock drain is constructed down the middle of the area to be filled, where a natural drainage course previously existed. When the fill is completed, this under-drain will form a continuous water run-off system from the upper end of the valley to the lower end of the fill. This poses its own problems due to the possibility of pollution generated by the fill that then leaks into these run-off systems. Typically head-of-hollow fills are graded and terraced to create permanently stable slopes.



Figure 5: Mountaintop removal mining (www.coal-is-dirty.com).

3.3.2. Sub-Surface Mining Methods

What follows is a brief description of the most common underground mining methods used in South African coal fields.

3.3.2.1. Bord-and-Pillar Extraction

The Bord-and-Pillar method of extraction is the primary mining method throughout the Mpumalanga Coalfields (Grobbelaar, 2001). Board-and-pillar mining consists of coal deposits that are mined by cutting a network of “boards” into the coal seam (Figure 6). “Pillars” of coal are left behind as roof supports. The pillars can make up as much as 40% of the total coal in the seam. These pillars are mined out mainly at a later stage. This mining method has several advantages:

- It requires comparatively little capital to get started.
- It allows access to the coal in a structured and organised way.
- It can be manoeuvred around geological or coal quality constraints.
- The extraction rate is reasonably high, ranging from 70% in the shallow mines to 50% in deeper areas (Grobbelaar, 2001).

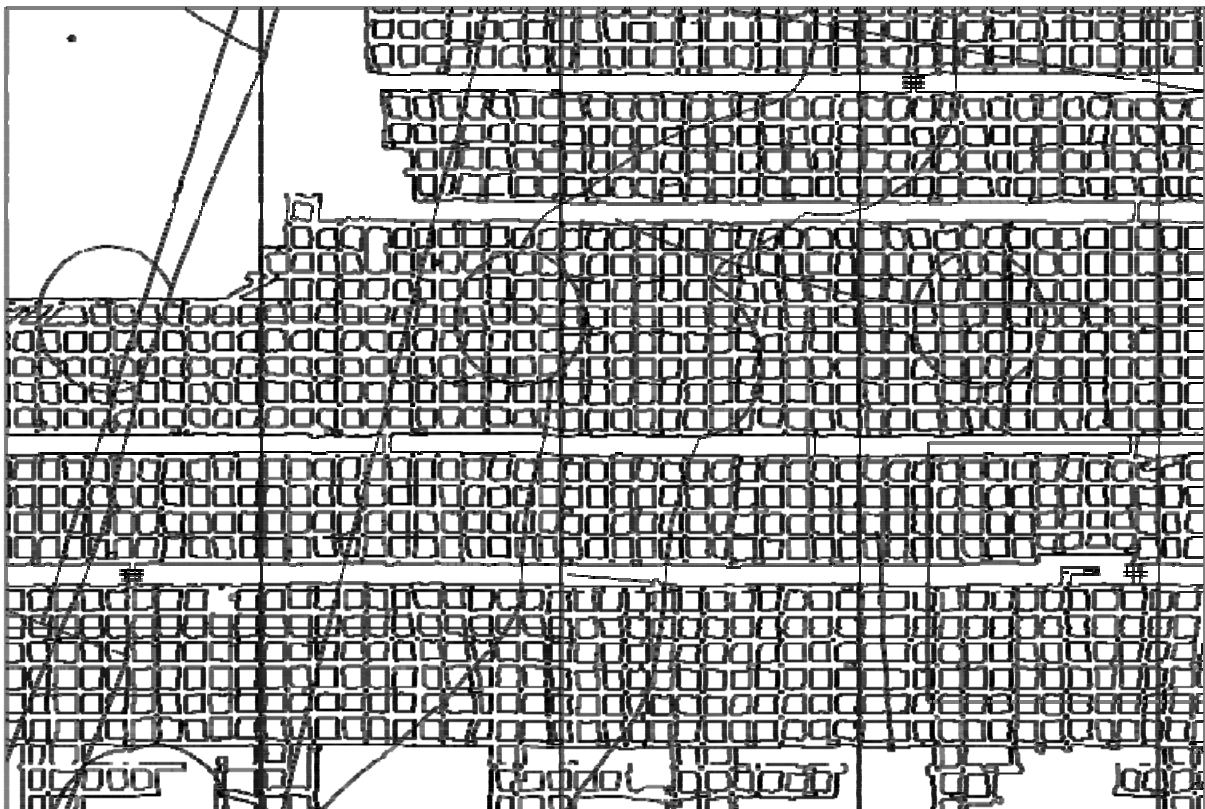


Figure 6: Example of board-and-pillar mining in a modern underground colliery taken from Grobbelaar, (2001).

3.3.2.2. Stopping

Stopping is a method for subsurface mining that has been used for at least 30 years in the Mpumalanga Coalfields (Grobbelaar, 2001). The Usutu Colliery was one of the first mines where this method was used on a significant scale (Figure 7). Stopping works by removing the required ore from an underground mine and leaving behind an open space known as a stope. Stopping is used when the overburden is sufficiently strong, so as not to cave into the stope, although artificial support is usually provided.

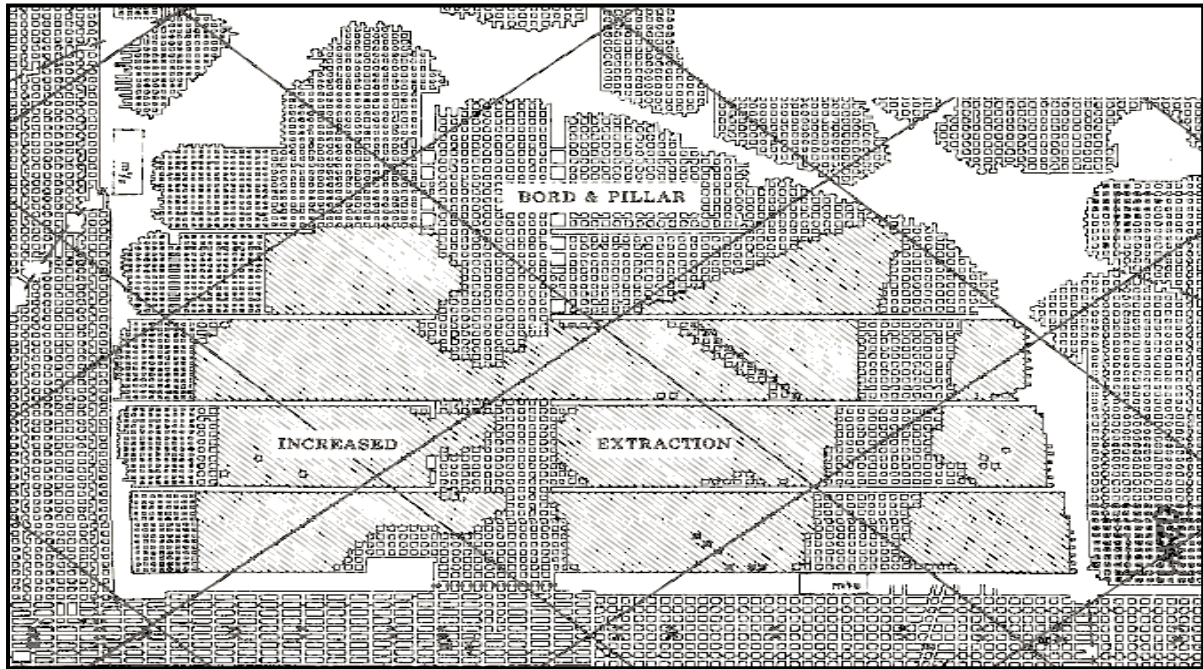


Figure 7: Example of stooped areas at Usutu Colliery taken from Grobbelaar, (2001).

Bord-and-pillar methods and stoping are often used in conjunction. The pillars left behind from bord-and-pillar mining may be halved, quartered or completely removed as time goes on and the mine progresses (Grobbelaar, 2001). The dominating factor regulating the extraction patterns of the pillars area safety constraints rather than economic considerations. According to Grobbelaar , (2001) the extraction rate per area is highly variable, being dependent on factors, such as mining depth, percentage extraction and rock competency. Due to the removal of the pillars, the overlying strata may collapse and these collapses may extend as far as the surface which in the case of the Waterberg coal fields might present a potential problem. Underground mining in the study area will only be used once all the coal capable of being removed by surface methods has been mined out. The sub-surface mines will be located either beneath the surface mines or in close proximity to them.

Accordingly, the thickness of the rocks overlaying the coal to be mined by underground methods will not be of a substantial thickness. If the overburden should crack or fracture as is the case in the Mpumalanga coal fields, surface runoff might enter into the underground workings of the mine. During the course of the modelling the surface runoff into a pit with an area of 800 ha was calculated by means of the rational equation for the estimation of runoff ($Q=CiA$, where Q is the run-off, C is a constant, i is rainfall intensity and A is the expected run-off area (in this instance C was selected as 0.07)). The results indicated an expected run off in the order of $43200 \text{ m}^3/\text{d}$ (Q was calculated to be $0.5 \text{ m}^3/\text{d}$).

This is a large volume of water that can flow into the pits and eventually might find its way into the underground mines. Care should be taken when selecting the type of subsurface mining to be employed to minimise the potential for forming vertical fractures.

3.3.2.3. Longwall Mining

Longwall mining (Figure 8) has been used in the Mpumalanga Coalfields since 1979 (Grobbelaar, 2001).



Figure 8: A longwall mining operation taken from Grobbelaar, (2001).

According to Grobbelaar (2001) the Matla and Secunda Collieries were first to introduce longwall mining in the Mpumalanga coal fields. Longwall mining is usually practised in areas that contain few or little structural disruptions. The method works by mining in panels that are usually 200 m wide, but according to Grobbelaar (2001), the width can vary depending on local considerations. The panels are mined by means of a cutting machine that is tipped with tungsten carbide teeth. These cut away the coal as it moves along the length of the panel. The mining height for this method is seam dependent, but according to Grobbelaar (2001), 3 m is usually the maximum height at which this method can be used. A positive factor when considering longwall mining as a mining method is that it is not constrained by depth (Grobbelaar, 2001). For example Grobbelaar (2001) remarks that at the Matla Colliery, “the shallowest longwall mining panel is less than 50 m below surface with the deepest planned longwall mining at the New Denmark Colliery, where a depth of 270 m will be reached”.

3.4. Coal Production

As stated in paragraph 2.5, coal is commercially mined in over 50 countries worldwide. According to British Petroleum (www.bp.com), some 6780 million tonnes of coal were produced in 2008 (Table 2). From these statistics one can see that there is a very large demand for coal. It is likely that this demand will increase as more African and Asian nations develop and expand.

The expansion in these countries goes hand in hand with the production of electricity for which coal is still one of the cheapest and most widely used fuel sources. Generally most of the coal produced in a country is used in the country of origin mainly for power generation or in the process of making steel. Some coal is however exported. Table 2 shows a sharp increase in the production of coal over the past 20 years, with Asia showing the largest increase in the tonnes of coal produced over the past 20 years.

3.4.1. Effects of Modern Mining on Production

The ceaseless advancement of technology has dramatically increased the production and efficiency of coal mining today. In order to keep up with the advancements in technology, and to extract coal as efficiently as possible, modern miners are required to be highly skilled and well trained in the use of complex and state-of-the-art instruments and equipment. This is likely to become even more necessary due to high cost associated with mining in this day and age, and mines must therefore be as efficient and as profitable as possible. The advancement in technology and training of miners has led to increases in the amounts of coal extracted from current mines. Additionally the advancements in other fields such as chemistry (processing of the coal and the manufacture of steel) and geology (better delineation of ore bodies) have greatly increased the efficiency of coal mines.

3.5. Environmental Effects of Coal Mining

According to the U.S. Department of the Interior (1979), coal mining has many damaging effects on the environment.

Some of these include:

- surface mining of coal completely destroys existing vegetation,
- destruction of the genetic soil profile,
- displacement or destruction of wildlife and habitat,
- degrades air quality,
- alters current land uses,
- permanently changes the general topography of the area being mined,
- noise pollution from blasting and machinery
- groundwater pollution
- surface-water Pollution

Mining in general often results in a scarred landscape with no scenic value which is of great concern for the Waterberg areas as the area is generally seen as a tourist attraction. If practised correctly, rehabilitation can mitigate some of these concerns but can never completely repair the damage that has been caused (U.S. Department of the Interior. 1979).

Mine tailing dumps can produce acid mine drainage which is a primary concern within the study area. This can seep into waterways and aquifers, with consequences for both the environment and human health. Great care needs to be taken to minimise the impact of mining.

3.6. Mining Methods in the Waterberg Coalfield

According to Dreyer (pers. comm. 2009), the entire area west of the Daarby fault will be mined using the opencast mining method due to the shallow coal depths. Open-cast mining refers to a method of extracting rock or minerals from the earth by their removal from an open pit (Figure 9 and Figure 10). The term is used to differentiate this mining from extractive methods that require tunnelling into the earth. The mining method currently being employed at the Grootegeluk mine is known as bulk mining, a form of opencast mining. Opencast mines are used when deposits of commercially useful minerals or rock are found near the surface; that is, where the overburden is relatively thin or the material of interest is structurally unsuitable for tunnelling, as is the case in the Waterberg coal fields, due to the high degree of faulting in the area. Opencast mines are typically enlarged until either the mineral resource is exhausted, or an increasing ratio of overburden to ore (stripping ratio) makes further mining uneconomic.



Figure 9: Opencast mine in the study area courtesy of the Grootegeluk mine.

Exhausted mines are sometimes converted to landfills for the disposal of solid wastes. However, some form of water control is usually required to prevent the mine pit from becoming a lake, and also to prevent the water from becoming acidic.

The problem of the open pit becoming a lake is of less concern in the study area, due to the low levels of annual precipitation, low transmissivities, high evaporation and the deep groundwater levels found in the area (which will be discussed later). The mining method used at the Grootegeluk mine is known as bulk mining, it is a form of open-cast mining that involves the removal of all relevant material and then processing all the material. This form of mining is practised as it has been found to be the most inexpensive and efficient way of mining the coal seams in the study area.

This is due to the fact that the coal occurs inter-bedded with thin layers of shale and mudstone. Selective mining is thus not seen as a viable option for the study area. The best possible surface mining method to use for the study area is the bulk mining method currently being employed at the Grootegeluk mine. The method is efficient and cost effective. However it is recommended that the new mines start with the mining of the deeper coals west of the Daarby fault. This will initially be expensive as the stripping ratio will be higher but this will be to the benefit of the mine at a later stage.



Figure 10: The opencast at the Grootegeluk mine curtesy of the Grootegeluk mine.

This method does however present a problem with the handling of the spoil as all the spoil is removed and dumped on big heaps outside the mine. Due to the way mining is conducted, selective spoil handling cannot be used to identify or separate rocks with high acid generation potential from those with lower acid potentials. It is therefore recommended that these high acid generation potential rocks be mixed with high base potential rocks to counteract any acid that will be generated. Detailed acid-base accounting analyses will need to be done to identify the acid generation potential for the different rocks.

Due to the high evaporation in the study area, the use of evaporation ponds is recommended for the disposal of waste water. However, the use of such ponds increases the salt content as the ponds are evaporated.

If these concentrated salts enter the groundwater or surface water system, they will be difficult to remove and this will increase the costs of rehabilitation after mining stops. It would be in the mines' best interest to isolate these ponds in areas that are "safe", and pose a low risk for groundwater contamination. These would comprise any areas that have very low transmissivities and vertical conductivities. Areas that should be avoided for the placement of such ponds are areas located near faults.

3.7. Proposed Mining Plans and Methods

The entire study area west of the Daarby fault is currently being prospected by different companies interested in the coalfield. It has been proposed by Dreyer (pers. comm. 2009) that the entire area north/west of the Daarby fault can be mined by opencast mining methods. According to Dreyer (pers. comm. 2009), all the mines in the area will initially be opencast, but might be converted into sub-surface mines at a later stage, once the open-castable coal has been removed.

The coal seams in the study area are sub-divided into eleven coal seams, one being the deepest and eleven being the shallowest of the coal seams. At Grootegeluk the mining process only mines down to beneath seam three. It has been deemed uneconomical to mine beneath seam three, as the seam below seam three is covered by thick sandstone layers and the additional excavation of these layers will increase the stripping ratio in the mine. It is recommended that the new mines planned for the area follow the example of the Grootegeluk mine with regard to mining methods, spoil handling, water management and rehabilitation.

3.8. Conclusion

There are many methods for the extraction of coal for both surface and sub-surface mining. Some of these methods will not be economically useful in the study area and it is recommended that the new mines use the same methods as those used by the Grootegeluk mine. As far as future sub-surface mining is concerned, there are three methods used elsewhere in South Africa that may be used at the same level in the study area. The specific conditions for the different mines will however need to be taken into account when planning for under sub-surface mining.

CHAPTER 4: Study Area Location

4.1. Introduction

The study area is located in the Waterberg region of the Limpopo Province of South Africa. The Limpopo Province is South Africa's northernmost province, lying within the great curve of the Limpopo River (Figure 11). It is a region of contrasts, from true bushveld country, to majestic mountains, primeval indigenous forests, unspoilt wilderness and a patchwork of farmlands.

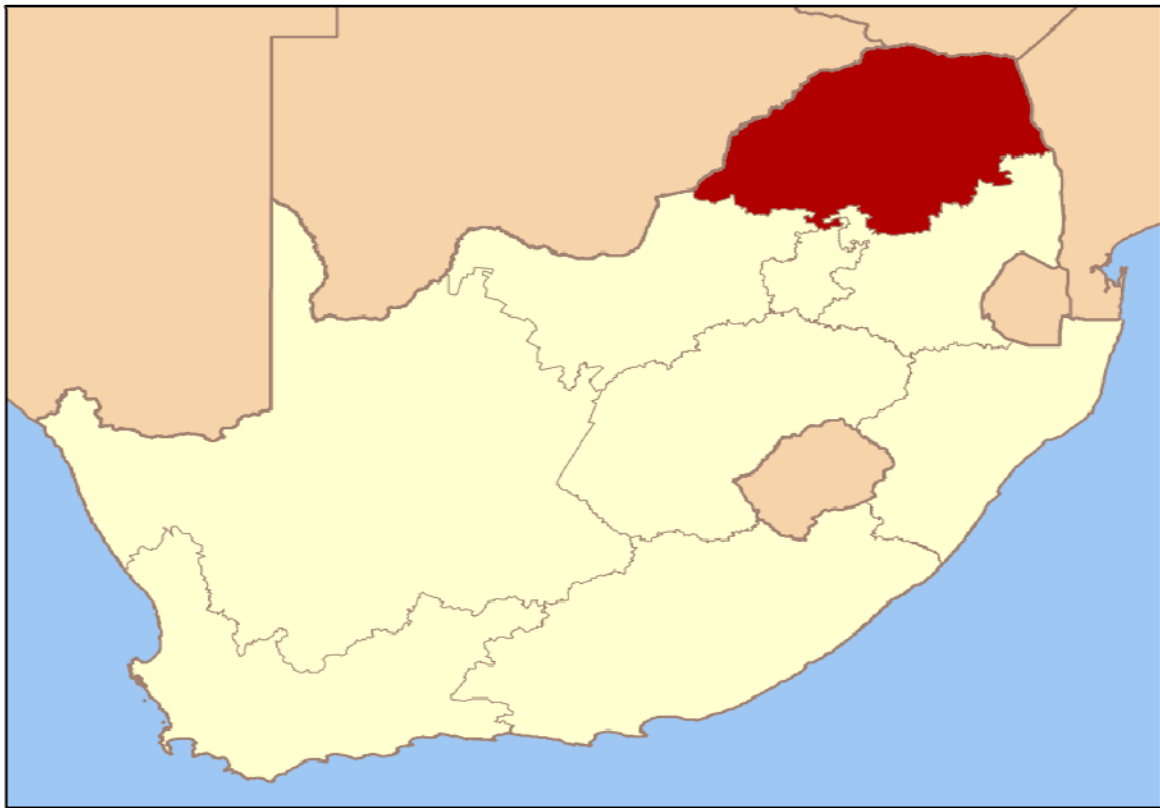


Figure 11: Location of the Limpopo province

The Limpopo Province is seen as the gateway to the rest of Africa, with its shared borders making it favourably situated for economic cooperation with other parts of southern Africa (www.southafrica.info). The Limpopo Province shares international borders with three countries namely; Botswana, Zimbabwe and Mozambique. The province also serves as a link between South Africa and these countries and other countries further afield in sub-Saharan Africa. On the southern tip of the province it is coterminous with the provinces of Mpumalanga, Gauteng, and the North West province. From the province's links with Gauteng (including the Johannesburg-Pretoria axis, the most industrialised metropole on the continent) and its links with Maputo development corridor, the province is ideally located for rapid development and expansion of economic opportunities (www.southafrica.info).

4.1.1. Mining and Minerals

Limpopo is a province that has been blessed with massive mineral riches. Some of these include the following: mineral deposits of platinum group metals, iron ore, chromium high- and middle-grade coking coal, diamonds, antimony, phosphate and copper, as well as mineral reserves like gold, emeralds, scheelite, magnetite, vermiculite, silicon and mica (www.southafrica.info). Base commodities such as Norite (known commercially as black granite), corundum and feldspar are also commercially exploited in the province. This wealth of resources has resulted in mining contributing to over a fifth of the provincial economy.

The province is generally classified as a developing area, exporting primary products and importing manufactured goods and services. It has a high potential for development with many investment opportunities in the mining and tourism sectors. According to South Africa Info (www.southafrica.info) the Lephalale region of the Waterberg has the third largest coal reserves in South Africa. The local municipality has identified this resource, and views it as lending a unique competitive advantage to the Waterberg District, rendering it a new powerhouse in the country for coal-fuelled electricity production.

This is where the importance of this project comes into play. Due to the planned expansion of the mining enterprises in the area and the accompanying developments, it is important to determine the extent of the impacts these developments will have in the study area. This study will focus specifically on the impacts which these developments will have on the groundwater quality and quantity in the area.

4.1.2. The Waterberg Region

The Waterberg region of Limpopo is vast, peaceful, incredibly beautiful, and possesses a rich cultural legacy and natural splendour. The region mainly comprises vast tracts of bushveld savannah, punctuated with clusters of trees and tall savannah shrubs. The Waterberg as we know it today is more than three million years old with archaeological finds and San paintings providing glimpses of the region's past (www.wheretostay.co.za). Presently, mining is an extremely important part of the economic structure of the Waterberg region, which constitutes one of the richest mineral deposits in the world and forms part of the Bushveld Igneous Complex.

4.2. The Study Area

The study area is located west of the town of Lephalale and near the Botswana border (Figure 12). The study area stretches from the town of Lephalale in the east, to just west of the town of Steenbokpan in the west and all the way to the border of Botswana in the north.

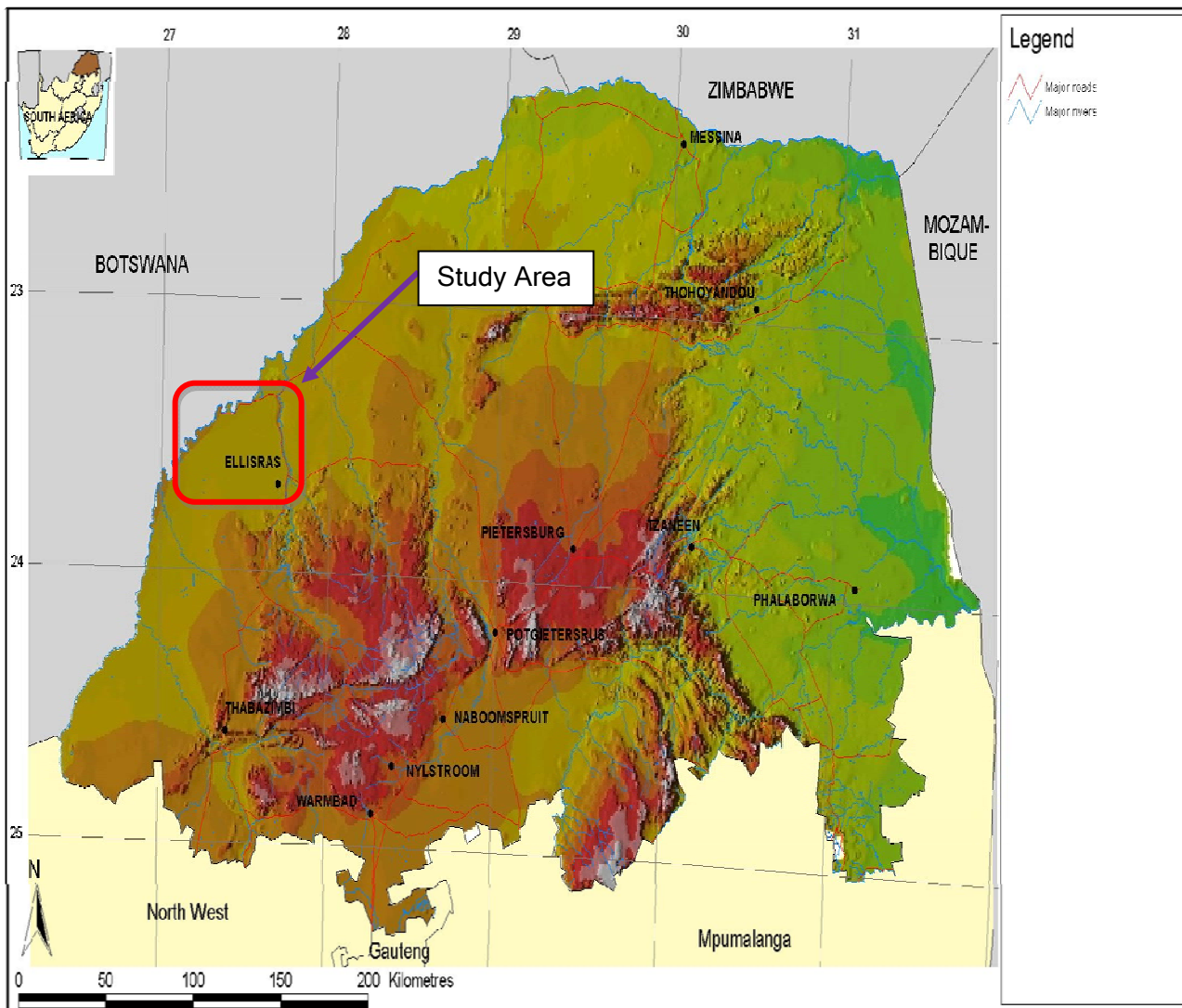


Figure 12: Location of the study area (regional), (<http://www.deat.gov.za/Maps>).

The study area is approximately 2300 km² in size and is mainly composed of farms. The Grootegeluk Coal Mine, Matimba Power Station and the Medupi Power Station Construction Project (Figure 13) are located within the study area.

According to Eskom, this power station (Medupi) is expected to commence its operations in 2015. The study area has a flat to gently undulating topography, surrounded by mountains to the east and the south. The main agricultural activities in the study area are farming with game and livestock (mainly cattle).

Crops such as peanuts and onions are cultivated to a small extent within the study area. Due to the low rainfall in the area, the crops are only planted in areas located near the rivers (the Mokolo, running north/south and the Limpopo, running roughly south/west - north). The crops must therefore be irrigated and need to be located close to major water sources.

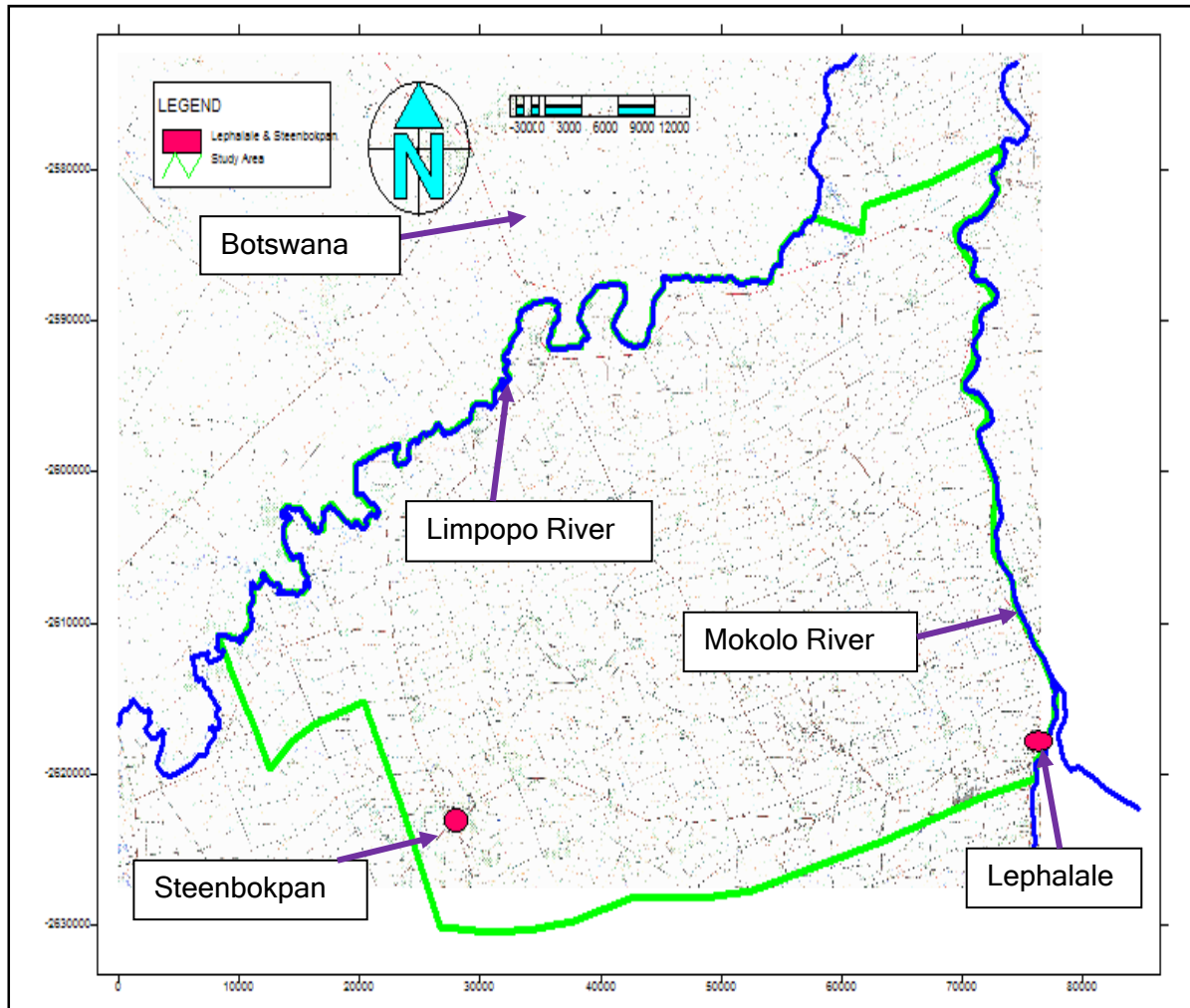


Figure 13: Location of the study area (Local).

4.3. Climate

The area has a generally dry climate, with temperatures reaching 40°C and higher during the summer months, and little rainfall during the year. The rainfall period is concentrated between September and March (summer rainfall area). The study area has a mean annual run-off of 150 mm - 397 mm and the MAE (evaporation) is 1800 mm - 2000 mm/a (SA Weather Service, 2008). Recharge is estimated at <10 mm/a or <1.5% of the annual rainfall (Vegter, 1995). As illustrated in Figure 14, the average rainfall is between 285 mm and 560 mm per year (SA Weather Service, 2008).

Rain is not evenly spread during the rainy season and occurs in the form of massive downpours that can last from a few minutes to several hours. During these times of intense precipitation, the soil becomes saturated very quickly and water pools on the surface in low-lying areas (Figure 15). Due to the small degree of vertical variation in the topography of the study area, the run-off is limited and in many situations is more local, which implies that the run-off does not move very far, only towards local depressions in the topography. The areas with elevated topography located near the rivers, show run-off towards the rivers.

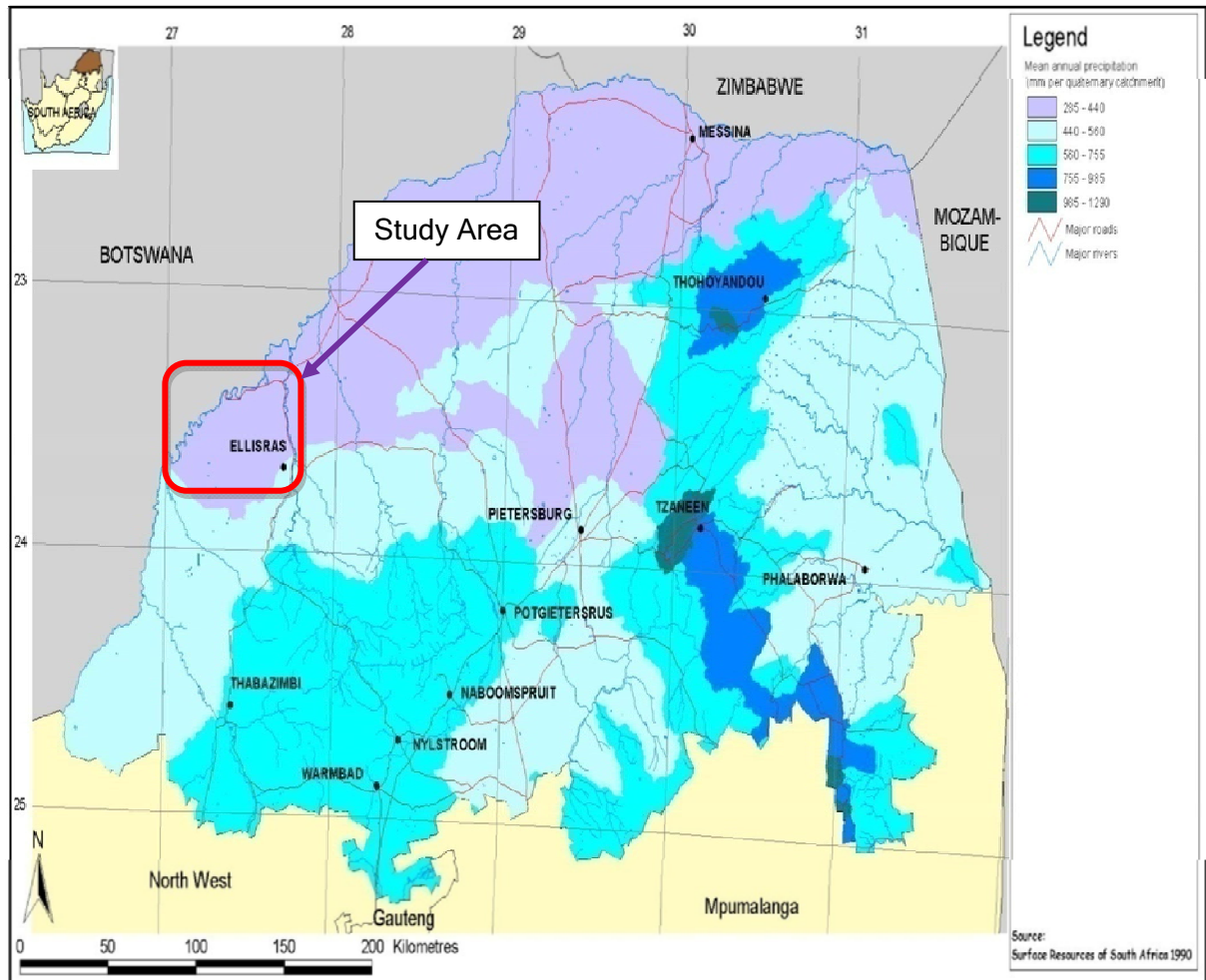


Figure 14: Rainfall in the study area (regional) (<http://www.deat.gov.za/Maps>).



Figure 15: Saturated soil with water pooling in the surface during the rainy season.

According to rainfall data (Figure 16) received from the Grootegeluk mine, October has the highest precipitation when compared to the other months of the year. Additionally, the data indicates a particularly problematic time for mines in terms of surface water influx into the pits and surface run-off from discard dumps and coal stockpiles.

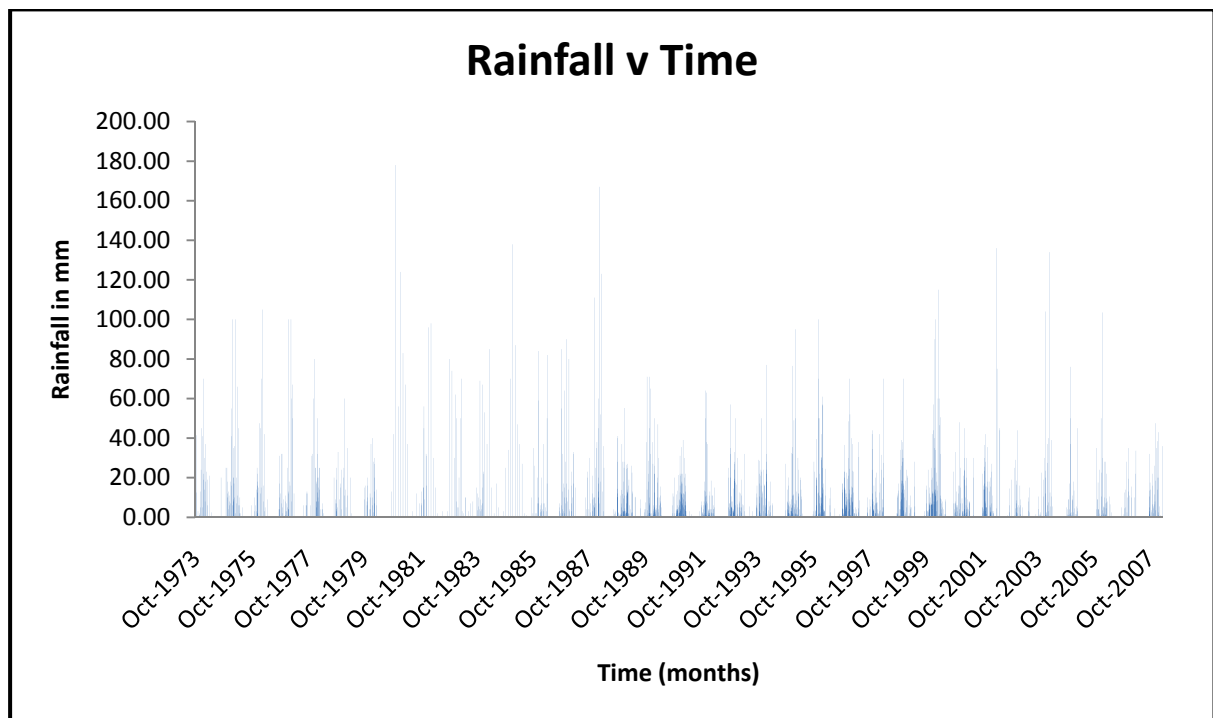


Figure 16: Rainfall figures for the study area (1973 - 2007).

The heavy rains are usually not sufficient to terminate mining operations, but in severe circumstances, the influx of water does pose a serious threat to the safety of miners (roads can turn to rivers of mud) (Dreyer 2008/2009). During these heavy precipitation events, the water is collected in the lowest areas of the pits in sumps from where it is pumped to be used in day to day operations of the mine. As the study area is a water scarce zone, water preservation should be a top priority. Of the large downpours, roughly 1.5% - 1.9% (according to Vegter, 1995) is recharged to the groundwater system. The recharge in the area will be discussed in a later chapter.

4.4. Surface Hydrology & Topography

The study area lies within the greater Limpopo River catchment (Figure 17), has a low rainfall and is drained by two rivers; the Mokolo running south-north and the Limpopo running roughly south/west-north. The Limpopo River can be classified as a non-perennial river. The Mokolo River is a non-perennial river. The study area is located within quaternary catchments A41E and A42J (Figure 18). It was expected that the runoff from the area would flow towards the river and other low-lying areas (for location of rivers, refer to Figure 13).

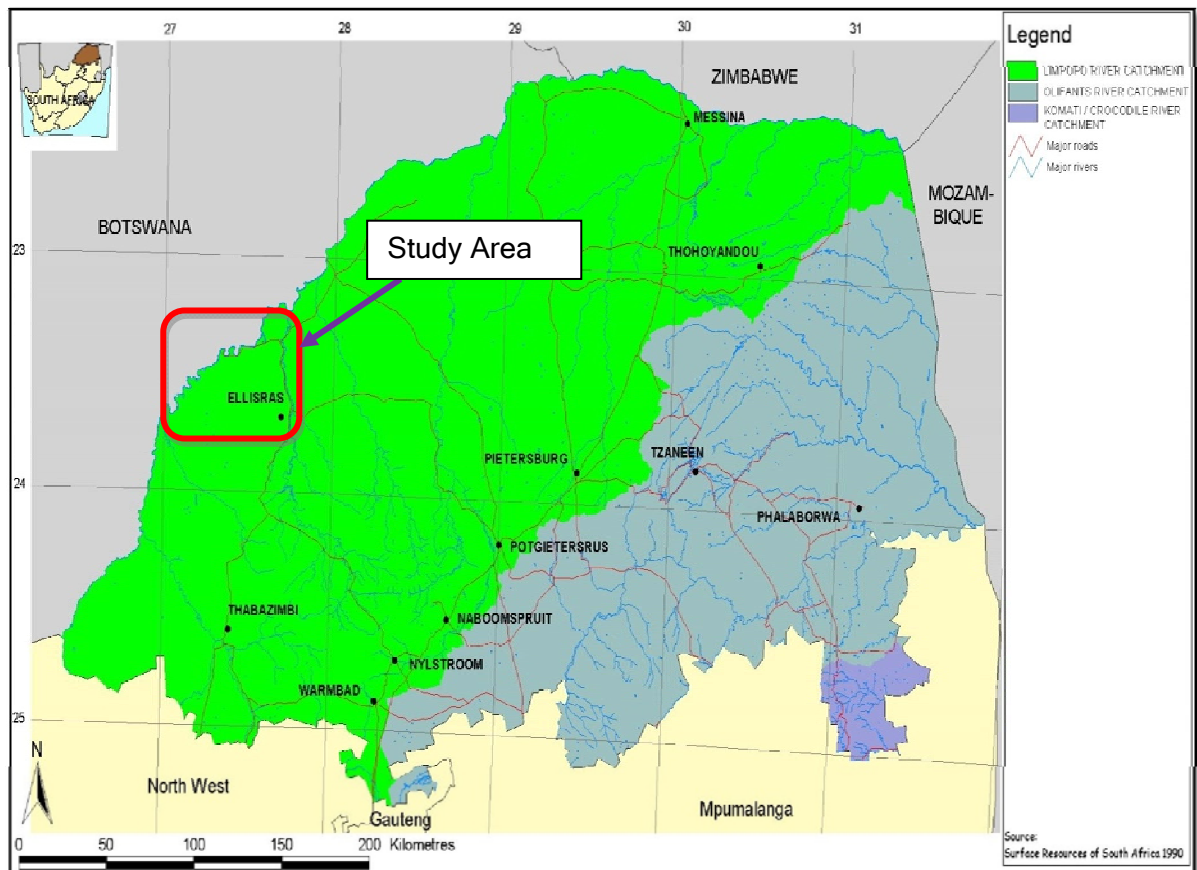


Figure 17: Location of the study area in the Limpopo catchment (<http://www.deat.gov.za/Maps>).

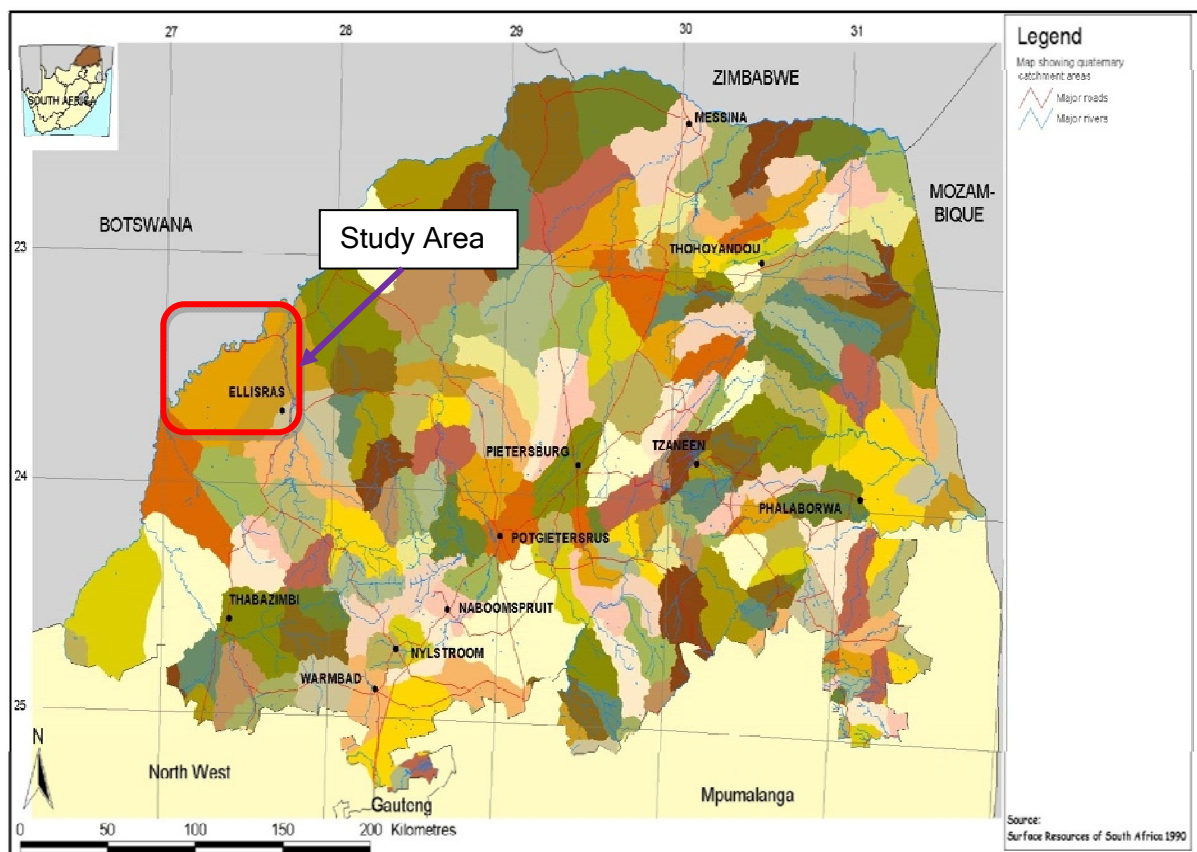


Figure 18: Location of the study area in the quaternary catchments A41E and A42J (<http://www.deat.gov.za/Maps>).

In order to confirm that the runoff would move towards the rivers, it was necessary to construct contour maps of the topography of the study area. The elevation information was obtained by means of the Global Mapper Version 10 software program. The information was contoured with the Windows Interpretative Software for the Hydrogeologist (WISH). Figure 19 indicates a flat to gently undulating topography, with the exception of an area near the centre of the study area that indicated an elevated topography (Figure 19).

From this it can be concluded that the central area of the study area acts as the driving force for water flow, with water flowing from areas with a high elevation, to areas with a low elevation. In order to confirm this flow vectors were added to the topographic contour using the WISH software (the results are displayed in Figure 20).

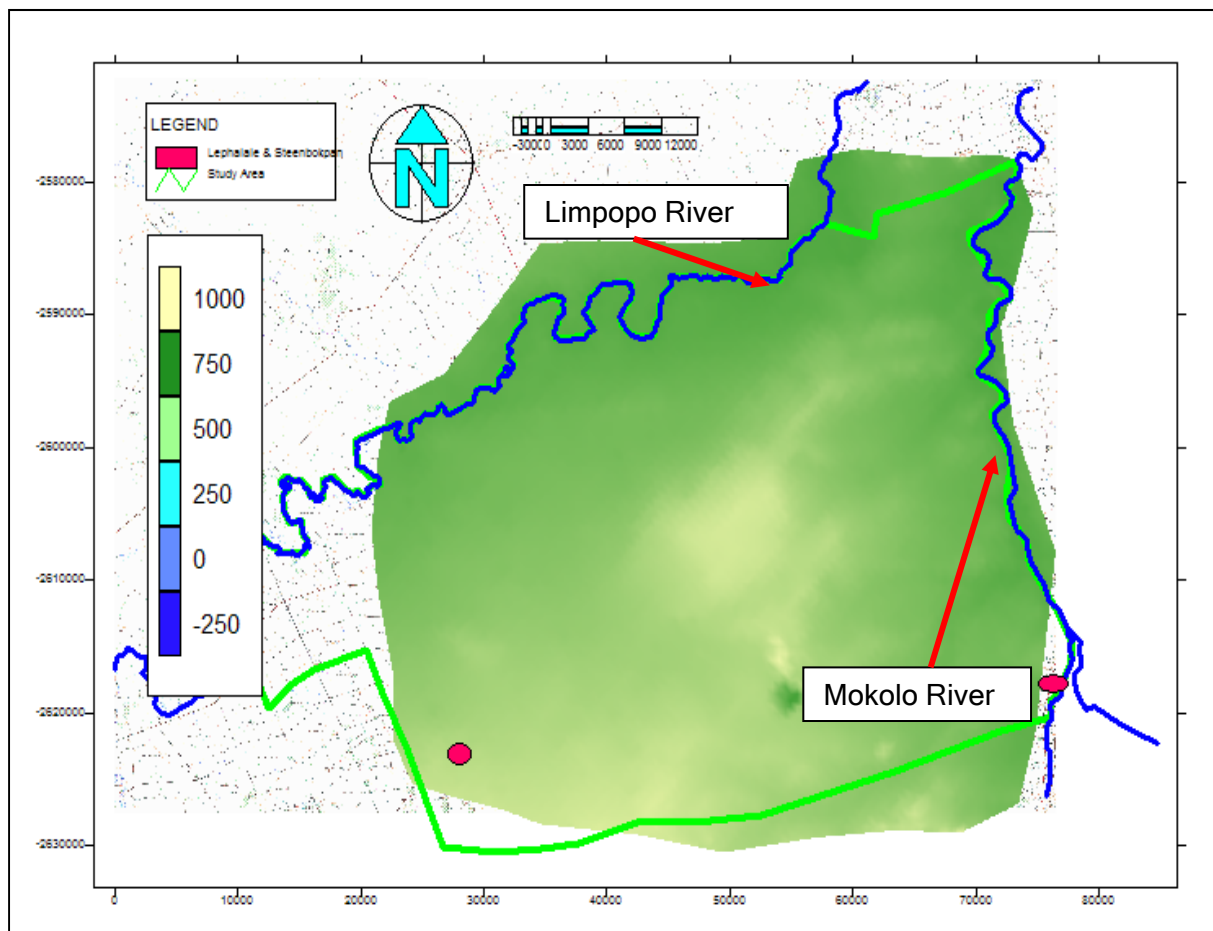


Figure 19: Topographic contour map generated for the study area.

From Figure 20 it can be concluded that surface run-off will drain towards the low-lying areas from the elevated areas, these predominantly being the two rivers in the study area. It is possible that the excavation of additional open pits in the area may alter the surface topography to such an extent, that the flow direction may change. If the size of the mines are sufficient, the flow maybe redirected towards the mines instead of the rivers. According to Dreyer (pers. comm. 2009) only the area west of the Daarby fault will initially be mined. (Figure 20).

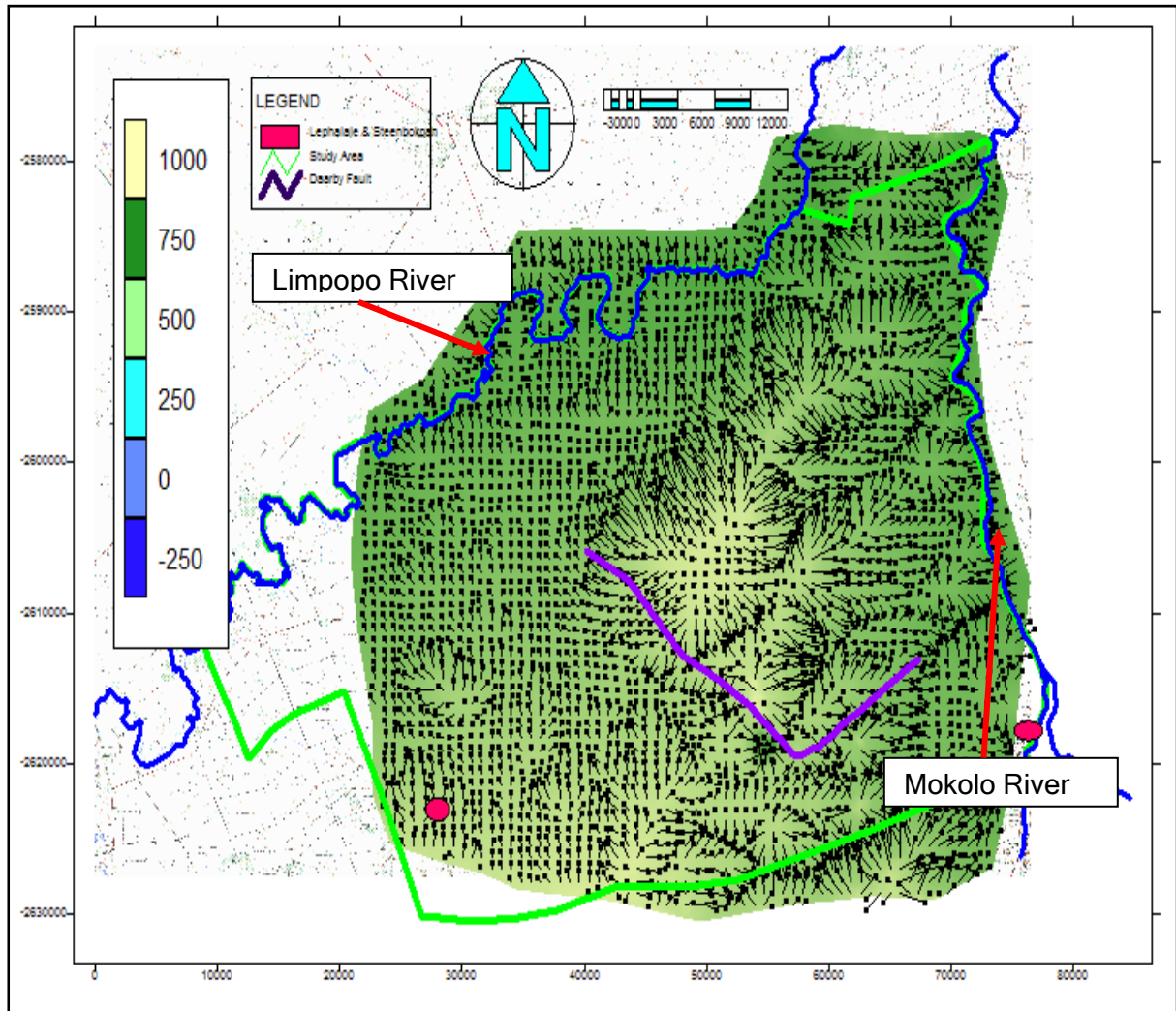


Figure 20: Topographic contour map of the study area showing flow vectors and the Daarby fault.

Figure 20 indicates that the impact of the mines will only be felt “down-stream” towards the town of Steenbokpan and only on the western side of the Daarby fault. The areas east of the fault will be unaffected by the mines with regards to surface runoff. Due to the location of the pits in the elevated areas, this would mean an increased influx of water into the pits during periods of high precipitation. In an exaggerated three-dimensional (3D) view of the contour map, some changes in elevation can be seen, although none of these are extreme (Figure 21).

Towards the south lies a very deep area compared to the rest of the study area. This area indicates the open pit at the Grootegeluk Mine. As indicated in Figure 21, the open pit has a impact on the surface of the study area and the addition of more open pits in the area will increase the impact. Additionally Figure 21 indicates that the areal extent of the pit is small when compared to the size of the study area as a whole. This will mean that in order for the pits to have a large enough impact on the topography to change the flow directions of surface runoff, there would need to be many pits of great size present in close proximity to one another.

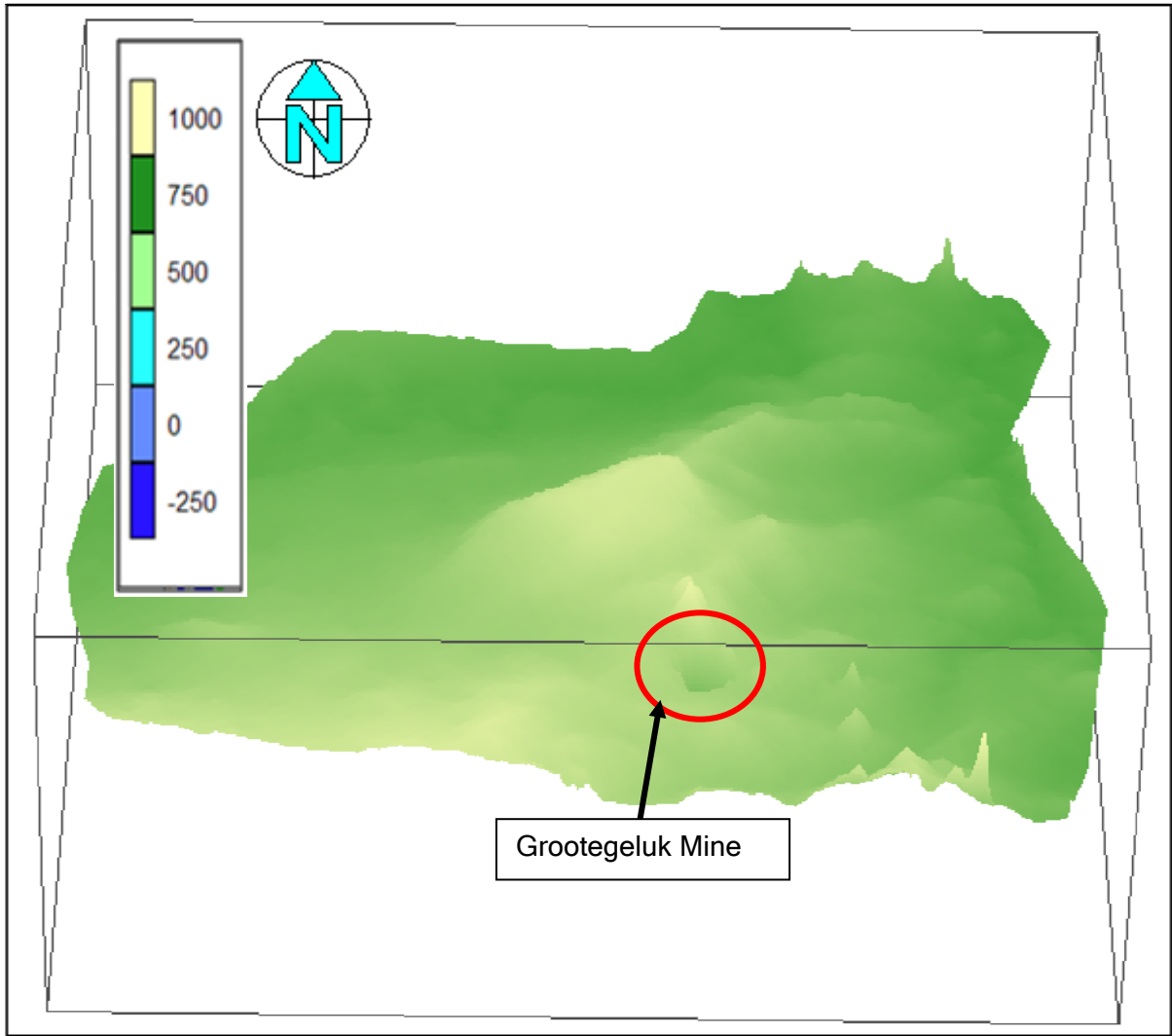


Figure 21: Exaggerated 3D view of the study area topography.

The number of additional mines planned for the study area is unknown, but it is doubtful that this number would be large enough to change the surface topography to such a dramatic extent that the mines would change the flow direction of surface runoff. Generally speaking, it is believed that the groundwater flow of an area mirrors the topography of that area.

Accordingly from the data in Figure 21 it would be safe to assume that the groundwater in the study area will be moving away from the central parts of the latter towards the lower-lying areas. The areas of higher elevation will therefore serve as the recharge zone for the lower-lying areas of the study area. It is expected that the excavation of large open pits in the study area will have an influence on the flow of ground water in the area west of the Daarby fault. In Figure 22 the area outlined in red indicates the location of the Grootegeluk Mine. Bearing the magnification of the image in mind, it can be expected that groundwater will flow in the direction of the pit.

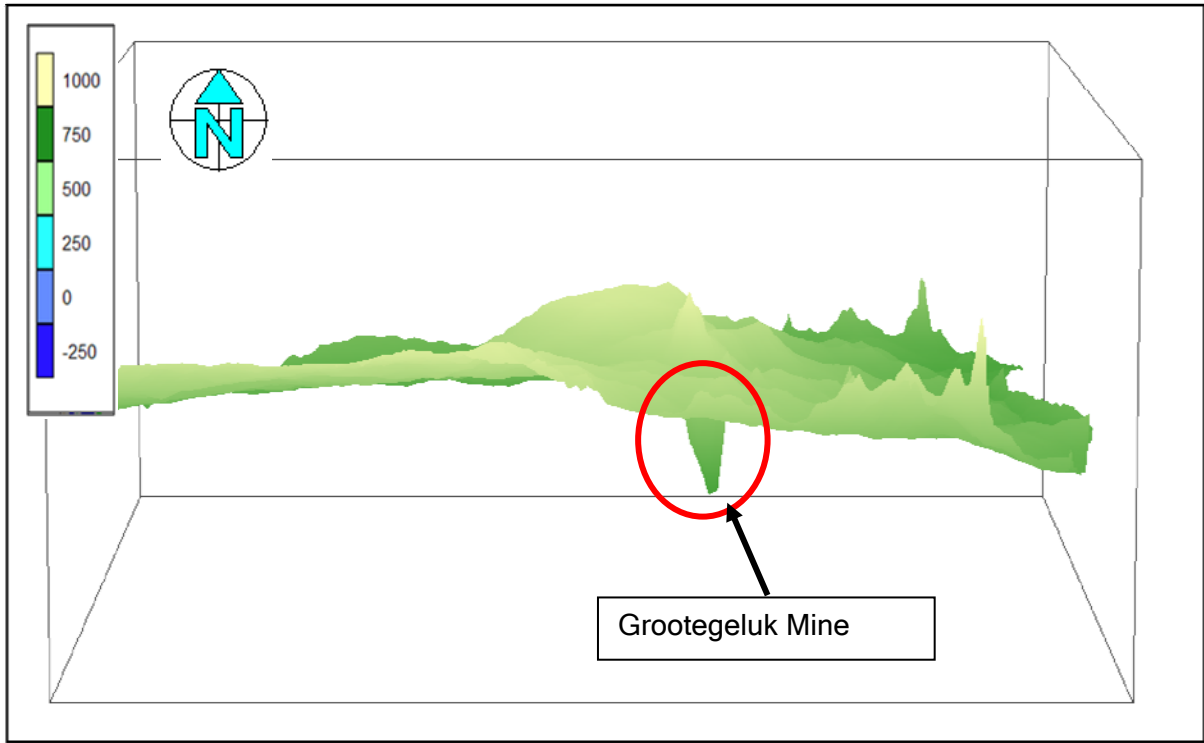


Figure 22: Exaggerated 3D view of the study area topography (Side view)

Figure 22 indicates that the water would move towards the Grootegeluk pit from the north-west and away from the Grootegeluk pit in the south-east. Due to the movement of water away from this area, it would therefore also be safe to assume that mines near the centre of the study area will have less influx of surface water and groundwater. We may then conclude that, due to the flat topography and the low rainfall, there will be little inflow of runoff into the pits.

4.5. Soil Depths, Soil Types and Land Cover

According to soil maps of the area (Figure 23), the soil depth of the study area is around 750 mm and beyond. Some of the soil's presence can be explained as being the result of strong winds and vast amounts of sand blown in from the Kalahari Desert. Much of the sand present in the study area have been formed in-situ as a result of weathering. Accordingly, the entire study area has deep top soils.

The study area has a flat topography which contributes to the movement of sand. The area is highly overgrown, which in turn slows the migration of sand. The thick layers of sand could be used as land cover once the mines reach a point of rehabilitation. The vast amounts of soil also present a problem in terms of dust, the suppression of which will require vast quantities of water. The soil in the study area varies between three main types; Red - yellow and greenish soils with high base status, soils with negligible to weak profile development (these types of soils usually occur on recent flood plains) and red massive or weak structured soils with a high base status (Figure 24).

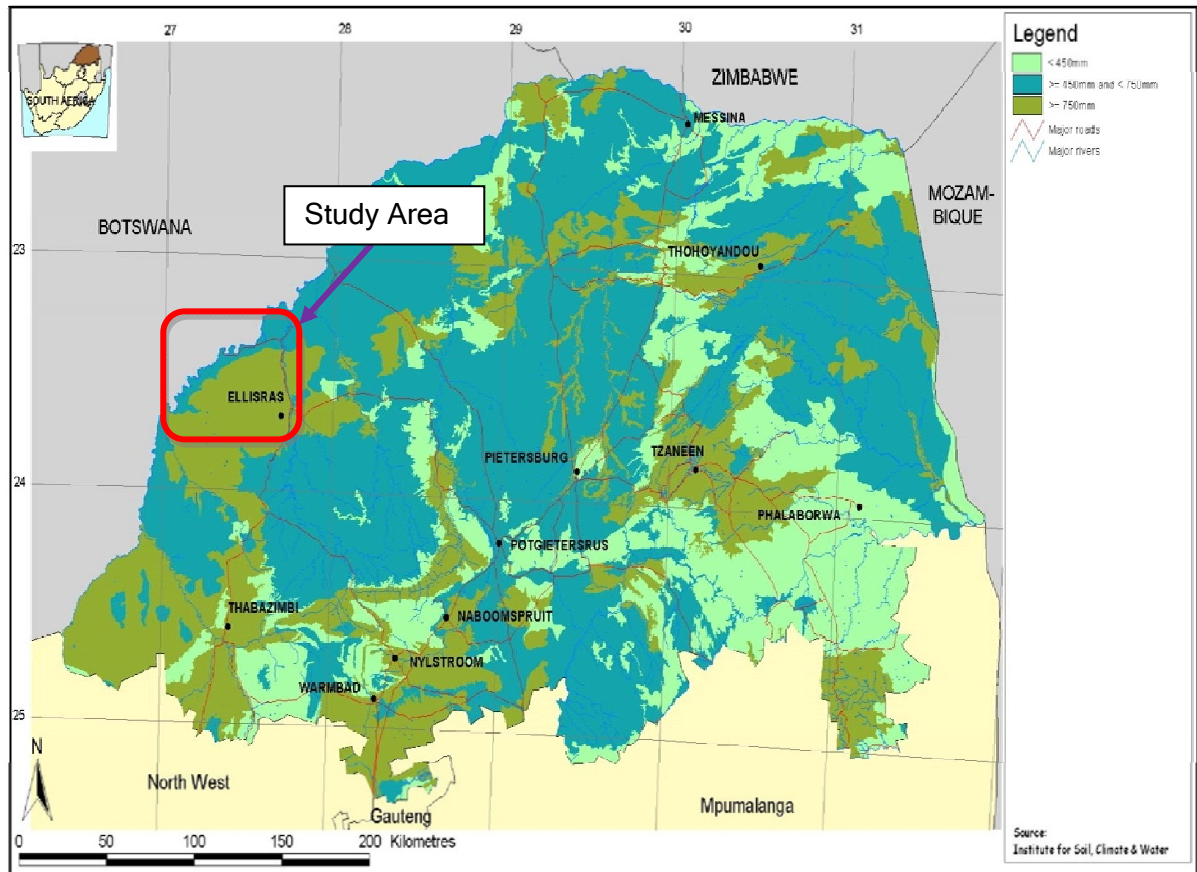


Figure 23: Soil depths in the study area (regional) (<http://www.deat.gov.za/Maps/>)

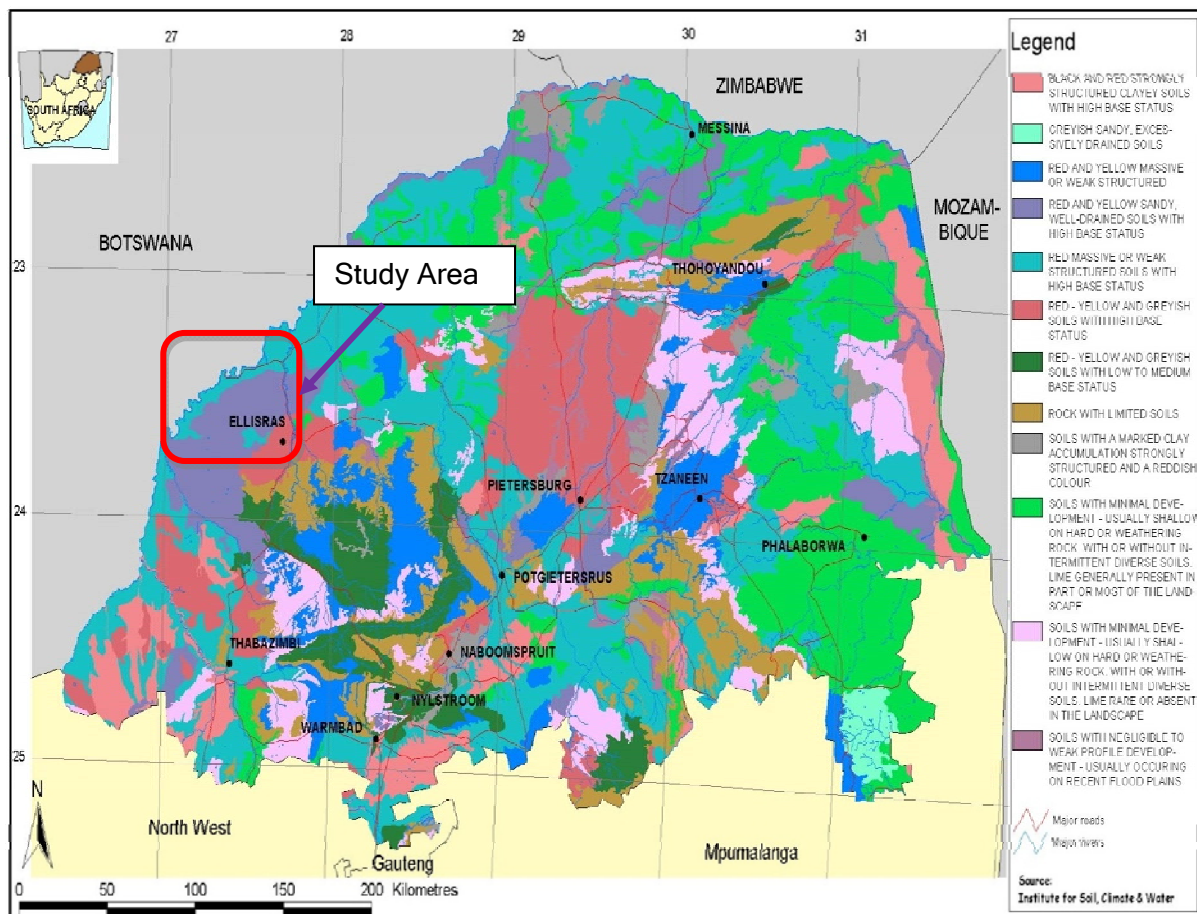


Figure 24: Soil types in the study area (regional) (<http://www.deat.gov.za/Maps/>)

The primary land cover in the study area is thicket and bushland, followed by woodlands and degraded land cover. Vegetation is mostly mixed bushveld forming part of the savannah biome. This bushveld represents a great variety of plant communities, with many variations and transitions. The vegetation varies from dense short bushveld, to open tree savannah. Protected tree species occur abundantly in the study area and includes the Baobab tree, Camel thorn, Shepherd's tree and Lead wood, Marula and Tamboti trees.

Efforts should be made by all parties to minimise the amount of damage done to the environment (Figure 25). This will be challenging, as all the mines located in the study area will be open-pit mines, which require the removal of overburden, plants and animals from the pit location. An effort should also be made to safeguard the endangered species that inhabit the area in question.

For example, in terms of the Medupi Power Station Construction Project, Baobab trees were identified in the construction area and successfully moved to a safe location.



Figure 25: Photo of the land cover of the study area.

CHAPTER 5: Methodology

5.1. Introduction

This chapter contains a discussion of the different methods analysed and sample collection used during the project. From a sampling point of view, the focus will be on groundwater sample collection and geological sample collection. With regard to the analytical methods used, the focus will be on acid-base accounting analyses and the analyses of pump test and slug-test results.

Additionally, the steps used in conducting a pump test and a slug test will be discussed. The discussion excludes the following: the use of the Inductively Coupled Plasma spectrometer for the analysis of the groundwater samples, and the use of X-ray Diffraction analyses to determine the mineral composition of the geological samples.

The methods used for the determination of recharge for the study area, namely the chloride mass balance method and the E.A.R.T.H. model, will be discussed.

5.2. Sampling

In order to conduct qualitative analysis of the groundwater found in the study area, and to gauge the potential of the geology of the area to generate acid mine drainage, two types of samples were collected, namely:

- Groundwater samples: samples were collected to determine the present status of the groundwater resources in the study area and to determine if, at present, there are any areas that have been affected by activities such as mining.
- Geological samples: samples collected for the use of acid-base accounting analyses, to determine if the rocks found in the study area will generate acid mine drainage if oxidized. Additionally, the analyses were conducted to determine if sufficient base potential exists in the rocks to counter the acid generation.

The samples were collected from a wide range of locations from within the study area. The collection of samples, or the quantity of samples collected, were often limited by a lack of access to sampling location (farms with locked gates), or due to confidentiality concerns (core samples containing coal)

5.2.1. Groundwater Samples

The water samples were obtained from boreholes by means of through flow bailers (Figure 26). These bailers were cleaned with de-ionised water before each sample was taken. The samples were stored in 500 ml plastic bottles and transported to the IGS laboratory for analysis. The samples were taken 5 m below the water level, or at fracture levels that had been determined by means of profiling. In addition to the sampling, the water levels and the pH and EC were measured in the field.



Figure 26: Groundwater sampling in the study area.

5.2.2. Geological Samples

A total of 84 samples (after separation) were collected from various localities throughout the study area. The samples varied from core samples to chip samples (Figure 27 and Figure 28). The samples also included two samples of processing plant waste from the Grootegeluk Mine and one sample of the sandstone layer located below the coal succession. The samples were collected in plastic sample bags and transported to the Institute for Groundwater Studies. Here the samples were crushed and used in acid-base accounting analysis and X-Ray diffraction analysis. X-ray diffraction (XRD) was performed on the samples to determine the exact mineralogical composition of the samples. The reasoning behind the testing for mineral composition, as well as the acid-base accounting, involved the identification of layers in the geology of the Waterberg Coal Fields which are prone to acid generation or have high base potentials.



Figure 27: Core sample from exploration borehole near the Grootegeluk mine (from the left Mr Claris Dreyer and Dr Danie Vermeulen).



Figure 28: To the left Core samples, to the right Chip samples.

5.3. Water Quality

Listed in Table 3 are the elements that were tested for, during the water quality analysis of the water samples.

Table 3: Elements analysed for during chemical analysis.

pH	EC	PAIk	MAIk	Ca	Mg	Na	K	F	Cl
NO3(N)	SO4	Cr6	Al	Fe	Mn	Cu	Co	Cr	COD

The elements listed in Table 3 cover a wide range and are effective indicators of potential pollution in the groundwater due to coal mining. The measurements of the pH and EC will indicate the acidity or alkalinity of the water samples (pH), as well as the overall salt loads of the water respectively. The EC only provides an indication of salt quantities, without an indication of the type. The water quality determinations were performed using an Inductively Coupled Plasma Spectrometer (ICP).

5.4. Acid-Base Accounting

Acid-base accounting analyses (ABA) are, according to Usher *et al.*, (2002), a first-order classification procedure only, during which the acid-neutralising and acid-generating potential of rock samples are determined and the difference, also known as the net neutralising potential (NNP), calculated. The NNP and / or ratio of neutralising potential to acid-generating potential is compared with a predetermined value, or a set of values. This is done in order to divide samples into categories that do, or do not require further ABA testing (Usher *et al.*, 2002). It was decided not to focus on the generation of poor quality leachate from the mines as it is anticipated that a certain level of acid generation at the mines would be inevitable.

This particular aspect should be covered in an additional study, as the current research is confined only to a scoping-level assessment. Different methods of conducting ABA test work will lead to different sets of sample data for evaluation. Rules and guidelines for testing have been developed by mine regulatory and permitting agencies (Usher *et al.*, 2002). Acid-base accounting indicates only the overall balance of acidification potential (AP) and neutralisation potential (NP) and is, in its most basic form, merely a screening process. Accordingly, it provides no information on the speed (kinetic rate) at which acid generation or neutralisation will take place. Due to limitations, ABA procedures are known as Static Procedures (Usher *et al.*, 2002). A given rock's potential to generate or neutralise acid is determined by its mineralogical composition (Usher *et al.*, 2002). This refers to not only the rock's quantitative mineralogical composition, but also to the individual mineral grain size, shape, texture, and spatial relationship with other grains in the rock (Usher *et al.*, 2002).

ABA can only yield a "worst case scenario" value for potential acid production and a "worst case", "most likely case", or "best case" value for potential neutralisation (Usher *et al.*, 2002). According to Usher *et al.*, (2002) the neutralisation potential is a measurement of the sum of the total carbonates, alkaline earths and bases available to neutralise acidity and therefore represents the most favourable condition. The calculations of the maximum potential acidity and neutralisation potential are structured in such a fashion that they equate the two measurements to a common basis for comparison.

The values resulting from these calculations, expressed as calcium carbonate equivalents, are compared in order to compute a net acid-producing or neutralising potential. According to Usher *et al.*, (2002), “material exhibiting a net acid production potential of 5 tons/1000 tons of overburden material or more as calcium carbonate equivalent, is classed as toxic or potentially toxic”. Studies have shown that “the application of the acid-base accounting methods to overburden handling and placement throughout the USA and Canada has generally been effective in eliminating or reducing adverse water-quality impacts”.

5.4.1. The Primary Advantages of ABA

- Short turn-around time for sample processing,
- Low cost,
- Relatively simple analytical procedures,
- Relatively simple interpretation of results (Usher *et al.*, 2002),

5.4.2. The Primary Disadvantages of ABA

- The method only predicts a maximum potential acidity and a maximum neutralisation capability, assuming a 1:1 acid to base reaction. According to Usher *et al.*, (2002), the actual acid production and neutralisation release rates cannot be predicted in this manner, nor can the completeness of the reaction be assessed.
- ABA assumes that all the acid production from a rock can be attributable to iron disulphide minerals (predominantly pyrite), with none being produced by sulphate or organic sulphur forms (Usher *et al.*, 2002).
- The measurement of NP utilises a hot acid extract to measure carbonates and bases.
- Acid-base accounting becomes a very powerful tool when used in conjunction with other data such as hydrologic data, mining and reclamation plans and mineralogy.

5.4.3. Prediction Methods

It is believed that an accurate form of prediction offers the most cost-effective means of reducing the potential impact of AMD. These impacts on the environment that are measured in the mining sector - as the costs associated with AMD - can be prevented by allowing advanced planning for prevention and control (Usher *et al.*, 2002). According to Usher *et al.*, (2002), the objective of a prediction programme is to reduce uncertainty to a level at which potential risk and liability can be identified and effective extraction, waste handling, and where necessary, mitigation and monitoring strategies, can be selected. The scope of a prediction programme will depend on site-specific conditions and factors. Some programmes may comprise a few simple tests, conducted in a relatively short period of time and with a modest budget. Others can involve extensive testing and analyses lasting several months to more than two years, at much higher cost.

The approach can include some or all of the following:

- Initial assessment and site reconnaissance.
- Sampling.
- Chemical, mineralogical and physical analyses.
- Short-term leaching tests.
- Geochemical static tests (ABA).
- Geochemical kinetic tests.
- Mathematical models.

With sufficient data the potentially higher accuracy of models and predictions can minimise the impact of acid generation in the mines. The most common method used by the IGA is the static peroxide method for ABA. This method is explained in more detail below (Usher *et al.*, 2002).

5.4.4. Static Methods (Acid-Base Accounting)

Static methods are some of the more common tests generally used for ABA calculations. These are screening methods to determine the difference between the acid-generating capability and the acid-neutralising potential of a particular sample or set of samples. The most common procedures used in static ABA testing are listed in Table 4.

Table 4: Most commonly used static ABA methods after Usher et al., (2002).

Paste pH	Static Net Acid Generation (NAG) procedure.
Peroxide methods.	BC Research Initial test
Sulphur content.	BC Research Confirmation Test.
Calculated NP.	Sobek Neutralisation Potential method.
Carbonate NP determination.	Modified acid-base accounting procedures for neutralising potential.
Lapakko neutralisation potential test procedure.	COASTECH modified biological oxidation test.
Net Carbonate Value (NCV) for acid-base accounting.	

5.4.5. Peroxide Methods

Several tests using hydrogen peroxide as an oxidant for sulphide minerals exist for use in ABA calculations. The one selected for use in this study is the Net Acid Production (NAP), or Net Acid Generation (NAG) test. The NAP, or NAG test, was developed to provide an alternative to acid-base accounting in order to predict acid-rock drainage.

The NAP test was used as it has the advantage of not requiring sulphur analysis, and therefore has the potential of being an expeditious method for use in the field if necessary. The NAP test can also provide an accurate quantitative assessment of acid-generating potential under controlled laboratory conditions. Current work indicates that NAP test results correlate well with ABA, particularly when the net neutralisation potential values are relatively low and negative.

These values constitute the range in which greater certainty is required (Usher *et al.*, 2002). When the NNP values are negative, the NAP values tend to underestimate the acid-generating potential. This should however not seriously affect waste management decisions. The test relies on the ability of hydrogen peroxide to oxidise sulphides such as pyrite, which in turn produce sulphuric acid in a mining-waste sample.

The acid produced is simultaneously neutralised by carbonates and/or other acid-consuming minerals in the sample. At the end of the reaction, the final pH of slurry provides a qualitative indication of acid-generating potential. Titration of the slurry to determine its acid content, allows the calculation of the net acid produced by the peroxide digestion and a quantitative assessment of the acid-generating potential. The pH recorded at the end of the H₂O₂ digestion step prior to titration can provide a qualitative indication of the acid-generating potential.

Table 5: Interpretation of final NAG test pH (Usher et al., 2002)

Final pH in NAG Test:	Acid-Generating Potential:
> 5.5	Non-acid-generating
3.5 to 5.5	Low risk acid-generating
<3.5	High risk acid-generating

Precaution should be exercised when interpreting NAP data in this way, since the pH values are dependent on the specific site lithology and mineralogy. Calibration with other tests and analyses is therefore recommended if the test is to be used in this way. Caution should also be exercised when interpreting NAG test results for coal reject samples and other materials that may contain high levels of organic material (such as potentially acid sulphate soils, dredge sediments, and other lake or marine sediments).

All organic material must be completely oxidised, otherwise the acid NAG results could be unrelated to sulphides. Several aliquots of H₂O₂ reagent may be added to the sample to break down organic acidity. Samples with a positive NAP value, high sulphur content and high ANC must be evaluated carefully (Usher *et al.*, 2002).

5.5. Aquifer Parameters

In order to obtain aquifer parameters for the study area, several slug tests and pumping test were conducted and analysed to determine and identify any trend or divergence from the expected norms for aquifers in Karoo-type rocks. These parameters were to be used for the construction of numerical flow models for the study area. The purpose of the models was to:

- Determine the volumes of water that would flow into the mines.
- Determine whether the mines would decant.
- Determine the impact the mines would have on the surrounding area.

The parameters that were analysed were applied to determine water levels and transmissivities, which were obtained from pump testing and slug testing. The pump and slug tests were performed primarily to obtain values for transmissivities and to determine the sustainable yields for the boreholes.

5.5.1. Slug Tests

A slug test is an efficient method which predicts the yield of the borehole by measuring the recovery rate of the water level after a sudden change. This test is performed by suddenly raising or lowering the static water level in the borehole with the aid of a closed cylinder or known volume of water. The volume of water in the borehole is displaced, therefore increasing the pressure in the borehole. The equilibrium in the water level is changed and will recover or stabilise to its initial value. By measuring the rate of recovery or recession (time to recover) of the water level, the borehole's transmissivity or hydraulic conductivity can be measured.

The recession time of the water level to recover to at least 90% of its initial value is used in a formula to determine the yield of the borehole. The formula indicates the possible yield of the borehole in L/h $y = 117155 x^{-0.824}$ (where x = recession time in seconds). The graph below was created from results obtained by testing 32 boreholes (Van Tonder *et al.*, 2002).

On the graph a straight line is obtained with the log-log scale. If the recession time for the borehole is entered on the x-axis, the possible yield can be read from the y-axis. If a slug test indicates the potential yield of a borehole at less than 0.3 l/s, additional tests should be considered. If the potential yield is more than 0.3 l/s, it is recommended that further tests such as step drawdown, multi-rate and constant rate pumping tests be conducted on the borehole.

The data gathered from the slug test was loaded into a software program developed by the Institute for Groundwater Studies, which works on a similar principal as the FC software program that is used to determine sustainable yields from pump testing data.

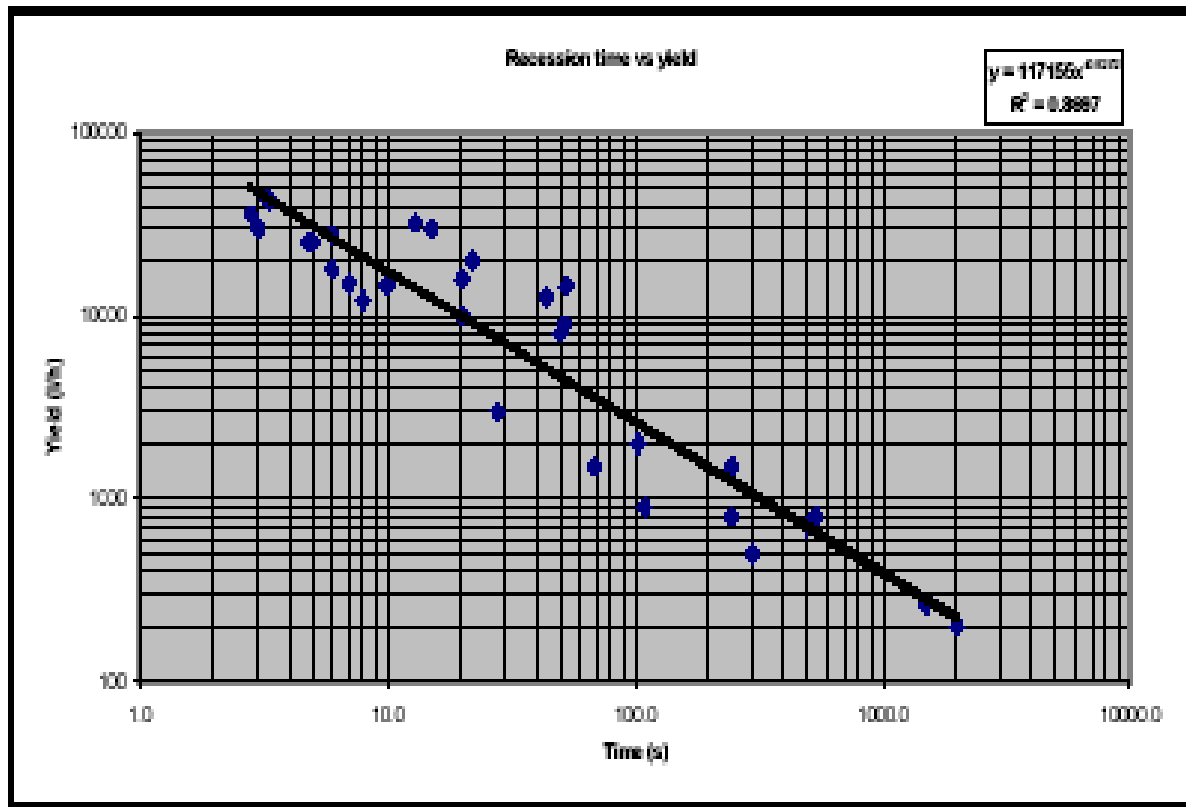


Figure 29: Slug test yield determinations.

The results are then interpreted and used as a quick estimate of the yield of a borehole. The data obtained from the slug tests were used as indicator parameters for the yields at which boreholes, that had been identified as candidates for pump testing, could be pumped.

5.5.2. Pump Testing

In an effort to obtain information on aquifer parameters for the study area, pump testing was conducted on several boreholes in the study area. The pump test can be divided into three stages; installing equipment and preparing the test, conducting the tests and measurements, and removing the equipment and checking the field data. Submersible pumps were used, as they handle easily in the field.

The pumps were fitted with lay flat pipes of approximately 50m length. The pumps were powered by generators and the time intervals for the test were measured with stop watches. The maximum yield of the pump was chosen so that sufficient drawdown was reached in time. During test measurements, the water levels and discharge rates were measured at fixed time intervals. The duration of the test, discharge rate and conditions of the measurement (manually, electronically) depend on the type and goal of the test (Van Tonder *et al.*, 2002).

Due to differences in transmissivities, depths and the available drawdown in the different borehole, the tests conducted by the researchers varied a great deal in terms of length. The time intervals were measured manually and the pumping rates were set to obtain the maximum possible drawdown. It is recommended that every measurement and observation on site should be recorded. Changes in the condition of the test, such as the discharge rate, heavy rainfall or interruptions of the test due to technical problems, must be recorded to ensure that the test is analysed correctly.

After completion of the tests, the equipment was removed from the boreholes, cleaned or decontaminated (where necessary) and the site was left in its original condition, prior to the test. The field data and information were checked directly after the test and again before beginning the analysis. As the objective of the pumping tests was to determine parameter values for the aquifer, the test was performed as follows:

- Firstly, a slug test was performed to obtain a first estimate of the possible maximum yield for the borehole (not done for every borehole)
- Secondly, a constant rate pumping test was conducted. It is recommended that the pumping rate should allow for sufficient drawdown during the constant rate test, without allowing the water level to reach the position of the main water strike. If the position of the main water strike or fracture is not known, a revised minimum one-hour step drawdown test should be performed.

According to Van Tonder *et al.*, 2002 no equal time steps are required, and the pumping rates can be increased at any time during the test. A flattening water level usually indicates the positions of the fractures.

- Thirdly, if the position of the fractures is known, a constant-rate pumping test can be performed. The abstraction rate should not allow the water level to reach the position of the main water strike.
- The minimum proposed pumping duration should be approximately 8 hours according to Van Tonder *et al.*, (2002), although this is a guideline value that can be adjusted when necessary. For the purpose of estimating the impact of inner boundaries (extent of fracture, matrix) or outer boundaries (no-flow or recharge boundaries), the duration of the constant rate pumping test should be several days. This is however not always practical and is subject to adjustment. (Van Tonder *et al.*, 2002). A pumping time of four hours was generally used for the pumping test, but longer tests were also conducted.
- Finally, the recovery inside the abstraction borehole was measured until the *water* level recovered to 95% of the original static water level. A recovery test has no external interferences.

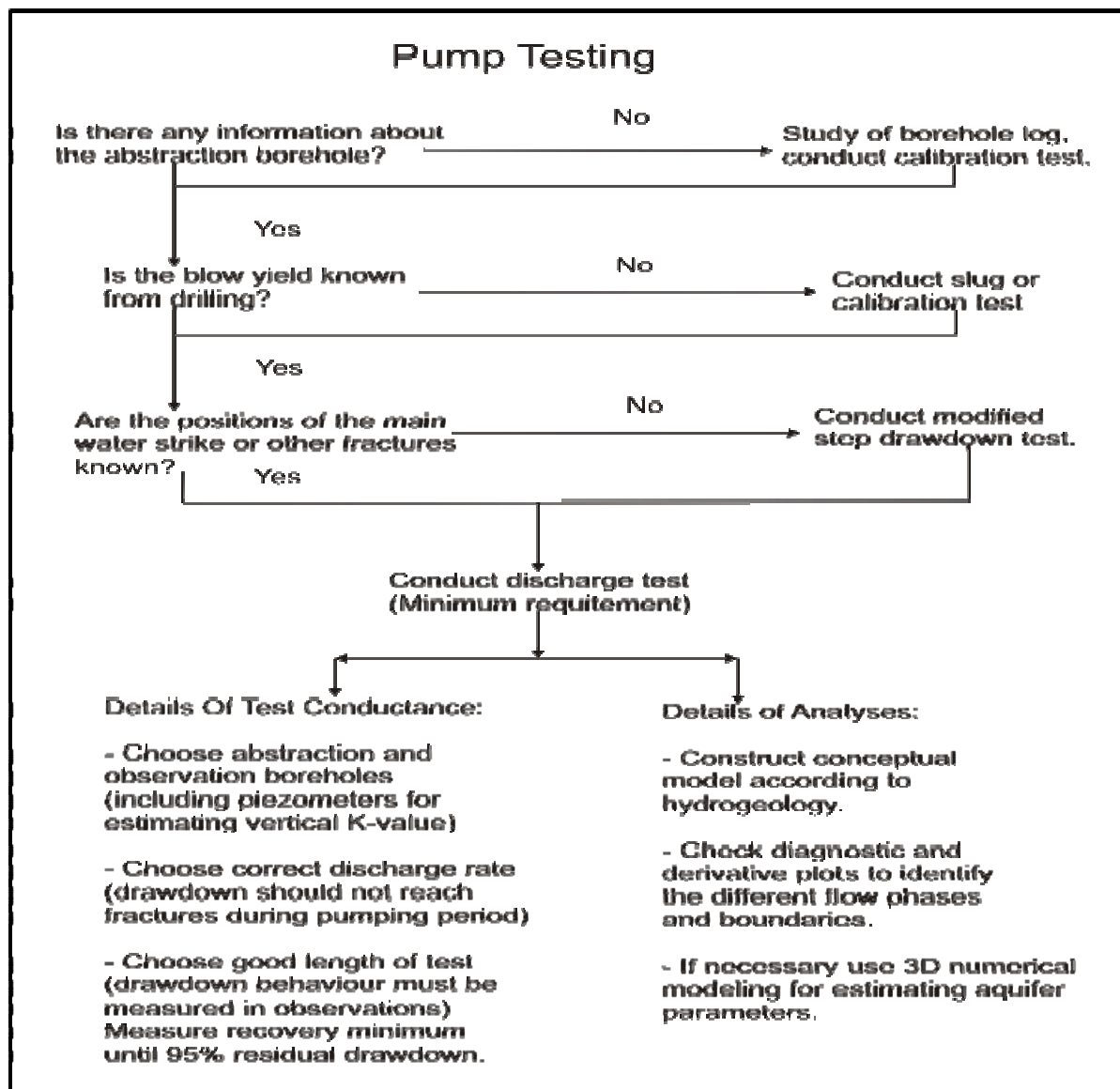


Figure 30: Process involved in pump testing after Van Tonder et al., 2002.

The pump test data was analysed using the FC software program developed at the Institute for Groundwater Studies in Bloemfontein. The software was used to determine sustainable yields for the boreholes that were tested. From the diagnostic plots generated by the FC program (log-log plots) it was concluded that the transmissivities of the boreholes were very low.

5.6. Recharge

The recharge for the study areas was required as an input parameter for the modelling phase of the project in order to simulate the real world scenario as closely as possible. Two methods were used for recharge determinations of the study area. The selection of methods was based on the accuracy of the methods for the prediction of recharge and the availability of data. The methods selected were the Chloride Mass Balance Method and the E.A.R.T.H. model for determining recharge.

5.6.1. The Chloride Mass Balance Method

The chloride method for determining recharge (also known as the chloride mass balance method) is one of the techniques which is often used to estimate groundwater recharge (Van Tonder and Xu., 2001). The chloride mass balance method has been used to evaluate recharge processes in a wide range of semi-arid environments, as these environments are more suited to this type of recharge estimation. Due to its conservative nature and the relative abundance thereof in precipitation, chloride is used for recharge estimation. (Van Tonder and Xu., 2001). According to Van Tonder and Xu (2001) “The application is based on comparison of the chloride deposition rate at the soil surface with the concentration in the soil water or groundwater. The Cl concentration increases relative to the concentration of rainwater as a result of interception, soil evaporation and/or root water uptake by the vegetation. The total (wet and dry) chloride deposition and the total precipitation depth determine the chloride concentration of the rainwater at the surface.”

The chloride method used in this study is as follows:

$$[\% \text{ Recharge} = 100 * Cl(\text{rain}) / Cl(\text{groundwater})]$$

The above-mentioned recharge calculations were used on the basis of information derived from 222 boreholes. From the analysed values, the data suggests that there is a large range for the Cl values found in the study area. The calculations indicated a recharge of 1.59% of the annual rainfall (see Appendix C).

5.6.2. The E.A.R.T.H. Model

In an effort to confirm the recharge values obtained from the Chloride method, the E.A.R.T.H. method for recharge estimation was used. What follows is a brief description of the method: According to Van Tonder and Xu (2001), the variability of the surface soil and plant characteristics often leads to a complex, three-dimensional, water and solute movement taking place in the upper part of the unsaturated zones.

They further observe that: “Soils which are formed by in-situ weathering often form a cover with a highly variable thickness adding to the complexity of determining accurate figures on the downward percolation (recharge) of soil water to the water table”. Van Tonder and Xu (2001) refer to the Van der Lee and Gehrels (1990; 1997) lumped parametric model which they named the E.A.R.T.H. model (**E**xtended model for **A**quifer **R**echarge and soil moisture **T**ransport through the unsaturated **H**ard rock).

This model was to be used for the estimation of groundwater recharge. The modelled space is schematically represented by a number of modules, or reservoirs, as illustrated by Figure 31. Each reservoir has an acronym, which roughly describes the main function or processes behind it (Van Tonder and Xu 2001).

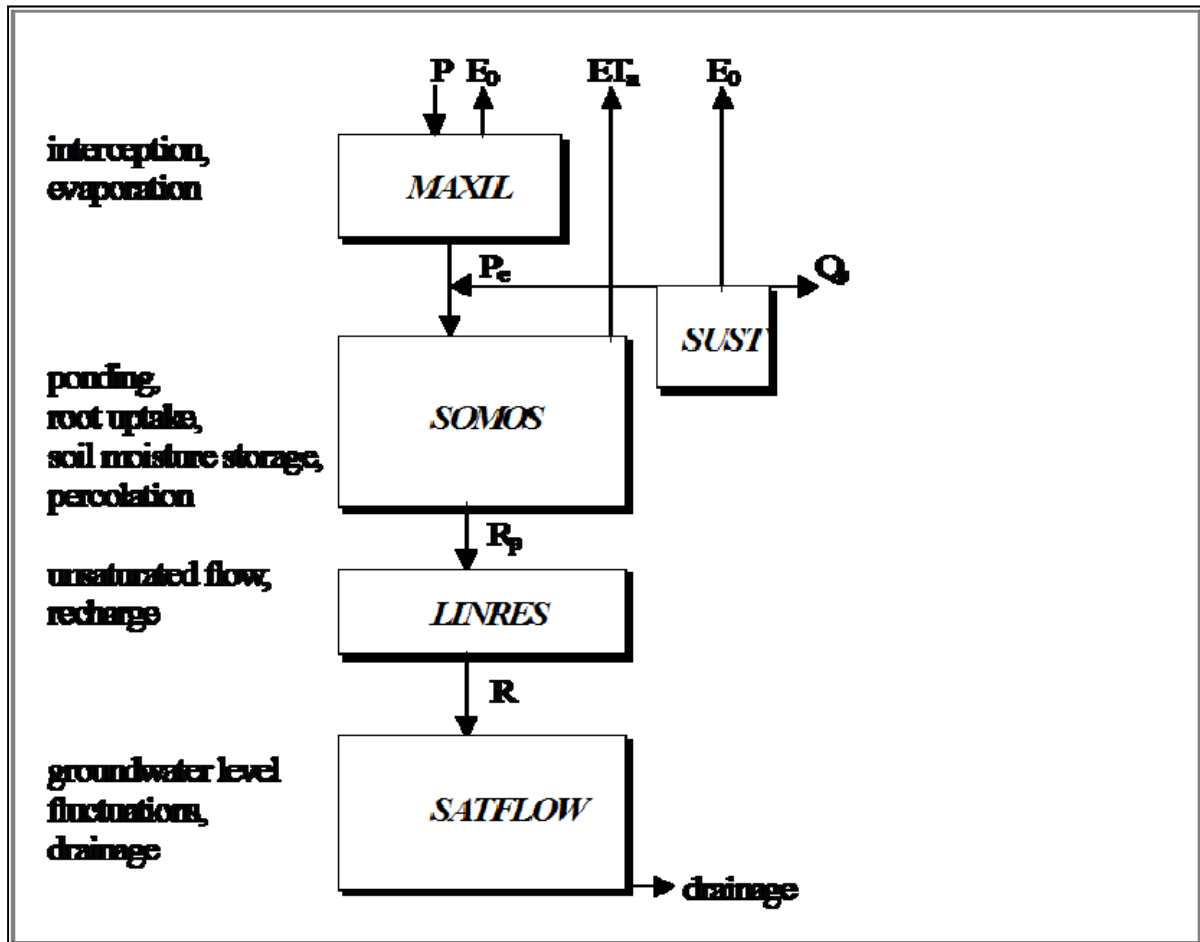


Figure 31: Illustration of the E.A.R.T.H. model.

Using the E.A.R.T.H. model, eight boreholes were used for the recharge determination. These boreholes were selected due to the availability of data dating back through time. Some of the boreholes have information dating back as far as 1973. Some of the other boreholes unfortunately have data which spans only five or eight years. The above-mentioned model was applied to the information collected, and a recharge of 1.51% was calculated for the study area (see Appendix D).

5.7. Numerical Groundwater Models

As the main goal of the study is to determine the impact of the mines and other activities planned for the study area, it was decided that models should be used to determine this impact. Given that models can sometimes be one sided and often differ from researcher to researcher, it was decided to construct both numerical-flow models and a conceptual model to serve as the concluding phase of the project.

What follows is a brief discussion on numerical modelling. The relatively recent development of the simulation of groundwater flow and transport by means of numerical modelling (dating from the 1970's according to Vermeulen and Dennis 2007), has evolved to the point where the study of complex groundwater problems is dominated by numerical modelling.

Due to the substantial advances in recent years in the domain of computer technology, the use of numerical models has become standard procedure for the solution of groundwater flow and mass transport. According to Vermeulen and Dennis (2007) numerical modelling can be used to solve both complex and simple problems. One of the major advantages of numerical modelling is the fact that various scenarios can be investigated without much effort. The large scale application of numerical modelling to groundwater-related problems has led to the synonymous use of the term *modelling* when referring to *numerical modelling*. What follows is a brief discussion of the steps involved in the construction of a numerical model.

5.7.1. Collection and Interpretation of Field Data

Field data plays an integral part in the understanding of the natural system and the specification of the groundwater problem that needs to be investigated. A numerical model can be developed into a site-specific groundwater model if the appropriate field parameters are assigned to the model (Vermeulen and Dennis 2007). The quality of the generated model generally depends on the quality of the input data used and the level of calibration achieved.

5.7.2. Conceptualizing the Natural System

It is recommended that a conceptual model be constructed in each numerical study. This model is then to represent the natural systems present in the area to be studied. The purpose of a conceptual model is to design and construct the equivalent (but simplified) conditions of the real-world problem to be modelled. The next step is to transfer the real-world situation into a model equivalent. This transferral is a crucial step in the domain of groundwater modelling.

The following parameters are generally included in a model (Vermeulen and Dennis 2007):

- The geological and geohydrological features and characteristics of the area being studied.
- The static water levels/piezometric heads measured for the study area.
- Interactions taking place between the geology and geohydrology on the boundaries of the study area.
- Processes and interactions taking place within the study area that potentially have influences on the movement of groundwater
- Simplifying assumptions necessary for the development of a numerical model such as for example a flat topography or homogeneous geology, and
- The selection of a numerical code suitable for the needs of the model.

5.7.3. Calibration and Validation

The importance of model calibration and validation lie at the core of the need to overcome the lack of input data. Additionally this is done to accommodate the simplification of the natural system in the model. During model calibration, simulated values of for example water levels or water level elevation are compared with the values measured in the field. The input data is then altered and modified within ranges, until the data simulated by the model, and the values observed in the field are fitted on a graph, within an acceptable tolerance (Vermeulen and Dennis 2007). The input data and the comparison of simulated and measured values can be altered either manually or automatically, although manual modification of the values is normally preferred.

The validation of a model is required in order to demonstrate the applicability of the model for use in making predictions. A practice commonly used for the validation of models involves the comparison of the model with a set of data that was not used during model calibration. Calibration and validation are, however, some of the more difficult aspects of numerical groundwater modelling. Often it is not possible to validate a model as there are no alternate data sets available for validation. In the case of the models constructed for the study area, calibration was done according to the amount of inflow currently being measured at the Grootegeluk mine. The model was, however, not fully calibrated as there was a general lack of input parameters with which to calibrate the model.

5.7.4. Modelling Scenarios

It is possible to assess alternative scenarios for a given area with relative ease by means of numerical modelling. When the application of numerical models is considered in a predictive sense, there are limitations to the application of the model. According to Vermeulen and Dennis (2007) models used for predictions should be applied to predictions of a relative rather than an absolute nature.

Five dewatering and accompanying decant models were constructed for the study area to illustrate different scenarios that may occur during the course of mining in the study area.

5.7.4.1. Scenario 1

- Three dewatering models were constructed using all the parameters collected for the study area (see Chapter 10) and only one pit (the northern pit).
- In the models, the faults found in the study area were not activated.
- The models were systematically dewatered, first to the second layer, then to the third layer and finally to the fourth layer to simulate the progression of the mine over time.

- All the models were constructed for all three transmissivities used for the models in general (0.4 m²/d, 0.28 m²/d and 0.12 m²/d) and would run for 10 years for each layer being dewatered.
- For the decant purposes the pits were filled and dewatered for 50 years.

5.7.4.2. Scenario 2

- The fourth dewatering model possessed the same parameters as scenario 1 (see Chapter 10) and in addition, contained one activated fault that ran through the pit. This was done to simulate a scenario where a zone of higher transmissivity might be encountered during the course of mining. Only a transmissivity of 0.4 m²/d for the model in general was used with higher transmissivities being applied to the faults.
- The decant model was run for 50 years simulating a time when mining activity had ceased.

5.7.4.3. Scenario 3

- The final model constructed had all three pits on the model and all the faults found in the study area activated. All the pits were dewatered to 110 m below surface.
- Once the models were dewatered they were run for 50 years. The models contained the parameters for use in decant models as stated in Chapter 10

5.7.5. Assumptions and Limitations of Numerical Modelling

In order to develop a model of an aquifer system, certain assumptions have to be made. The following assumptions were made while developing the model:

- The aquifer system is represented by a two-dimensional system consisting of four layers with dominating horizontal flow. This horizontal flow is the result of the lateral extent of the area modelled (tens of kilometres) compared to the depth of the aquifers.
- The geology was assumed to be homogeneous.
- The system was taken as being in steady state, even though the natural conditions had been disturbed.
- The available information on field tests and predominant geological structures was assumed to be correct.
- No abstraction boreholes were included in the model.
- Many of the aquifer parameters could not be determined in the field and were estimated accordingly
- It was assumed that the entire study area had an average water level of 28 m below ground level.

It must be noted that a numerical model simulating groundwater flow is merely a representation of the real system. Accordingly it can be viewed at most as an approximation, with the accuracy depending on the quality of the available data. This implies that errors are always associated with numerical groundwater models. This is largely due to uncertainties in the data and the inability of numerical methods to accurately describe natural physical processes (Vermeulen and Dennis 2007).

5.7.6. Generation of a Finite Difference Network

5.7.6.1. General

According to Vermeulen and Dennis (2007) “in order to investigate the behaviour of aquifer systems in time and space, it is necessary to employ a mathematical model”. The software program MODFLOW developed by Harbaugh and McDonald, (1996) as referenced by Vermeulen and Dennis (2007), was used for this investigation. The programme is an internationally accepted modelling package, capable of calculating the solution of the groundwater flow equation by means of the finite difference approach.

A professional graphical-user-interface (GUI), PMWIN, developed by Chaing and Kinzelbach (1999) as referenced by Vermeulen and Dennis (2007), was used for the creation of the model. It was additionally used to analyse and display the modelling results. According to Vermeulen and Dennis (2007) “The finite difference (FD) method was the first method to be used for the systematic numerical solution of partial differential equations”.

In order to construct an FD model, the user creates a regular grid covering the entire study area. The model area is then subdivided into rectangular sub domains commonly referred to as cells. The cell values are assigned individually and can contain such parameters as, water level, transmissivity and recharge area. Each cell may hold a value for each parameter, but cannot have different values for the same parameters.

5.7.6.2. Boundary Conditions

One of the first and most demanding tasks in groundwater modelling is that of identifying the model area and its boundaries. Consequently, a model boundary is the interface between the model area and the surrounding environment. Conditions on the boundaries, however, have to be specified. Boundaries occur at the edges of the model area and at locations in the model area where external influences are represented, such as rivers, wells and leaky impoundments. Criteria for selecting hydraulic boundary conditions are as follows: primarily topography, hydrology and geology.

The topography, geology, or both, may yield boundaries such as impermeable strata or potentiometric surface controlled by surface water, or recharge/discharge areas such as inflow boundaries along mountain ranges.

The flow system allows the specification of boundaries in situations where natural boundaries are a great distance away. Boundary conditions must be specified for the entire boundary and may vary with time. At a given boundary section just one type of boundary condition can be assigned. As a simple example, it is not possible to specify groundwater flux and groundwater head at an identical boundary section. Boundaries in groundwater models can be specified as:

- Dirichlet (also known as constant head or constant concentration) boundary conditions
- Neuman (or specified flux) boundary conditions
- Cauchy (or a combination of Dirichlet and Neuman) boundary conditions

A box model was used, in which the northern, eastern, southern and western borders of the model were set to constant head boundaries. This was done to simplify the model. For the dewatering models, constant head boundaries were placed on the lowest levels of the layer that was to be dewatered. For the decant models, these boundaries were removed.

5.7.6.3. Initial Conditions

The determining of initial conditions is vital for addressing modelling flow problems. Initial conditions must be specified for the entire area. Generally, the initial water level/head distribution acts as the starting distribution for the numerical calculation. The initial water level was set to surface level (for the model zero (0) as the modelling program can only simulate saturated flow.

5.7.6.4. Sources and Sinks

Sources and sinks can be defined as recharge and abstraction sources in the aquifer, respectively. Examples of sources are precipitation and inflow from surface water and recharging boreholes. Sinks may comprise abstraction boreholes, springs, evapotranspiration, mines and outflow to surface water.

The groundwater recharge (R) for the area was calculated using the chloride method and the E.A.R.T.H. method. Accordingly the recharge for the study area was calculated to be 1.5% of the annual rainfall. The recharge entering into the model in general was determined at 0.023 mm/y, and at 20% of the annual rainfall in the open pits (Hodgson *et al.*, 2007), amounting to 0.31mm/y.

5.7.6.5. Aquifer Parameters

Two main parameters are used to describe the physical properties of the aquifer, namely transmissivity (T) and storage coefficient (S). Transmissivity is a measure of the ease with which groundwater flows in the subsurface. Transmissivity is related to hydraulic conductivity (K): $T = Kd$ where d is the saturated thickness of the aquifer. Storage coefficient is the volume of water from which an aquifer releases, or takes into storage per unit surface area of the aquifer per unit change in head. For a confined aquifer, the storage coefficient is equal to the product of the specific storage and aquifer thickness of the saturated porous medium. For an unconfined aquifer, the storage is the ratio of the volume of water that drains by gravity to that of the total volume, and is known as specific yield.

- The calculated harmonic mean of the transmissivities was $1.6 \text{ m}^2/\text{d}$ as calculated from pumping test data.
- This was taken as the total transmissivity for the system and divided among the layers for an even distribution of $0.4 \text{ m}^2/\text{d}$ for each layer.
- Two additional transmissivities were taken to test the model (different scenarios).
- It was decided to take transmissivities of roughly $1/3$ ($0.12 \text{ m}^2/\text{d}$) and $2/3$ ($0.28 \text{ m}^2/\text{d}$) respectively.
- The reason for taking these transmissivities was to simulate different scenarios as it was felt that the transmissivity of $0.4 \text{ m}^2/\text{d}$ was too high and did not correspond to the volumes of water entering into the pit.
- An additional factor was that the model could not be calibrated due to lack of data.
- These transmissivities were used for the area as a whole, with the transmissivities in the pits set at $100 \text{ m}^2/\text{d}$ for the dewatering models, and $500 \text{ m}^2/\text{d}$ for the decant models respectively.
- The transmissivities selected for the faults were $500 \text{ m}^2/\text{d}$.

A general storage coefficient of 0.003 was selected for the model in general and storage coefficients of 1 and 0.25 for the dewatering and decant models in the pits themselves. These values were selected on the basis of their conformity with the expected norms for Karoo aquifers. Vertical hydraulic conductivity was set to 1E^{-5} for the model as a whole, and at 10 in the pits to simulate worst case scenario situations.

5.7.6.6. Time

For the dewatering models, a time frame of 10 years was determined for the purpose of simulating the dewatering of each layer as mining tends to penetrate ever more deeply into the geology. The 10 years were divided into lengths of 360 days (to remove leap years from the modelling calculations), with the time steps set to 12 (12 months). For the decant models, a time frame of 50 years divided into lengths of 360 days and 12 time steps was selected.

5.7.6.7. Pits

Initially only one pit was simulated with the three different transmissivity values. This was finally expanded to three pits; one to the north, one towards the south-east and one between the other pits. The sizes of the pits vary, with the northern pit being 1750 ha, the central pit 2793 ha, and the south-eastern pit 2070 ha. The large pit sizes were chosen to simulate the absolute worst case scenario situations.

CHAPTER 6: Geology of the Waterberg Coalfields

6.1. Introduction

In 1920, coal was discovered while drilling for water on the farm Grootegeluk. Since then a large number of exploration boreholes have been drilled in the study area. There are also large numbers of boreholes being drilled as part of ongoing prospecting programmes within the study area. Iscor began the development of the Grootegeluk colliery, currently the only active mine in the study area, in the 1970s. Figure 32 indicates the regional geology of the study area. As indicated in Figure 32, the study area includes most of the Karoo Supergroup. The predominant structures (the three main faults) namely the Daarby, the Zoetfontein and the Eenzaamheid faults, are indicated on the map.

The Waterberg Coalfield trends east / west and is heavily faulted (Figure 32 & Figure 33). It is composed of sedimentary rocks of the Karoo Sequence and forms a graben structure bounded in the north by the Zoetfontein fault and in the south by the Eenzaamheid fault. The Daarby fault subdivides the coalfield into the shallow open-castable western part and the deeper north-eastern part of the coalfield (a displacement of approximately 400 m).

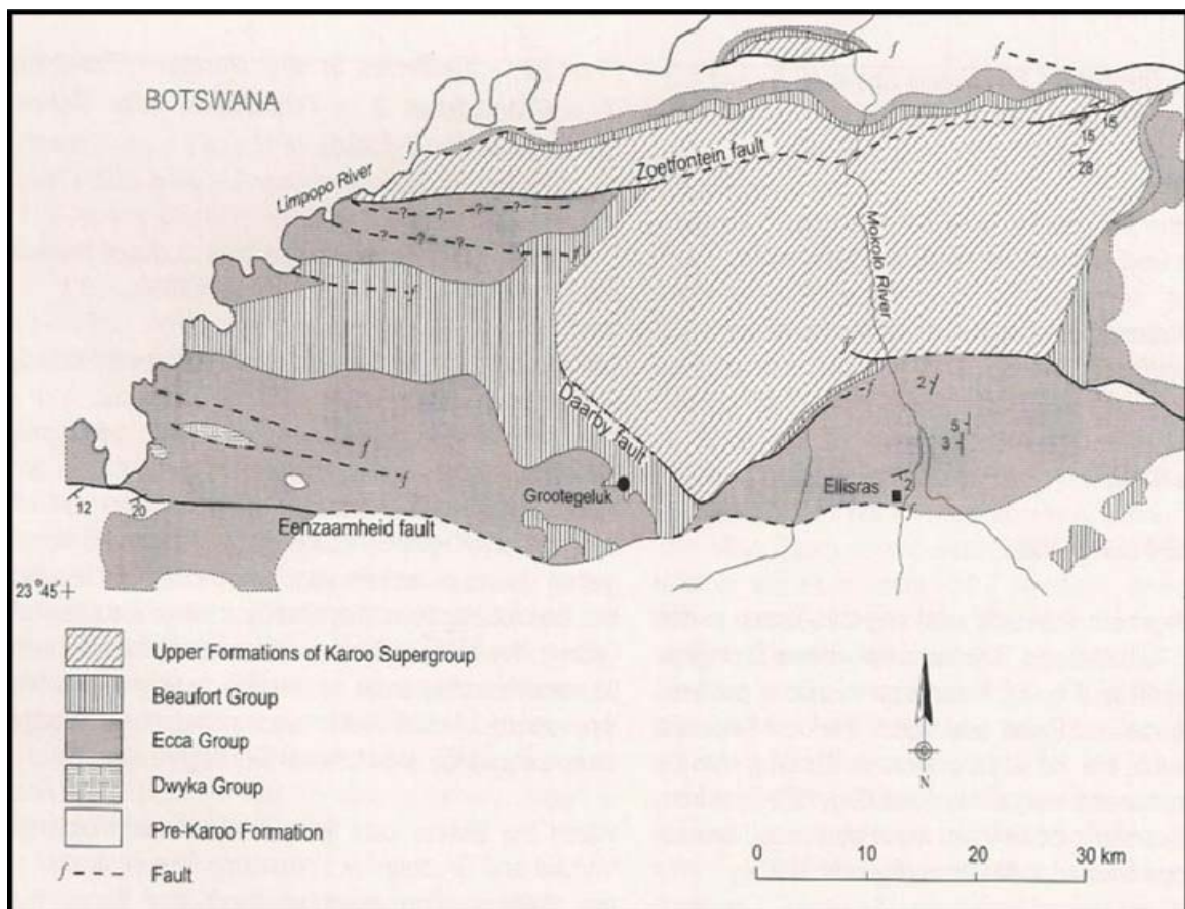


Figure 32: Simplified geological map of the Waterberg Coalfield after Snyman (1998).

The Zoetfontein fault resulted from pre-/during Karoo depositional tectonism, whilst the Enzaamheid and Daarby faults resulted from post-Karoo depositional tectonism. Figure 33 displays a phase magnetics map of the study area (courtesy of the CSIR), indicating all the dominant structures found in the study area with the three main faults indicated on the map. The map indicates faults as well as igneous intrusions with pre-Karoo topography also playing a role.

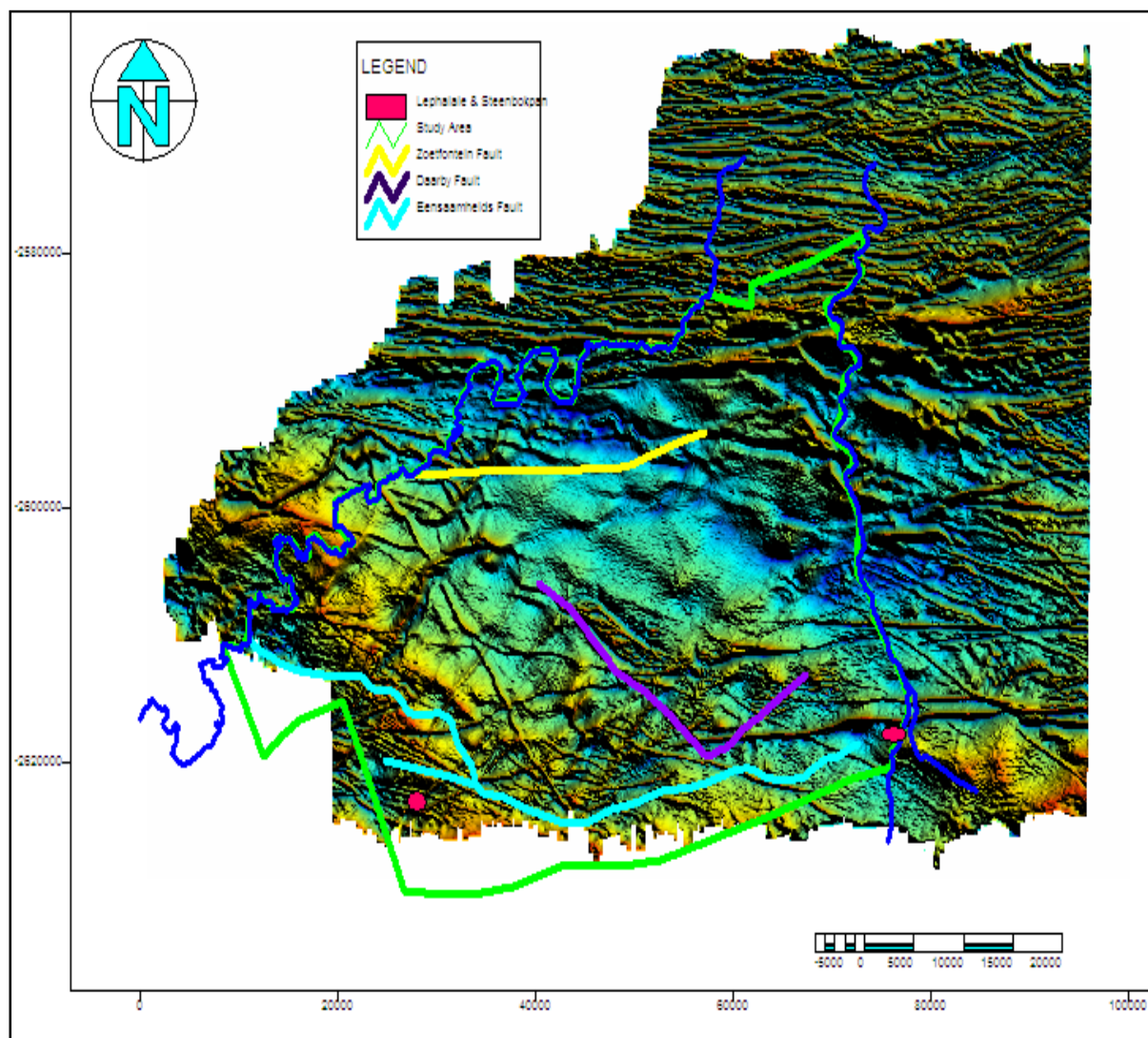


Figure 33: Phase magnetics map of the study area indicating the dominant structures, courtesy of the CSIR.

All the units of the Karoo Sequence are present in the coalfield and the subdivision of this Sequence is mainly based on lithological boundaries, consisting from top to bottom of the Stormberg Group (Letaba Formation), followed by the Beaufort Group, the Eccca Group and the Dwyka Group. Within the Waterberg Coalfield, coal occurs in both the Vryheid and Grootegeluk formation, which are equivalent to the Volksrust formation of the Karoo Supergroup. In addition to the Karoo Supergroup rocks, there are also rocks present in the study area from the Mokolian Supergroup, as represented in the study area by the Waterberg group rocks.

6.2. Coal-Bearing Successions in the Coalfield

The coal-bearing sequence is 115 m thick (Figure 27 & Figure 34) and subdivided into 11 zones (Snyman, 1998). The lower four form part of the Vryheid formation. These zones coincide with the four lower seams of predominantly dull coal, with an average thicknesses of 1.5 m - 5.5 m. The ash content of these seams increase upwards from 20% to roughly 45%.

Zones 5 to 11 occur in the Grootegeluk formation, which consist of rapidly alternating mudstone and thin coal seams. This consists mainly of bright coal. The run-of-mine coal from these zones ranges from about 45% - 65% in ash content and has to be beneficiated to obtain a blend of coking coal and a middling suitable for steam raising. There is a sharp peak in the P_2O_5 content of up to 10% in the coal ash of zones 4 and 5, which makes these two zones unsuitable as a source of metallurgical coal. The P_2O_5 spikes coincide with the boundary between the Vryheid and Grootegeluk formations. According to Dreyer (pers. comm. 2009), the coal in the area will be mined down to a level known as Coal Zone 2 (Figure 34). Figure 35 shows the position of the coal floor with regards to the topography, indicating the deepest level to which the coal will be opencasted.

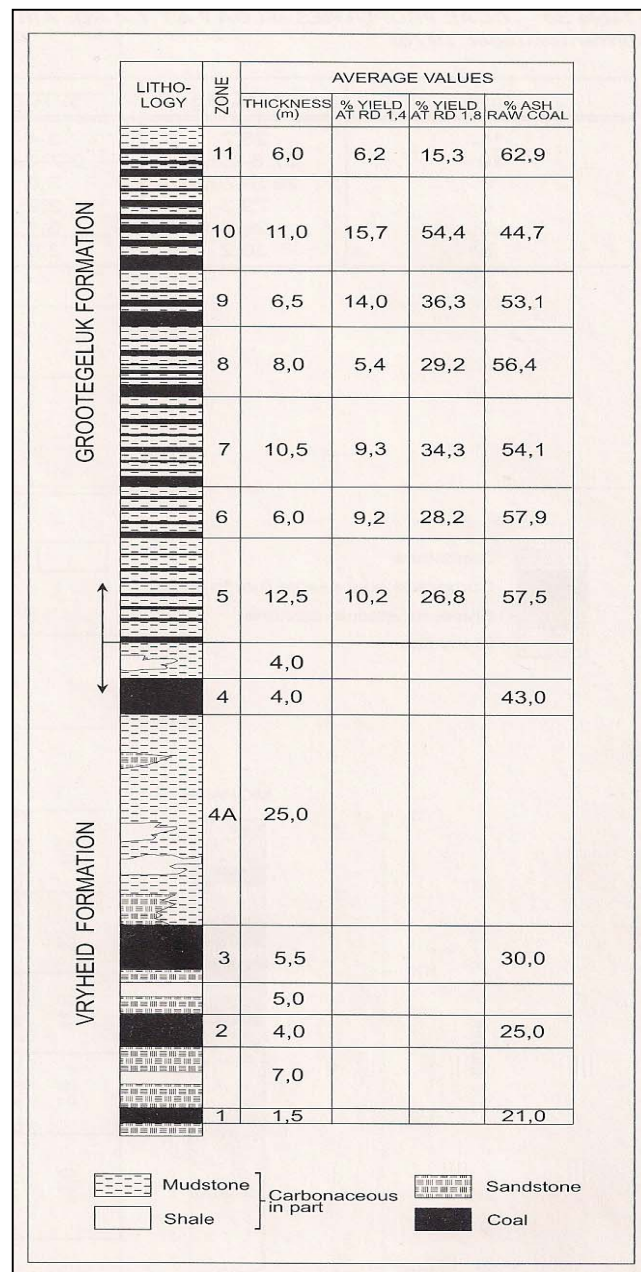


Figure 34: Generalized stratigraphic column of the coal-bearing interval in the Waterberg coalfield (Snyman, 1998).

According to Dreyer (pers. comm. 2009). It should be noted that due to the thickness of the last coal seam (1.5m) it would be possible to remove the coal by means of underground mining methods. This remains a future option, and is not currently considered to be an economically viable option.

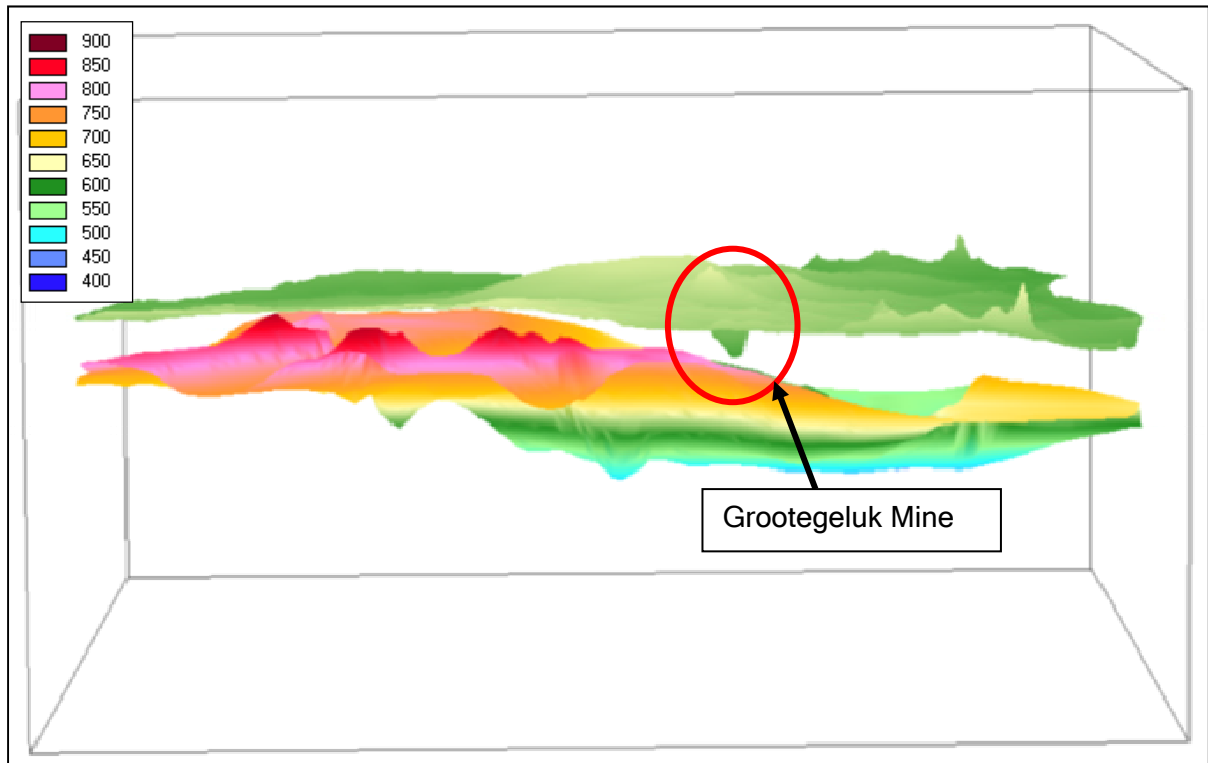


Figure 35: Exaggerated 3D side view of the topography and Coal Zone 2 (legend).

From Figure 36, it is apparent that the coal seams are located at shallower depths in the west and at much deeper depths in the east and north/east. The cut-off between the deeper and shallower coal (the Daarby fault) can also be seen.

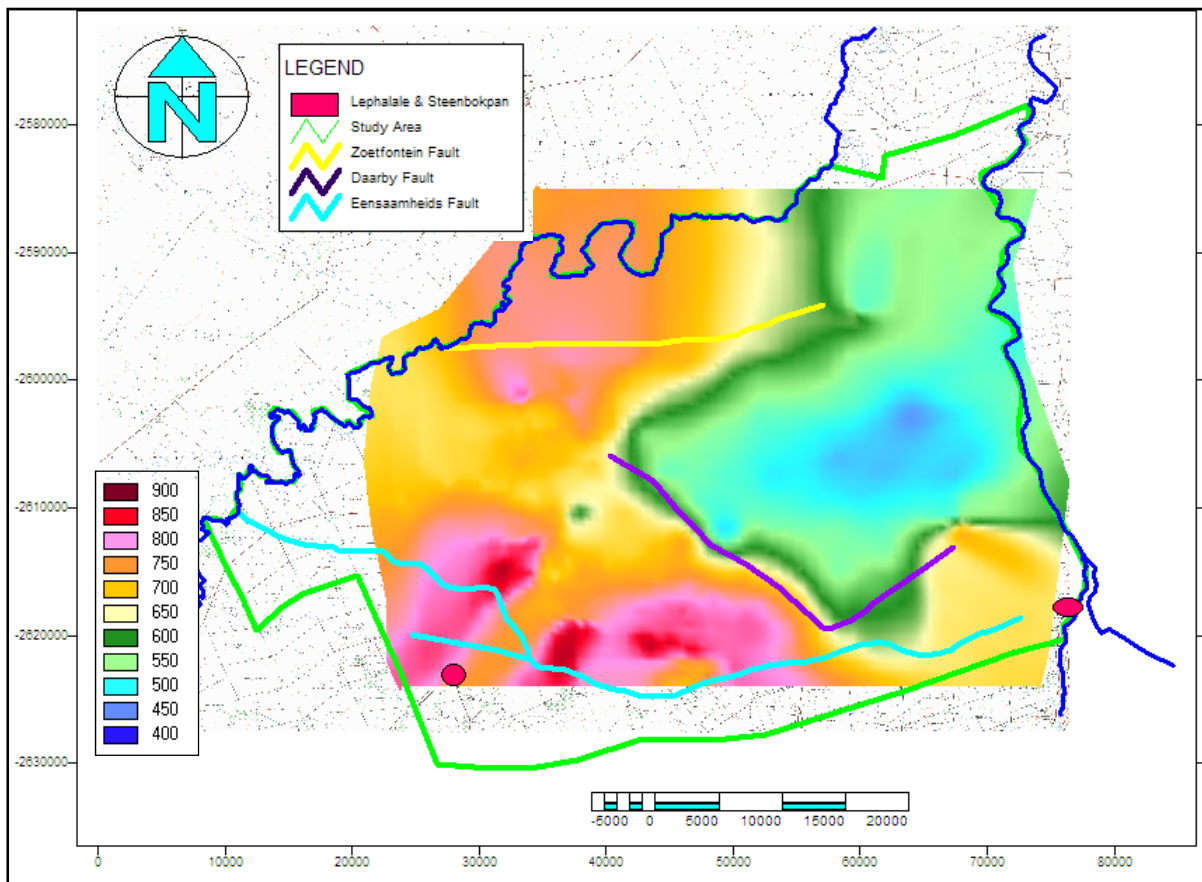


Figure 36: Plan view of Coal Zone 2.

Figure 37 indicates cross-sections through the study area. The north/south cross-section was made through the Grootegeluk pit and the figure clearly shows that the water levels follow the topography of the area. The pit at Grootegeluk has a significant impact on the movement of groundwater in the area. In both sections deeper and shallower coal-bearing strata can be seen. The zones are separated by the Daarby fault that divides the coal-bearing strata into deeper eastern area and shallower western area.

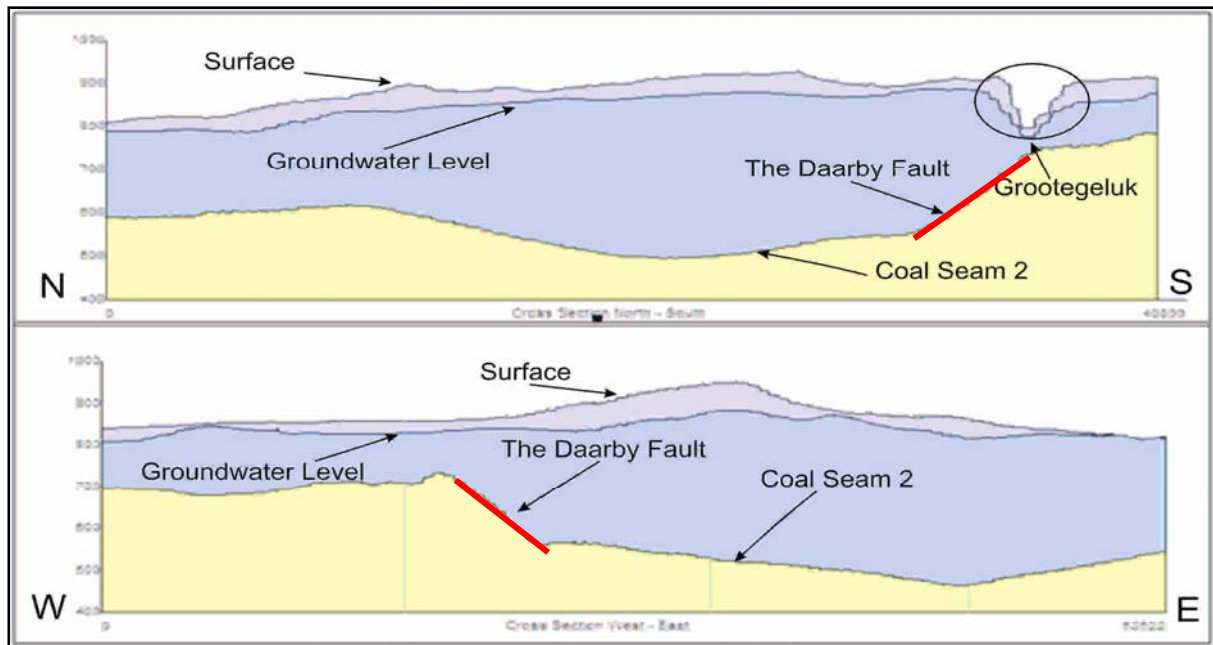


Figure 37: North/south and west/east cross-sections of the study area.

The study area was further divided into three main categories according to weathered geology. These are:

- Areas that contain the full succession of coal (Figure 38)
- Areas that have been weathered down to the Vryheid formation (Figure 38)
- Areas that have been weathered down to the Pietermaritzburg (Figure 38).

Figure 38 shows that there is significant variation in the level to which the geology has been eroded and thus also the depth of the coal which varies greatly in the study area. From the information gathered, it is clear that there are large volumes of coal that can be economically extracted from the Waterberg Coalfield. However, the coal is of such low quality that it will need to be beneficiated to maintain profitability (pers. comm. Dreyer 2009). The necessity for beneficiation plants gives rise to other potential problems. The plants will require large volumes of water to operate, which will increase the strain on groundwater systems if the required water is to be abstracted from boreholes. In an area where there is already a shortage of water (including usable groundwater), this would present a serious problem. Furthermore, the discard from the beneficiating plants contains minerals that are prone to acid generation.

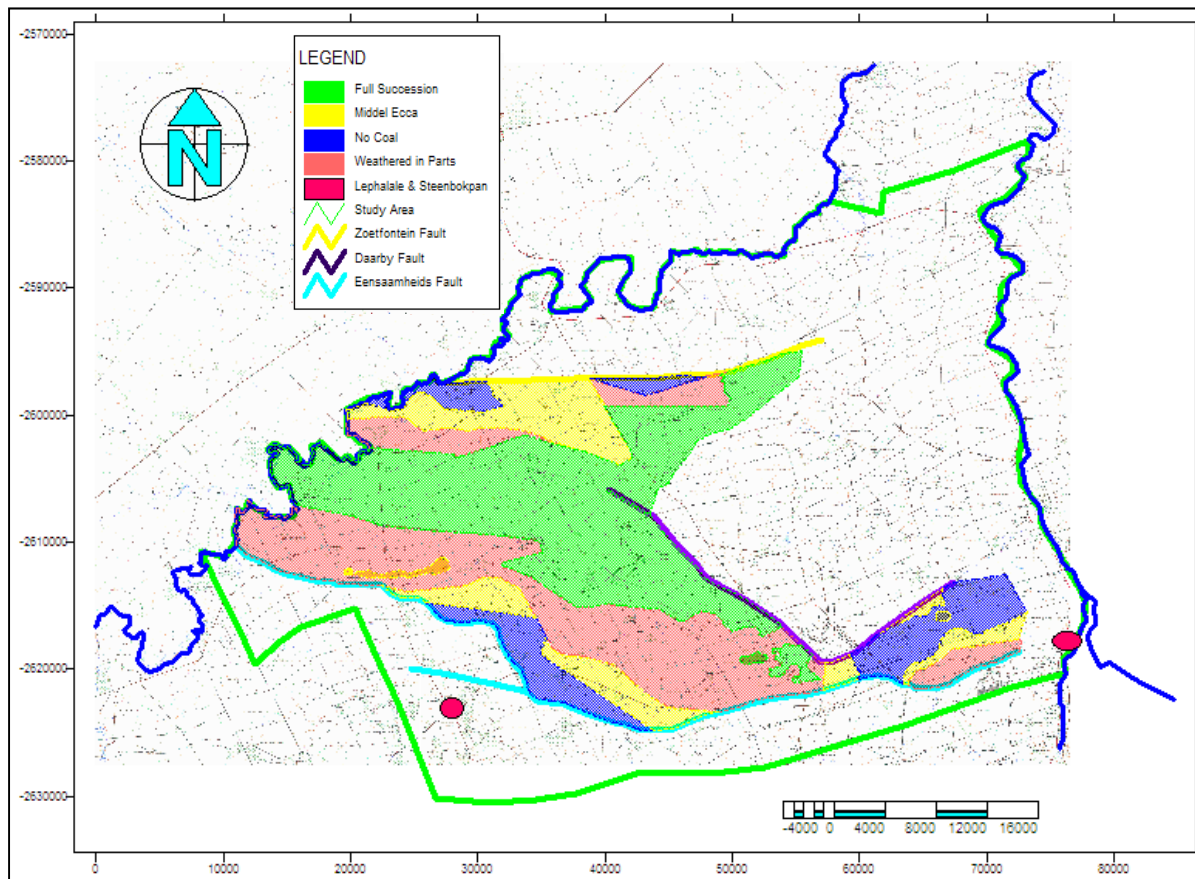


Figure 38: The weathered zones and major faults in the study area.

Large volumes of this discard will be produced during the life of the mines. It is recommended that the discard be placed in such a manner that they minimize the possibility for pollution of groundwater resources. The main rock types in the area are blue/green mudstone, shales and white Ecca formation sandstones. These formations are divided into different layers, and the coal is intermixed with the mudstones and shale. The overburden (and in some cases interburden like Ecca sandstones) will be used to backfill the pits once mining has stopped. It is therefore important to know the characteristics and potential for acid generation, or neutralisation, of the interburden.

6.3. Conclusion

From the gathered and assessed data, it becomes clear that there are large quantities of coal available for mining in the Waterberg coalfield. The coalfield is contained between boundaries formed by the three main faults, of which the Daarby fault divides the coalfield into a deeper eastern half and a shallower western half. Only the western area will be mined initially. The coal is subdivided into 11 zones and the deepest level to which surface methods of extraction can economically be used is coal layer two (pres. comm. Dreyer 2009). Only one method will be applied in the mining of the coal, and beneficiation will be required due to the low quality of the coal. The discard produced from the beneficiation plants will be used as back fill along with other material removed from the pit.

CHAPTER 7: Acid-Base Accounting

7.1. Introduction

Acid-base-accounting analyses were conducted on geological samples gathered from the study area. The goals of these analyses were threefold:

- Firstly; to determine whether the rocks (geological units) in the study area that will be removed during mining, will become acidic upon oxidation, or if the rocks contain a high enough base potential to prevent this from happening.
- Secondly; to determine if a correlation exists between the depth of weathering in the different parts of the study area and the acid potential of the rocks of these areas.
- Thirdly to determine if there are any “problem” layers that have a higher acid potential than the other rocks found in the study area.

In order to achieve these goals geological samples were collected from various localities throughout the study area. These samples consisted of various core and chip samples. Additionally the samples included two processing plant discard samples (one from each plant) obtained from the two plants at the Grootegeluk mine. These samples were taken to the lab at the Institute for Groundwater Studies for static acid-base accounting tests. To assess the geochemical nature of the most likely reacting components, several laboratory tests were undertaken. Detail on the objectives, methodology and interpretation of each type of test is provided in the sections to follow. Analytical tests to determine the acid-generating potential of rock samples are either static or kinetic in nature. A static test determines both the total acid-generating and total acid-neutralising potential (NP) of a sample. The capacity of the sample to generate acidic drainage is calculated as either the difference of the values or a ratio of the values, as will be discussed in the following section.

These tests are intended to predict acid-producing potential, and not the generation rate of acid. Static tests can be conducted quickly and are inexpensive compared to kinetic tests. Acid-base accounting is a screening procedure whereby both the acid-neutralising and acid-generating potential of rock samples is determined and the difference (net neutralising potential) is calculated. The NNP and/or the ratio of neutralising potential to acid-generation potential are compared with a predetermined value, or set of values, to divide samples into categories that either do or do not require further determinative acid potential test work. Rules and guidelines were developed (e.g. Price and Errington, 1995, Steffen, Robertson and Kirsten, 1989 and Brady *et al.*, 1994) for ABA procedures by mine regulatory and permitting agencies and presented by Usher *et al.*, 2002). In its most basic form, ABA is a screening process.

It provides no information on the speed (or kinetic rate) with which acid generation or neutralisation will proceed, and because of this limitation, the test work procedures used in ABA are referred to as Static Procedures (Ziemkiewicz, 1994). The potential for a given rock to generate and neutralise acid is determined by its mineralogical composition and other mineralogical properties. This includes the quantitative mineralogical composition and individual mineral grain size, shape, texture and spatial relationship with other mineral grains. The term "potential" indicates that even the most detailed mineralogical analysis, when combined with ABA, can give only a "worst-case" value for potential acid production and, depending upon the NP procedure, a "worst-case", "most likely case" or "best-case" value for potential neutralisation capability (Usher *et al.*, 2002). The NP measures the total carbonates, alkaline earths and bases available to neutralise acidity, and represents the most favourable condition. Calculations of maximum potential acidity and NP are structured to equate the two measurements to a common basis for comparison. The resulting values, expressed as calcium carbonate equivalents, are compared to compute a net acid-producing or acid-neutralising potential. Material exhibiting a net acid-production potential of 5 tons/1000 tons of material or more as calcium carbonate equivalents are classed as toxic or potentially toxic (Hunter, 1997a and Sobek *et al.*, 1978).

7.1.1. The Primary Advantages of the ABA Methods are:

1. Short turn-around time for sample processing.
2. Low cost.
3. Relatively simple analytical procedures.
4. Relatively simple interpretation of results (Hunter, 1997a).

7.1.2. The Principal Disadvantages of ABA are:

1. The method predicts maximum potential acidity and maximum neutralisation capability, thus implying a 1:1 acid to base reaction. Actual acid production and neutralisation release rates (Usher *et al.*, 2002) cannot be predicted with this technique, nor can the completeness of the reaction be assessed.
2. Acid-Base Accounting assumes that all acid production is attributable to iron disulphide minerals (chiefly pyrite) and that no acid is produced by sulphate or organic sulphur forms.
3. It only provides a possibility of occurrence.
4. Reaction rates are ignored (ABA generally tests the fast-reacting species; slow-reacting neutralising species will usually not prevent acidification).

5. Instant availability of reactive species is assumed. However, nearly all rock samples lacking or possessing carbonates (which are fast-reacting and thus instantly available) of dunite composition (predominantly olivine + serpentine) have insufficient NP to be classifiable as “not potentially acid generating” if the minimum limit for this category were to be set at, for example, 20 kg CaCO₃ equivalent/tons of material.
6. Size effects are ignored (Limestone particles of greater than 6.4 mm are coated with precipitates and are only 20% utilised when acid conditions are in evidence (Scharer *et al.*, 2000).
7. Extrapolation to the field is uncertain when volumetric calculations cannot be made.

The widespread use of static tests in AMD prediction has been justified on the basis of historical - and generally successful - applications to North American coalfields. Overall, the static test can be regarded as a first screening level for mine drainage prediction, which provides a very good indication of acid-generating potential. Most non-carbonate minerals can participate in the attenuation of acidity, but only to a modest degree, and only in the longer term, after an AMD scenario has already been developed (Usher *et al.*, 2002).

Since static tests involve only single analyses and the procedures are simple, they are rapid and relatively inexpensive. Thus, although the amount of information provided by kinetic tests exceeds that of static tests, the latter are much more widely used in terms of number. Usher *et al.*, (2002) cite several researchers who indicate the value of ABA as a legitimate tool for mine-drainage quality prediction across the world, including South Africa. It becomes a very powerful tool when used in conjunction with other data such as hydrologic data, mining and reclamation plans, and mineralogy data, as proposed in the ABATE strategy, and in the study specifically focused on ABA (Usher *et al.*, 2002).

7.1.3. Static Tests Used in this Study

The following methods were used for this study:

- Determination of reactive %S using hydrogen peroxide oxidation
- Neutralising potential using a sulphuric acid adaptation of the Sobek method (Sobek *et al.*, 1978)
- Calculation of acid-base accounting
- Determination of liberated elements during oxidation.

Mineralogy of each sample using X-ray Diffraction (XRD) and X-ray Florescence (XRF) determination.

7.2. Overview of ABA Data Types Obtained

In the procedure followed, the pH of the pulverised samples is measured in water (start or initial pH), and after complete oxidation (final pH) (Table 6). This is the first indicator of the overall behaviour of the sample. High-risk acid generators are samples which turn acidic upon oxidation. These results are indicated in the tables below:

Table 6: Initial and Final pH and Interpretation

Site Name	Initial pH	Final pH	Interpretation
Sample 1	8.4	6.7	Lower Acid Risk
Sample 2	8.66	6.28	Lower Acid Risk

If the initial and final pH values (the pH of the sample after complete oxidation using hydrogen peroxide) are alkaline, then the sample will not be acid producing, but will have a potential to buffer acid. When the final pH turns acidic, the acid-generating processes consume all the available neutralisation in the sample upon oxidation. Under these conditions, the sample is net acid producing. With an initial pH that is already acidic, this means that the sample has already undergone oxidation in the field, resulting in acid mine drainage. The initial and final pH values are plotted together with the overall difference between the acid potential and neutralisation potential in kg/tonne (NNP). Conventionally, CaCO_3 rather than H_2SO_4 is used to express acid or neutralisation potential. If the NNP value is negative, there is no neutralisation potential and acid generation will take place, and vice versa. The determined pH values, together with the NNP (whether open or closed) indicate a similar scenario, as shown in Figure 39.

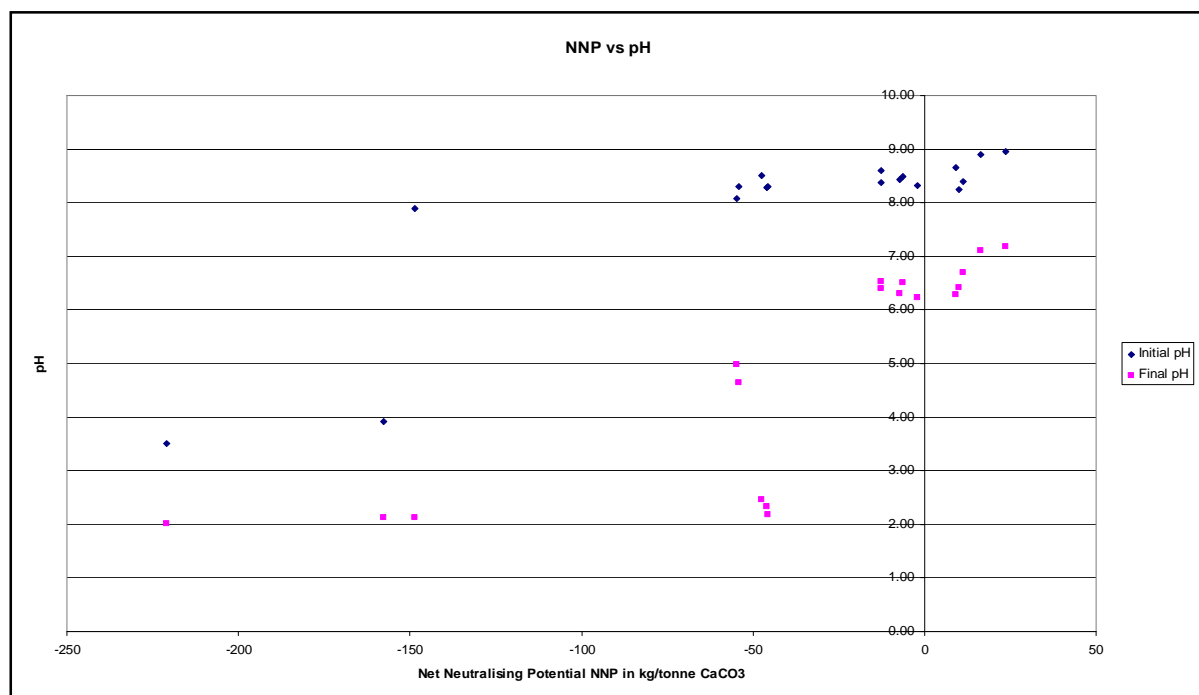


Figure 39: NNP vs. pH (initial and final) (closed system).

To the far left on the graph, the samples are already oxidised in the field and have a high acid potential. Closer to values of -50 NNP on the graph, samples have an alkaline initial pH, which will become acidic upon oxidation, but will not produce as much acid as the first. On the positive side, the final pH did not become acidic upon oxidation. These samples contain a neutralisation potential with a lower likelihood of producing AMD.

It is important to differentiate between so-called “open” and “closed” systems. The carbonate system is predominant in controlling the buffering intensity and neutralising capacity of natural waters, and represents a complex system that involves the transfer of carbon among three phases: solid, liquid and gas. When $\text{CO}_{2(g)}$ comes into contact with water, it will dissolve and form carbonic acid (H_2CO_3) until equilibrium is reached. Depending on the pH of the solution, the carbonic acid will dissociate to hydrogen, bicarbonate (HCO_3^-) and carbonate (CO_3^{2-}) ions.

7.2.1. In an Open System

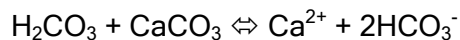
$\text{FeS}_2 + 2\text{CaCO}_3 + 3, 75\text{O}_2 + 1.5\text{H}_2\text{O} \Leftrightarrow \text{Fe}(\text{OH})_3 + 2\text{SO}_4^{2-} + 2\text{Ca}^{2+} + 2\text{CO}_2$ (carbon dioxide exsolves into the atmosphere).

Acidity produced from 1 mole of FeS_2 (64 g sulphur) is neutralised by 2 moles of CaCO_3 (200 g) or 1 g sulphur: 3.125 g CaCO_3 (Brady *et al.*, 1994).

7.2.2. In a Closed System

$\text{FeS}_2 + 2\text{CaCO}_3 + 3, 75\text{O}_2 + 3, 5\text{H}_2\text{O} \Leftrightarrow \text{Fe}(\text{OH})_3 + 2\text{SO}_4^{2-} + 2\text{Ca}^{2+} + 2\text{H}_2\text{CO}_3$ (carbon dioxide dissolve in water)

H_2CO_3 reacts with carbonate in the following reaction:



A second reaction depicting the maximum calcium carbonate requirements for acid neutralisation in a closed system may therefore be written as:

$\text{FeS}_2 + 4\text{CaCO}_3 + 3, 75\text{O}_2 + 3, 5\text{H}_2\text{O} \Leftrightarrow \text{Fe}(\text{OH})_3 + 2\text{SO}_4^{2-} + 4\text{Ca}^{2+} + 4\text{HCO}_3^-$ (Usher *et al.*, 2001).

In this reaction, 1 mole of FeS_2 is neutralised by 4 moles of CaCO_3 , which results in a mass ratio of 1 g pyrite: 6.25 g calcite. It is therefore very important that the correct conceptual model be applied when interpreting the results.

7.3. Calculated Parameters from ABA

Based on the above tests, the following parameters can be calculated:

Net Neutralising Potential (NNP) = Neutralising Potential (kg/t CaCO₃) - Acid-Generating Potential (kg/t CaCO₃), and Neutralising Potential Ratio (NPR) = NP/AP.

The results for these determinations are given in Table 7.

Table 7: Calculated parameters from ABA

Sample number	Net NP (Open system)	Net NP (closed system)	NP ratio (NPR) NP/AP for open system	NP ratio (NPR) NP/AP for closed system
Sample 1	21.185	11.259	3.13	1.57
Sample 2	21.978	9.245	2.73	1.36

The table indicates that a differentiation exists between open and closed systems. The open system is indicative of the waste rock piles, while the tailings will have areas that vary between open and closed conditions. Negative values indicate insufficient neutralisation potential and a potential for acid production, and vice versa.

7.4. Interpretation of Results

7.4.1. Screening Criteria

Details of the screening criteria for each type of test are given in publications such as Price and Errington (1995) and summarised in Usher *et al.*, (2001).

The most important criteria are as follows:

For NNP

- If $NNP = NP - AP < 0$ The sample has the potential to generate acid, and
- If $NNP = NP - AP > 0$ The sample has the potential to neutralise produced acid.
- More specifically, any sample with $NNP < 20$ is potentially acid generating, and any sample with $NNP > -20$ might not generate acid.

There is a strongly defined “grey area” between -20 and = 20 kg/t CaCO₃, since the nature of static testing and the field variability makes it risky to assign potentially acid- or non-acid generating properties to such samples.

For NPR, the following guidelines are used for the classification of samples (Table 8).

Table 8: Guidelines for ABA screening criteria (from Price et al., 1997b)

ARD POTENTIAL	NPR SCREENING CRITERIA	COMMENTS
Likely	<1:1	Likely AMD generating
Possibly	1:1 - 2:1	Possibly AMD generating if NP is insufficiently reactive or depleted at a faster rate than sulphides
Low	2:1 - 4:1	Not potentially AMD generating unless significant preferential exposure of sulphides along fracture planes, or extremely reactive sulphides in combination with insufficiently reactive NP
None	>4:1	No further AMD testing required unless materials are to be used as a source of alkalinity

7.4.1.1. Interpretation of Individual Samples

Table 9 and Table 10 provide an interpretation of selected samples, based purely on screening criteria.

Table 9: Interpretation of each sample according to NNP criteria.

Site Name	NNP (Open)	NNP (Closed)	Interpretation
Sample 1	21.18	11.26	Verify with other tests
Sample 2	21.98	9.25	Verify with other tests

Table 10: Interpretation of each sample according to NPR criteria.

Site Name	NP Ratio(NP/AP) for Open System	NP Ratio(NP/AP) for Closed System	Interpretation Open System	Interpretation Closed System
Sample 1	3.13	1.57	Acid under certain conditions	Acid under certain conditions
Sample 2	2.73	1.36	Acid under certain conditions	Acid under certain conditions

7.4.1.2. Interpretive Diagrams

As an initial step in the interpretation of these data, interpretive diagrams will be used. There is an internationally recognised zone of uncertainty, where values should be interpreted with circumspection of NNP values between -20 to 20 kg/t CaCO₃. Figure 40 shows the subdivision according to the ratio between AP and NP (NPR). This diagram for all the Waterberg samples indicates that, for the bulk of the samples, there is the potential for acid production for those plotting above the red and blue lines. An alternative way to indicate the results are shown in Figure 41. Most of the samples have sufficient sulphide to yield long-term acidity (most samples contain more than 0.3 % S) (red area on the graph). This implies that, although some neutralisation potential is possible according to international findings, acid mine drainage will be produced. It is therefore clear that the majority of samples can be regarded as acid producers, and that the ABA results should be interpreted in conjunction with the on-site conditions, leaching rate and long-term conceptual models.

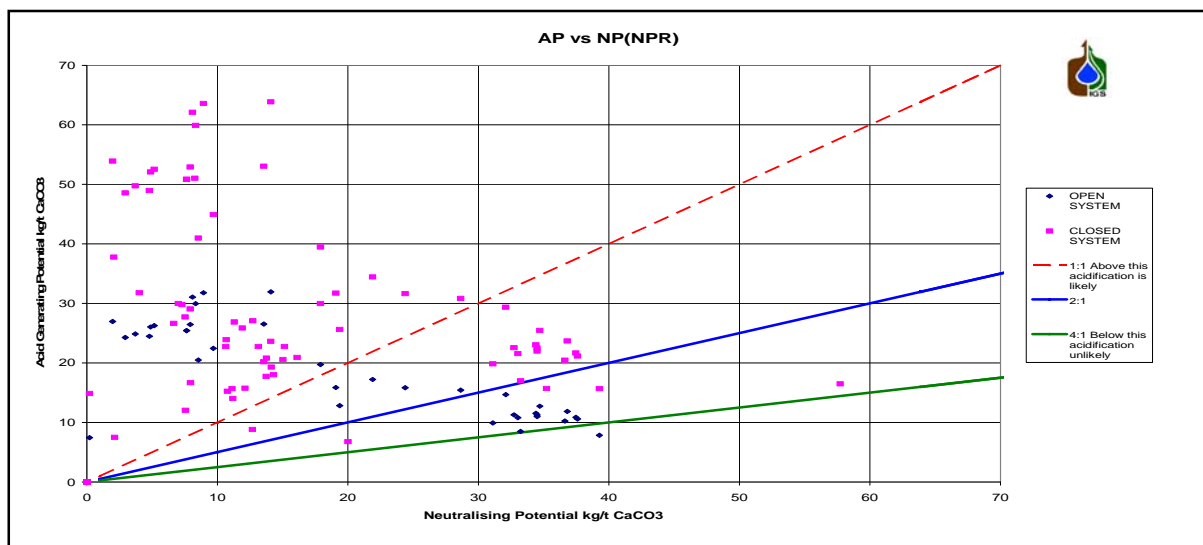


Figure 40: NP vs. AP graph, indicating areas of likely and unlikely acid generation.

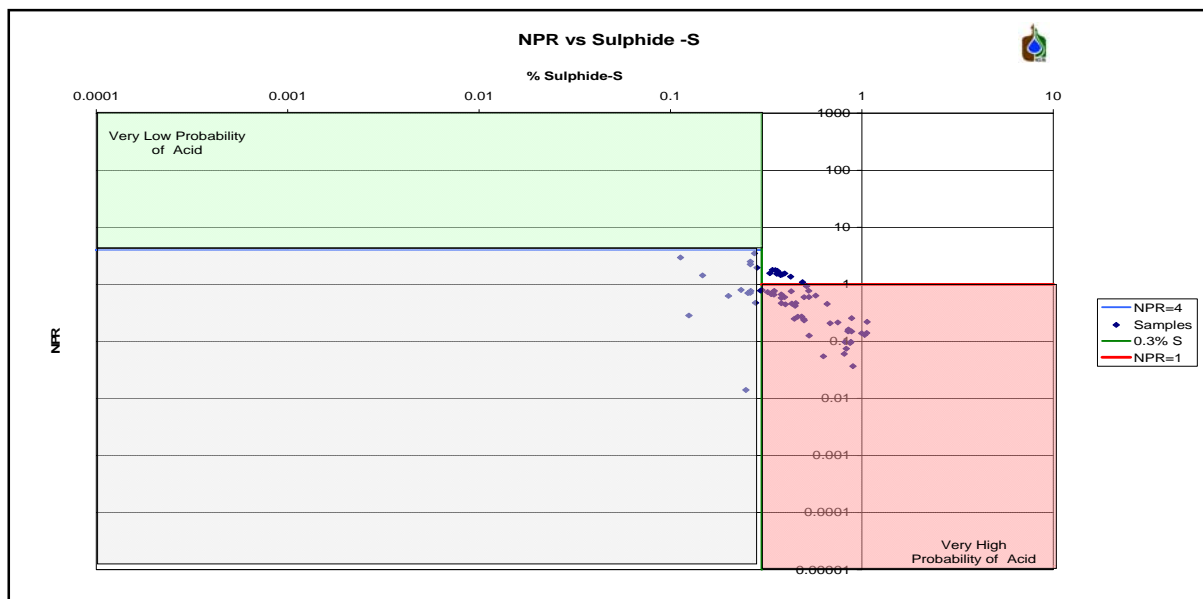


Figure 41: %S vs. NPR.

7.5. Results for the Waterberg Samples

Chip and core samples were obtained from the existing colliery and core samples were obtained from a second company at present prospecting in the study area. The samples were subjected to static ABA testing to determine acid- or base-generating potential and analysed by means of x-ray diffraction to obtain their mineral composition.

7.5.1. Acid-Base Accounting

A summary of the static acid base results is displayed in the following graphs. The graphs indicate that both base potential and acid mine drainage potential exist for samples from the Waterberg area.

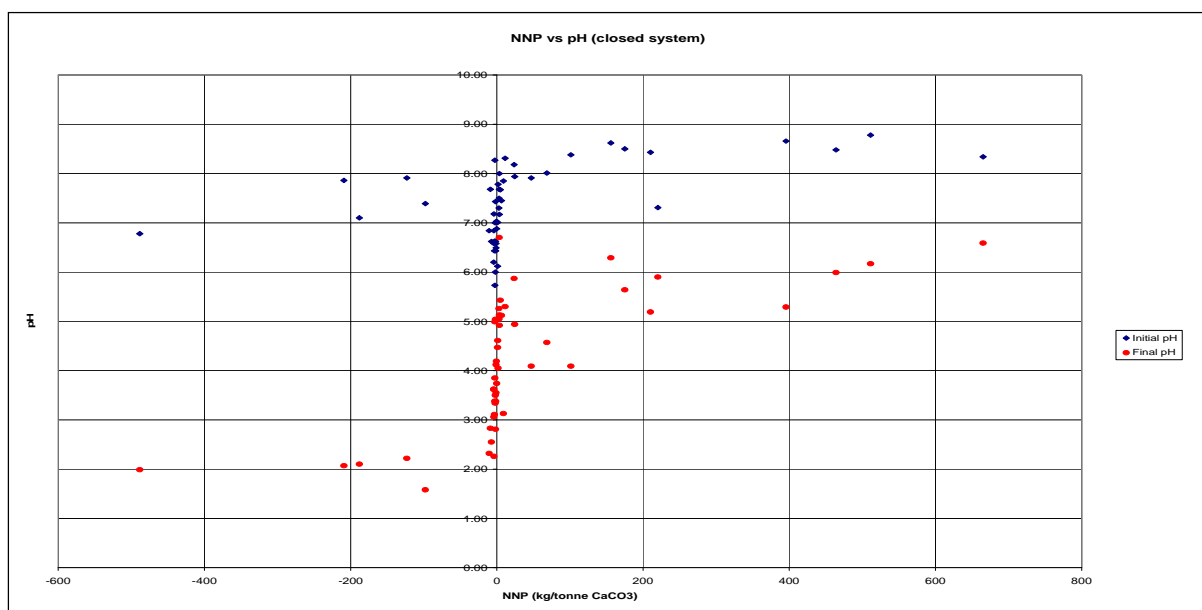


Figure 42: NNP vs. pH for all samples tested.

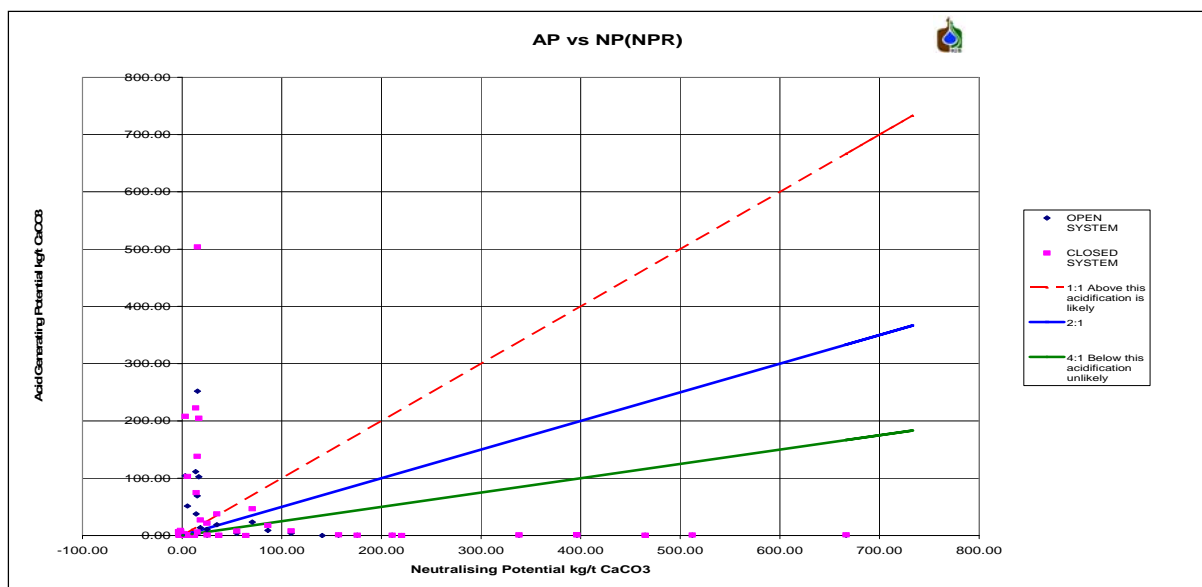


Figure 43: AP vs. NP for all samples tested.

7.5.2. Mineralogy

The XRD results indicate that Quartz and Ferroan Chlorite are the major components of the core & chip samples. Other minerals that are present include Calcite, Siderite, Ankerite, Goethite/Hematite, Illite and Pyrite. The northern chip samples contain dominant calcite.

Occurrence classification of the minerals is indicated as follows:

Table 11: XRD classification table.

Dominant	XX	>40%
Major	X	15-40%
Minor	xx	5-15%
Accessory	x	2-5%
Rare	<x	<2%

7.5.3. Weathering Zones

The study area was divided into three distinct zones with regards to sampling and weathering. The study area comprises areas that:

- Have the full succession present, (green areas)
- Areas that have been weathered down to the middle Ecce and (yellow areas)
- Areas that have been only weathered in parts (red areas).

This division governed the selection of sampling locations in an effort to identify trends with regards to weathering level and the degree of acid/base potential. The study area was further divided into sampling locations in the northwest, the north and to the south east.

The ABA results for each of these areas will be discussed separately and then compared.

7.6. Full Coal Succession Areas (Green Areas)

7.6.1. North western Samples

Core samples were collected from one borehole located in the north western sampling location as indicated in Figure 44. The core was divided into 20 representative samples spanning the length of the core (some 200 m). Some of these samples indicate a high risk of acid generation, with the final pH values becoming acidic upon complete oxidation, while others indicate a lower risk. The net neutralising potential for both closed and open systems is summarised in Tables 31 & 32 of Appendix A. The negative values indicate acid mine production while the positive values indicate neutralising potential.

The NNP (for a closed system) and pH values from the above mentioned tables are plotted in Figure 45 & Figure 46, indicating a mixture of acid producers, as well as some with neutralising capabilities.

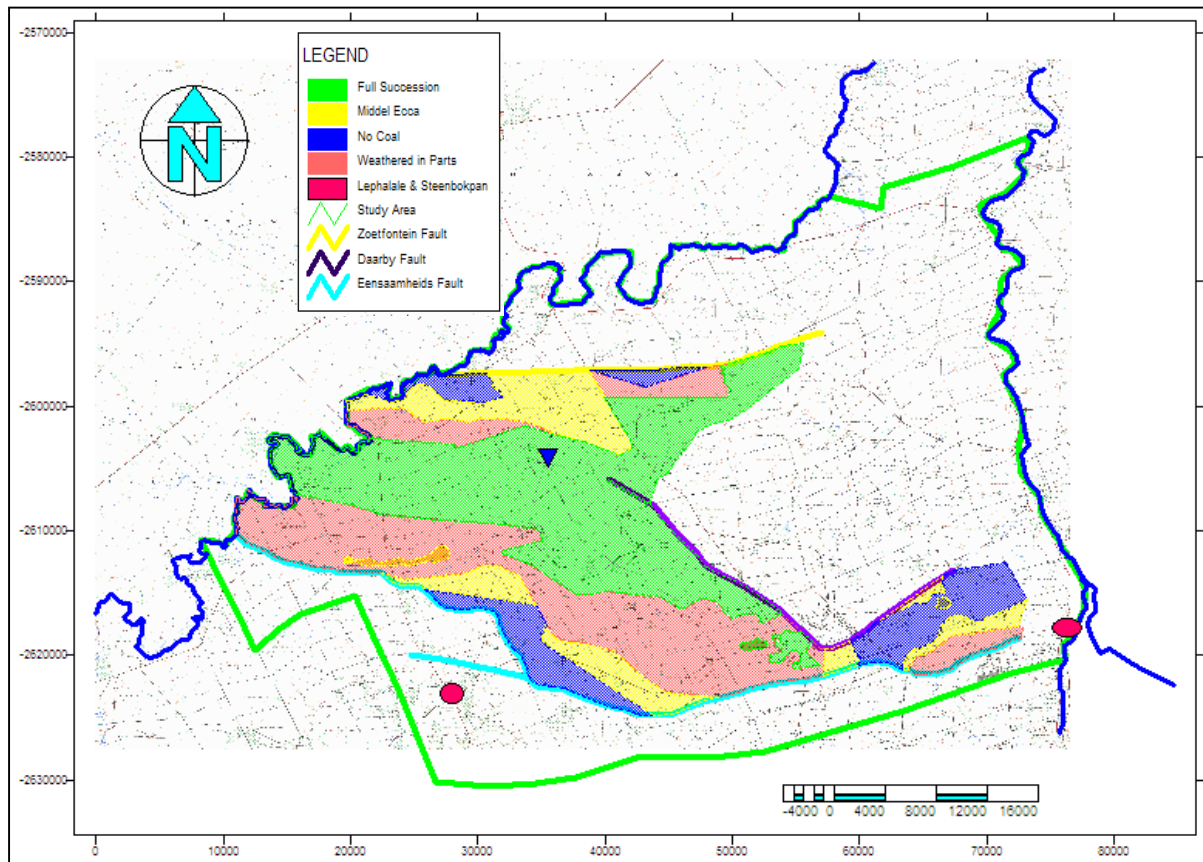


Figure 44: Borehole position of the north western sample.

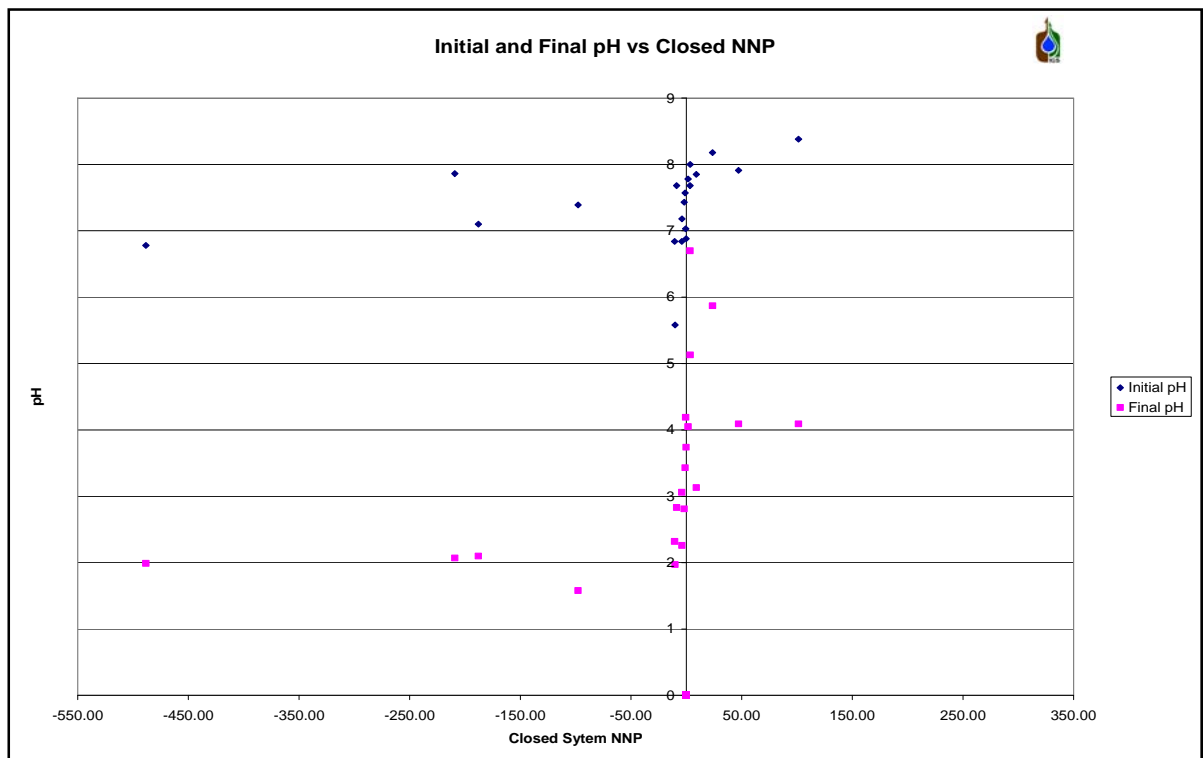


Figure 45: Net neutralizing potential (closed) vs. pH for north/western core.

The percentage sulphur in the samples plotted against the NPR also indicates a high risk of acid production, with some of the samples plotting in the red area. Other samples plot in the neutralising capacity region (green). The neutralising potential ratio for the North western samples can be seen in Table 33 of Appendix A. Those samples with values close to zero indicate no neutralising potential, while those with values greater than four indicates no acid potential. This is also indicated in Figure 47.

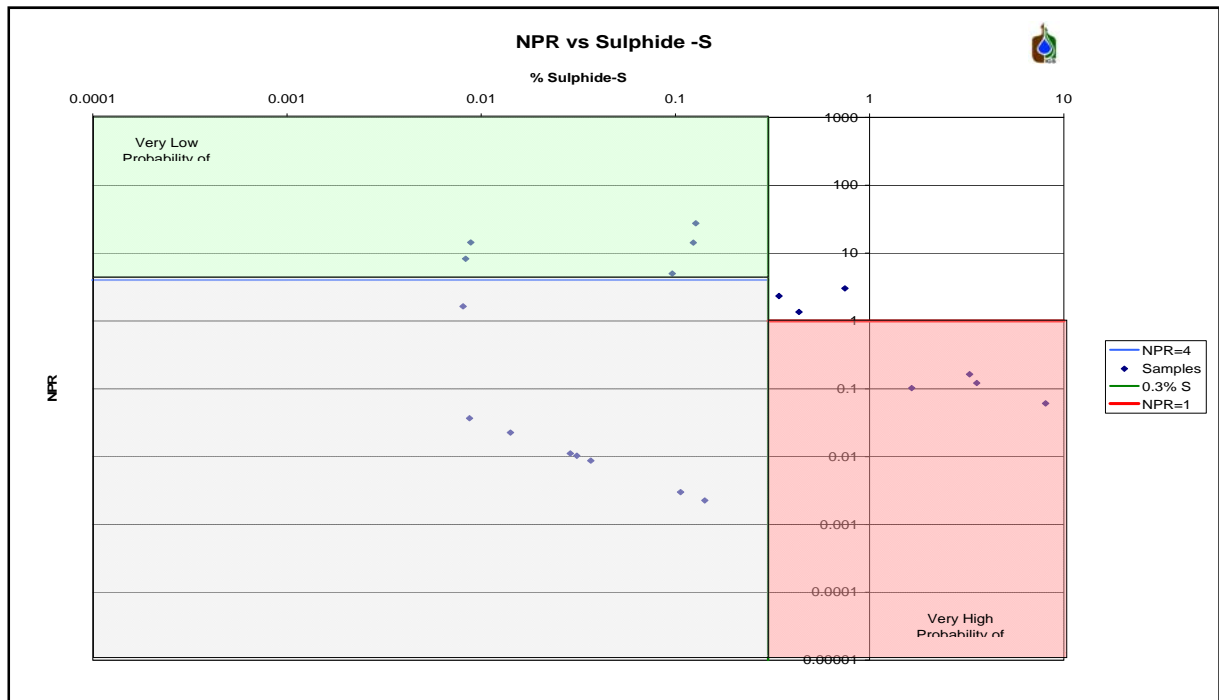


Figure 46: %S vs. NPR for the north/western core.

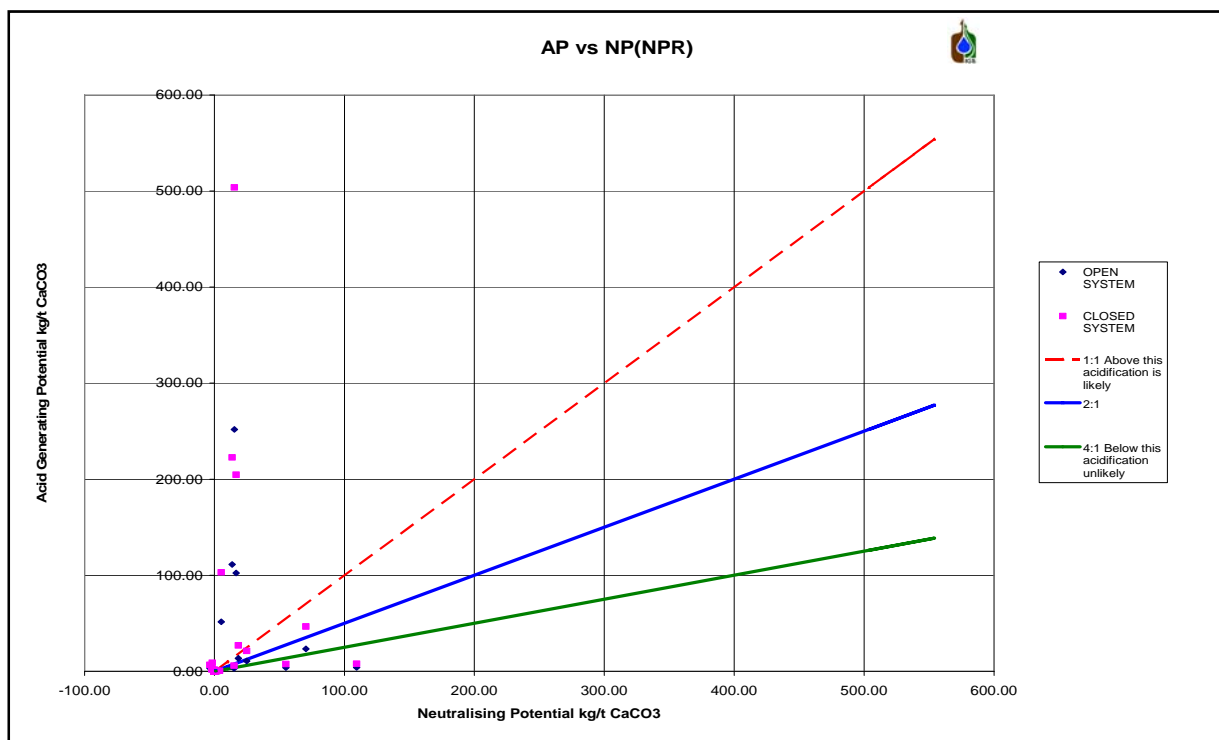
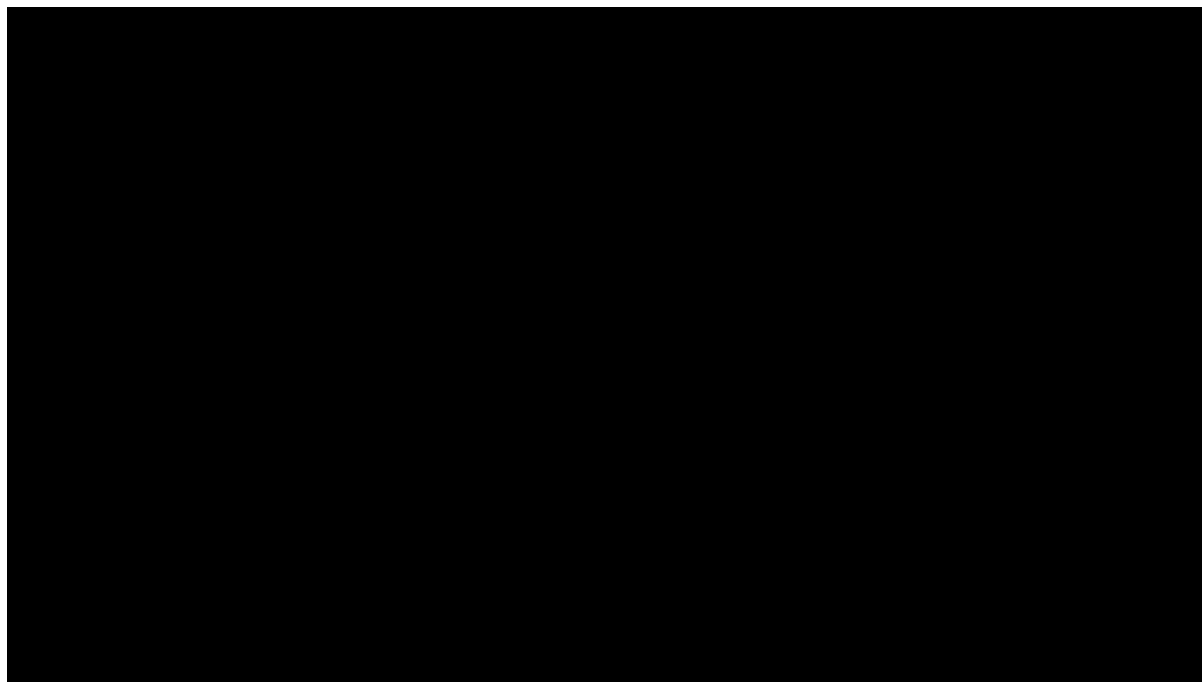


Figure 47: NP vs. NA (NPR) for the north/western samples.

The XRD analyses indicate the dominant mineral as quartz and Ferroan Chlinochlore (Table 12). The samples containing 2-10% calcite vary in terms of base potential. The three samples (SS7, 11 and 15) with 1-2 % pyrite have a high acid-generating potential.

Table 12: XRD results for the north western samples.



From the static tests conducted on the core samples from the north/western site in the Waterberg area, it is clear that acid mine drainage will be produced upon oxidation in some of the samples, although there is some buffering potential in some of the samples. The volume of production will depend on the thickness of the geological successions in the area.

7.6.2. South Eastern Samples

Samples were collected from boreholes as indicated on the map (Figure 48). Four core samples were collected from one borehole over a depth of 160 m (green area/full coal succession). One chip sample was collected from one other prospecting borehole (green area / full coal succession) and four additional samples from an area falling into the area which exhibits erosion in parts (red areas/weathered in parts). These different samples will be discussed as a whole as they were collected and analysed at the same time. Their differences will be discussed later in the report. Initial and final pH values are summarised in Table 34 of Appendix A. Some of these samples indicate a high risk of acid generation, with the final pH becoming acidic upon complete oxidation, while others indicate a lower risk. The NNP for both closed and open systems is summarised in Table 35 of Appendix A. The negative values indicate acid mine production, while the positive values indicate neutralising potential.

The NNP (for a closed system) and pH values from the above tables are plotted in Figure 49, indicating one major of acid producer (GGS2) and one with neutralising capabilities (GGS4).

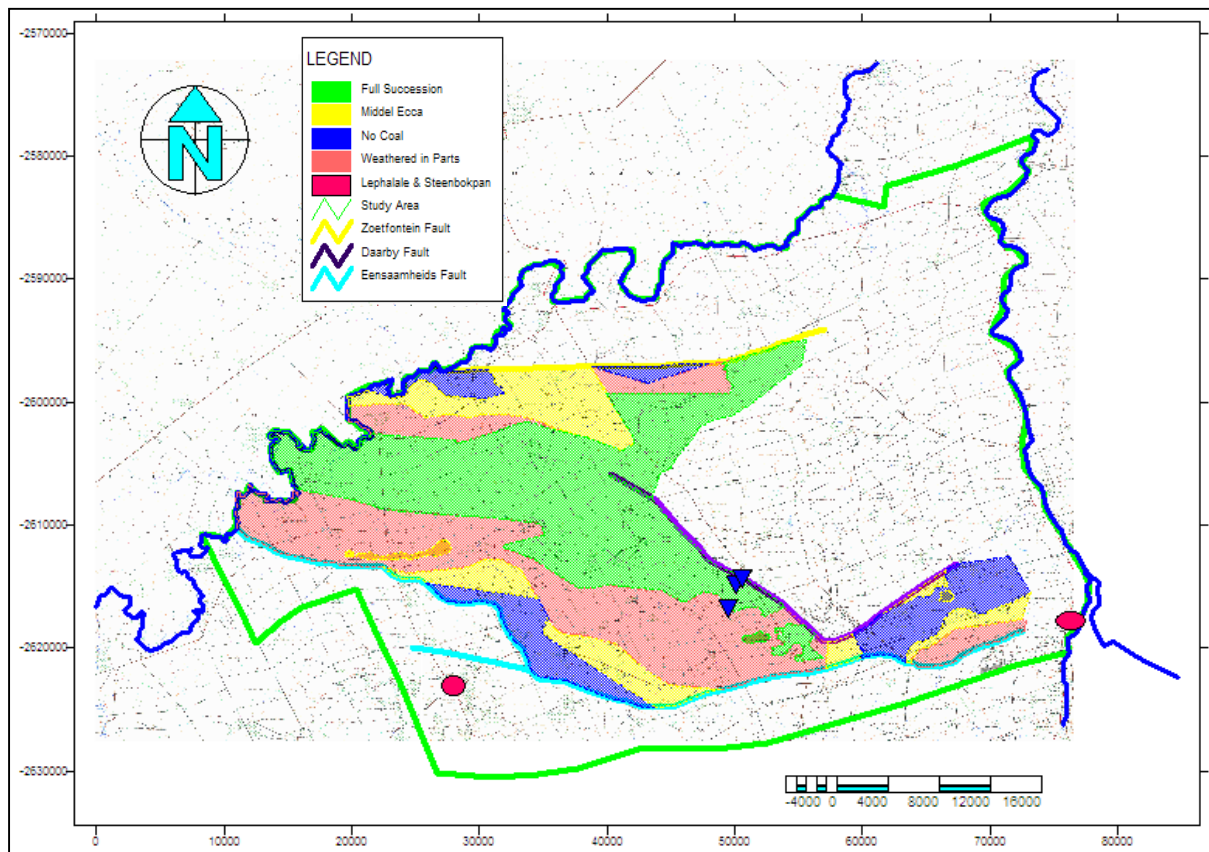


Figure 48: Borehole positions of the south eastern boreholes.

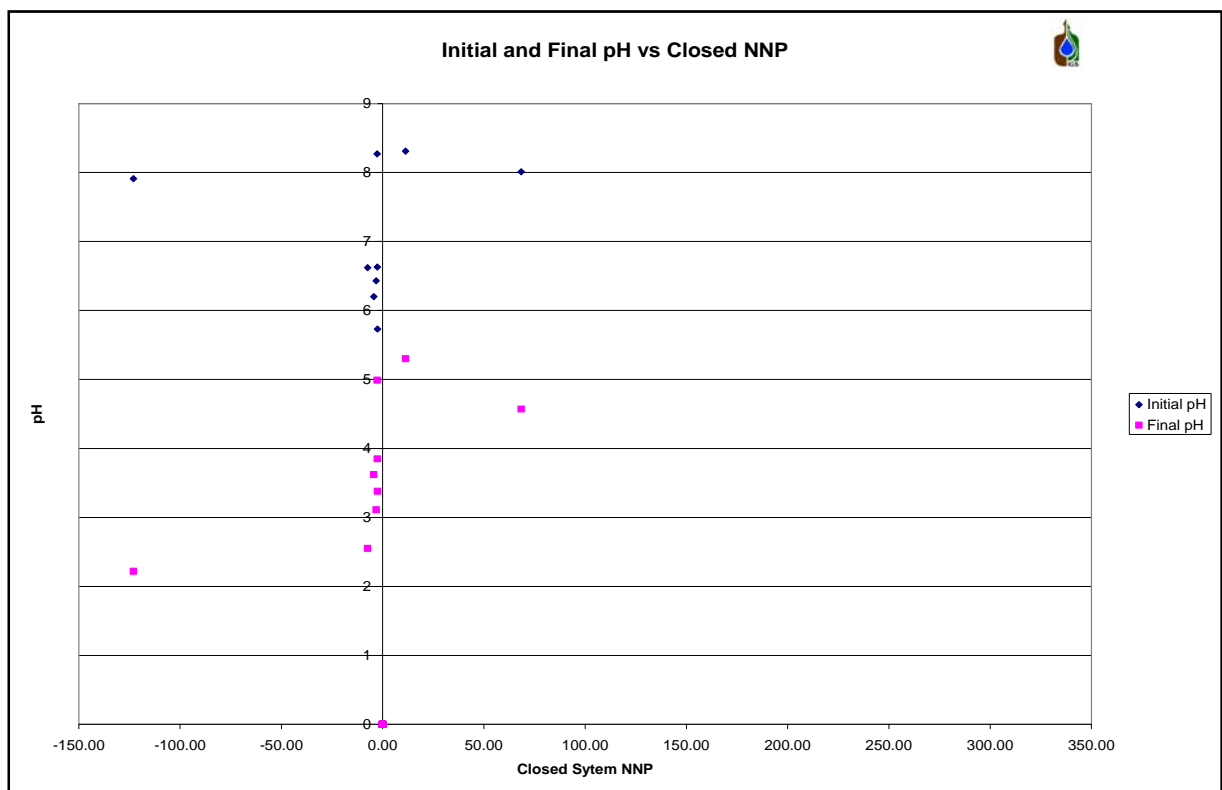


Figure 49: NNP (closed) vs. pH for south/eastern core.

The percentage sulphur in the samples plotted against the NPR also indicates a high risk of acid production, with the GGS2 sample plotting in the red area and GGS4 plotting in the neutralising capacity region (green) (Figure 50).

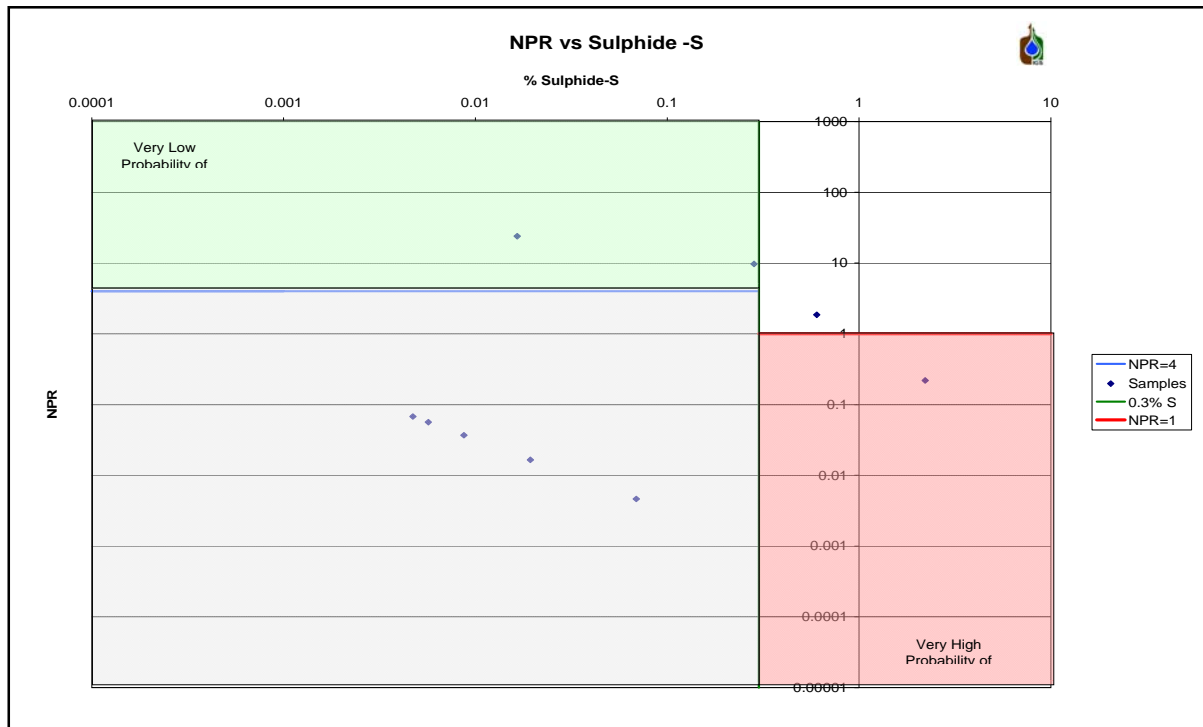


Figure 50: % S vs. NPR for the south/eastern core samples.

The NPR for the south eastern samples can be seen in Table 36 of Appendix A. Those samples with values close to zero indicate no NP, while those with values greater than four indicates no acid potential. This is also indicated in Figure 51.

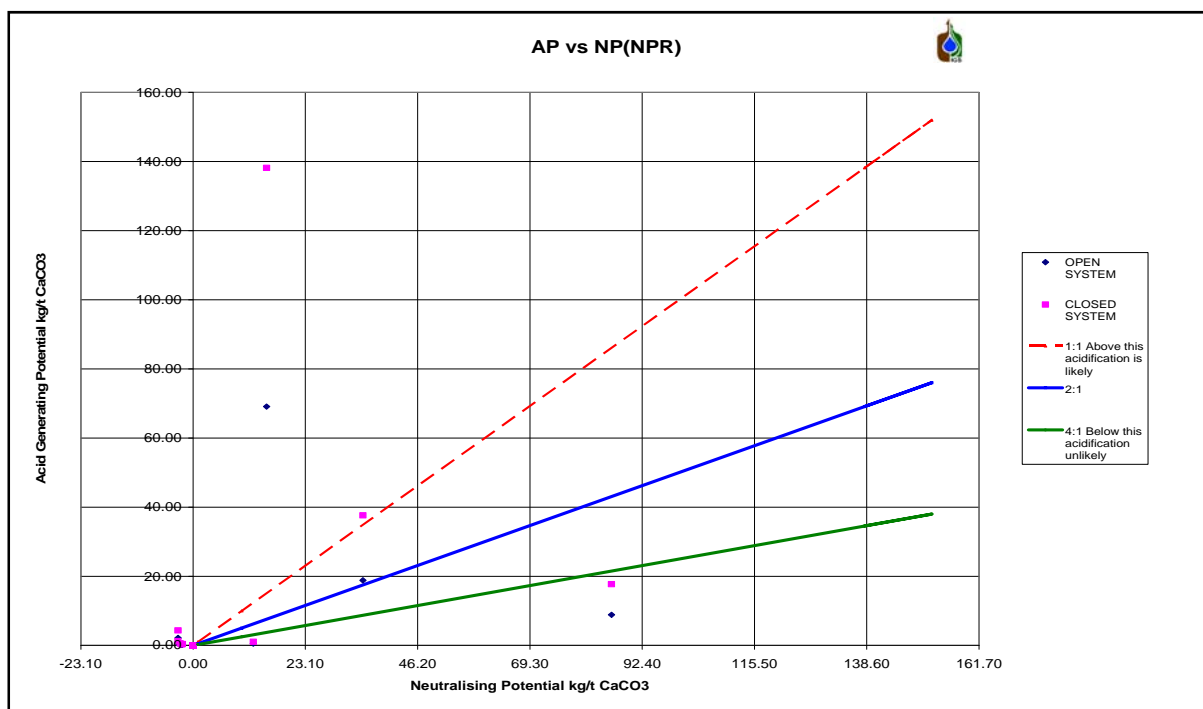
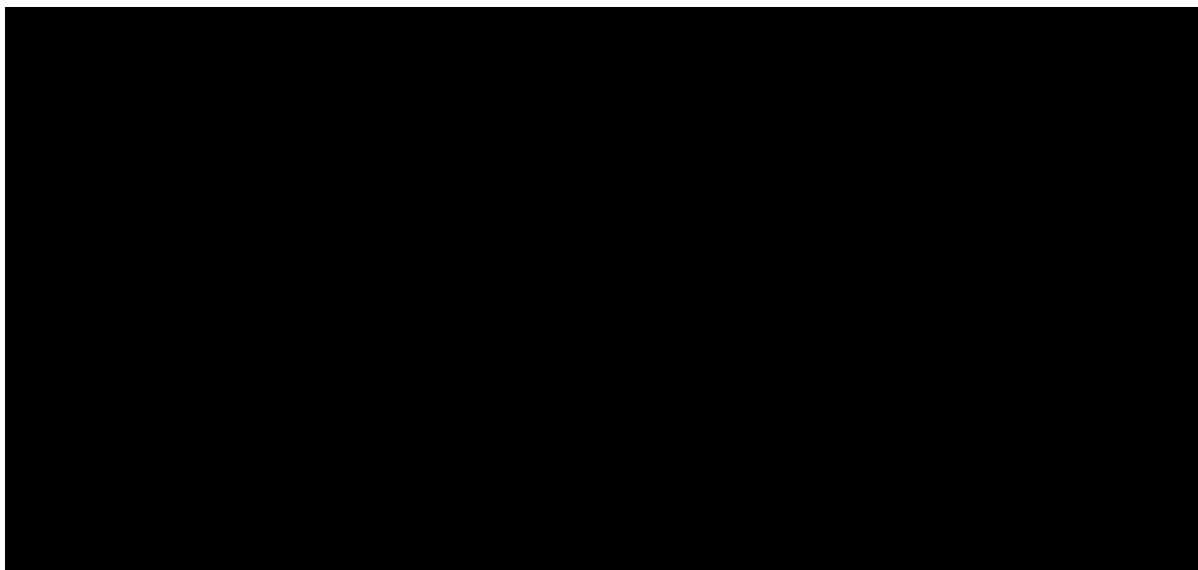


Figure 51: NP vs. NA (NPR) for the south/eastern samples.

The XRD analysis indicates the dominant mineral as quartz and Ferroan Chlinochlore (Table 13). The sample containing 2-10% calcite (GGS4) is the only one with a base potential. No pyrite could be identified in any of these samples.

Table 13: XRD results for the south/eastern core samples.



From the static tests conducted on the samples from the south eastern site surrounding the Grootegeluk mine, it is clear that acid mine drainage will be produced upon oxidation in some of the samples, although there is also some buffering potential in other samples. The volume of production will depend on the thickness of the geology over the area. As these samples were taken from the area surrounding the currently active mine, and fall into the same weathering grouping as the mine, it is concluded that the rocks which are to be used as backfill for the mine will generate acidity. The volumes generated will accordingly depend on the thickness of the rocks replaced in the pit.

7.7. Vryheid Formation Weathering (Yellow Areas)

Chip samples were collected from boreholes in the northern site, as indicated on the map (Figure 52). The samples were collected from five different prospecting boreholes on the farm Goedgedacht. The depths of the samples range from 1 m - 14 m below the surface. This area contains geology that has been eroded down to the Vryheid formation. Initial and final pH values are summarised in Table 37 of Appendix A. Some of these samples indicate a high risk of acid generation, with the final pH of these samples becoming acidic upon complete oxidation; some indicate a lower risk. The net neutralising potential for both closed and open systems is summarised in Table 38 of Appendix A. The negative values indicate acid mine production, while the positive values indicate neutralising potential. Most of the samples indicate a base potential. The table indicates that each site appears to have similar properties.

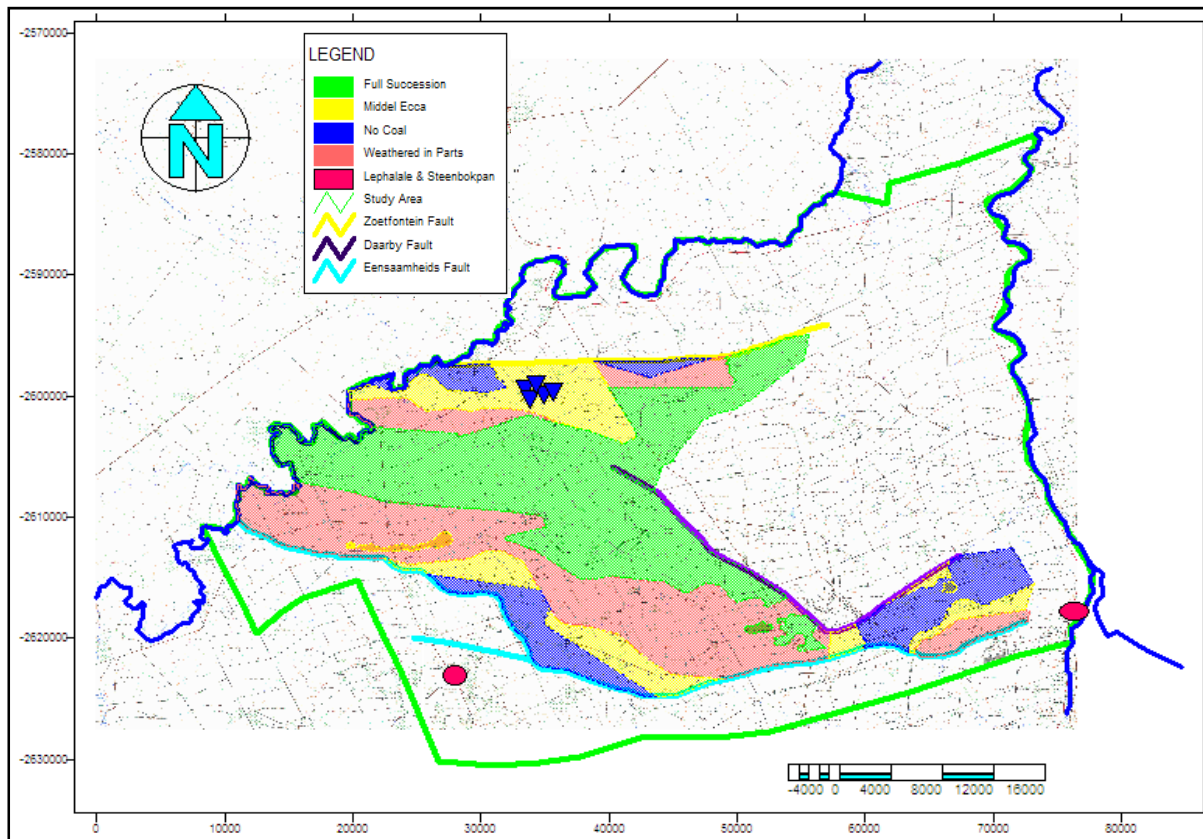


Figure 52: Positions of the chip sampling points.

The NNP (for a closed system) and pH values from the above-mentioned tables are plotted in Figure 53, indicating a neutralising capacity in most of the samples, with some just acidifying, although this is not a major concern regarding acid production.

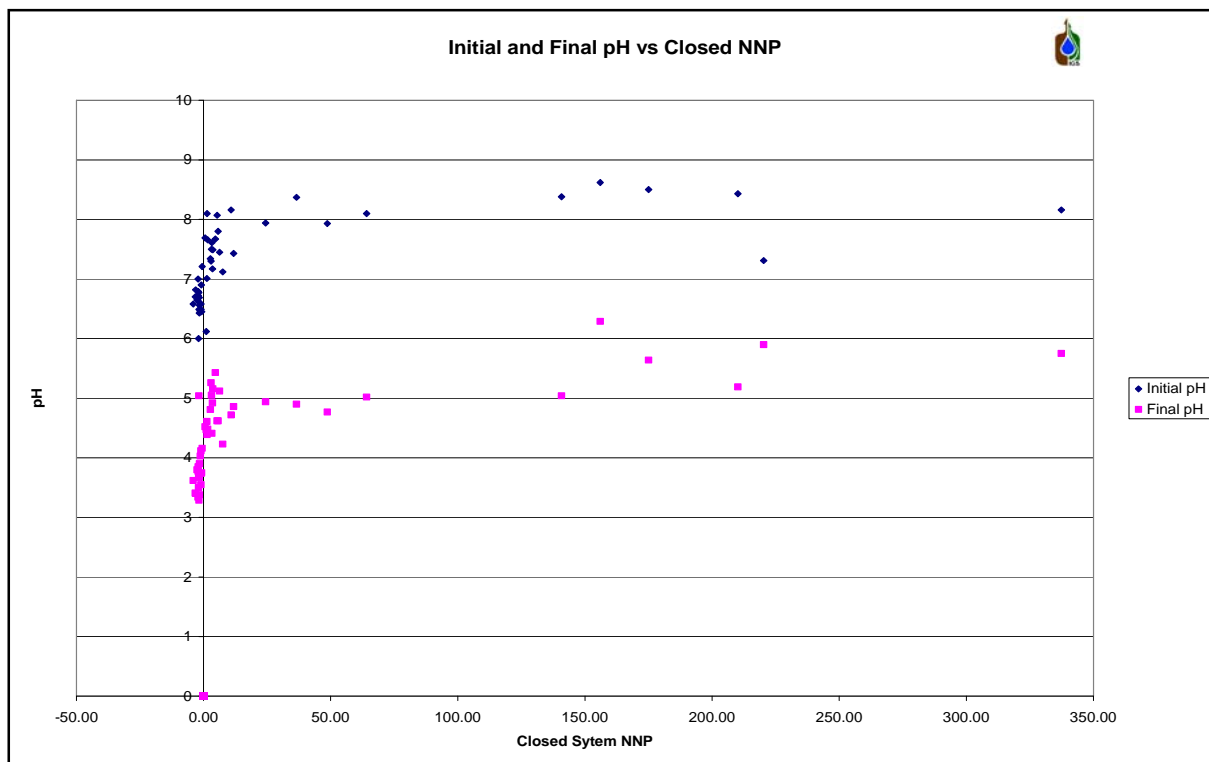


Figure 53: NNP (closed) vs. pH for northern chips samples.

The percentage sulphur in the samples plotted against the NPR also indicates a low risk of acid production, with no sample plotting in the red area and a batch plotting in the neutralising capacity region (green) (Figure 54).

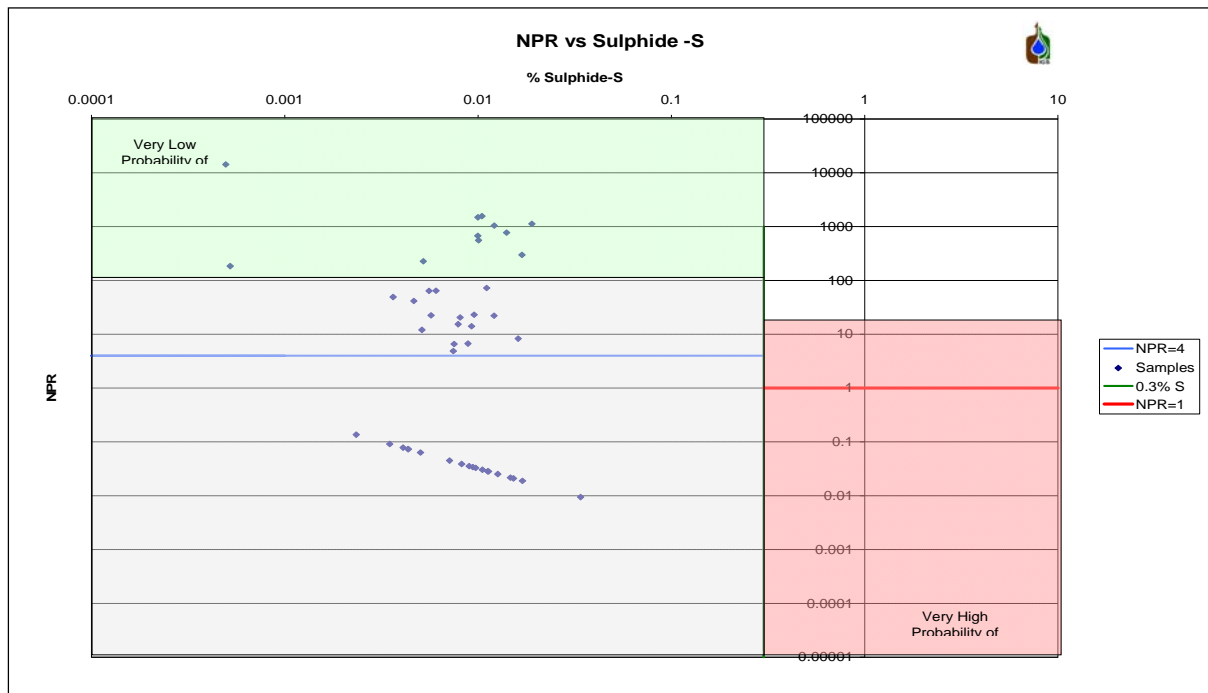


Figure 54: %S vs. NPR for the northern chip samples.

The neutralising potential ratio for the northern samples can be seen in Table 39 of Appendix A. Those samples with values close to zero indicate no neutralising potential, while those with values higher than four indicate no acid potential. This is also indicated in Table 39 of Appendix A, where it can be seen that most samples show an acid-neutralising capacity.

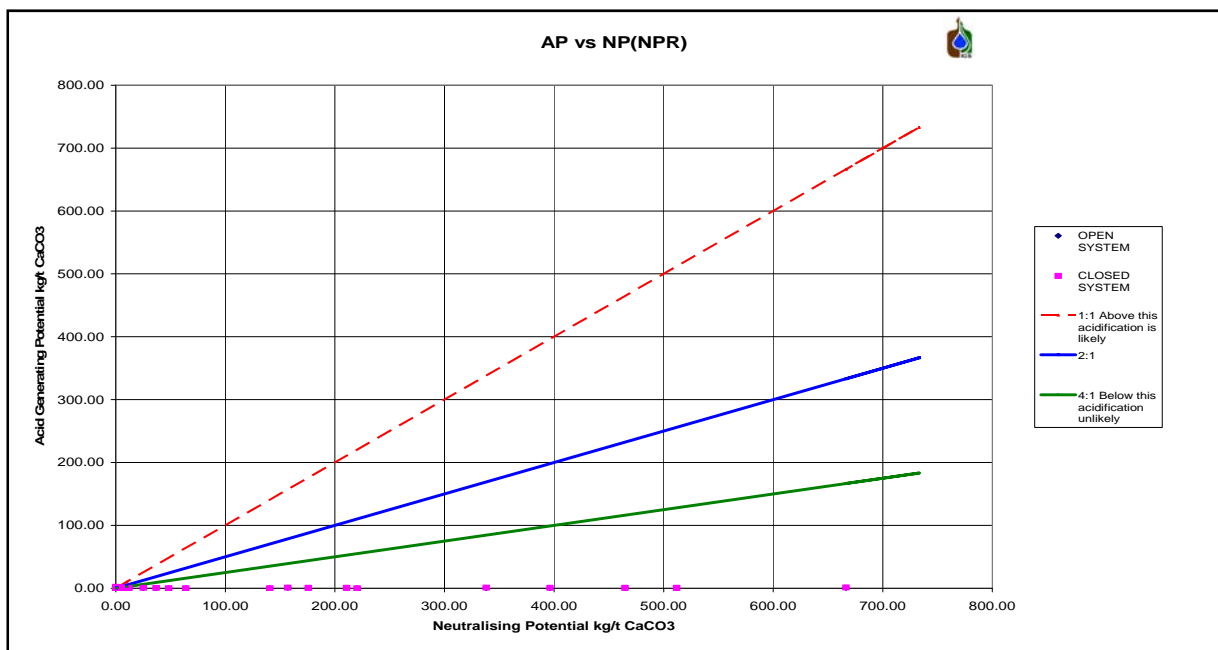
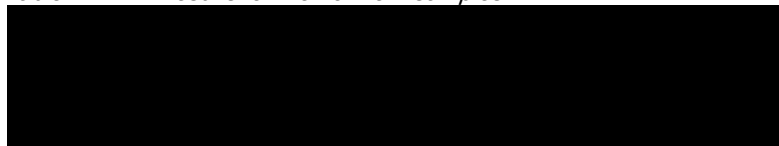


Figure 55: NP vs. NA (NPR) for the northern samples.

The XRD mineralogy indicates the dominant mineral of the GT2 range as calcite (Table 14). This mineral contributes to the neutralising potential of the sample.

Table 14: XRD results for the northern samples.



7.8. Sandstone Samples

A sample of sandstone located beneath Coal Zone 2 (the base of current mining operations) was collected for ABA analyses. The sample represents sandstone with a thickness of 60 m. The initial and final pH values are summarised in Table 40 of Appendix A. The sandstone sample indicates a risk of acid production after oxidation. The NNP for both closed and open systems is summarised in Table 41 of Appendix A. These values are around zero NNP, which will require confirmation through kinetic testing. The latter, however, does not fall within the scope of this project. The NNP (for a closed system) and pH values from the above-mentioned tables are plotted in Figure 56, and indicate that there is no major acid or neutralising capacity.

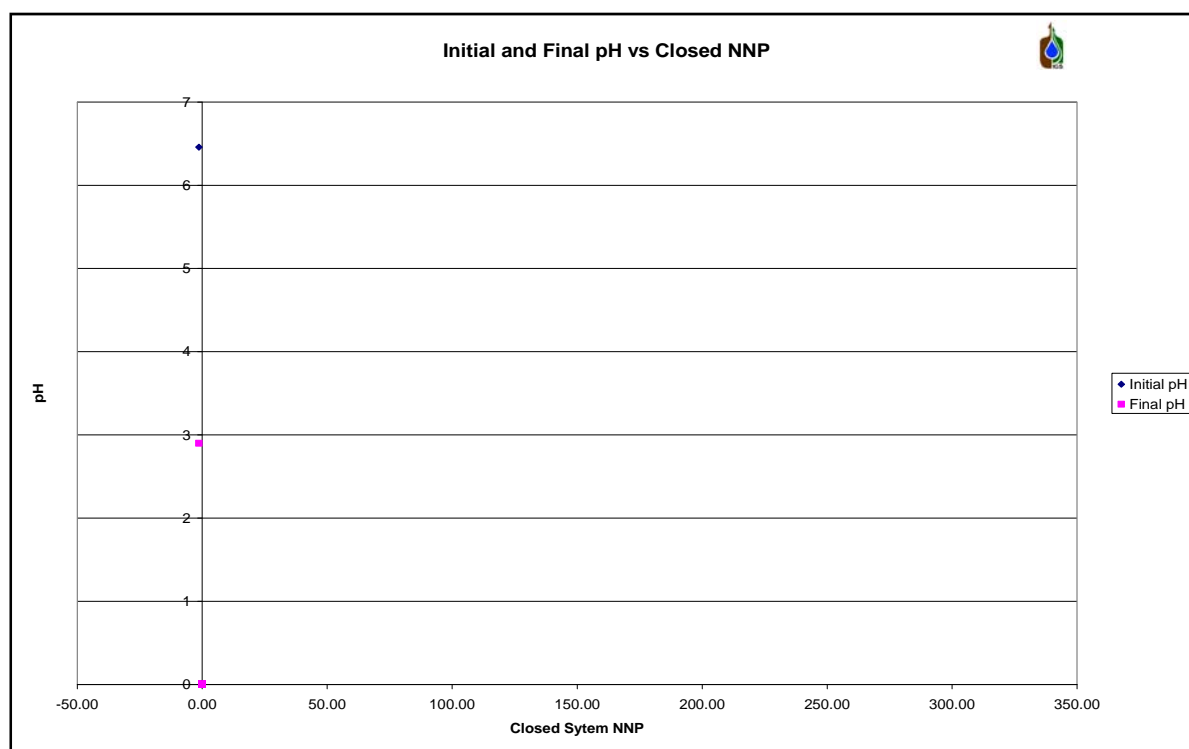


Figure 56: NNP (closed) vs. pH for Sandstone.

The percentage sulphur in the samples plotted against the NPR indicates a very low risk of acid production (Figure 57). The NPR for the samples can be seen in Table 42 of Appendix A.

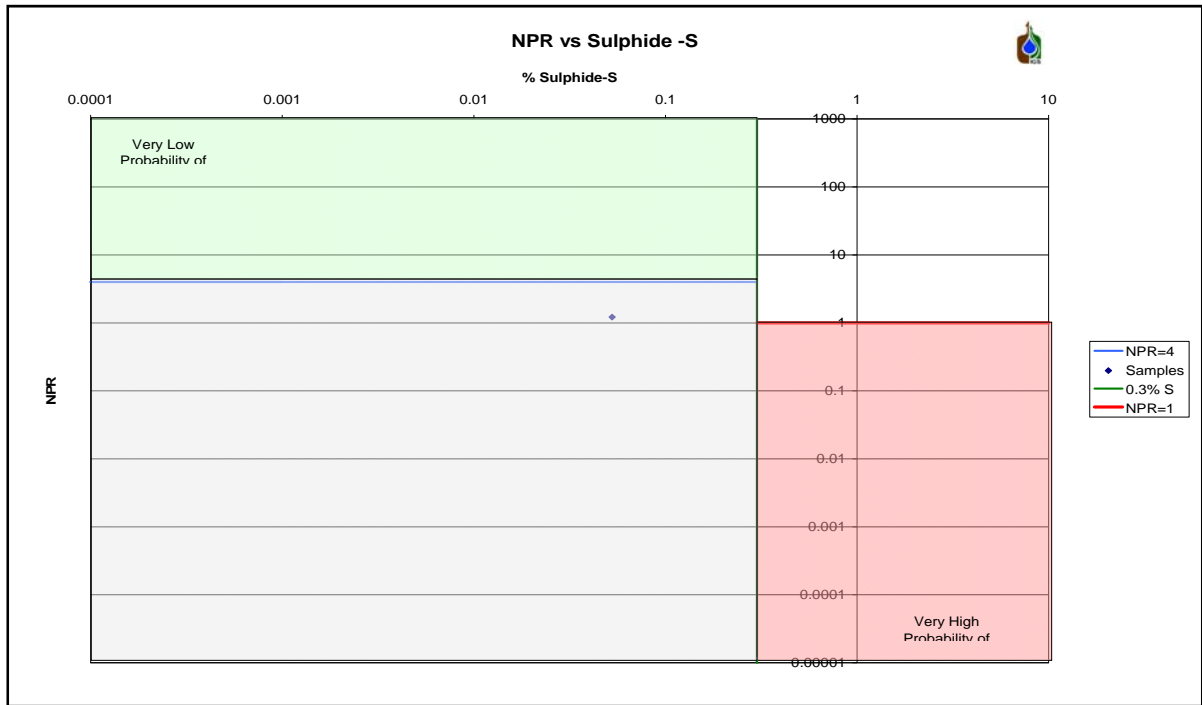


Figure 57: %S vs. NPR for the sandstone samples.

Those samples with values close to zero indicate no neutralising potential, while those with values >4 indicate no acid potential. This is also indicated in the NPR (NP/AP) graph (Figure 58).

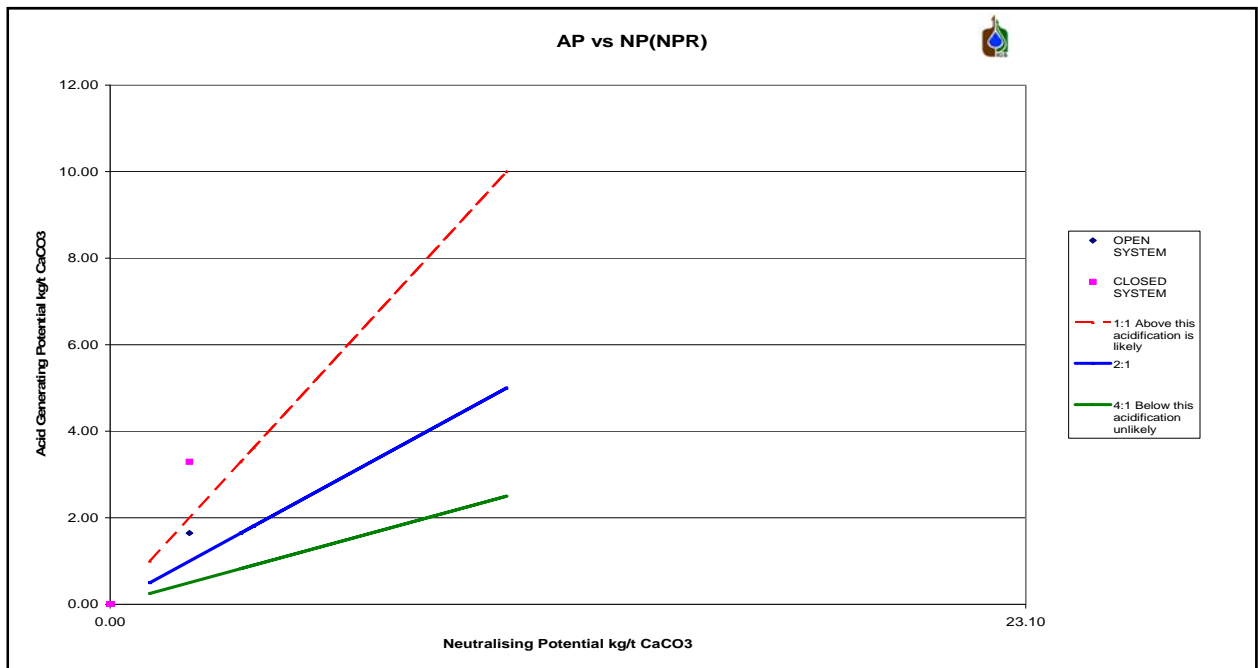


Figure 58: NP vs. NA (NPR) for the sandstone samples.

The mineralogy of the sandstone sample is not known, as no XRD analyses were conducted. From the static tests on the sandstone samples in the Waterberg area, it is clear that a small quantity of AMD will be produced per mass of the specimen.

7.9. Discard Samples

Two samples of discard material from the two beneficiation plants at the Grootegeluk mine were collected for ABA analyses. The samples collected were compiled over a period of time in order to obtain a better level of distribution in the sample. No XRD analyses were conducted on the samples. The initial and final pH values are summarised in Table 43 of Appendix A. This discard samples indicate a high risk of acid production after oxidation. The NNP for both closed and open systems is summarized in Table 44 of Appendix A. These values are negative, indicating a potential for acid generation. The NNP (for a closed system) and pH values from the above- mentioned tables are plotted in Figure 59, indicating that there is a high acid-producing potential.

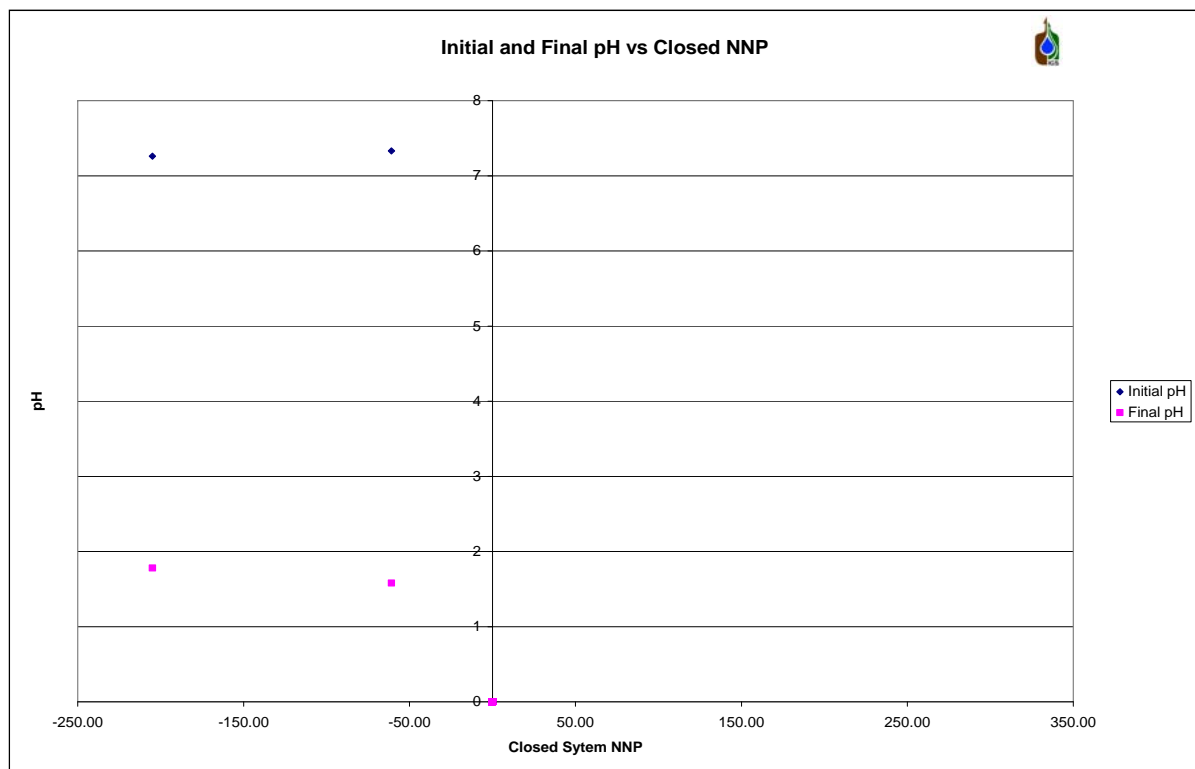


Figure 59: Net neutralizing potential (closed) vs. pH values for discard samples.

The percentage sulphur in the samples plotted against the NPR also indicates a high risk of acid production (plotting in the red area), with sulphur percentages of over 1% (Figure 60). The NPR for the discard samples can be seen in Table 45 of Appendix A. All the samples have an NP: AP ratio of less than one, indicating potential acid production.

From the static tests conducted on the discards from the Waterberg area, it is clear that acid will be produced upon oxidation of the samples. This has been observed in the field by Dreyer (pers. comm. 2009), who indicated that there is acidic effluent flowing out from the discard dumps at the Grootegeluk mine. Dreyer (pers. comm. 2009) stated that the volume of effluent was small and that many of the primary polluting components have been removed via burning of the discard dumps due to spontaneous combustion.

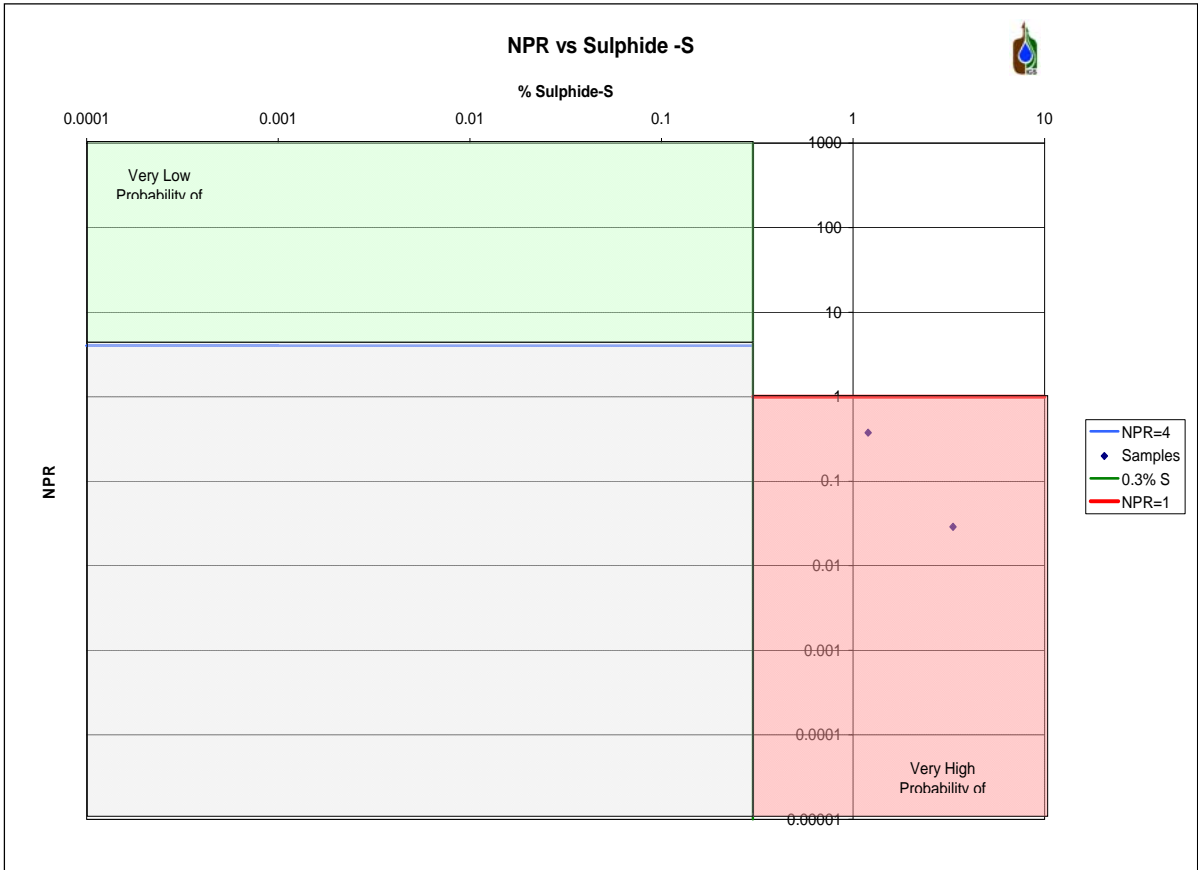


Figure 60: %S vs. NPR for the discard samples.

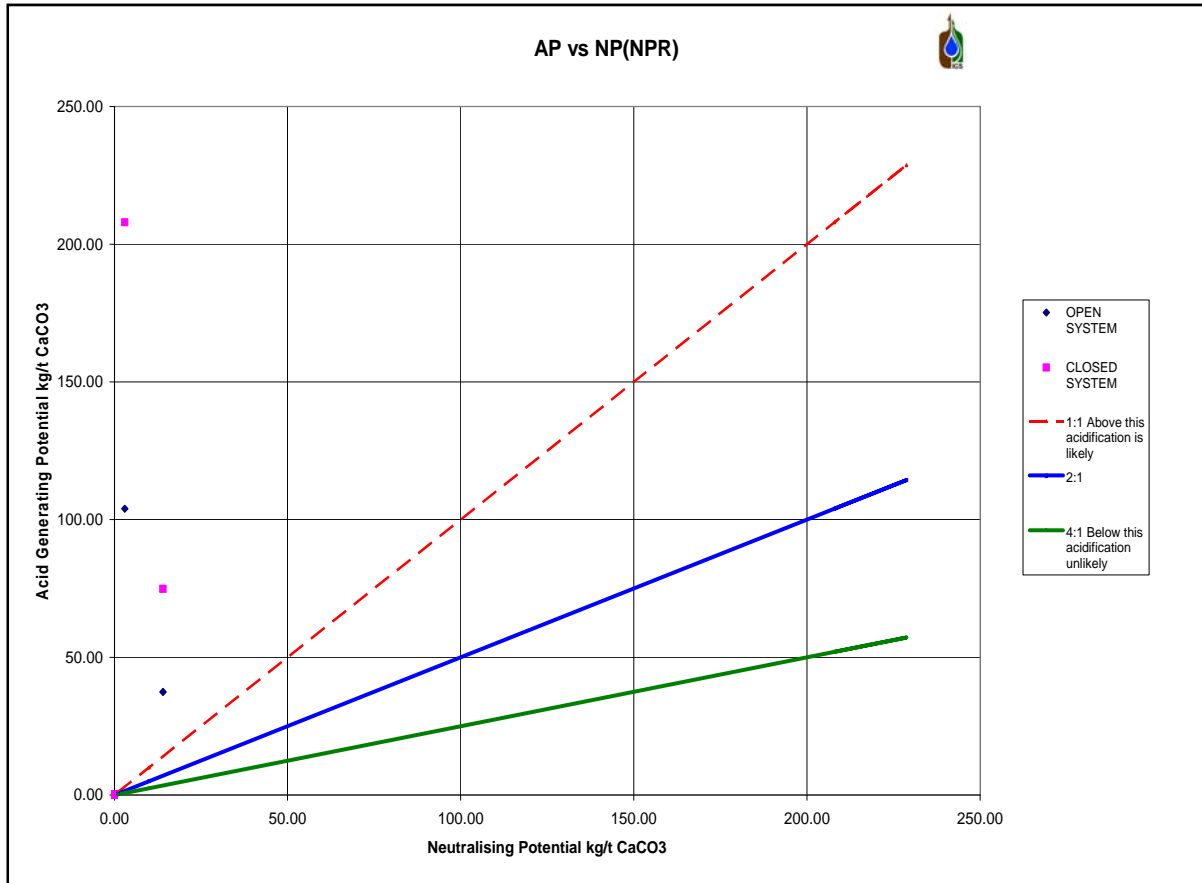


Figure 61: NP vs. NA (NPR) for the discard samples.

7.10. Discussion of Results

From the results of the ABA analyses one can conclude that, in most cases, there is sufficient neutralisation potential to account for any acid generated if a constant ratio is maintained (every ton of acid rock should be mixed with a ton of base-potential rocks). There are, however, some exceptions:

7.10.1. The North Western Samples

The analyses of the samples taken from the north western sampling location indicate that there is sufficient pyrite to generate acid. The data further indicates the existence of calcite to serve as a buffer which limits the amount of acid generated, depending on the thickness of the successions that contain the pyrite (in general, the pyrite exists in the form of disseminated deposits in the sandstones and in the coal). It is recommended that care be taken when handling the spoil. The current method used at the Grootegeluk mine, - whereby the rocks (geology) are replaced in the pit in the same successions as when they were removed - should be practised.

7.10.2. The Northern and South Eastern Samples

Four sets of samples were collected, and ABA analyses were conducted. It was found that the samples have the potential to generate acid, although they also contain buffer potential. Care should be exercised when re-depositing the spoil in the pit in these locations. Three other sets of samples were collected and analysed. The data for the samples from the farm Goedgedacht indicate that there is sufficient buffer potential in most cases to limit the level of acid production. The samples collected from the farm only represent the top 14m of the geological succession in the study area, and were collected from the weathered zone, in which a certain level of leaching had likely occurred.

It is therefore recommended that more detailed work be done and that ABA be conducted on core samples at greater depth. The third set of samples collected and analysed includes a sandstone sample from beneath the second coal seam. This sandstone indicates the lowest level to which opencast mining in the study area will take place. The ABA analyses of these samples indicate that some acid will be generated for any given mass of the sandstone. The sandstone will not be removed in the near future, accordingly it is recommended that sandstones be placed near the bottom of the pits to reduce or limit the potential for acid generation.

A best-practice scenario would be to place the sandstone beneath the water table, followed by an attempt to flood the sandstone as soon as possible in order to substantially reduce the potential for acid generation. This will however not be possible in the study area due to the low volumes of water available, both from groundwater and surface-water sources.

It is therefore recommended that the sandstone be placed at a higher level in order to keep it “dry” and thus minimising the potential for acid generation. The final set of samples collected for analyses includes two samples of discard generated by the processing plants at the Grootegeluk mine. These samples were analysed by static ABA methods. It was found that the samples had a high acid generation potential, and if oxidised, the samples would produce acid. It is recommended that the same steps be taken as those relating to the sandstone. The discard should be placed above the water table in order to keep the discard “dry” and thus minimise the generation of acid. It is furthermore recommended that the discard not be mixed with other rocks, unless these have a high base potential.

7.11. Comparison of ABA Results to Weathering Depth

It was decided that a comparison between the depth of weathering and the results from the ABA analyses be conducted in an effort to identify any patterns of potential problem layers that are prone to acid generation. Accordingly, the study area was divided into three areas with regards to weathering (Figure 62). From the map, the areas indicated in green contain the full succession of geology and all the coal seams. The area in yellow indicates areas that have been eroded down to the middle Ecca geology with some of the coal-containing strata missing. The area in red includes areas that have been badly eroded, with much of the coal succession removed.

7.11.1. The Green Areas (N/W & S/E Sampling Locations)

The samples from the green areas on the map (Figure 62) indicate that there is a general increase in the potential to generate acid up to a depth of roughly 80m below surface. From this point, the acid potential begins to diminish as the neutralisation potential increases, with the deepest samples having very little acid-generating potential. Both core samples collected from the green area show a predisposition to generate acid at depths of between 50m and 80m below the surface.

It must also be made clear that the increases in the acid generation potential of the rocks coincide with the increased presence of pyrite in the rocks. In fact, the increase of acid-generating potential by the rocks coincides with the presence of pyrite in most cases (Figure 65), while the base generation or neutralisation potential increases with the increase of calcite content in the rocks.

The rocks at a depth of between 50 m to 80 m, (Figure 63 & Figure 64) beneath the surface contain alternating layers of mudstone and shale inter-bedded with coal.

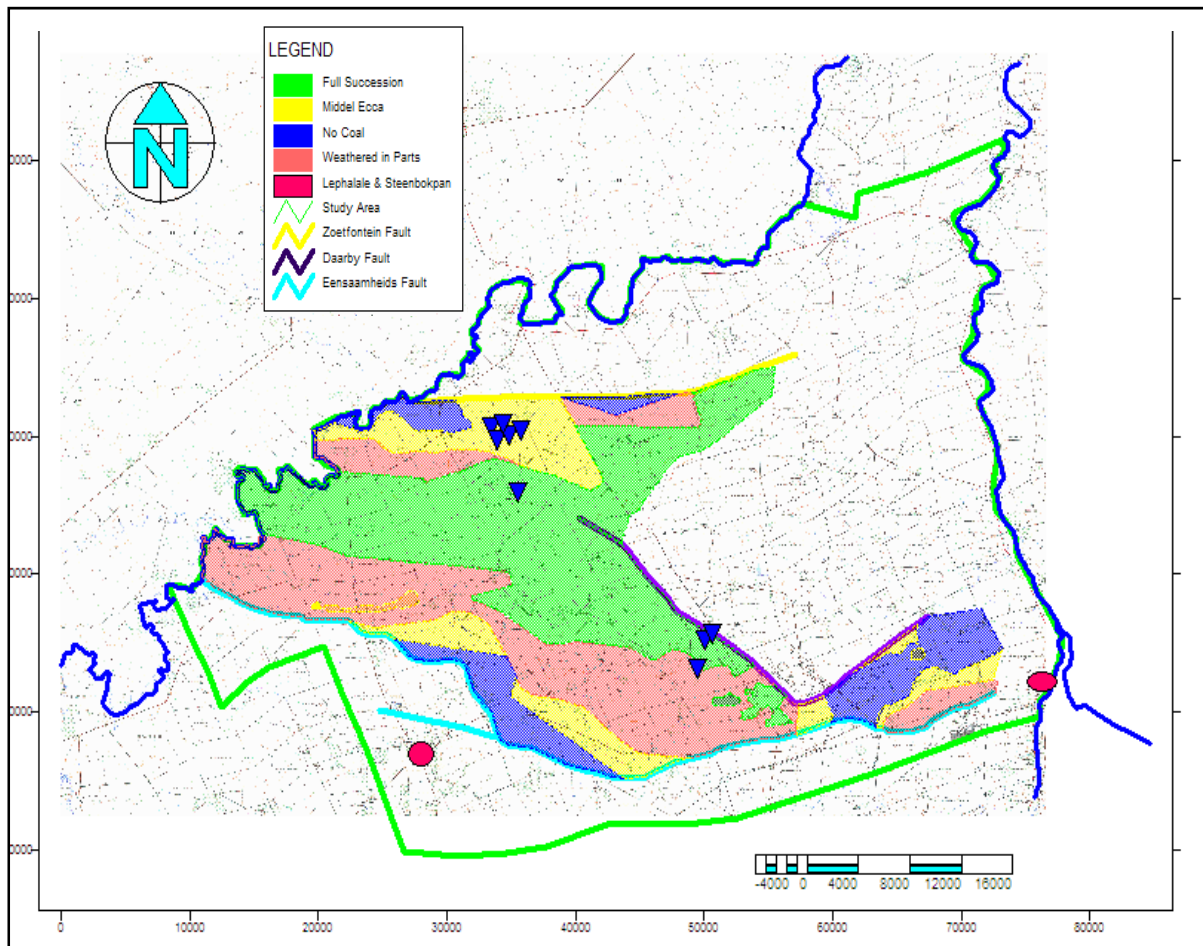


Figure 62: Location of the sample localities with regards to weathering.



Figure 63: Sample GGS 2 Taken 52 m below the surface in the south eastern area.



Figure 64: Samples SS5 & SS6 Taken 54 m & 66 m respectively below the surface in the north western area.



Figure 65: Sample SS6 showing the presence of pyrite.

The data indicates that the highest potential for acid generation is found in the areas of the succession that have the highest concentrations of pyrite. According to the data this area is concentrated in the areas that contain the full succession, between 50 m and 80 m below the surface. At present, management options, with regard to minimizing acid mine drainage, at the only active colliery in the study area, is to replace the rocks in the pit in the same order as their prior removal. It is recommended that the geology from this area be carefully noted for future reference once the new mines open, in order to follow the same procedure for backfilling of the pit. It is further recommended that these rocks be mixed with rocks that have a high base potential to further minimise the acid potential of the pyrite-containing rocks. This should be done in an effort to minimise the potential for acid generation, should the acid-generating layers oxidise.

7.11.2. The Yellow Areas (Northern Sampling Locations)

The geological samples collected from the yellow comprised chip samples only, as no core samples were available at the time of sampling. There is no identifiable pattern to the acid potential from these samples. Samples, GT1 (Figure 66 & Figure 67) and GT4 show a tendency to start generating acid from roughly 5m below the surface. From this depth, the acid potential steadily increases with depth. With the exception of the first sample, the samples from Borehole GT7 (Figure 66 & Figure 67) show a similar pattern.

Acid-generation potential starts at a depth of roughly 11 m below surface. Unfortunately, the boreholes from which these samples were collected were shallow and the acid potential at increasing depth may only be guessed.



Figure 66: Samples GT1.1 & GT7.5, respectively, with no acid potential.



Figure 67: Samples GT1.9 & GT7.1, respectively, with acid potential.

Samples from Borehole GT2 (Figure 68) show a very high base potential and no acid generation potential.



Figure 68: Sample GT2.12 with no acid potential.

Sample GT3 (Figure 69) fluctuates greatly. Some samples from the very top of the succession indicate acid-generation potential, together with those near the centre and near the bottom of the succession. This is interspersed with samples that have high base potential.



Figure 69: Sample GT3.2 (on the left) with acid potential and sample GT3.3 (on the right) with no acid potential

According to the data from the boreholes located in the yellow areas, there is too great a variation in the acid and base potential of the samples to be indicative of a specific layer with higher than expected acid-generation potential. It is recommended that further ABA studies be conducted in this region, and that core samples be used in an effort to ascertain the location of any layers with the potential for acid generation at greater depth.

7.11.3. The Red Areas (South Eastern Sampling Location)

Only one set of samples was collected from the red areas. The samples collected were chip samples and were collected down to a depth of 4m (Figure 70 & Figure 71). According to the results of the ABA tests, there is a high degree of certainty that the samples from the red areas will generate acid in both open- and closed-system conditions. The samples also contain no potential for buffering the acid once it is generated. It is however recommended that core samples are taken from this area and that further ABA analyses be conducted in an effort to identify any potential problem layers located at deeper levels in the succession.



Figure 70: Sample GGVZ1, collected 1 m below the surface with acid potential.



Figure 71: Sample GGSVZ1.4 4 m below the surface with acid potential.

7.12. Conclusion

7.12.1. The North Western Samples

- The analyses of the samples taken from the north-western sampling location indicate that the rocks in the area contain sufficient pyrite to generate acid.
- The data further indicates that there is sufficient calcite present to serve as a buffer to limit the amount of acid generated, but not enough to completely eliminate the potential for acid generation.

7.12.2. Northern and South Eastern Samples:

- It was found that the samples have the potential to generate acid, although they also contain buffer potential.
- The ABA analyses of the sandstone samples indicate that some acid will be generated for any given mass of the sandstone.
- For the discard it was concluded that these samples had a high acid-generation potential, and if oxidised, the samples will indeed produce acid.

7.12.3. ABA Compared to Weathering

The results of the comparison between the ABA results at the level of weathering are inconclusive.

- In the areas that contain the full succession there is correlation between rocks from the zone 50 m - 80 m below the surface.
- The rocks at this depth have a higher potential for acid generation in both the north-western sampling location as well as the south-eastern sampling location.
- The lack of additional samples for both the yellow areas and the red areas makes comparison difficult and no concrete conclusions can be drawn.
- It is therefore recommended that additional samples be collected and the same analyses be done on these samples in order to identify potential correlation.

CHAPTER 8: Pre-Mining Water Quality of the Waterberg Coalfields

8.1. Introduction

The primary goal of this project was to determine the pre-mining groundwater quality for the study area and how it would be affected by mining. In order to achieve this, chemical data on the current quality of the groundwater in the study area was necessary. Chemistry data for the study area was obtained from various sources. Much of the data obtained was collected from existing data bases, and compiled by companies that have been active in the study area in the past, or that are currently active in the study area. Companies such as Exxaro, Eskom, Sasol and Anglo Coal were the major contributors to the data base. There were however "gaps" in the data that needed to be filled in. These gaps were rectified by sampling of boreholes for which no data was available. These samples were transported to and accordingly analysed at the laboratory of the Institute for Groundwater Studies at the University of the Free State.

8.2. Sampling

8.2.1. Water Samples

The water samples were obtained from boreholes by means of flow-through bailers. The bailers were cleaned with de-ionised water before each sample was taken. The samples were stored in 500 ml plastic bottles and transported to the IGS laboratory for analysis. The samples were taken 5 m below the water level, or at fractures as identified by multi-parameter profiling where possible.

8.3. Water Quality Determination

Table 3 lists the elemental parameters that were tested for and measured during the water quality analyses. The analyses were done by means of an Inductively Coupled Plasma Spectrometer (ICP). The elements listed above cover a wide range and are good indicators of potential inorganic pollution in groundwater as a result of coal mining. The EC and pH measurements were taken both in the field and in the laboratory. The pH gives indications of the acidity or alkalinity of the water, whereas the EC gives an indication of the salt content of the water.

The EC can, however, only give the total dissolved salts and can provide no indication of the types of salts. In total, chemical data for 509 boreholes scattered throughout the study area was gathered. The data from the boreholes included information on the parameters listed in Table 3. However, not all the boreholes could yield information on all of the parameters mentioned earlier, but were analysed only with regard to the information that was available.

To determine the impact which mining and power generation has on the quality of groundwater in the study area, the rest of the chapter will be discussed as a comparison between areas that have been affected by the aforementioned activities and areas that have not been affected by these activities.

8.4. Discussion of Results

8.4.1. pH

Figure 72 indicates that, with the exception of a few boreholes, the observed pH values of the sampled boreholes is well within safe limits (averaging 7.27) and does not vary to a great degree. Within these exceptions one does, however, find a large degree of variation, being 2.40 at the lowest point and 9.80 at the highest. The low pH is likely to be the result of a spill or some other point source pollution, for when one compares the other pH values for the same borehole over time one finds that the pH gradually increases to a value of 6. This large degree in variation is only found in a small number of boreholes (Figure 72).

There is no discernable pattern with regard to the locations of the high or low pH values. The lower pH values are located “near” areas of active mining or power generation. This cannot be given as a reason for the low pH values, as only a few of the boreholes show acidic pH levels and the boreholes located within close proximity to the acidic ones do not show any signs of acidification. There is additionally no correlation between the pH values and the depth of the borehole or the geology in which the boreholes are situated (almost all the boreholes have been drilled through sandstone and shale and only a few have acidic pH values).

It is therefore concluded that the acidic pH values are either the results of spills or of unknown geological conditions local to the boreholes displaying acidic pH values. From the data collected, a contour map of the pH values for the study area was constructed (Figure 73). There are no discernable patterns noticeable in the distribution of the pH values, with the exception of the boreholes with low pH values being located near areas of active mining or power generation.

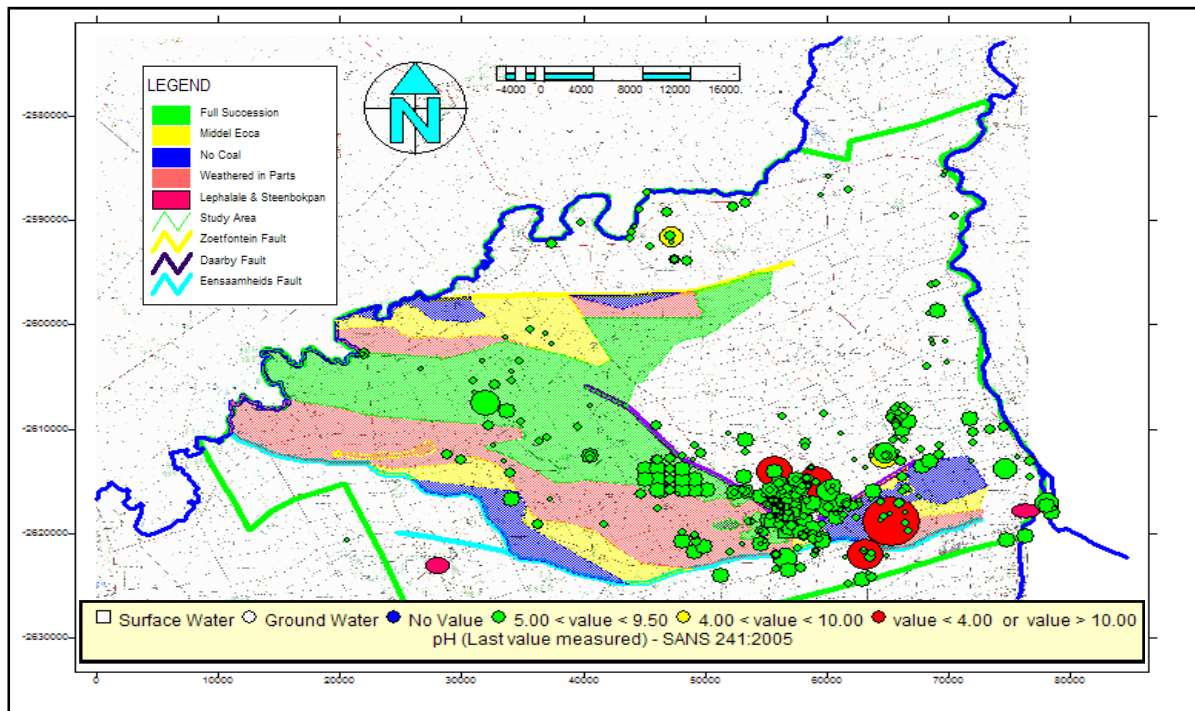


Figure 72: Groundwater pH levels in the study area.

From Figure 72 and Figure 73 it can be concluded that there is no definitive impact on the groundwater pH from the activities taking place in the study area. There is no visible difference between the values observed for areas where there are activities at present, and areas where there are none. The exceptions found in the areas currently displaying activities such as mining or power generation are likely to be the result of spills or of local unknown geological phenomena, and cannot be taken as an indication of the impact of the activities on the groundwater.

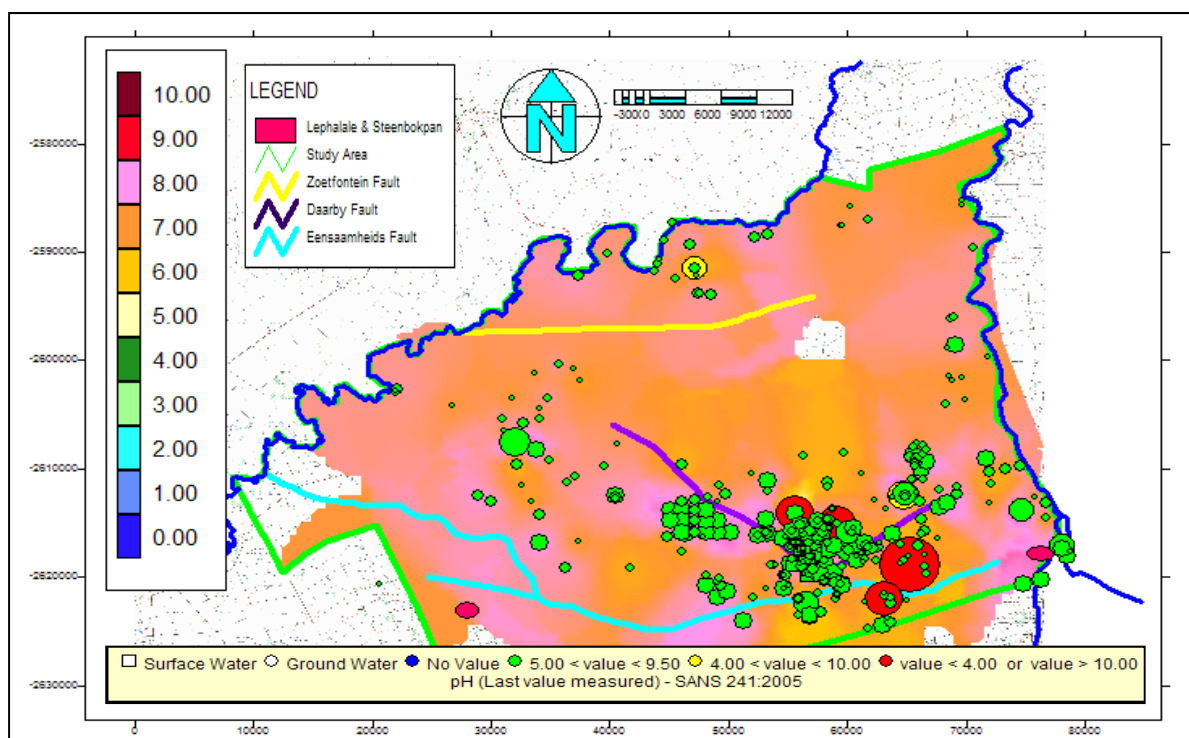
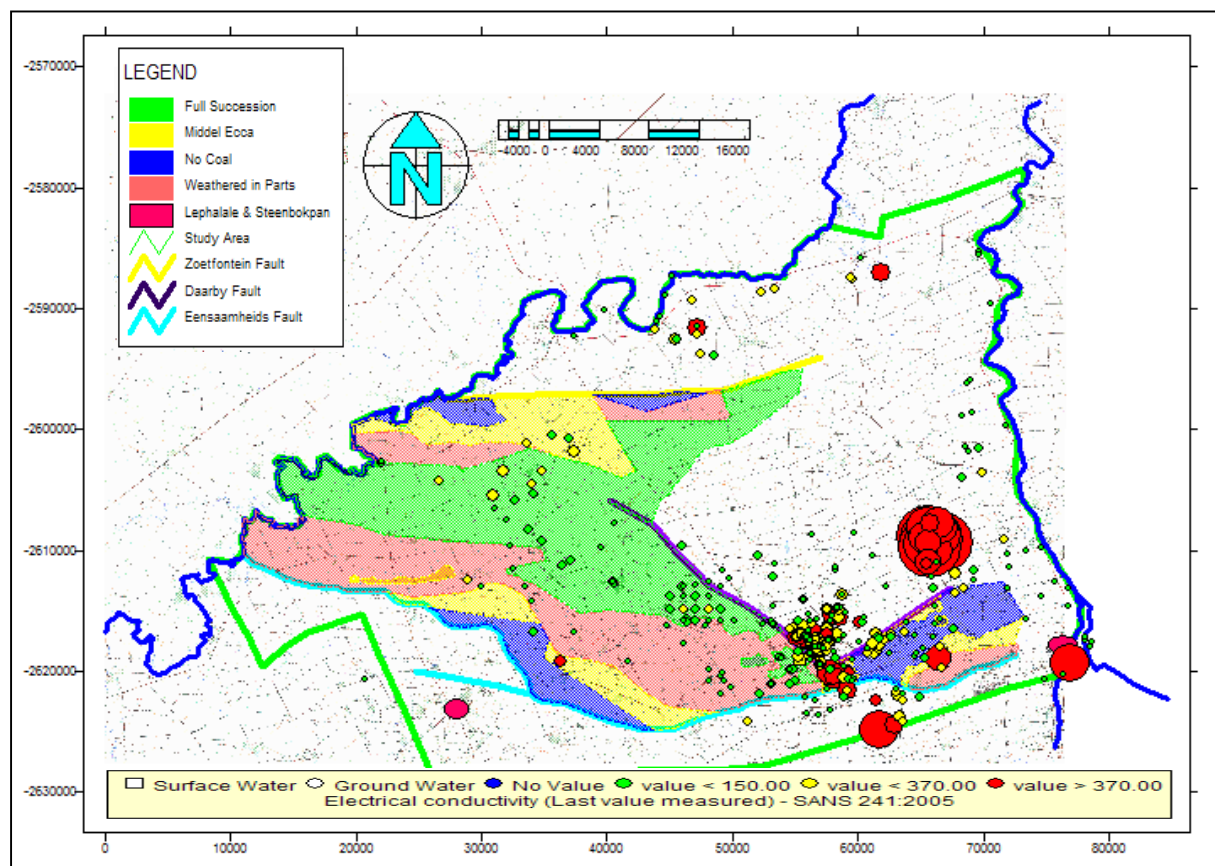


Figure 73: pH contour map of the study area.

8.4.2. Electrical Conductivity (EC)

The electrical conductivity (EC) of the groundwater in the study area varies greatly, with the highest levels located on the farms towards the east of the Daarby fault, predominantly located on the farm Zonderwater (Figure 74). The largest concentration of mid-range EC values are located in the vicinity of the Grootegeluk mine and the Matimba power station near the central south east of the study area, indicating the impact of these activities on the groundwater. There is no discernable pattern to the distribution of EC values in the area.



8.4.2.1. Groundwater in the Waterberg Group Rocks (Areas with Current Activities)

The data indicated that the EC values for the boreholes located on the farm Zwartwater are much higher than the EC values in the surrounding area. This farm marks the location of the fly-ash dump for the Matimba power station. The data indicates that the boreholes on this farm have high EC values. The reasons for this are twofold:

Firstly:

- The boreholes were drilled south of the Eenzaamheid fault.
- The Eenzaamheid fault marks the transition from Karoo rocks north of the fault into Waterberg Group rocks south of the fault.

- The Waterberg Group rocks have a generally higher salt content than the rocks from the Karoo groups. This has been observed at other boreholes close to the town of Lephalale that have been drilled into the Waterberg Group rocks.
- Accordingly it is possible that the salts from the rocks have leached into the groundwater resulting in the higher EC values.

Secondly:

- The farm is the location of the fly-ash dump for the Matimba power station and it is very likely that the salts have leached from the dump and have ended up in the boreholes.
- These boreholes are drilled in the Waterberg Group rocks and are located in the shallow aquifer.
- These salts would have entered into the upper weathered aquifer during periods of high recharge (large precipitation events) and would move through the un-weathered aquifer.

Figure 76 shows the data for boreholes drilled at the site of the new Medupi power station. The boreholes were drilled in pairs, one deep borehole and one shallow borehole per site. This was done to determine whether water from the shallow, weathered aquifers flowed to the deeper, fractured aquifers, and to assess if there was a difference in water quality between the shallow and deeper aquifers.

Figure 76 indicates that with the exception of boreholes MBH4D, MBH2S and MBH6D there are no significant differences in the measured EC values for the boreholes. For the most part the shallow boreholes and the deeper boreholes display EC values that are very similar. This indicates that there is movement between the shallow and deeper aquifers.

When discounting borehole pairs 1 and 5, due to a lack of data for the shallow boreholes (dry boreholes), and taking only the four remaining pairs, one finds that boreholes MBH2S and MBH6S, - boreholes drilled in the shallow aquifers - have higher EC values than those drilled in the deeper aquifers. Additionally boreholes MBH3D and MBH4D, drilled into the deeper aquifers, indicated higher EC values than the ones drilled into the shallow aquifers. Borehole pairs MBH4 and MBH6 were drilled into the Karoo group rocks and pairs MBH2 and MBH3 were drilled into the Waterberg group rocks.

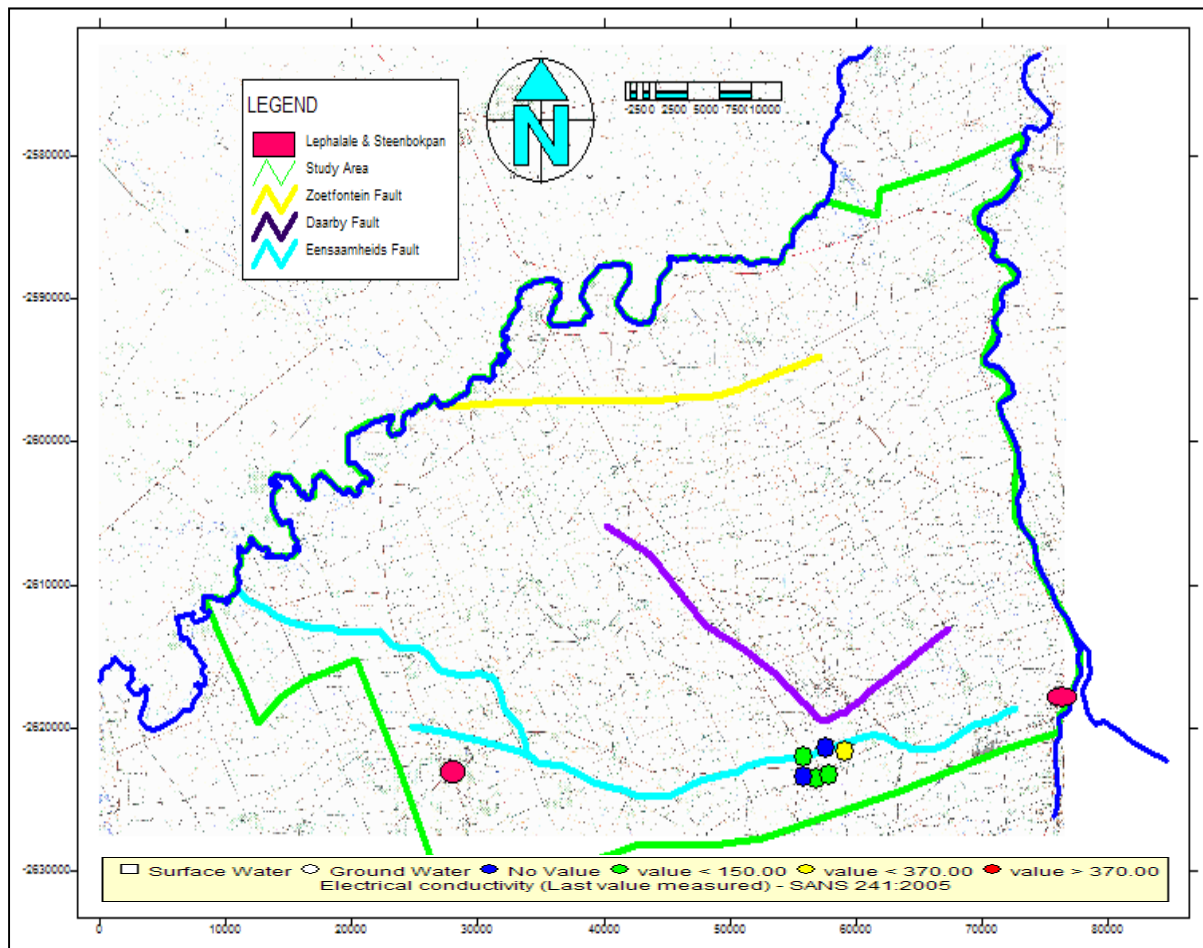


Figure 75: Location of the 6 borehole pairs at the Medupi power station.

The data shows that for the boreholes drilled in the vicinity of the Medupi power station, there is movement between the deeper and shallower aquifers. It was initially expected that the shallow boreholes (drilled in the weathered zone) would display lower values than the deeper boreholes (Hodgson *et al.*, 2007).

This was found to be true with the exception of two of the boreholes namely MBH6S and MBH2S. With both boreholes indicating elevated EC values in the shallow aquifers. It is expected that due to the difference in transmissivities, the time it takes for the water to move in the different rocks will differ greatly, with water movement in the Karoo group rocks expected to be more rapid than in the Waterberg Group rocks.

It is suspected that boreholes MBH4D and MBH2S were drilled on an unknown geological anomaly (most likely a dyke) which is responsible for the elevated EC values. Accordingly it is concluded that the elevated EC values found in the borehole near the Matimba ash dump is the result of downward movement of effluent draining from the dump. Vermeulen and Dennis (2007) also noted these elevated EC levels in the vicinity of the ash dump during a survey conducted for the Matimba power station.

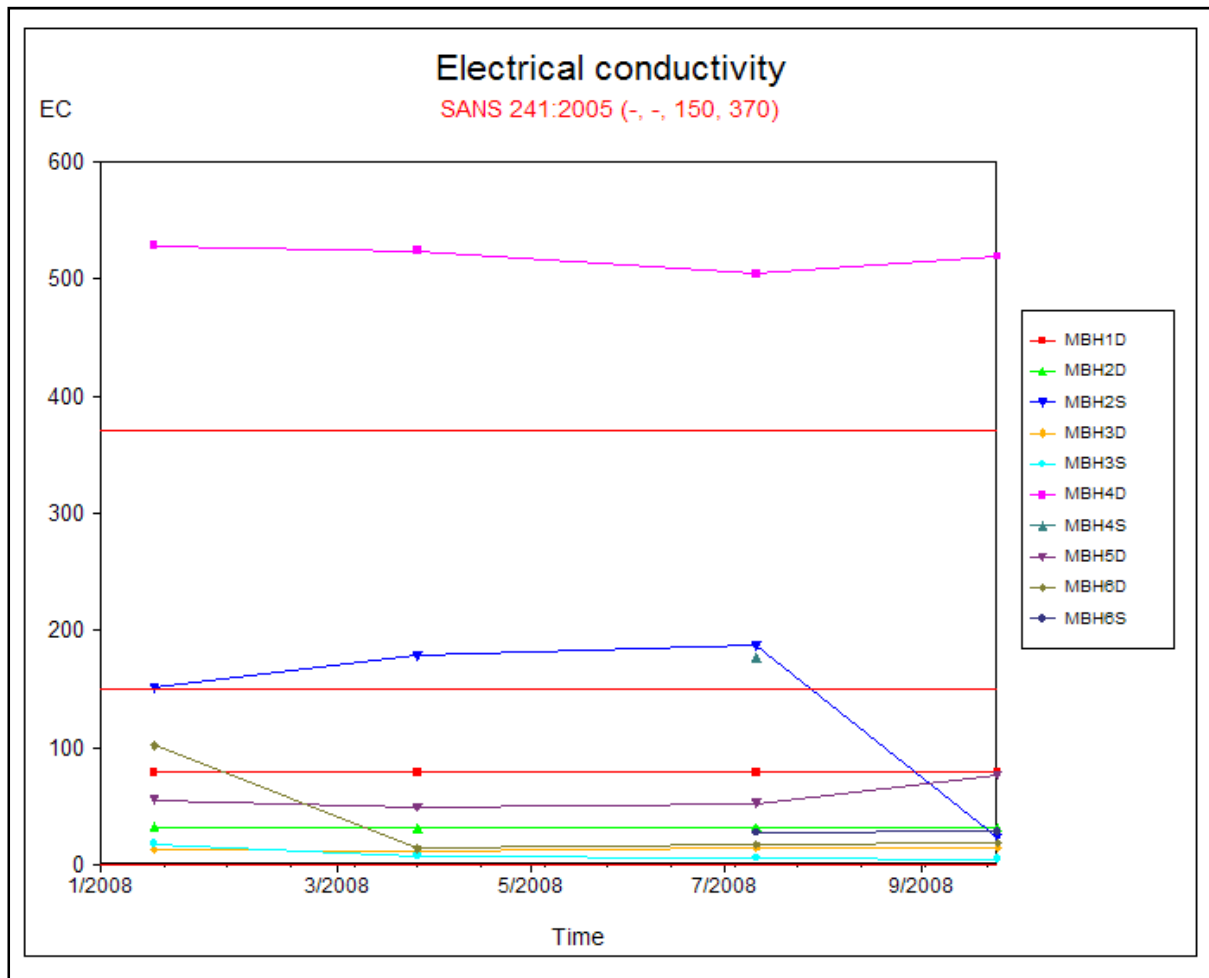


Figure 76: Graph of the EC for the deep (D) and shallow (S) boreholes drilled at the Medupi power station.

Vermeulen and Dennis (2007) additionally noted that “According to the point size distribution of electrical conductivity values around the ash dump, the dump has a definite impact on the groundwater quality of the monitoring boreholes near the structure. The boreholes further away, show no elevation and are currently unaffected”. This is illustrated in Figure 77.

Additionally, Figure 77 indicates a general increase of the EC values in the boreholes located near the ash dump over a period of eight years. The ash dump is situated on Waterberg Group rocks and according to Dreyer (pers. comm. 2009), all of the newly planned infrastructure for the new mines and the new power station are to be located on the Waterberg Group rocks, west of the Eenzaamheid fault. The data suggests that the same forms of contamination - slow seepage from the ash dumps and coal stock yards into the groundwater - may be expected at the location of the new power stations.

It is recommended that monitoring boreholes be drilled at the sites of the new power stations, and their infrastructure be carefully planned. Additionally it is recommended that the boreholes be monitored regularly and that measures (such as lining of the dump areas with bentonite) be taken to prevent the leached salts from entering into the upper aquifers.

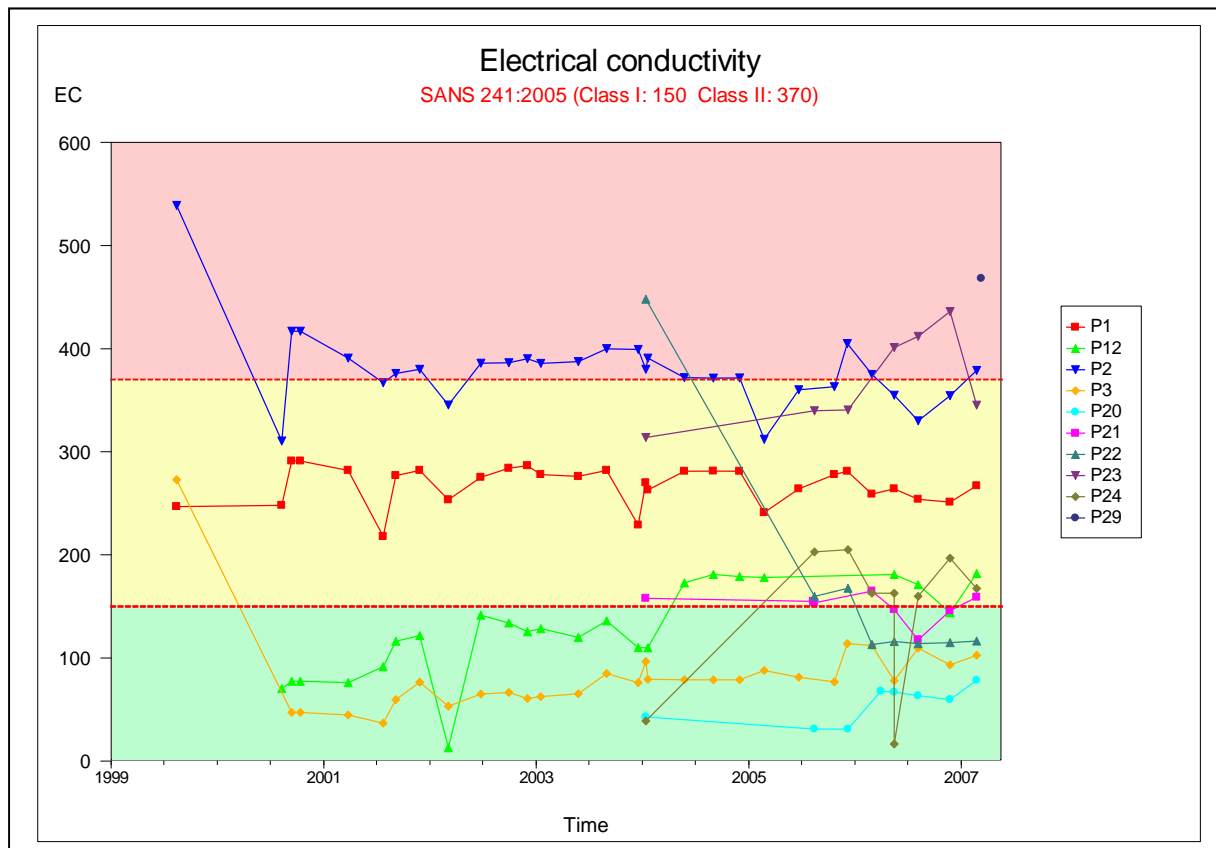


Figure 77: Graph of electrical conductivity at the ash dump boreholes (taken from Vermeulen and Dennis 2007).

8.4.2.2. Groundwater in the Karoo Aquifers (Areas with Current Activities)

The data from Figure 78 (outlined in red) indicates areas found in the Karoo group rocks that have elevated EC values. Figure 78 displays the contour map of the EC values for the study area. The area outlined in black indicates an area for which no data could be gathered. Additionally, the data from Figure 78 indicates that, with the exception of the boreholes towards the east and the central south east, the area displays generally low EC values. The areas towards the east and south east are cause for concern and show the influence of activities on the groundwater.

The area to the east indicates the area in which Anglo Coal is presently testing the viability of hydro fracturing to remove methane from the subterranean coal deposits. The area to the south east, marks the location of the Grootegeluk mine and the Matimba power station. There is also the area to the south near the Matimba fly-ash dump located between the Daarby and Eenzaamheid faults. This area is not directly linked to the Matimba ash dump and is spatially far removed from the dump. The area is located too far away from the mine infrastructure at Grootegeluk to have been contaminated by, for example, a spoils dump. Furthermore the boreholes are located south of the Daarby fault, which, according to Dreyer, (2009) is impermeable. It is therefore likely that these boreholes are very deep boreholes and are naturally saline, with the high EC values not being the result of pollution.

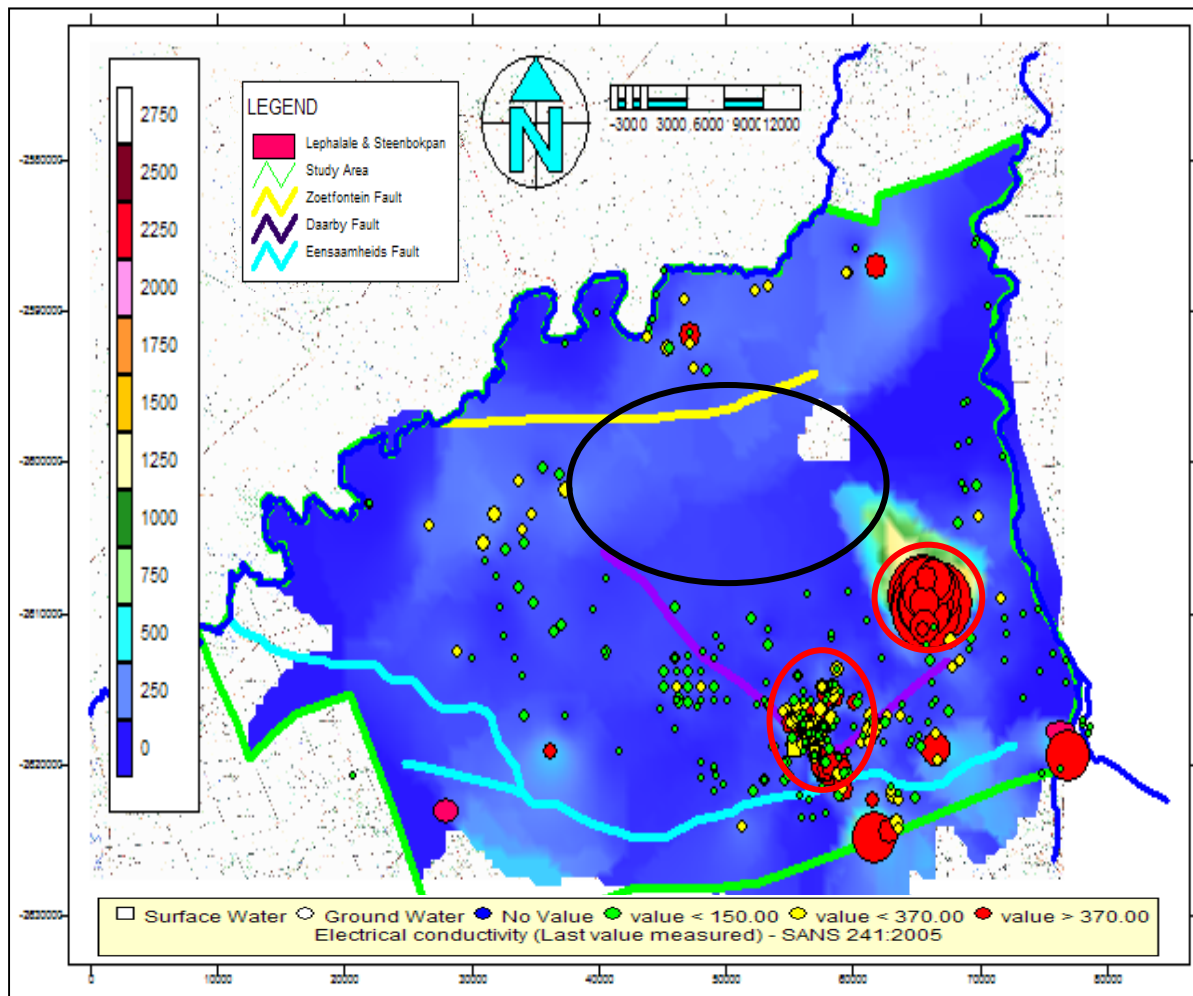


Figure 78: Contour map of the EC values encountered in the study area.

8.4.2.2.1. Far Eastern Boreholes

The boreholes drilled in the far east of the study area, display the highest EC values in the study area (Figure 79). According to a study done by Usher *et al.*, (2005), the anomalously high EC values found in the groundwater for these boreholes are naturally saline.

According to Usher *et al.*, (2005) the high EC values are the direct result of the depth of the boreholes (some reaching depths of 420 m) and not the result of pollution. The data from Figure 80 indicate that the EC values are much higher than the values for the boreholes drilled into the Waterberg Group rocks. There is, however, insufficient data on the surrounding farms to determine the extent of the elevated EC values.

These values appear to remain constant according to Figure 80 with the exception of three boreholes in which the values fluctuate. These boreholes fall outside the primary focus area of the project, but the effect which the activities in the area exert on the water quality should be noted.

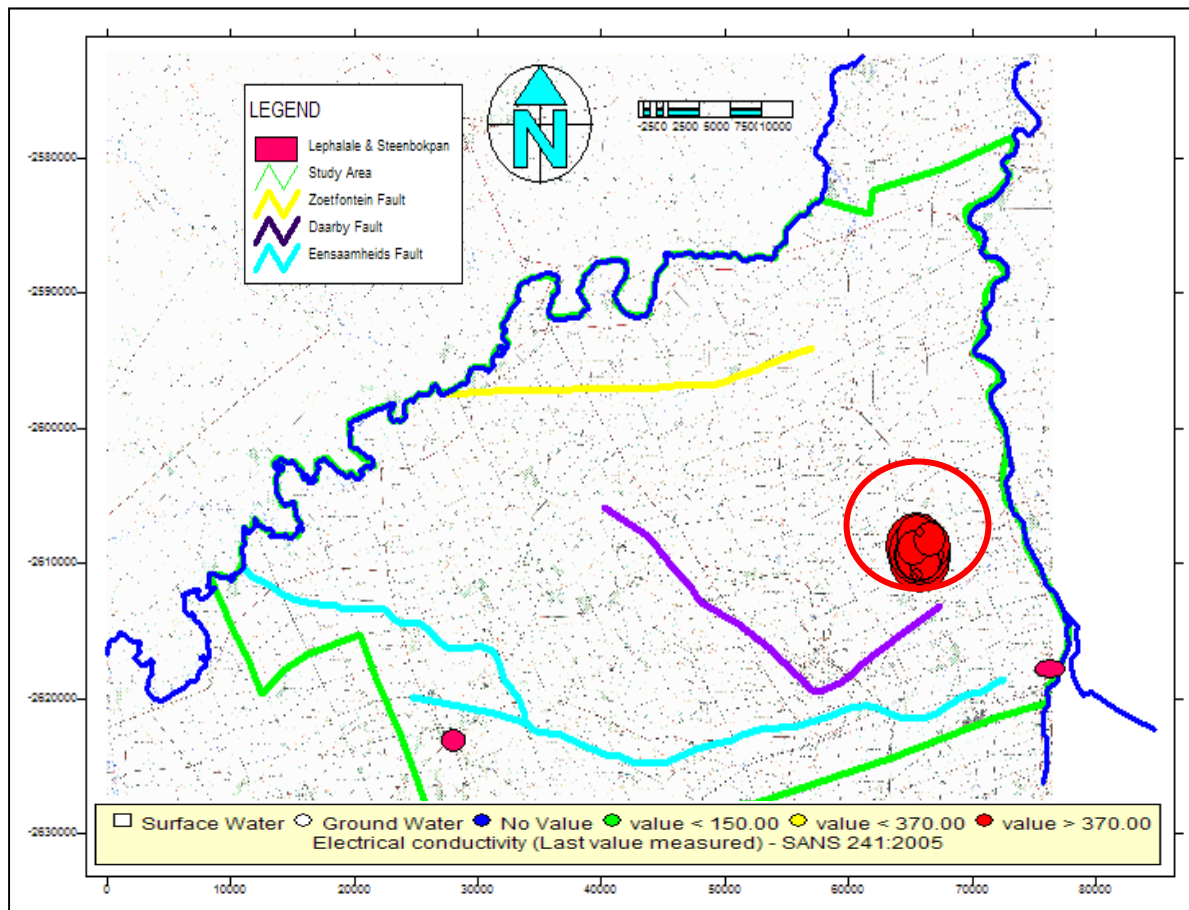


Figure 79: Location of the eastern boreholes with the high EC values.

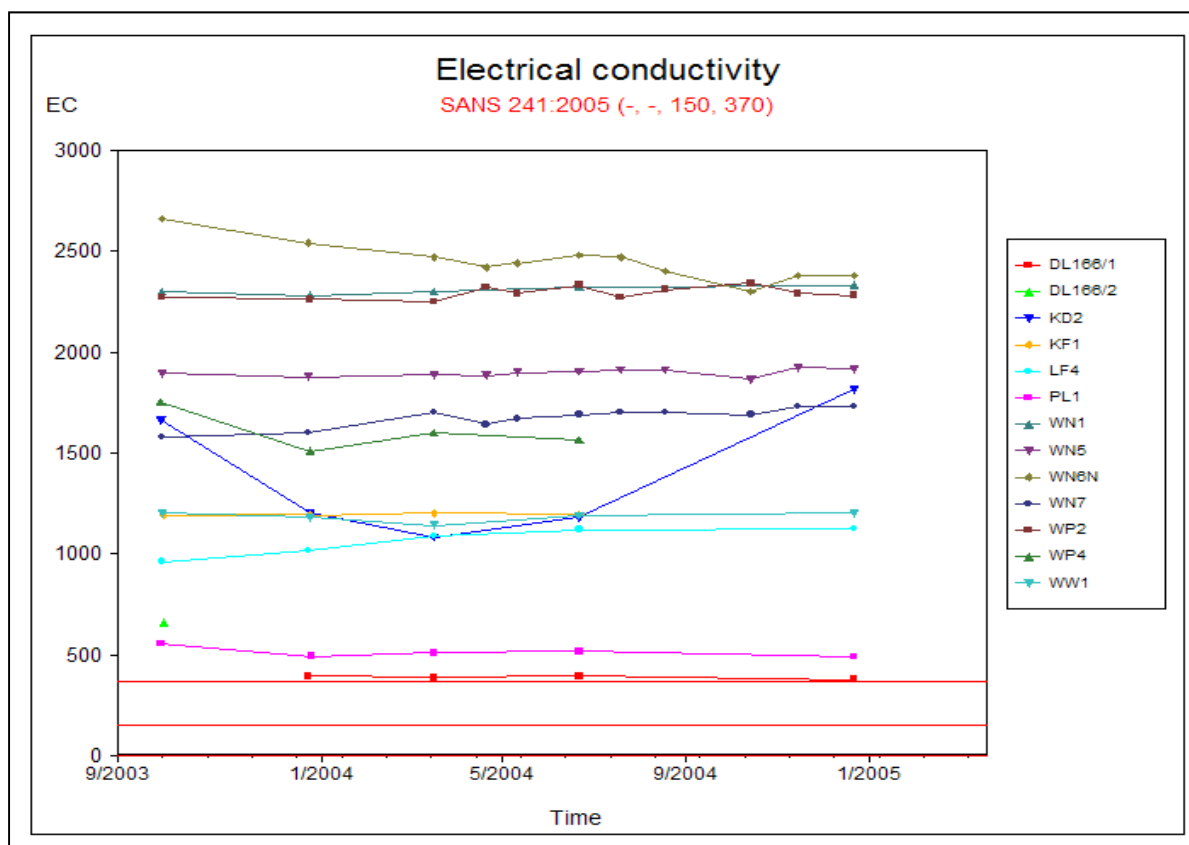


Figure 80: Time series data for the eastern boreholes.

8.4.2.2.2. The Current Mining Area (Grootegeluk)

The areas towards the south east around the Grootegeluk mine indicate elevated EC levels (Figure 81) and in some of the boreholes elevated sulphate values are evident. These elevated values are associated with the activities at the mine (coal washing, stockpiling, and evaporation ponds). Accordingly it can be expected that similar effects will be present at the new mines planned for the study area.

Figure 82 indicates the EC values recorded for the boreholes drilled on the site of the Grootegeluk mine. The values fluctuate between high and low values and all the values show a large decline to nearly zero between the years 2004 and 2005. This reduction in values coincides with a period of high rainfall. It can therefore be concluded that the water in the boreholes was “flushed” during this time of elevated precipitation.

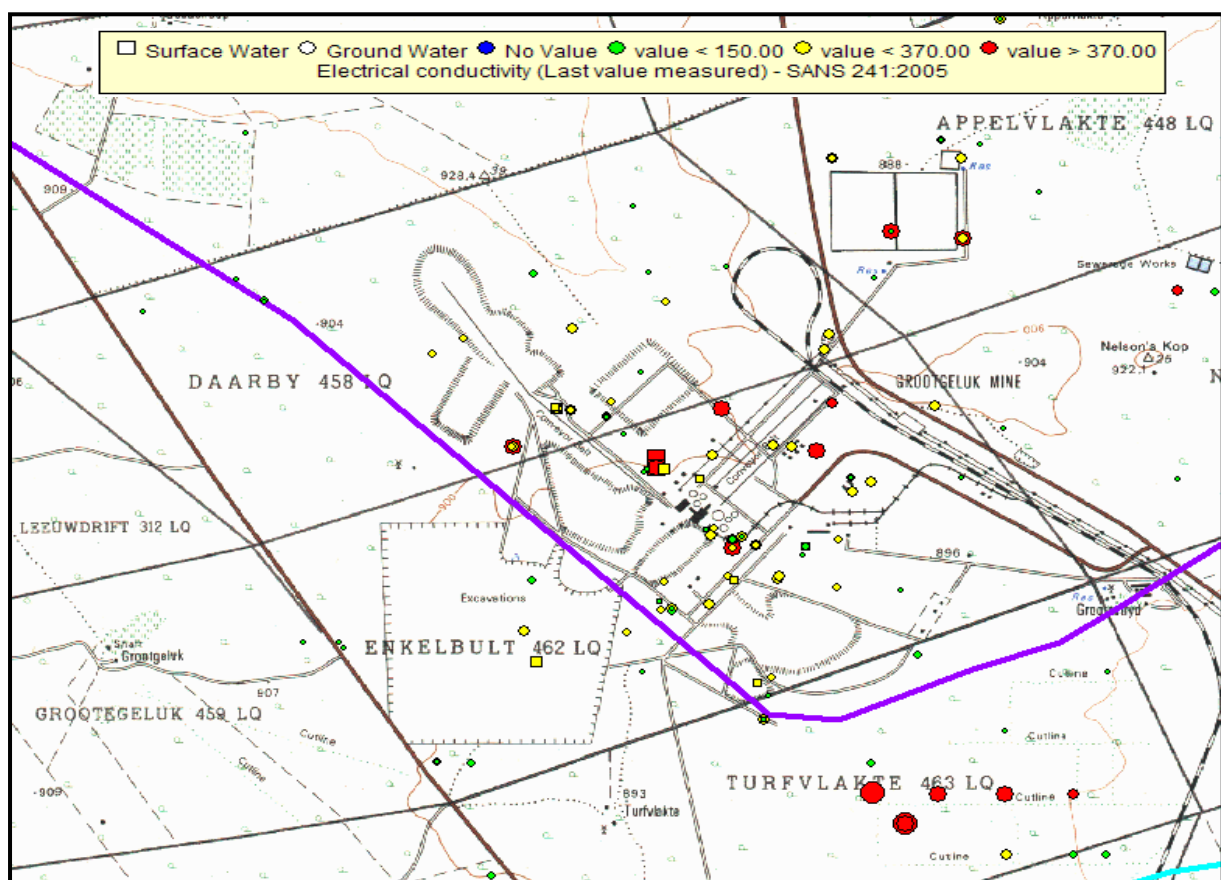


Figure 81: Size distribution for EC values of boreholes and evaporation ponds at the Grootegeluk mine.

This could be indicative of sufficient movement in the aquifers to “displace” the salts recorded in the form of the elevated EC values. The decline of the EC values, was accompanied by an increase of the sulphate values over the same period (Figure 83). This may be viewed as indicative of runoff from discard dumps and coal stockpiles infiltrated into the aquifers during this period of high rainfall. The same type of scenario can be expected at the new mines.

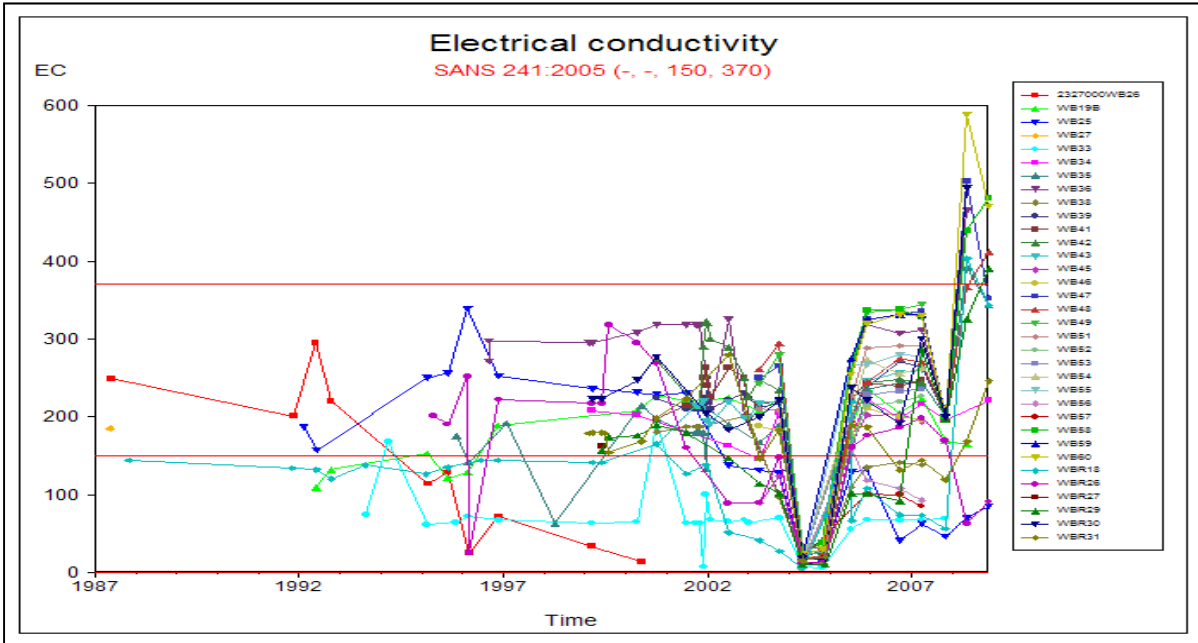


Figure 82: EC values for the boreholes drilled on the Grootegeluk mine site.

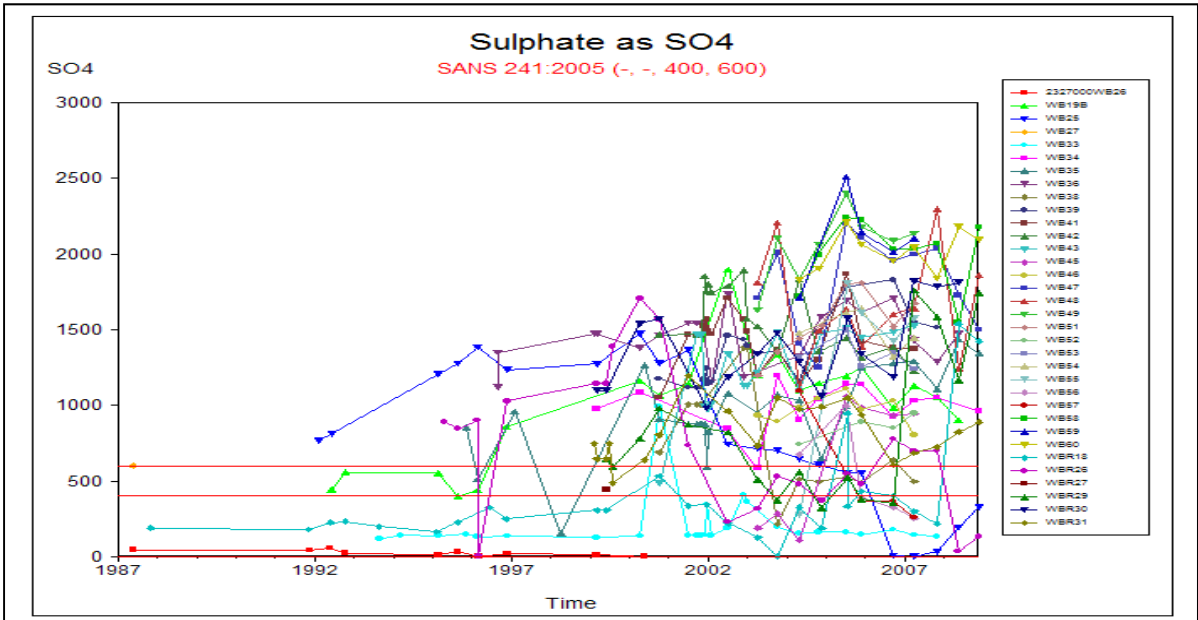


Figure 83: SO₄ values for boreholes drilled on the Grootegeluk mine.

The data from the previous figures indicate that in the Karoo aquifers, there is sufficient movement to allow for the infiltration of dissolved inorganic pollutants. The data in Figure 83 indicates a large increase in the SO₄²⁻ levels since 1992. It is expected that these values will continue to rise while the operations at the mines continue. This poses problems for groundwater resources located outside of the faults that delineate the coal field. The reason for this is that all of the infrastructure for the mines and the power stations will be constructed south of the Eenzaamheid fault and thus outside the coal field. The groundwater resources located in the vicinity of the mining infrastructure are likely to be affected by the vertical movement of these pollutants, but the low transmissivities of the rocks along with the low recharge, will effectively retard the horizontal movement of these pollutants.

8.4.2.3. The Areas West of the Daarby Fault (Unaffected by Mining)

For the areas that have been unaffected by activities such as mining or power generation the general groundwater quality ranges from fair to good (Figure 84).

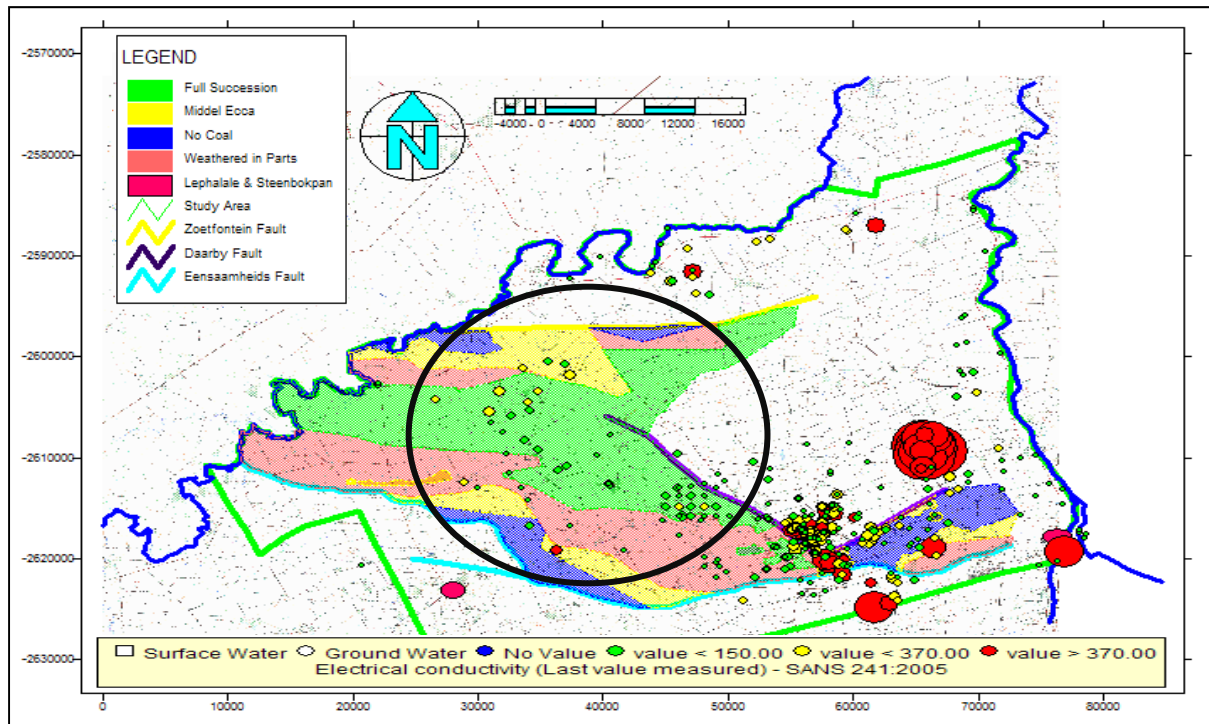


Figure 84: EC map of the study area showing the areas that have not been affected by activities such as mining or power generation (outline in black).

Figure 84 indicates that, in general, the EC values for the area that has not been influenced by activities ranges between values that can be classified as low and medium, with the medium values likely to be the result of abstraction. Figure 85 indicates that there is no visible trend in the EC values, with the values remaining stable over time. There are exceptions to this, with the predominant rise and fall in the values coinciding with precipitation events.

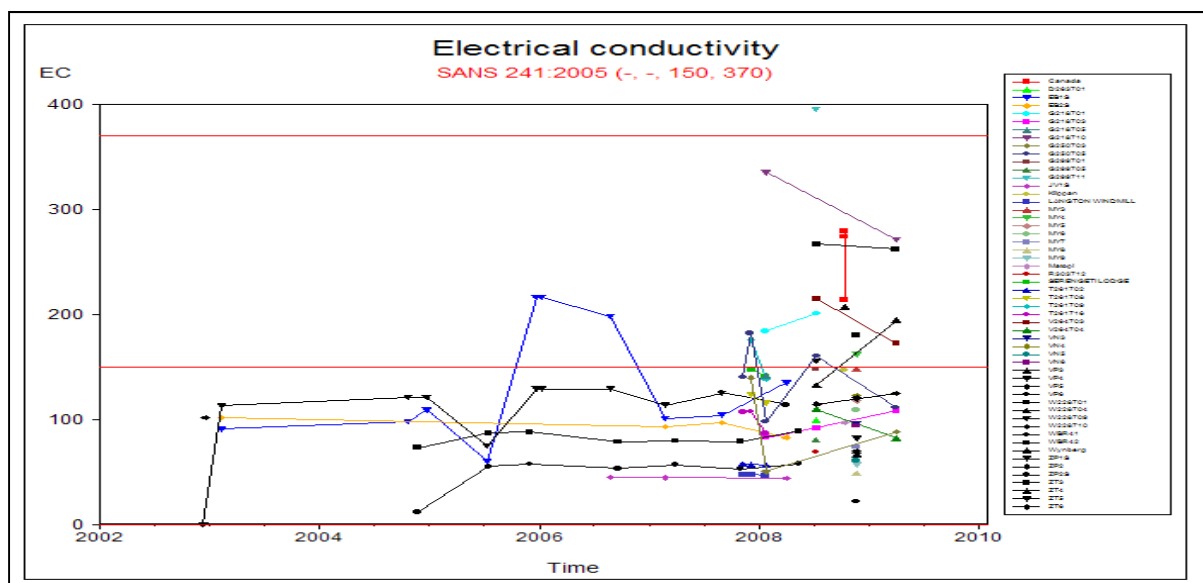


Figure 85: Time graph for EC values in areas that have not been affected by activities.

The CI values displayed in Figure 86 are generally above medium for the groundwater in the study area. There are areas that have lower CI values but the values are related to the geology and it is unclear to which degree the CI levels in the groundwater will be affected by activities such as mining or power generation. Interestingly enough, in the vicinity of the Grootegeluk mine the CI values are very low.

According to Dreyer (pers. comm. 2009), this is the result of artificial recharge being generated by the workings at the Grootegeluk mine. It is anticipated that the same situation might occur at the new collieries with infrastructure located on the eastern side of the Daarby fault. Further investigation may be necessary, as the conditions at the new collieries may differ from those found at the Grootegeluk mine as a result of local geological conditions.

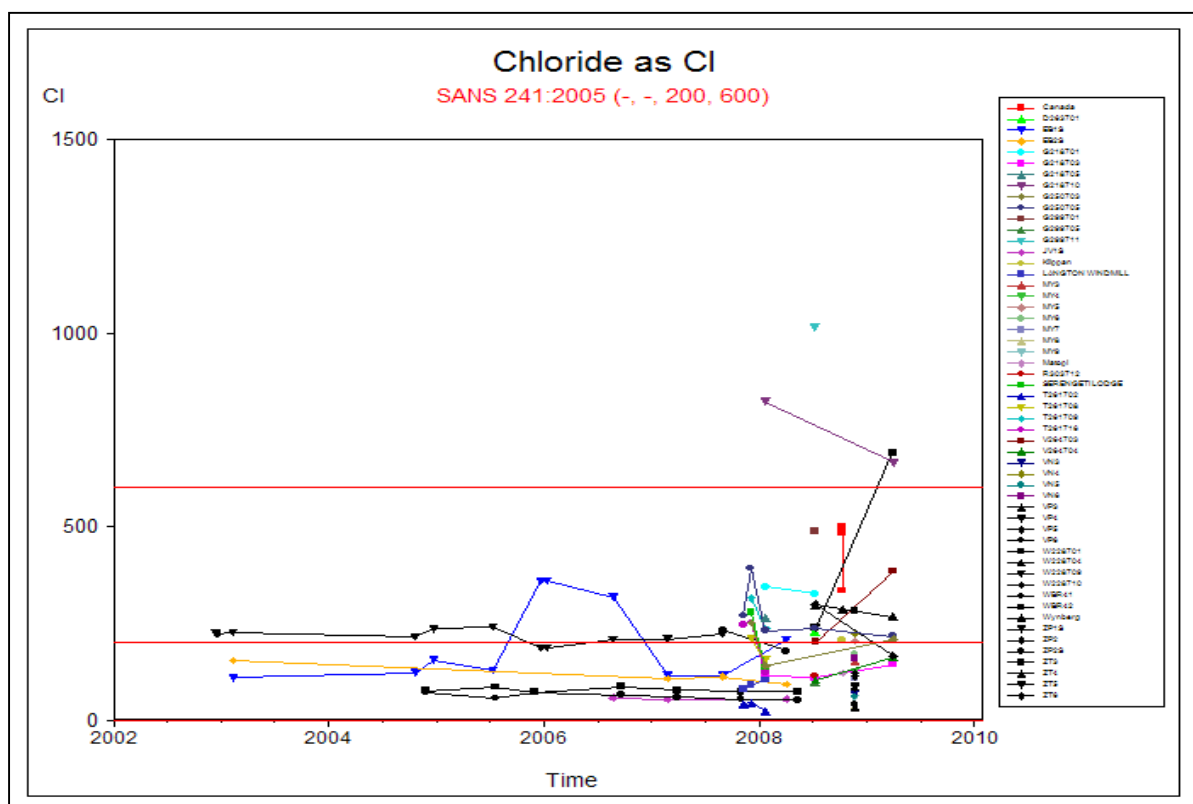


Figure 86: Time graph for CI values of groundwater unaffected by activities.

The same observations made for the EC values in unaffected areas, can be made for the sulphate values in the same areas (Figure 87). The values are generally low with the exception of a few boreholes. The large values such as those found in the vicinity of the Grootegeluk mine are not present with the exception of areas where boreholes have been drilled into the coal seams. It is expected that the sulphate values for the groundwater will increase with the addition of new mines. The higher sulphates are most likely not the result of direct groundwater pollution, but are more likely caused by runoff from the dumps into the groundwater system or into the boreholes from where the measurements are taken.

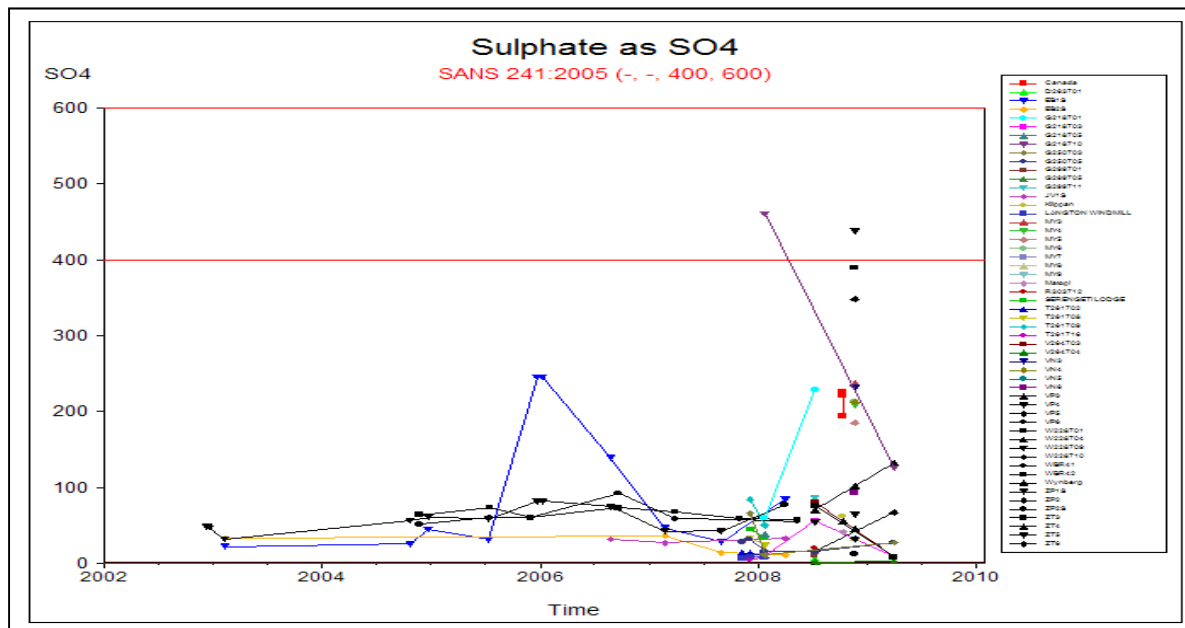


Figure 87: Time graph of SO₄ values for areas that have not been affected by activities.

8.5. Conclusion

In conclusion, it is expected that the addition of new mines and power stations will diminish the quality of the groundwater in the study area. It is expected that the EC values will rise along with the SO₄²⁻ values in the vicinity of the mines. It is also expected that the Cl values may fall depending on the activity and the local conditions near the mines (geology, elevation). The water quality of the study area that has remained unaffected by activities such as mining and power generation, can be classified as moderate at best. Generally, the area as a whole has high EC and Cl values with near neutral pH values. At present a fine line exists between usable groundwater and unusable groundwater in the study area. It is predicted that the addition of the new mine to the area will have an adverse effect on the groundwater in the immediate vicinity of the mines.

8.5.1. Power Generation and its Impacts on Groundwater Quality

Possible sources of groundwater pollution at power stations are mainly fly ash disposal, coal stockpiling and dirty water dams. The Matimba power station is well equipped with monitoring boreholes. Such monitoring boreholes will also need to be drilled for future power stations. These boreholes should be monitored frequently (once every 6 months) to monitor potential pollution from occurring or spreading beyond the perimeters of the power stations (Hodgson and Krantz (1995). In this regard, the geology of the study area plays a significant role. The proposed power stations, south of Steenbokpan, as well as the Medupi power station currently under construction, are located on the much denser Waterberg Group quartzites south and west of the Eenzaamheid fault. These formations have very low transmissivities and effective porosities, making the movement of groundwater in these quartzites very slow.

According to Hodgson and Krantz (1995), the following impacts on the groundwater can be expected from power stations and its supporting bodies (stockpiles and ash dumps) :

- The ash water chemistry is unstable in the presence of open air. Accordingly it readjusts by a decrease in pH (from > 12.0 to around 8.0) and the precipitation of calcium carbonate.
- This precipitation of calcium carbonate and the near neutral pH, have been cited as parameters that would qualify fly-ash as possible remediation for AMD.
- The heavy metal leachability from ash at normal pH levels is insignificantly low.
- The base potential of fly ash is usually 2 - 5 times higher than that of spoil in opencast mines. The introduction of fly ash into mining environments can therefore add additional base potential.
- A prerequisite for fly ash disposal within mining environments is that the system as a whole will remain alkaline.
- Under acidic conditions, the heavy metal leachability from fly ash is very high.
- Heavy metal availability occurs at pH levels below 3.0.
- It is concluded that great care should be exercised in instances where fly ash is introduced into coal mines.
- Alkaline systems should be maintained.
- A well-managed dry-ash dump does not pose any threat to groundwater pollution.
- Although no pollution is generally found at the modern coal stockyards at some power stations, this does not imply that pollution does not occur.

8.5.2. Coal Mining and its Effect on Groundwater Quality

According to (Hodgson and Krantz (1995), the main problems identified at collieries around South Africa (mainly in the Witbank area) are:

- Heavy metals found in the mines may become available for leaching under certain chemical conditions (low or high pH values depending on the metals involved).
- The metals that pose a potential for leaching may include iron, aluminium, manganese, copper, zinc and, in rare instances, nickel, cobalt and cadmium. Lead, arsenic, selenium, molybdenum and chromium, which are normally only present in trace amounts according to (Hodgson and Krantz (1995).
- On the basis of the present scale of opencast mining in the Witbank Catchment, this amounts to 70 t/d of sulphate. It must be mentioned that the Witbank area has many more rivers and much higher levels of rainfall that contribute to the distribution of the sulphates, than the Waterberg study area.
- According to (Hodgson and Krantz (1995) pits that have been mined out in the Witbank coal fields, fill up with water to their decant level within 5 - 10 years after

mining has stopped. According to modelling of possible decant scenarios in the study area, the pits in the Waterberg coal field will not reach decant level.

- When the pits reach decant level, the polluted water flows out onto the surface, contaminating surface water sources.
- Recharge averages 20% of the rainfall, of which 12% is run-off into the mine and 8% infiltration through the spoil (in the pits).
- In the Witbank area, saturation levels for salts have not been reached in any of the opencast mines, due to the significant dilution of the pit water by rainfall. Sulphate levels are typically between 2000 - 3000 mg/L in backfilled opencast areas.
- This will however not occur in the study area due to the low levels of rainfall. Saturation might take place at a much higher rate and take much longer than in the case of the Witbank coalfields (Hodgson and Krantz (1995)).
- According to (Hodgson and Krantz (1995) the mineral most likely to precipitate upon saturation is gypsum.
- Once gypsum precipitation occurs, a cycle of chemical instability is initiated, precipitating most of the calcium, while magnesium and sulphate concentrations in these open pits could rise in excess of 2 000 mg/l and 10 000 mg/l respectively.
- This would create a problem in the study area, as the groundwater already contains high levels of magnesium and calcium.
- This situation can be avoided by dilution from rainwater, which is already problematic in the study area, due to the low rainfall levels (average rainfall is between 285 mm and 560 mm per year).
- Mixing cell modelling of open pits in the Witbank area has indicated that the inclusion of coal discards into the unsaturated zone in opencast pits creates local acid conditions that will lead to acidification above and below the water level.
- This method of isolating the discard from the water level is proposed as a water - quality management measure for the study area, as there will be (according to modelling done by the researcher) a minimal and slow influx of water into the mines.
- The primary inflow of water into the pit will be from surface runoff.
- This, in conjunction with the results from acid-base-accounting (which indicated that the discard will become acidic over time), show that there will be substantial acid generated from the discard stored in the unsaturated zone in the Waterberg coal fields.

Under these conditions, acid pits have the potential of becoming acidic. It is concluded that coal discard disposal constitutes a very serious problem, because of the vast volumes of material discarded over time.

CHAPTER 9: Geohydrology

9.1. Introduction

In order to make accurate determinations about the characteristics of the aquifers in the study area, tests were done on several boreholes throughout the study area. The tests were limited to pumping tests and slug tests as these can be accurately interpreted and give good quality results if conducted properly. The southern boundary of the study area is formed by the Eenzaamheid fault. This fault divides the study area into two areas of distinct geology; the Karoo Supergroup geology to the north of the fault, and the Mokolian Supergroup to the south of the fault, both of which are represented in the study area by the Waterberg Group quartzites.

According to Dreyer (pers. comm. 2009) the Eenzaamheid fault acts as a watershed for groundwater flow in the study area, dividing it into two distinct groundwater compartments with very little (if any) flow across the fault boundary. It was observed from water chemistry data collected in the study area that the water found in these boreholes have very high chloride values which can be indicative of low recharge and little flow. These observations apply specifically to the chloride values for the borehole water located between the Daarby and the Eenzaamheid faults.

This cannot be construed as an indication of no flow across the fault boundary however, as there are many boreholes present in the same vicinity that do not display the same elevated Cl values. It is concluded that the most plausible explanation derives from the presence of high Cl values of the geology into which the boreholes have been drilled.

From observations in the study area, the faults serve as preferred pathways for the flow of water, having much higher transmissivities than the surrounding rock, with boreholes (in most cases) drilled near the faults showing higher yields than boreholes drilled further away from the faults.

According to Dreyer (pers. comm. 2009) the Eenzaamheid fault and the Daarby fault are impermeable (according to testing done by Dreyer, pers. comm. 2009) as evidenced by the difference in water levels displayed by boreholes drilled along the Daarby fault. Boreholes on the western side of the fault have deeper water levels than boreholes drilled on the eastern side of the fault. The assumption can therefore be made that the three main faults in the study area (the Eenzaamheid, Daarby and Zoetfontein faults) serve as no flow boundaries, although the faults themselves act as zones of higher transmissivities.

Consequently the study area can be divided into four distinct groundwater compartments by the faults. (Figure 89)

The compartments are:

- South of the Eenzaamheid-fault
- The area between the Eenzaamheid-fault, the Daarby-fault and the Zoetfontein-fault
- The area north of the Zoetfontein-fault
- The area to the east of the Daarby-fault

According to Dreyer (pers. comm. 2009) all the surface mining planned for the area will be carried out in the area north and west of the Daarby fault, the area delineated by the three major faults found in the study area. Taking the impermeability of the faults into consideration it can be concluded that any abstraction which takes place is confined to the area between the Daarby fault in the east, the Eenzaamheid fault in the south, the Zoetfontein fault in the north and the Limpopo River to the west, and will not influence the water levels outside the boundary formed by the faults and the river.

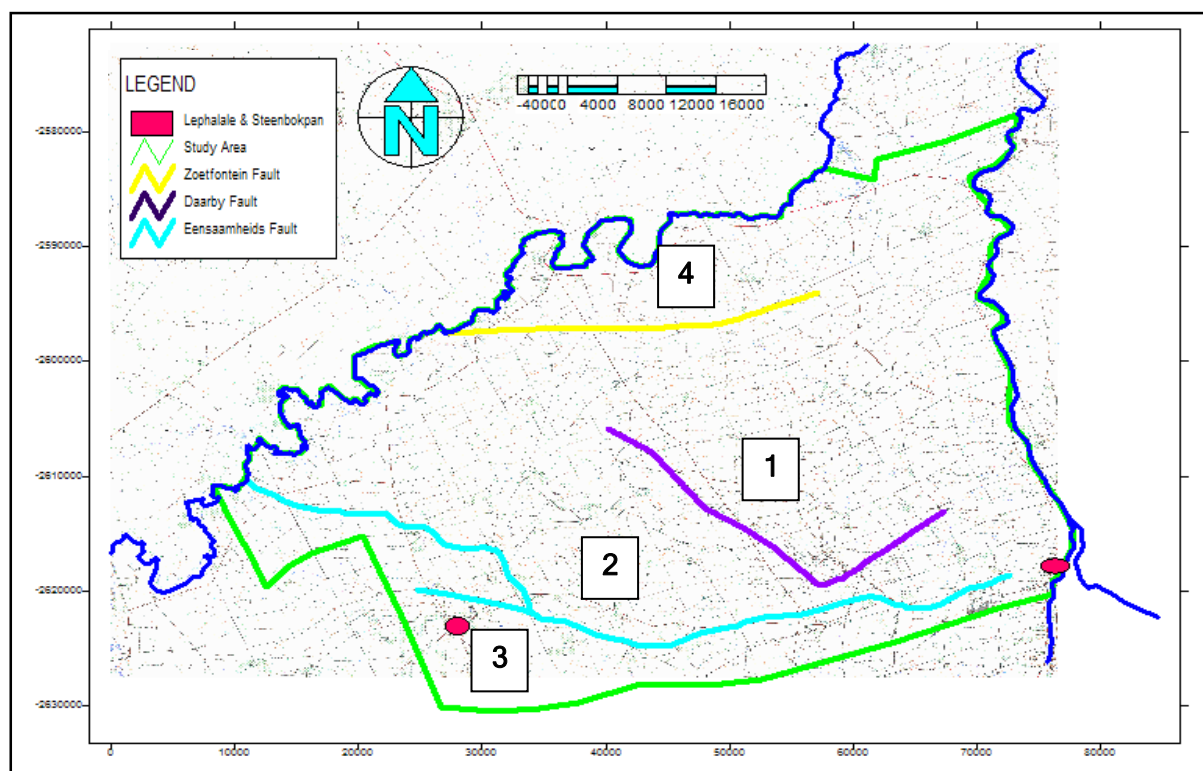


Figure 88: The groundwater compartments numbered 1 - 4, formed by the faults in the study area.

9.2. Aquifers

As described by (Hodgson and Krantz (1995) there are two distinct and superimposed groundwater systems in the geological formations of the coalfields in South Africa. These are the upper weathered aquifer and the system in the fractured rock below.

9.2.1. The Weathered Groundwater System

The top 5 - 15 m normally consists of soil and weathered rock (Figure 89). The upper aquifer is associated with the weathered horizon. In boreholes, water may often be found at this horizon. These aquifers are recharged by rainfall (Hodgson and Krantz (1995)).



Figure 89: Rocks from the weathered aquifer zones of the study area.

Rainfall that infiltrates into the weathered rock reaches impermeable layers of solid rock underneath the weathered zone. Movement of groundwater on top of the solid rock is lateral and mirrors the topography. This water reappears on the surface at fountains, where the flow paths are obstructed by barriers such as dolerite dykes, paleo-topographic highs in the bedrock, or where the surface topography cuts into the groundwater level at streams. The Waterberg Coalfields have a more arid climate when compared to other coal fields in South Africa, receiving only between 280 mm and 560 mm of rain annually.

The effect is less significant, although still visible during high rainfall. This effect can most clearly be seen during periods of high rainfall in boreholes, drilled into the Waterberg Group geology. The rainwater infiltrates through the weathered zones until it reaches an impermeable layer. Once the water reaches an impermeable layer, it will continue to flow along the layer to emerge later as a spring where the surface topography cuts into the groundwater level. It has also been observed in the study area that during times of high precipitation the recharge of these shallow aquifers is so high that boreholes that have been drilled into the aquifers are transformed into “artesian” boreholes. The weathered zone is generally low-yielding, because of its insignificant thickness.

The quality of the water is normally excellent and can be attributed to many years of dynamic groundwater flow through the weathered sediments. Leachable salts in this zone have been washed from the system a long time ago. It is recommended that aquifer testing not be done in the study area during the rainy season, as the above-mentioned phenomenon may impair the accuracy of the tests.

9.2.2. The Fractured Groundwater System

The grains in the fresh rock below the weathered zone are well cemented and do not allow significant water flow. All groundwater movement therefore occurs along secondary structures such as fractures, cracks, joints or intrusions in the rock (Figure 90) (Hodgson and Krantz (1995)). These structures are best developed in sandstone and quartzite, hence the better water-yielding properties of the latter rock types. Dolerite sills and dykes are generally impermeable to water movement, except in the weathered state. In terms of water quality, the fractured aquifer always contains higher salt loads than the upper weathered aquifer. The higher salt concentrations are attributed to longer contact times between the water and rock.



Figure 90: Rocks from the fractured aquifer zone, showing a bedding plane fracture outlined in red.

9.3. Water Levels

Water level data is available for the 1067 boreholes surveyed in the study area (Figure 91). Significant differences in the water levels have been observed in the study area with the extremes ranging from artesian boreholes, to boreholes that have water levels as deep as 154 m below surface (Figure 92). The average water level of the study area however is approximately 28 m below the surface.

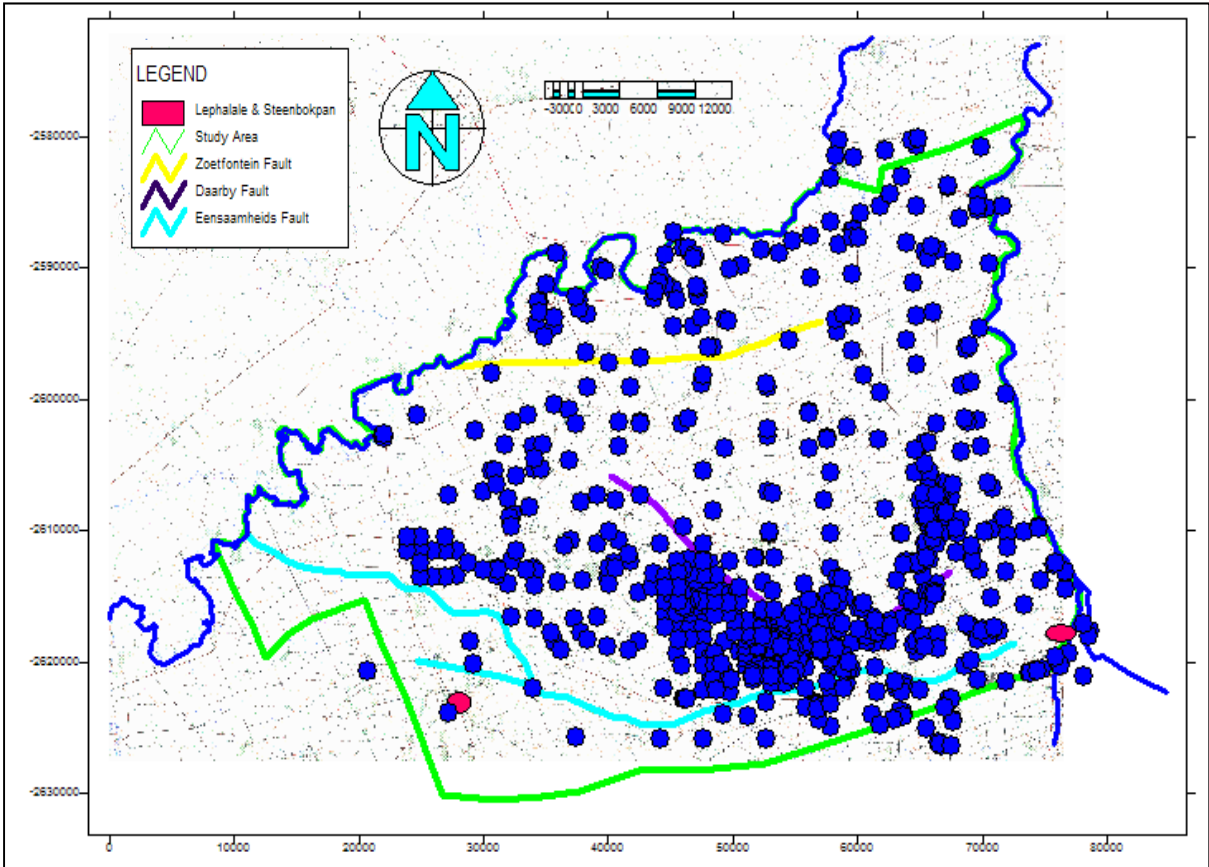


Figure 91: Boreholes in the study area for which water level data is available.

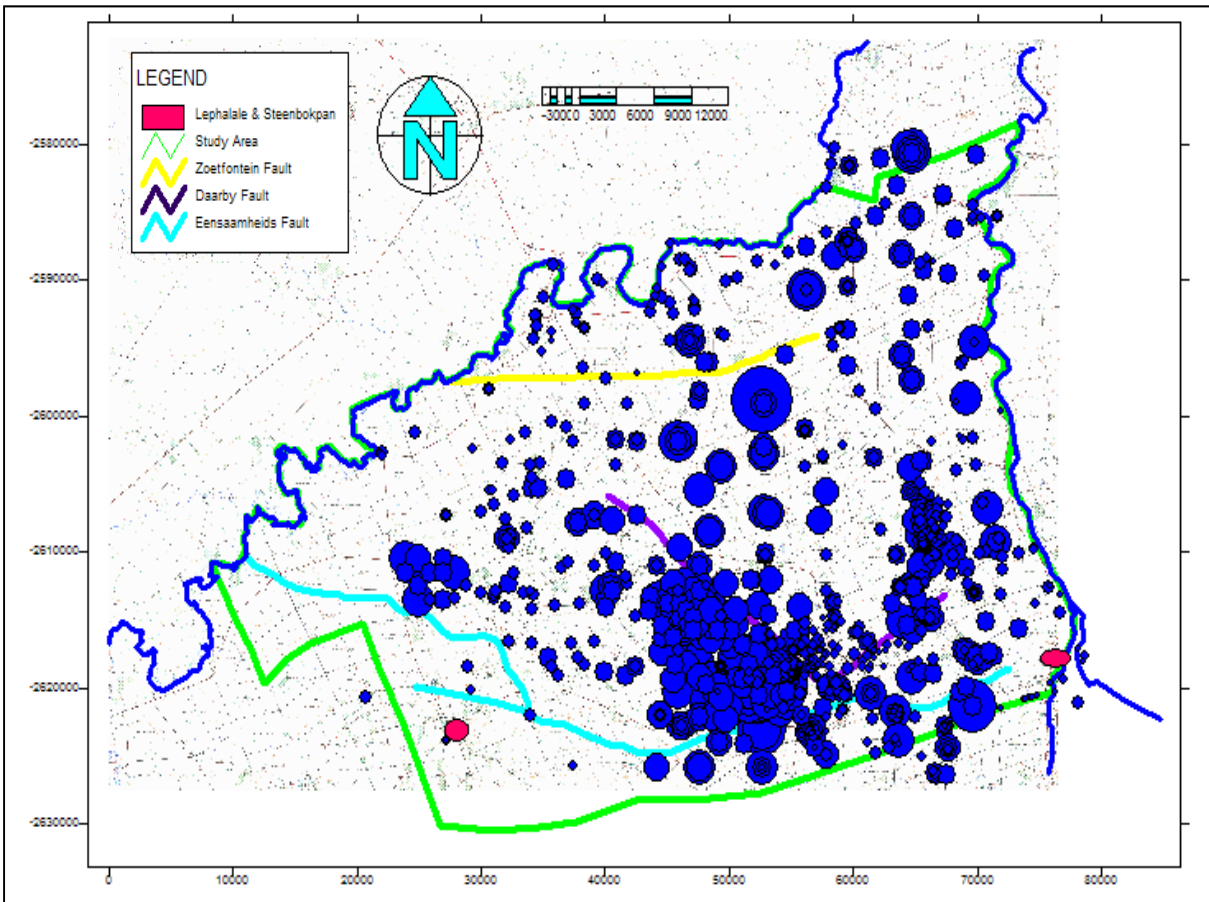


Figure 92: Map showing boreholes with proportional distribution of water level data.

The major contributors to increased water level depth are three fold;

- Firstly, the areas located near the centre of the study area have an elevated topography which leads to an increase in water-level depth.
- Large-scale abstraction taking place from boreholes in certain areas of the study area. The water abstracted from these boreholes is used for the watering of livestock, game and in some cases for domestic use.
- Due to the mine dewatering taking place at the Grootegeluk Mine, currently the only operational colliery in the study area.

In order to achieve a higher level of accuracy with regards to the groundwater levels and to determine if the water levels truly mirror the topography, the water level data was interpolated by means of the Bayesian interpolation methods.

These values along with the originally gathered data were contoured and plotted together with contour maps of the surface topography. From these maps the level of correlation could be better determined and deviation from the expected norms for Karoo type aquifers could be better observed.

The results are as follows.

9.3.1. Water-Level Contouring

A contour map of the water-level depth was constructed from the data that had been gathered (Figure 93). Figure 93 shows the contour map of the water level distribution found in the study area. The map displays water levels in meters below the surface. From Figure 93 one can observe that there are areas with deeper water levels and areas with shallower water levels.

The central areas show deeper water levels than the surrounding areas and the elevated nature of the central area is the likely cause of this. Additionally Figure 93 indicated that the average water levels for the study area are between 20 m and 40 m below the surface (numerically determined to be 28 m).

To this contour map, a map of the surface topography was added, the results of which are displayed in Figure 94. Figure 94 indicates that the water levels do mirror the topography. The elevated regions of the study area near the centre, along with the increased water levels can also be seen. It is interesting to note that the elevation near the centre of the study area has a north/south trend which is reflected by the water levels.

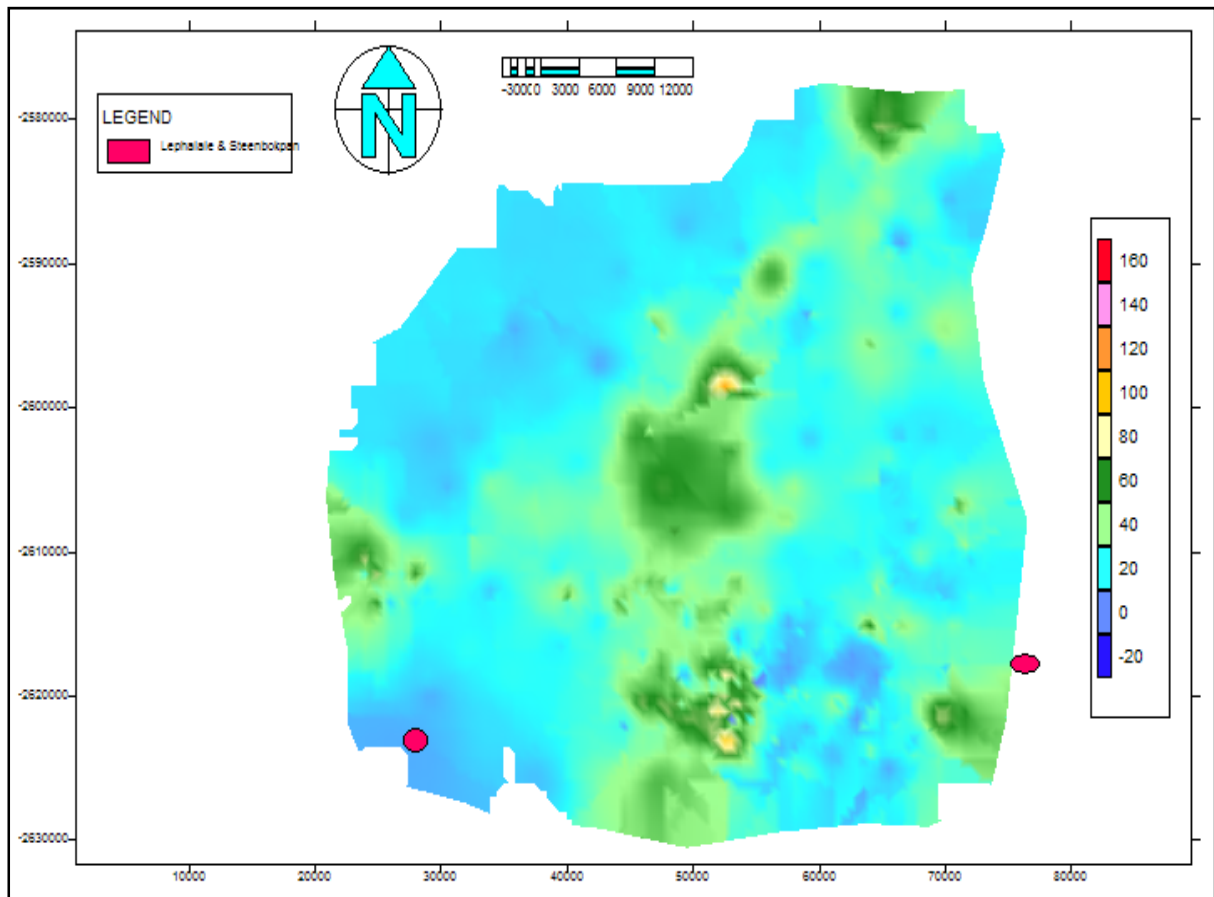


Figure 93: Contour map of the depth of water levels found in the study area (m below surface)

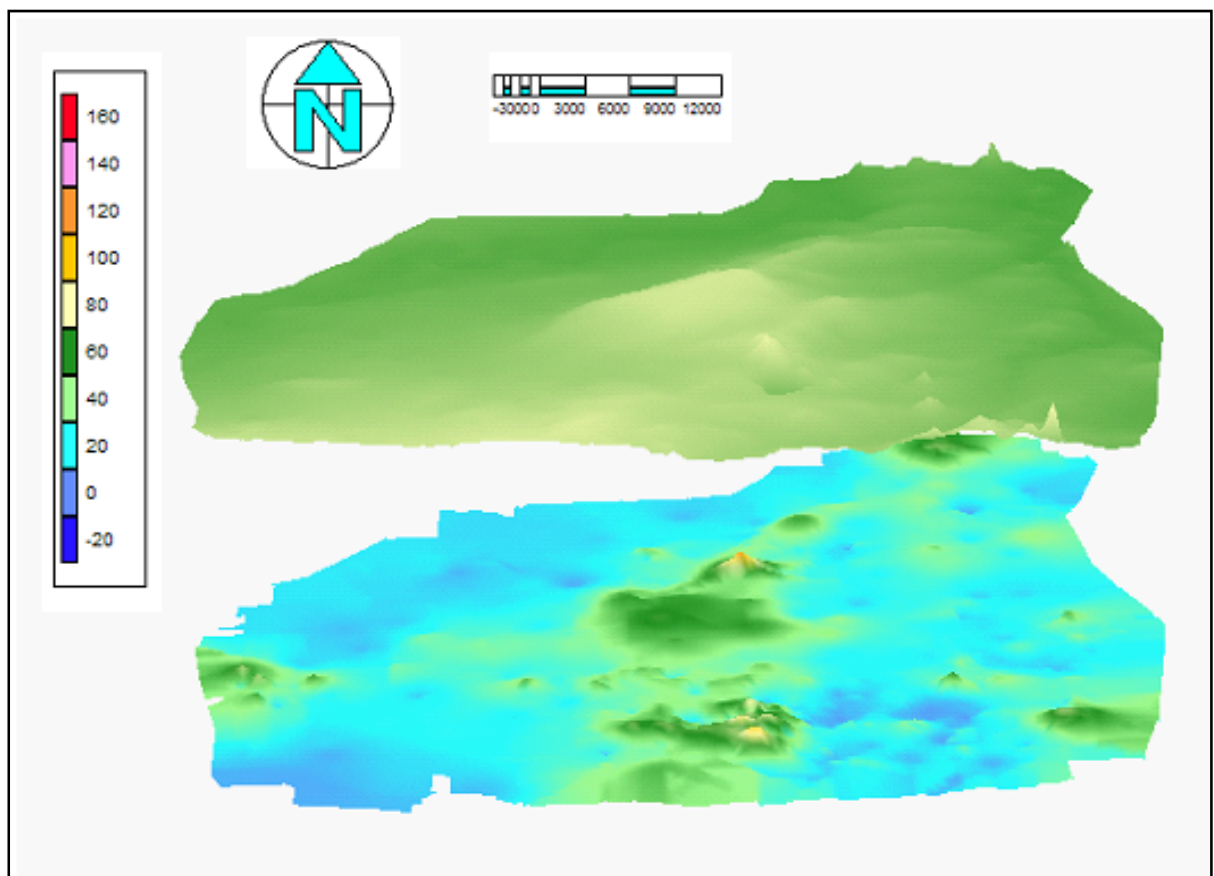


Figure 94: Topography and water level contour maps.

9.3.2. Water Level Elevation Contouring

Once it had been established that the water levels do follow the topography, contour maps of the water level elevations for the study area were constructed (Figure 95).

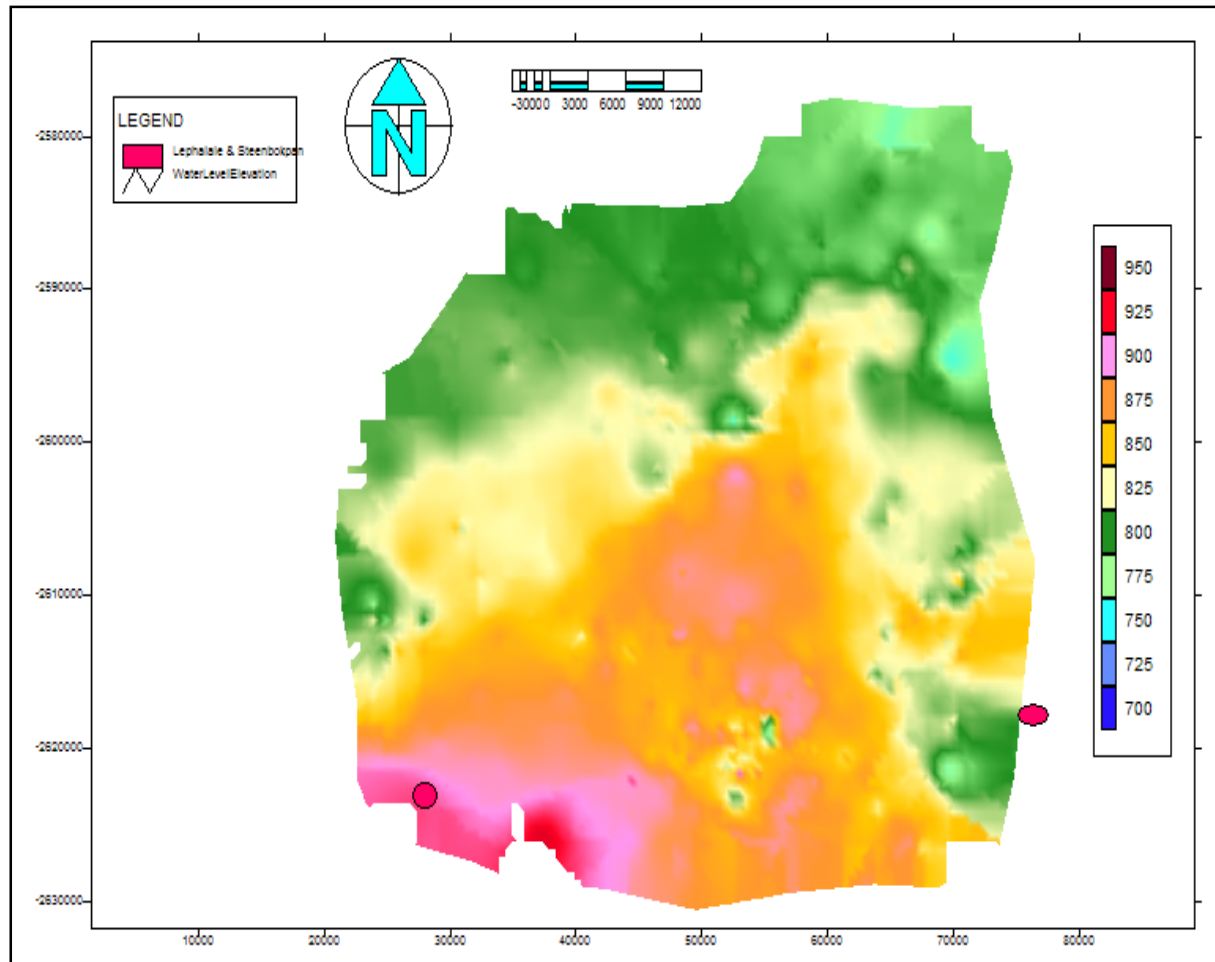


Figure 95: Water level elevation contour map for the study area.

Figure 95 displays much the same characteristics as Figure 93, with the centrally elevated areas displaying deeper water levels than the lower areas of the study area. Again when Figure 95 is added to a contour map of the topography, one observes that the water levels mirror the topography, as is the case in Figure 94.

9.3.3. Bayesian Interpolated Water-Level Contouring

The final set of contoured water level data was that which had been interpolated by means of Bayesian interpolation. This was done to achieve more accurate water level data for the study area. The results were plotted as a contour map and displayed in Figure 97. The correlation between the groundwater level data used during the Bayesian interpolation and the topography is displayed in Figure 96.

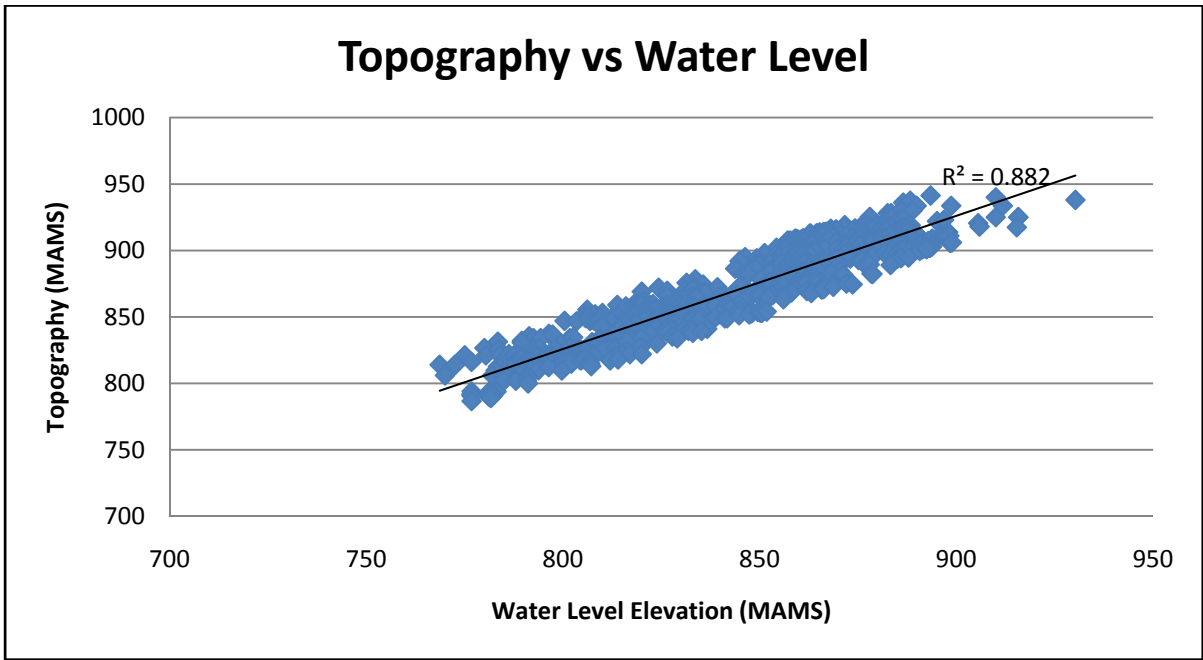


Figure 96: Correlation between Topography and water level data used for Bayesian interpolation.

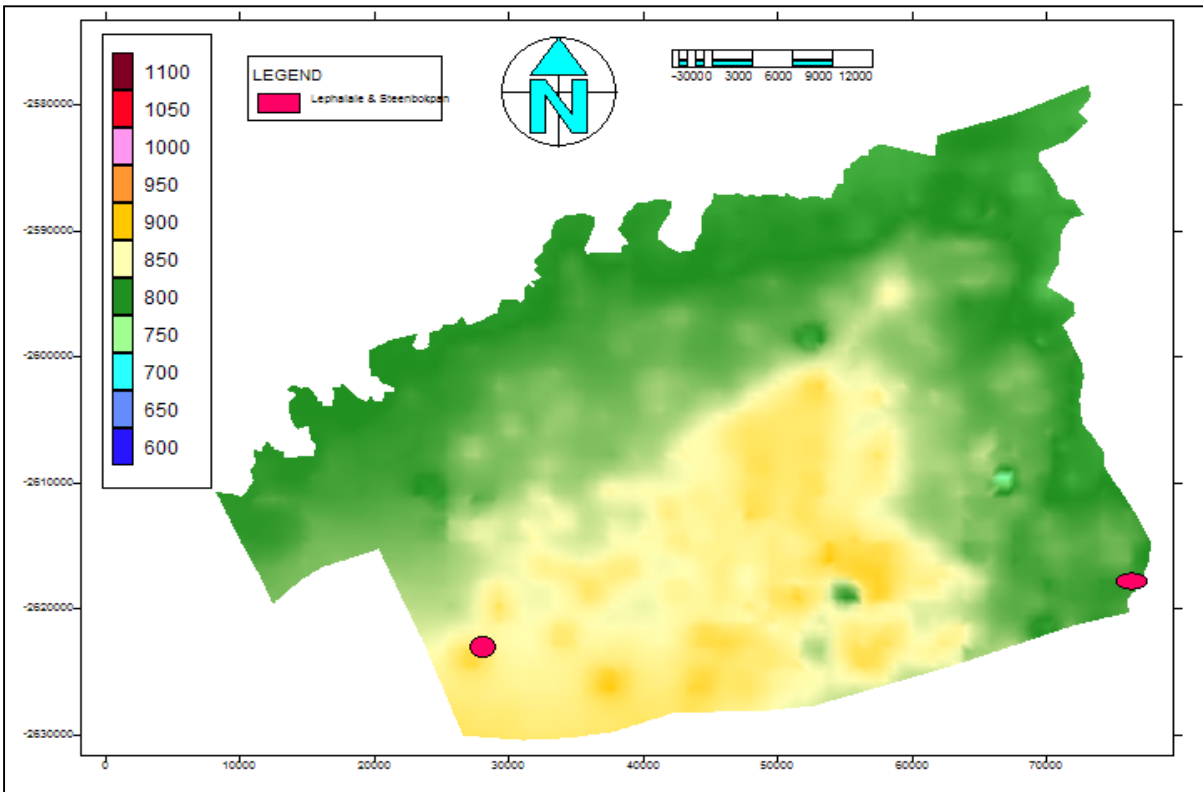


Figure 97: Bayesian interpolated water levels for the study area.

From the observation of the contour maps of the topography, the groundwater levels, the groundwater elevations and the Bayesian interpolated water levels of the study area, it becomes clear that the water levels in the area follow the topography. Furthermore all three different water-level contour maps exhibit the same trends, namely, that there is an elevated ridge of water levels (and topography) near the central part of the study area that runs roughly north/east south/west.

Using the water level elevation data and Bayesian data, flow vectors were added to the contour maps to determine the predominant flow directions for ground water in the study area (Figure 98). According to these flow vectors, the central areas of the study area are the driving force for groundwater flow in the area. From the data shown in Figure 93 to Figure 98, there can be no doubt that the groundwater flow in the study area follows the topography and would therefore flow away from the central part of the study area towards the low-lying areas near the boundaries of the study area, namely the two rivers.

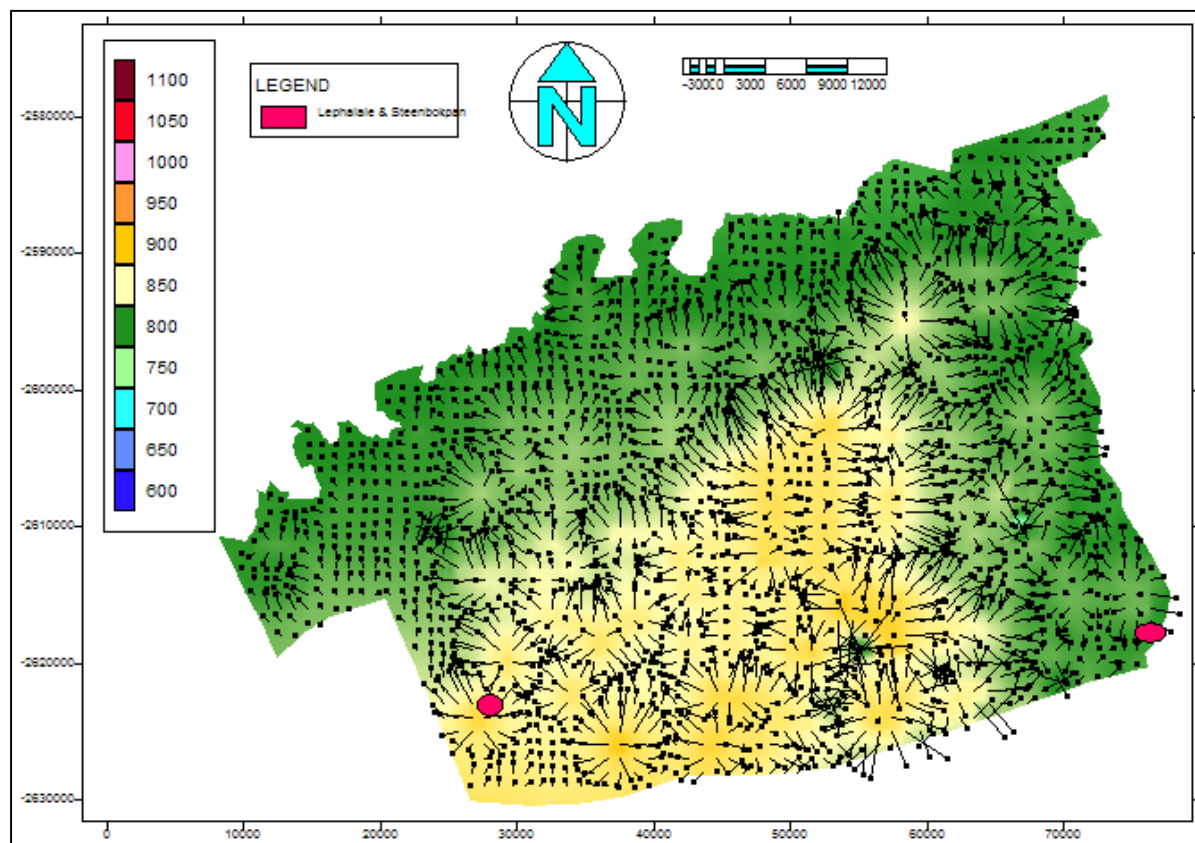


Figure 98: Bayesian interpolated water level contour map with flow vectors, indicating flow away from the central parts of the study area.

According to the flow vectors in Figure 98 the predominant flow directions of groundwater in the study area will be towards the east, the west and to the north, away from the central elevated regions with little if any flow towards the south. From observations made at the Grootegeluk Mine with regards to the influence which the mine and the dewatering of the mine may exert on the surrounding aquifers, it is expected that the addition of new open pits to the area (specifically in the central areas) will change the flow direction of groundwater (Figure 99) (These aspects will be discussed in more detail in Chapter 10). The changes which the open pits will effect in the topography (the excavation of big holes in the ground) will have an impact on the direction of flow of the groundwater. For example, if all the mines that are planned for the area were to be located near the centre of the study area, the excavation of the pits would lower the topography to such an extent that the flow direction of the groundwater would be influenced.

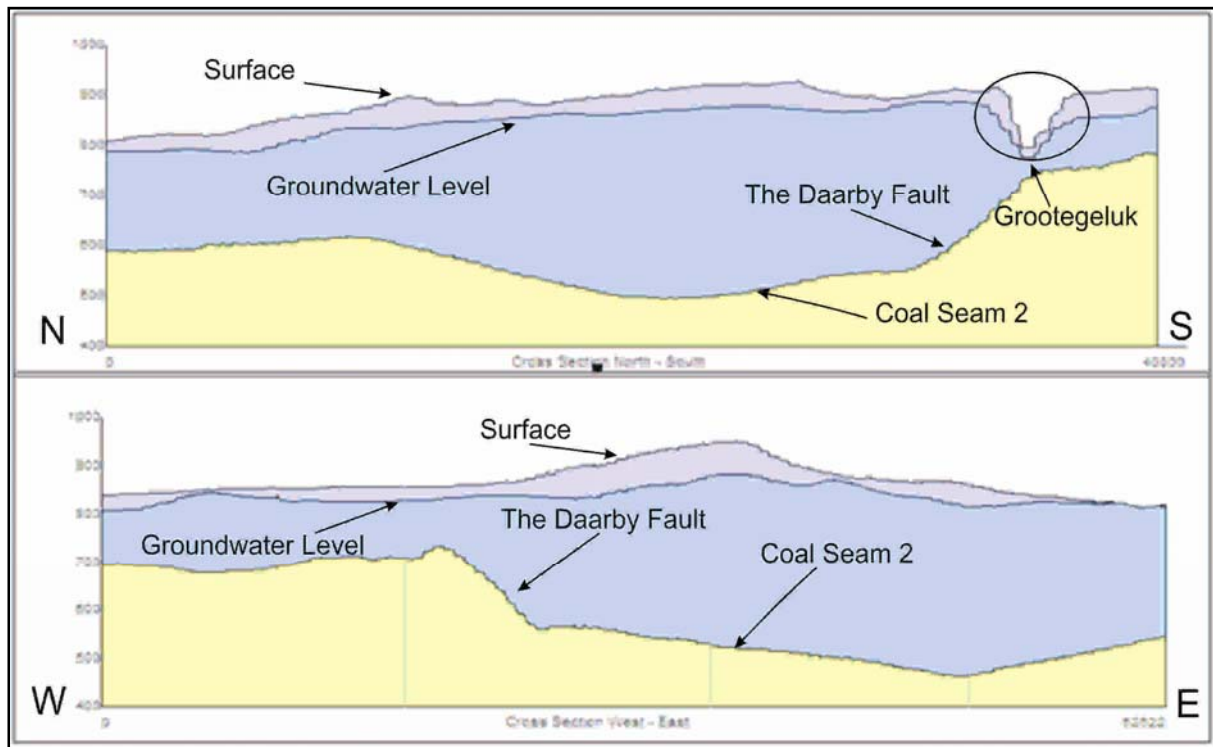


Figure 99: Sections through the study area, with the top section running through the Grootegeluk mine.

It is suspected that given the data displayed in Figure 99, the lower topography that will have been artificially created by the excavations of the mines will reverse the flow of groundwater. To put it differently, the groundwater will not be flowing away from the central areas, but towards them, more specifically towards the mines. The degree to which this will impact the rest of the study area is unknown and will be determined by factors such as the depth, size and locations of the open pits. This will be discussed in more detail in Chapter 10.

9.4. Aquifer Parameters

In order to obtain aquifer parameters for the study area, several slug and pumping tests were conducted and analysed to determine and identify any trend or divergence from the expected norms for Karoo type aquifers. These parameters were additionally required to serve as input parameters for the numerical modelling of the groundwater flow in the study area, used to predict dewatering cones and decant times.

9.4.1. Slug Testing

As slug testing can only give an indication of the parameters of a certain aquifer, only four such test results will be discussed. The four boreholes that were slug tested are located on the farms Vlakfontein, Tambotievley & Groenfontein (Figure 100).

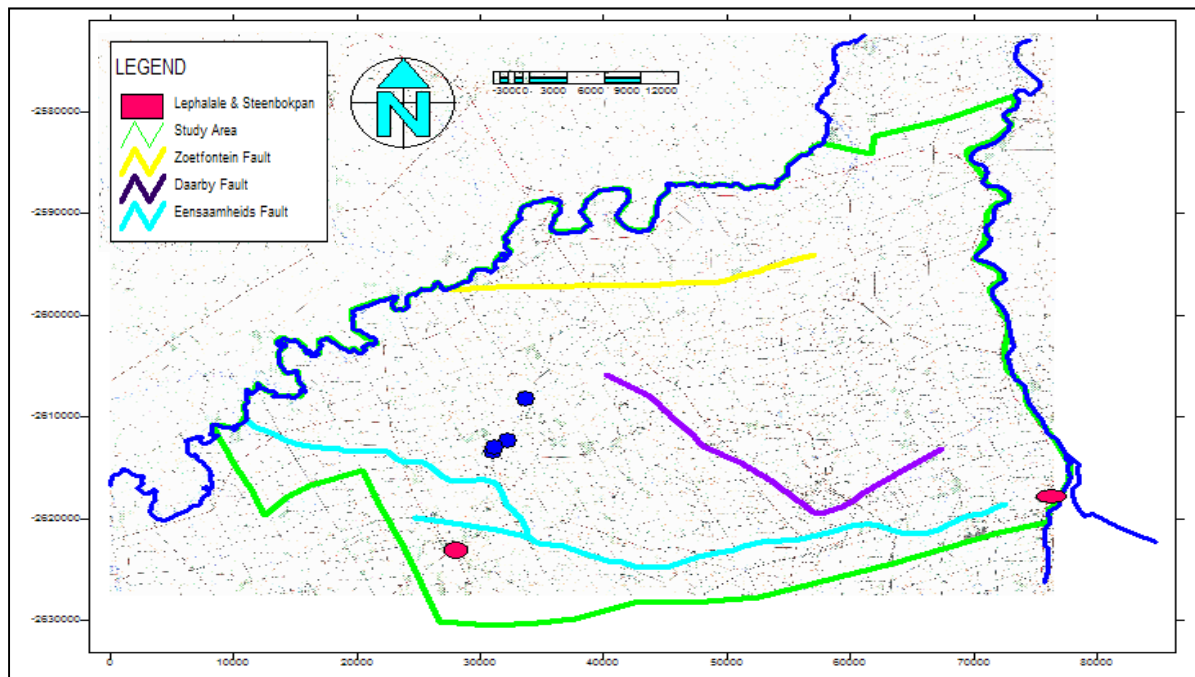


Figure 100: Location of the slug tested boreholes.

These farms are located in the north/western part of the study area. Three of these boreholes were subsequently pump tested as well. The slug test results indicated that the transmissivity of the boreholes varies greatly, keeping in mind that slug test data is inconclusive for determining the transmissivity of the whole area. These tests were conducted during a period of very high precipitation and it is expected that the results are only indicative of the transmissivities of the weathered aquifer zone. Accordingly the results may differ if the same boreholes are tested during the dry season. Table 15 provides a summary of results of the slug tests for the four boreholes.

Table 15: Summary of slug test results for the study area.

Borehole Name:	Yield (l/s):	Transmissivity (m ² /d):	Transmissivity (m ² /d) of Formation - Average:
Slpmt 1	26.22	131.08	65.54
Slpmt 2	2.09	10.45	5.22
Slpmt 3	1.97	9.87	4.93
Slpmt 4	4.88	24.4	12.20

As can be seen from the table, the transmissivities and yields of the boreholes vary greatly. However, the trend of boreholes with high yields having high transmissivities may be observed. A brief discussion of the findings of each individually slug tested borehole follows.

9.4.1.1. Borehole Slpmt 1

The borehole Slpmt 1 was slug tested and recovered to its initial water level in 1.3 seconds, accordingly the estimated yield for the borehole was calculated to be 26.22 l/s. A transmissivity of 131.08 m²/d was calculated for the formation in the vicinity of the borehole. A transmissivity of 65.5 m²/d was calculated for the formation in the vicinity of the borehole on average (Table 16).

Table 16: Slug test results for Slpmt1

SLUG TEST - YIELD ESTIMATE									
Note: All the estimates are qualified guesses and could be wrong									
BH Name =	BH1 (Sasolpmt1)								
Recession time (s) for 70% recovery	1.3								
Yield of BH (L/s) =	26.22								
T (m ² /d) of formation in vicinity of BH =	131.08								
T (m ² /d) of formation - Average =	65.54								
<table border="1" style="margin-left: auto;"> <tr> <td colspan="2" style="background-color: #FF0000; color: white; text-align: center;">RECOMMENDATION</td> </tr> <tr> <td colspan="2" style="background-color: #FF0000; color: white; text-align: center;">Conduct a Pump test on BH</td> </tr> <tr> <td colspan="2" style="background-color: #FF0000; color: white; text-align: center;">First estimate of sustainable yield (L/s)</td> </tr> <tr> <td style="width: 50%;"></td> <td style="text-align: center; background-color: #FF0000; color: white;">5.24</td> </tr> </table>		RECOMMENDATION		Conduct a Pump test on BH		First estimate of sustainable yield (L/s)			5.24
RECOMMENDATION									
Conduct a Pump test on BH									
First estimate of sustainable yield (L/s)									
	5.24								
<table border="1" style="margin-left: auto;"> <tr> <td style="width: 50%;">K-value of fracture (m/d) =</td> <td style="background-color: #008000; color: white;">50243.70</td> </tr> <tr> <td>T-value of fracture (m²/d) =</td> <td style="background-color: #008000; color: white;">10048.74</td> </tr> </table>		K-value of fracture (m/d) =	50243.70	T-value of fracture (m ² /d) =	10048.74				
K-value of fracture (m/d) =	50243.70								
T-value of fracture (m ² /d) =	10048.74								

9.4.1.2. Borehole Slpmt 2

The slug test for the borehole displayed a yield of 2.09 l/s with a transmissivity of 10.45 m²/d for the formation in the vicinity of the borehole and a transmissivity of 5.22 m²/d for the formation in the vicinity of the borehole on average (Table 46 of Appendix B). The borehole recovered to its initial level after 2.09 seconds.

9.4.1.3. Borehole Slpmt 3

From the slug test of Slpmt3, the yield of the borehole was 1.97 l/s with a transmissivity of 9.87 m²/d for the formation in the vicinity of the borehole and a transmissivity of 4.93 m²/d for the formation in the vicinity of the borehole on average (Table 47 of Appendix B). The borehole recovered to its initial water level of 1.97 s. This borehole is located at a point furthest away from the other boreholes that were slug tested. The borehole also has a low yield and a correspondingly low transmissivity.

9.4.1.4. Borehole Slpmt 4

From the slug test of Slpmt4, the yield of the borehole was 4.88 l/s with a transmissivity of 24.40 m²/d for the formation in the vicinity of the borehole and a transmissivity of 12.20 m²/d for the formation in the vicinity of the borehole on average (Table 48 of Appendix B).

The borehole recovered to its initial water level of 4.88 seconds. Borehole Slpmt 4 is located between boreholes Slpmt 1 and Slpmt 2. The borehole has a higher yield and transmissivity than borehole Slpmt2 but nowhere near the values observed for borehole Sasolpmt1. It is likely that this borehole is located on, or near the same fracture system as Slpmt1 even though a distance of approximately 100 m separates the two boreholes.

From the slug tests, the transmissivity in the formations varies greatly, although two of the transmissivity values do fall within the same range. There is no clear indication of the transmissivity from the slug test results, taking into account that a slug test is at best only a guess of the parameter values.

9.4.2. Pumping Tests

A total of 51 boreholes located throughout the study area have been pump tested and analysed (Figure 101) in order to obtain parameters for the aquifers of the study area. As it is impractical to discuss all of the analysed boreholes, the methods used will be shown by means of using the data and analyses of the three boreholes Slpmt1, 2, 3 & 4. A summary of the results of the analyses for the boreholes is given in Table 17.

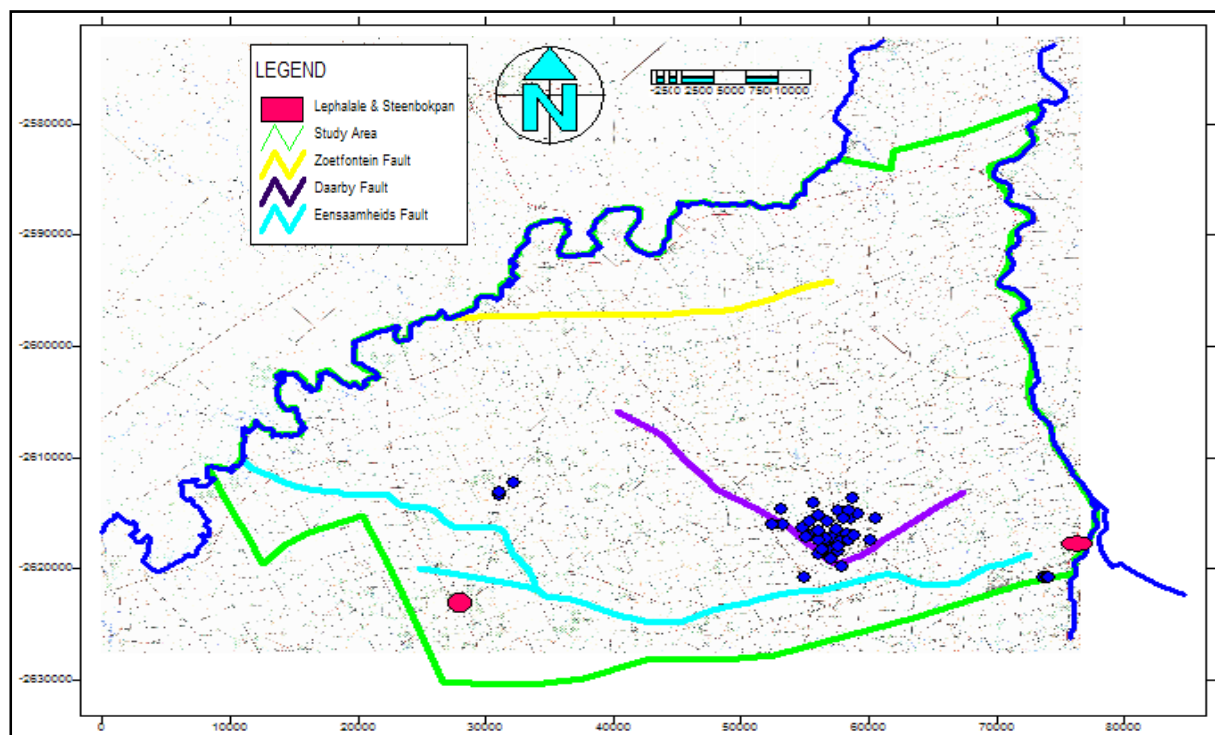


Figure 101: Location of the pump tested boreholes.

Three of the four boreholes that were slug tested were subsequently pump tested and the results of these tests were analysed by means of the FC software program that has been developed at the Institute for Groundwater Studies at the University of the Free State.

Table 17: Summary of pumping test results for the boreholes in the study area.

9.4.2.1. Borehole 1 (Slpmt1)

The borehole is located on the farm Vlakfontein. The depth of the borehole is 45 m and the static water level was at 21.07 m below surface after the pump had been lowered into the borehole. During the slug test, the water level recovered almost instantly, indicating a yield of approximately 20 l/s. A pumping rate of 2 l/s was chosen due to constraints on pump size. The borehole was pump tested for three hours and then left to recover. The water level recovered to within 90% of its original level within 15 minutes. The pumping test data was analysed with the FC software programme developed by the Institute for Groundwater Studies. The results indicate a yield of 6.35 l/s and the recovery tests indicated a high transmissivity of 600 m²/d (Table 18).

Table 18: Sustainable yield for Slpmt1.

Method	Sustainable yield (l/s)	Late T (m ² /d)
Basic FC	5.10	632.4
Cooper-Jacob	7.59	497.5
Barker	0.54	
Average Q_sust (l/s)	6.35	

When analysing a logarithmic plot of the analysed pumping test data, the graph displays three areas where the data levels off (underlined in red). These areas indicate possible fractures. Accordingly, Figure 102 indicates three fractures located below the water level located approximately 27 cm, 32 cm and 35 cm below the water level respectively (fracture zone).

These fracture zones contain large quantities of water as is evident from the low level of drawdown that was achieved during the test. The fracture zone is located very close to the water level surface and will be in danger of running dry during either a drought, or from over abstraction. It is unknown if there are more fractures present further down the borehole, as very little drawdown was achieved during the test.

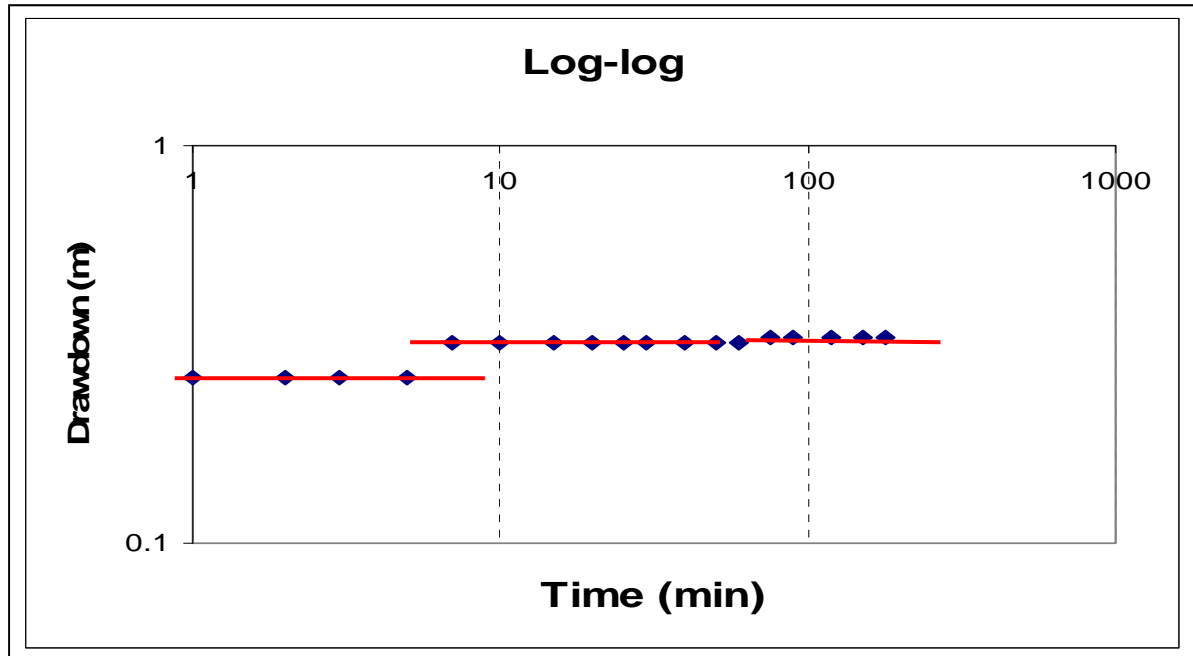


Figure 102: Log vs. Log plot of the analysed pump test data.

To obtain the recommended sustainable yield by means of the Cooper-Jacob method for yield estimation, the drawdown data obtained from the pumping test of the borehole was entered into the FC software programme. The data was fitted accordingly. The fitted graph is displayed in Figure 103 and the results of the analyses are displayed in Table 18.

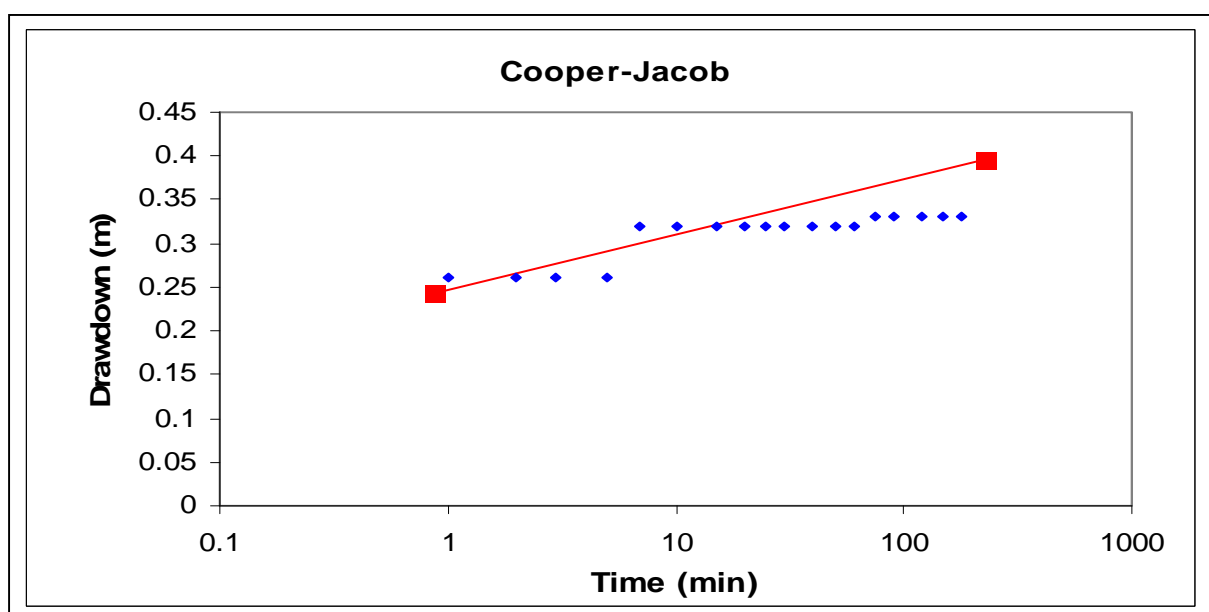


Figure 103: A Cooper-Jacob graph of the drawdown at Borehole 1 (Slpmt1).

The water level and the cluster of fractures is located at a depth of between 21 m and 22 m below the surface. From the pumping test it could not be determined if this area forms part of the weathered zone, in which case the yield obtained is not a true reflection of a safe yield for the borehole and it is recommended that the borehole be retested during the dry season.

Table 19: Pumping test result summary for Slpmt1

Recommended abstraction rate (L/s)		7.00	for 24 hours per day		
Hours per day of pumping	8	12.13	L/s for	8	H/d
Amount of water allowed to be abstracted per month		18144	m ³		
Borehole could satisfy the basic human need of		24192	persons		

Due to precipitation during the summer months, more water will assemble in the weathered zone than during the dry season. If this is the case, the borehole yield may drop, or even run dry during winter months. However, if the water level is below the weathered zone, the yield obtained will be a true reflection of the yield of the borehole. The pump used for this test did not have the capacity to stress the borehole to its limits, to determine the additional fractures, or to determine the location of the weathered zone. No boundaries could be identified. The findings for this borehole are inconclusive, but do give an indication of conditions of the aquifers found in the study area. The test further indicates that there are boreholes present in the study area that have very large yields and high transmissivities.

9.4.2.2. Borehole 2 (Slpmt2)

This borehole is located near the entrance of the farm Tambotievley. The depth of this borehole could not be determined. The borehole had a static water level of 26.39 m. The borehole was slug tested and indicated a yield of 2.5 l/s. The pumping test was performed at a pumping rate of 1.5 l/s after the slug yield had been determined at 2.5 l/s, with the pumping test lasting 90 minutes. Once the pumping had stopped the borehole was recovered for 60 minutes. The results of the test indicated a yield of 0.19 l/s, (Table 20) with the recovery tests indicating a transmissivity of 3 m²/d.

Table 21: Sustainable yield for Slpmt2.

Method	Sustainable yield (l/s)	Late T (m ² /d)
Basic FC	0.19	2.2
Cooper-Jacob	0.17	2.2
Barker		
Average Q_sust (l/s)	0.18	

The test results indicate a low-yielding borehole with a low transmissivity. The log vs. log graph of this borehole, indicate two areas of possible fractures, the first is located 8 m below the water level (a small fracture) and the second 16 m below the water level (Figure 104). The borehole could however not be stressed enough to dewater the second fracture due to pump limitations. There may be additional fractures deeper down the borehole, which could not be determined.

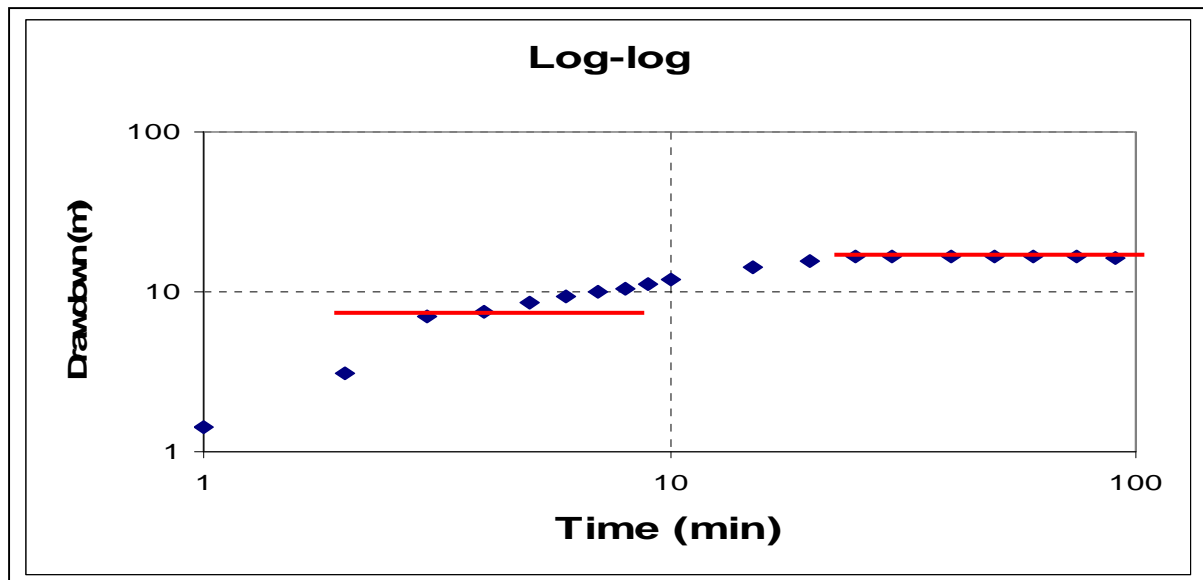


Figure 104: Log vs. log plot of borehole Slpmt 2.

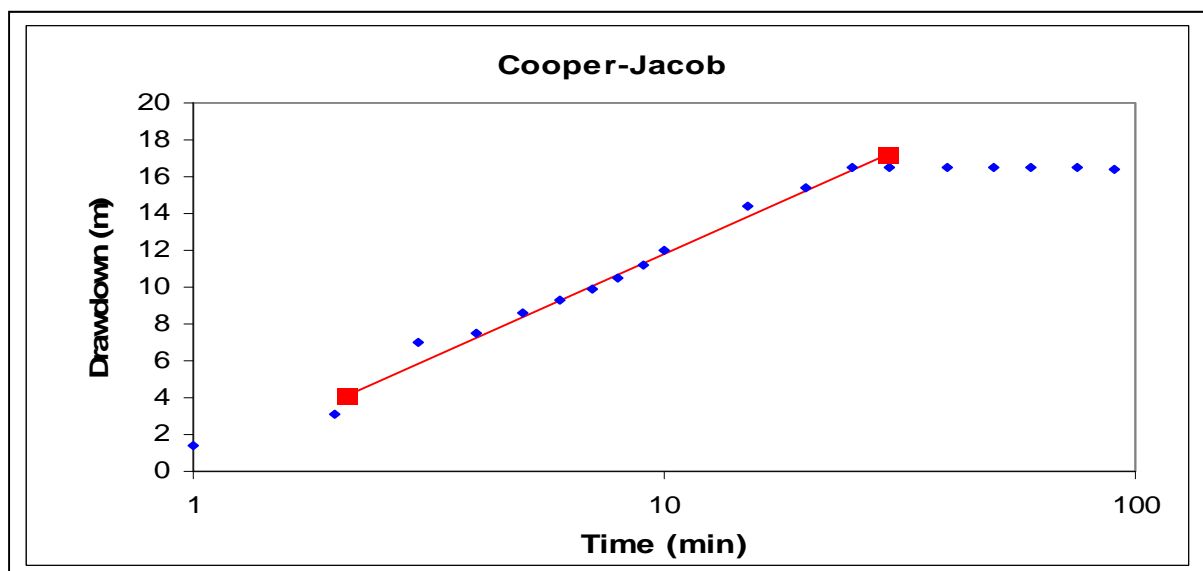


Figure 105: A Cooper-Jacob graph of the drawdown for Borehole 2 (Slpmt2).

The results from the testing indicated a low-yielding borehole, and that the initial slug test yields were incorrect. Once again due to the shallow water depth there is uncertainty about the depth of the weathered zone for this borehole. It is likely that the initial high yields observed from the slug test were the result of the water level being in the weathered zone and not the result of high-yielding fractures.

Two fractures were observed in the borehole, but the latter of these could not be stressed to the extent that an accurate yield could be calculated for the borehole. It is recommended that the borehole be tested during the dry season and that the results be compared to the results obtained during this study in order to determine a more accurate yield for the borehole. No boundaries could be identified during the course of the test.

Table 22: Pumping test result summary for borehole Slpmt2.

Recommended abstraction rate (L/s)	0.50	for 24 hours per day		
Hours per day of pumping	8	0.87	L/s for	8 hour s per day
Amount of water allowed to be abstracted per month	1296	m ³		
Borehole could satisfy the basic human need of	1728	persons		

9.4.2.3. Borehole 3 (Slpmt4)

This borehole is located on the farm Vlakfontein. The static water level for this borehole was located at 19.57 m, with a depth of approximately 40 m. The slug test indicated a yield of 4.5 l/s. From the slug test a pumping rate of 2 l/s was determined and the pumping test lasted for 3 hours after which the borehole was allowed to recover for 3 minutes, Thereafter the water level recovered to 90% of its original level. A summary of the test indicates a yield of 0.72 l/s, with the recovery tests indicating a transmissivity of 15 m²/d (Table 23).

Table 23: Sustainable yield for Slpmt4.

Method	Sustainable yield (l/s)	Late T (m ² /d)
Basic FC	0.74	22
Cooper-Jacob	0.7	25
Barker		
Average Q_sust (l/s)	0.72	

The yield and transmissivity of this borehole is considerably higher than that of borehole 2 (Slpmt 2) and might be an indication that the borehole is located near the same fracture network as borehole 1 (Slpmt 1). However, once again the borehole could not be stressed to a large enough degree due to pump constrictions.

The log vs. log graph for this particular borehole indicates two potential fractures which could also potentially be interpreted as one large fracture. In all likelihood these are not two different fractures but a zone of fractures located 2 m below the water level.

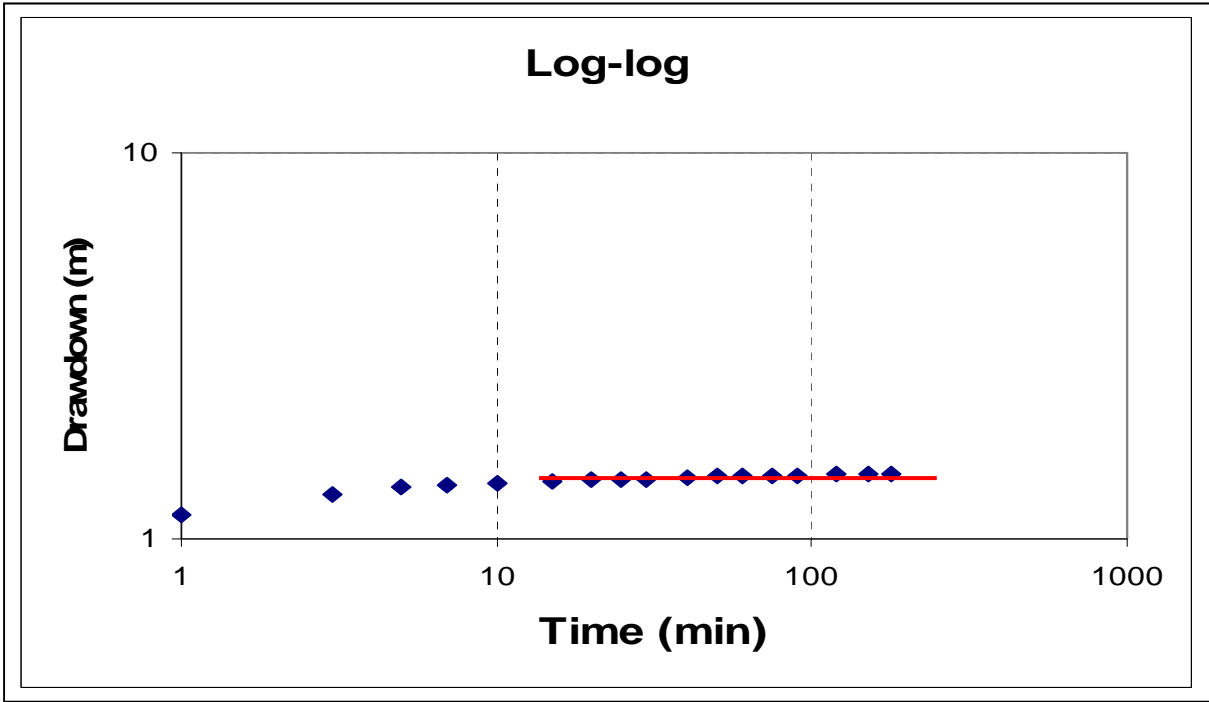


Figure 106: A Log-Log graph of the drawdown observed at Slpmt3, the red line indicating a possible fracture.

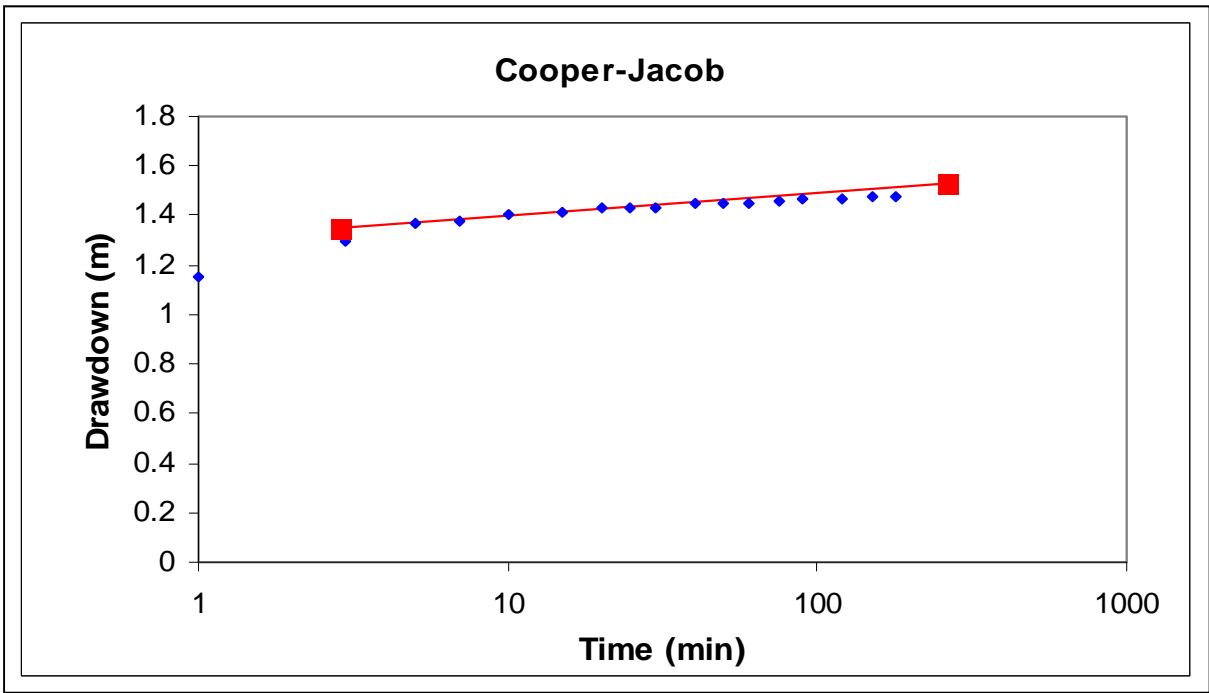


Figure 107: A Cooper-Jacob graph of the drawdown at Slpmt3.

The results for borehole Slpmt 4 are inconclusive (Table 24). From observations in the field it was determined that the water level of the borehole is well within the suspected weathered zone for the study area (top 30 m). This fact combined with the high precipitation that took place during the time of testing has, more than likely, influenced the outcome of the tests. The high yield of the borehole, combined with the inadequate strength of the pump, resulted in insufficient draw down for the borehole to make any accurate conclusions about the yield or the location of potential boundaries.

Table 24: Pumping test result summary for Slpmt4.

Recommended abstraction rate (L/s)		1.00	for 24 hours per day		
Hours per day of pumping	8	1.73	L/s for	8	hours per day
Amount of water allowed to be abstracted per month		2592	m ³		
Borehole could satisfy the basic human need of		3456	persons		

9.4.3. Discussion of Aquifer Parameter Testing Results

According to the slug and pumping tests of the western parts of the study area, there are vast differences in the transmissivities of the area and yields of the boreholes. It must however be kept in mind that these test results could have been influenced by the high quantities of rainfall during the time of testing. A total of 51 boreholes have been pump tested in the study area from 1987 to the present.

A greater quantity of boreholes has been tested around the Grootegeluk Mine than in any other location in the study area. Some tests have been conducted to the west (Slpmt1 - 4) and some to the east (H21-0637, H21-0638 and H21-0663). Those to the east were drilled by the Department for Water Affairs and Forestry and are located in the Waterberg Group. The north-eastern parts of the study area have not been tested, as this area will not be mined (Dreyer 2009).

The pumping test results indicated that the transmissivities and yields of the boreholes in the study area vary greatly, with transmissivities as low as 0.31 m²/d to as high as 600 m²/d. The harmonic mean for the transmissivity values for all the tested boreholes was calculated to be 0.4m²/d. This low transmissivity is a result of the geology of the study area (mostly alternating layers of shale and mudstone interspersed with sandstone and coal) and the fact that these geological formations are very dense, and allowed for very little through-flow.

From the findings it is predicted that regardless of the location of the mines in the study area, with the exception of a mine being located on a fault, there will be very little influx of water into the mines. The low trends in transmissivity result in the slow movement of water and will result in the slow influx of groundwater to the mines (30000 l per month at the Grootegeluk Mine), with the exception of the mines located in the areas that have much higher transmissivities such as fault zones. Additionally the data indicates that there are only a few areas displaying large transmissivities, and most commonly found in the vicinity of faults. Accordingly it is expected that in at least some of the cases, where mines are located near faults, they stand to have a much greater influx of groundwater into their workings.

For example, the boreholes drilled in the vicinity of the Grootegeluk Mine - which has the highest yields and transmissivities - are drilled either on, or in close proximity to the Daarby and Eenzaamheid faults. Some of the other boreholes that have large yields and high transmissivities are the ones that have been drilled into the Waterberg Group of Rocks. As indicated, these boreholes have much higher yields and transmissivities than other boreholes found in the study area. It must be noted that even these boreholes are located near faults. The data for the three boreholes drilled in the Waterberg Group show higher transmissivity than the boreholes drilled into Karoo rocks in the rest of the study area (Table 17). This happens regardless of the fact that the Waterberg Group rocks are much denser than the Karoo rocks and should accordingly have lower transmissivities. These higher transmissivities are likely due to a larger degree of fracturing in the Waterberg Group, compared to the Karoo rocks.

These fractures provide flow conduits for groundwater moving through the formations at much faster velocities than the water in the Karoo formations. It could however also be caused by higher levels of piezometric pressure in the Waterberg rocks than in the Karoo rocks.

From these results, in conjunction with the deep water levels, the low rainfall and the high evapotranspiration, it is predicted that the pits in the study area will display similar characteristics as the Big Hole in Kimberly (Figure 108). This means, in essence, that the pits in the study area may have water flowing into them, but will never decant.



Figure 108: The Big Hole located in the city of Kimberley in the Northern Cape province of South Africa.

9.5. Recharge

In order to determine the impacts of the current activities, and to predict the potential impacts of the planned new activities in the study area, it was necessary to determine the recharge of the aquifers in the study area. In order to calculate the recharge for the study area, two methods for determining recharge were used. The first was the chloride-mass-balance method. This method was used due to the availability of data and the effectiveness of this type of recharge calculation. The second method used was the E.A.R.T.H. model. Once again, the availability of data and the reliability of the calculations were the deciding factor in selecting this method.

9.5.1. Chloride in the Study Area

Before a discussion of the recharge itself, the Cl values in the study area will firstly be briefly discussed.

The data for the recharge determinations was gathered from various sources; these included data received from the Grootegeluk Mine, other companies currently operating in the study area and from groundwater samples taken from the study area which were analysed at the IGS laboratory. The distribution of the samples is displayed in Figure 109.

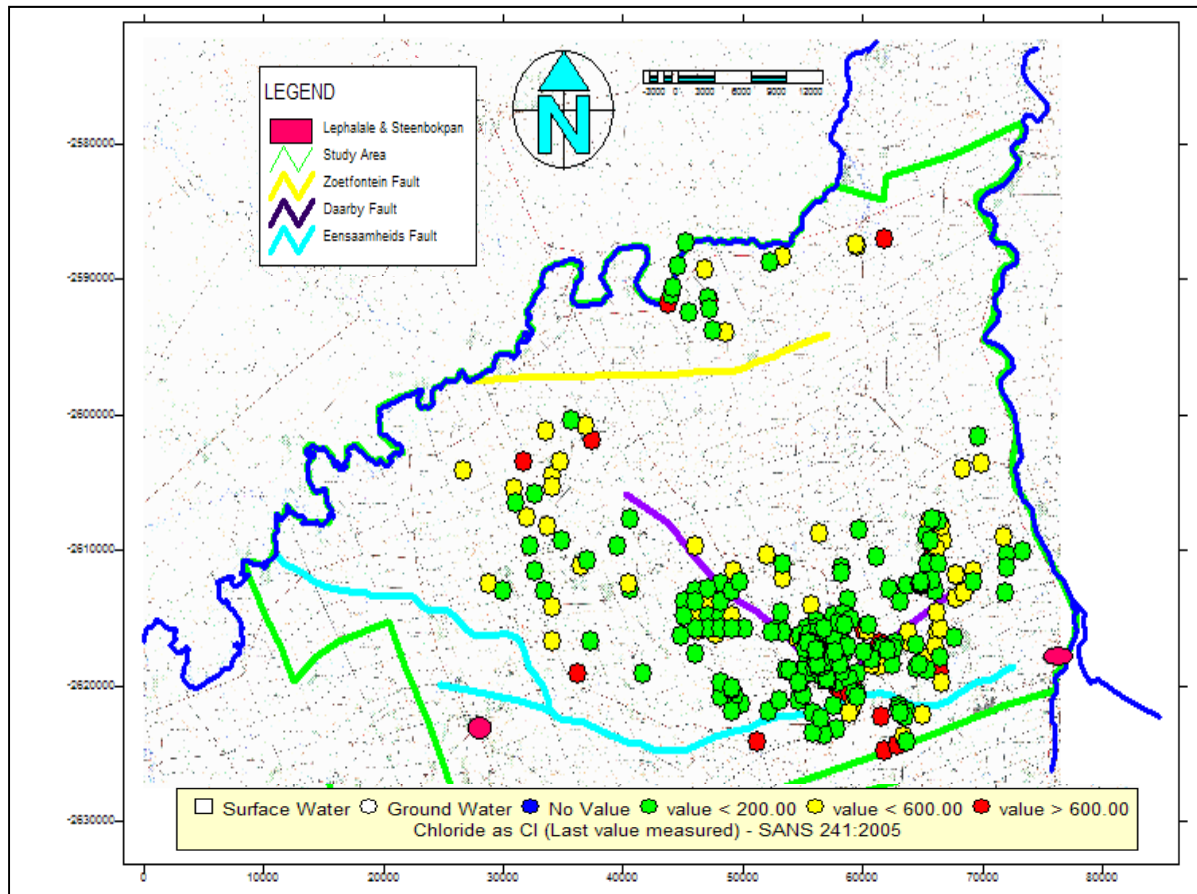


Figure 109: Distribution of the samples boreholes in the study area.

Due to the lack of access of some parts, samples covering the entire study area could unfortunately not be obtained. A total of 222 samples were analysed for their chloride content, the results of which are given in Appendix C. From the values analysed, the data suggests that there is a large range for the Cl values found in the study area, with the lowest value being only 6 mg/L and the highest value a soaring 2573 mg/l (Figure 110).

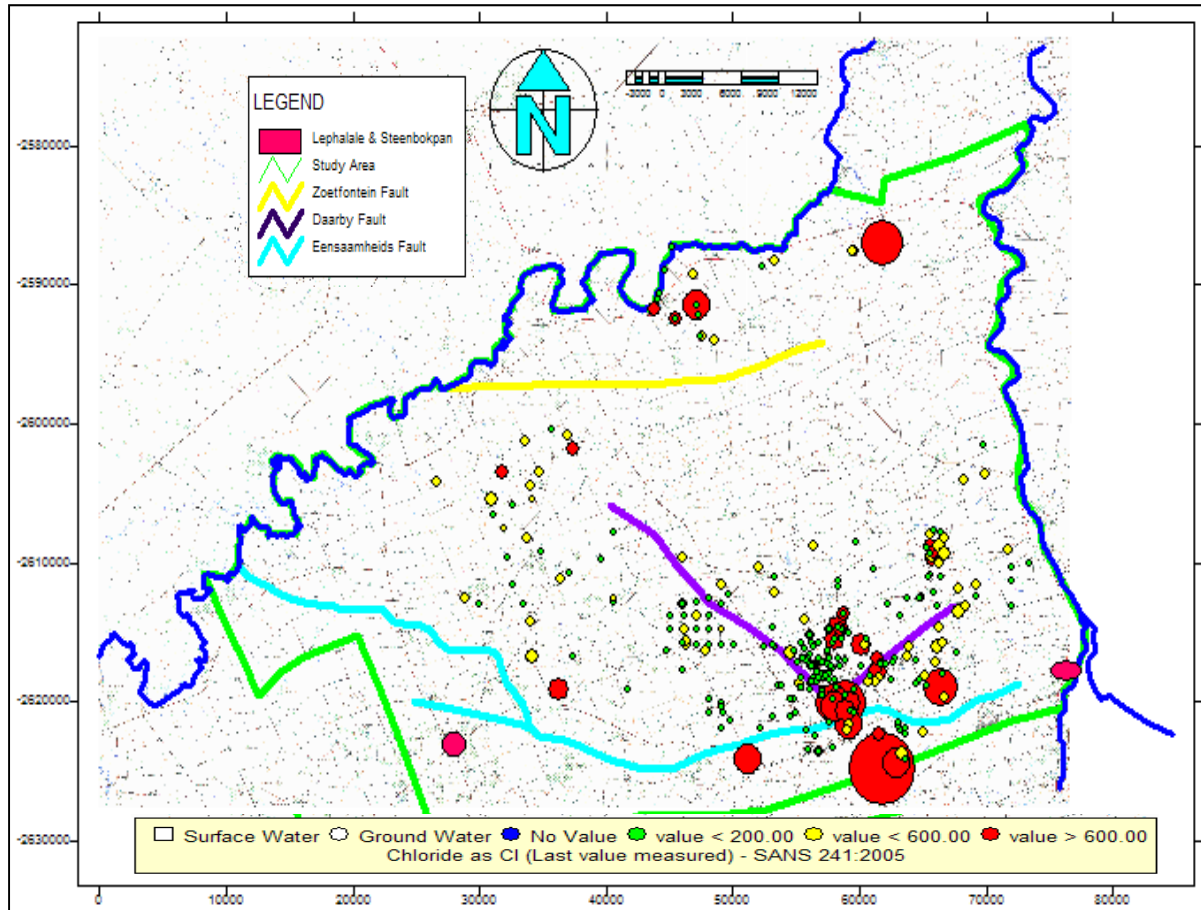


Figure 110: Value distribution for the measured Cl in the study area.

The causes for these variations are unknown.

Some of the theories that account for the high Cl values are:

- The high Cl values found are related to geology (the rocks have salt contents).
- Due to large levels of abstraction the Cl in the water has become concentrated resulting in these high values.
- The high values are possibly related to power station activities.
- The waters are naturally saline with the boreholes being of great depth (Usher *et al.*, 2005).

In an effort to better gauge the overall Cl levels for the study area, a contour map of the Cl values for the study area was constructed (Figure 111).

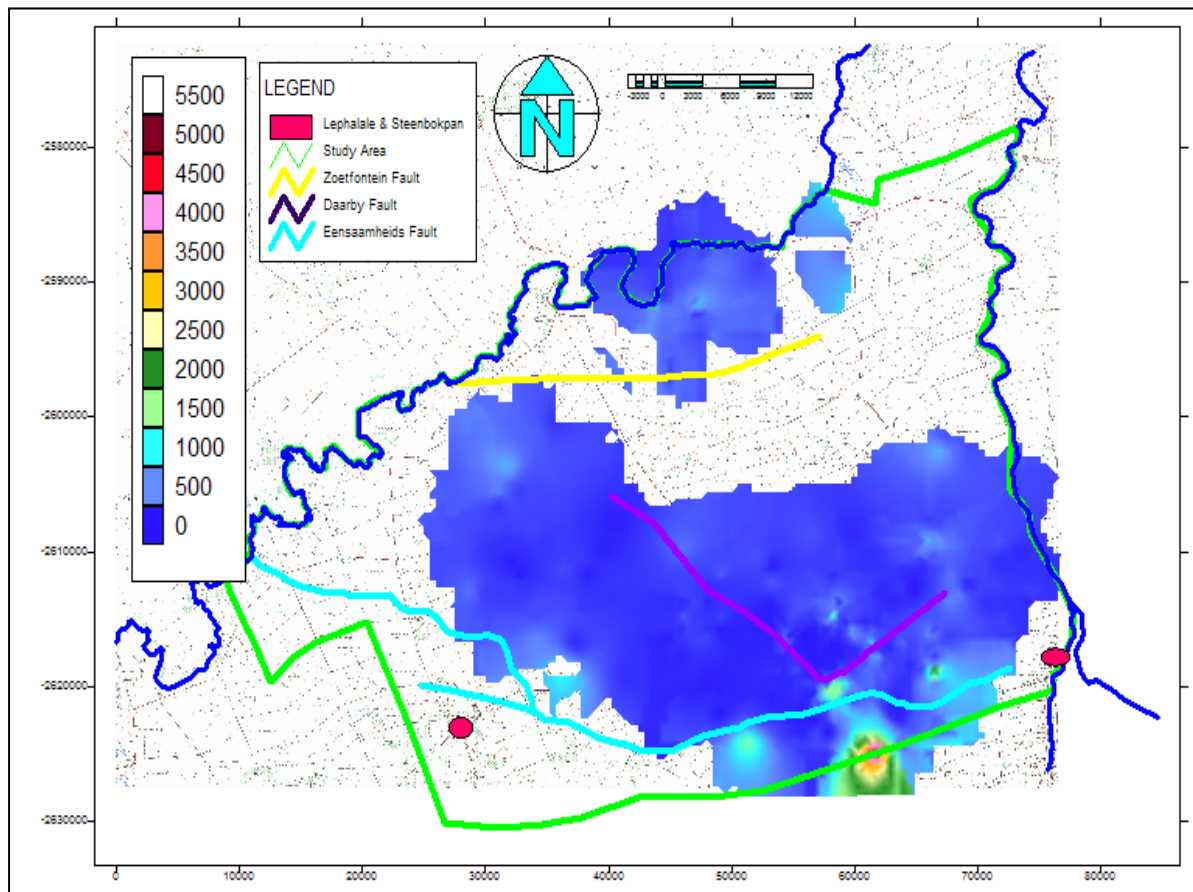


Figure 111: Contour map for CI values in the study area.

Figure 111 shows that with the exception of the extreme values, the CI levels in the study area are generally high. This has been observed in the field by the salty taste of the water samples from the boreholes. When the data was analysed it indicated six boreholes that have been drilled between the Eenzaamheid fault and the Daarby fault with high CI values (Figure 112 & Figure 113). This was initially suspected as being indicative of no flow taking place between these two faults. Dreyer (pers. comm. 2009) indicated that the faults are impermeable.

This hypothesis was however discarded upon closer inspection of the data, This indicated that there were boreholes which displayed low CI values in the vicinity of the boreholes with the high CI values. It is suspected that the six boreholes located between the faults displaying the elevated EC values, are located in geology that is responsible for the elevated EC values.

According to Dreyer (pers. comm. 2009) there is an extension of the Daarby fault the runs along the same area where the boreholes displaying the elevated EC are located. It is possible the inorganic pollutants may have moved along this extension and contaminated the boreholes. Dreyer (pers. comm. 2009) additionally indicated that this extension connects the Daarby and Eenzaamheid faults in this vicinity. It is therefore plausible that the elevated

CI values are the result of groundwater flowing from the contact zone between the Karoo and Waterberg group rocks.

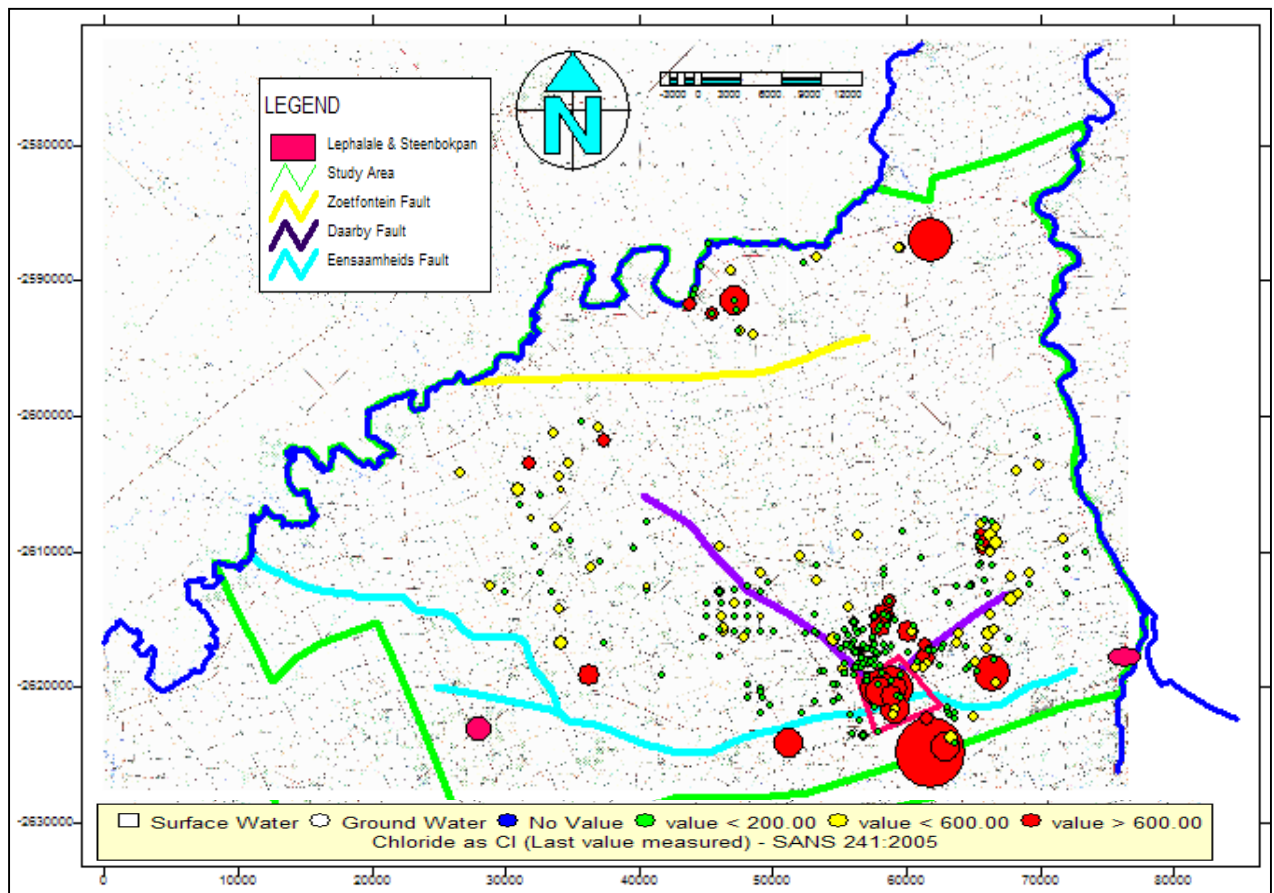


Figure 112: Boreholes located between the faults.

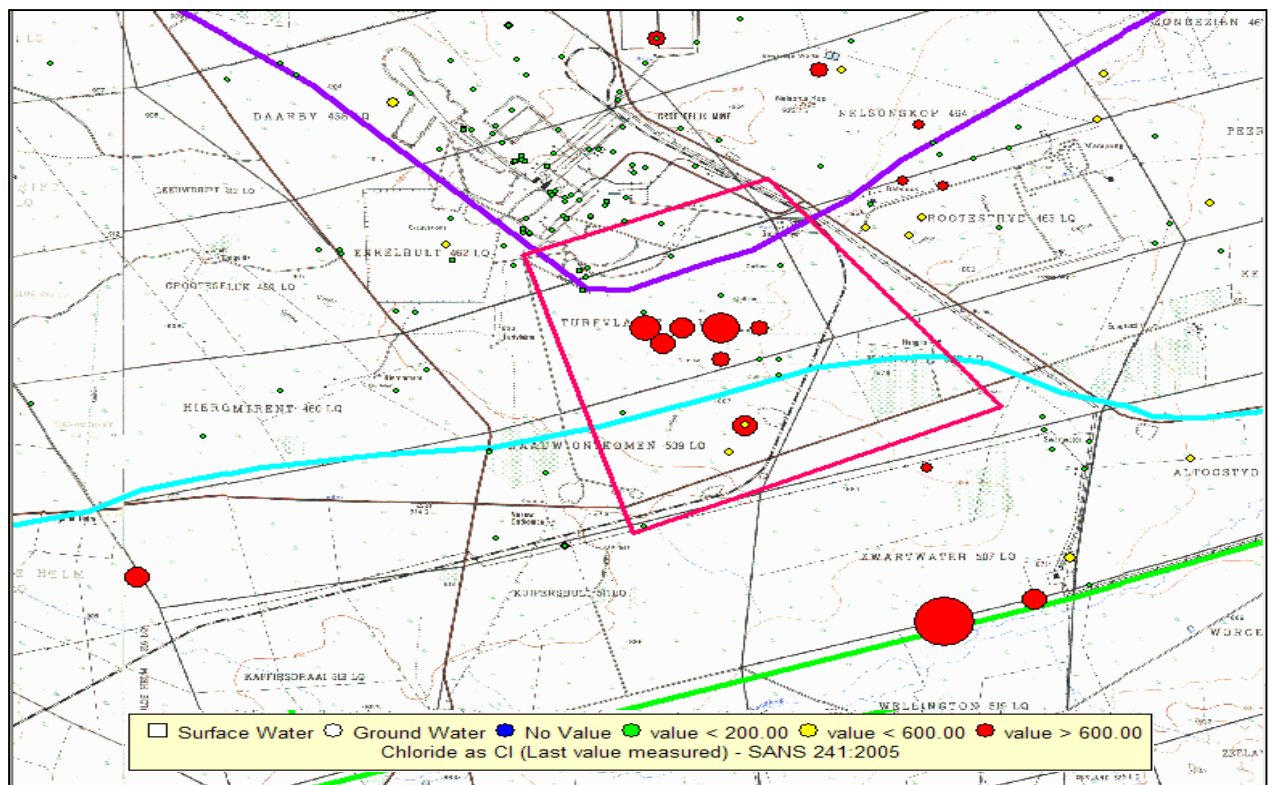


Figure 113: Close-up look at the boreholes located between the faults.

9.6. Recharge Determinations

9.6.1. The Chloride- Mass- Balance Method for Determining Recharge

As previously mentioned information on 222 boreholes was collected for use in recharge determination with the CI method. From the analysed values the data suggests that there is a large range for the CI values found in the study area, with the lowest value being a mere 6 mg/l and the highest value a substantial 2573 mg/l. The harmonic mean was calculated and used for the recharge determinations of the study area. This came to a value 62.76 mg/l CI. From the calculations using this harmonic mean value, a total recharge of 1.59% for the study area was calculated. The marked degree of variation in the CI values lead to a substantial variation for the recharge calculations, dependent on whether the recharge was calculated for the individual boreholes. The results ranged from recharge as high as 18% (6 mg/L CI), to as low as 0.4% (2573 mg/l CI) depending on the location of the boreholes and the CI content of their waters.

The results obtained from the recharge calculations for each individual borehole were plotted against the boreholes (Figure 114) and the same was done for the CI values (Figure 115). This was done for the purpose of obtaining a better understanding of the distribution of the recharge percentages and the CI values. These two graphs were then combined to produce Figure 116, which indicated that an inverse correlation between the percentage recharge and the CI values exists, as one would expect. The data therefore indicates a good correlation between the present recharge and the CI values (Figure 116).

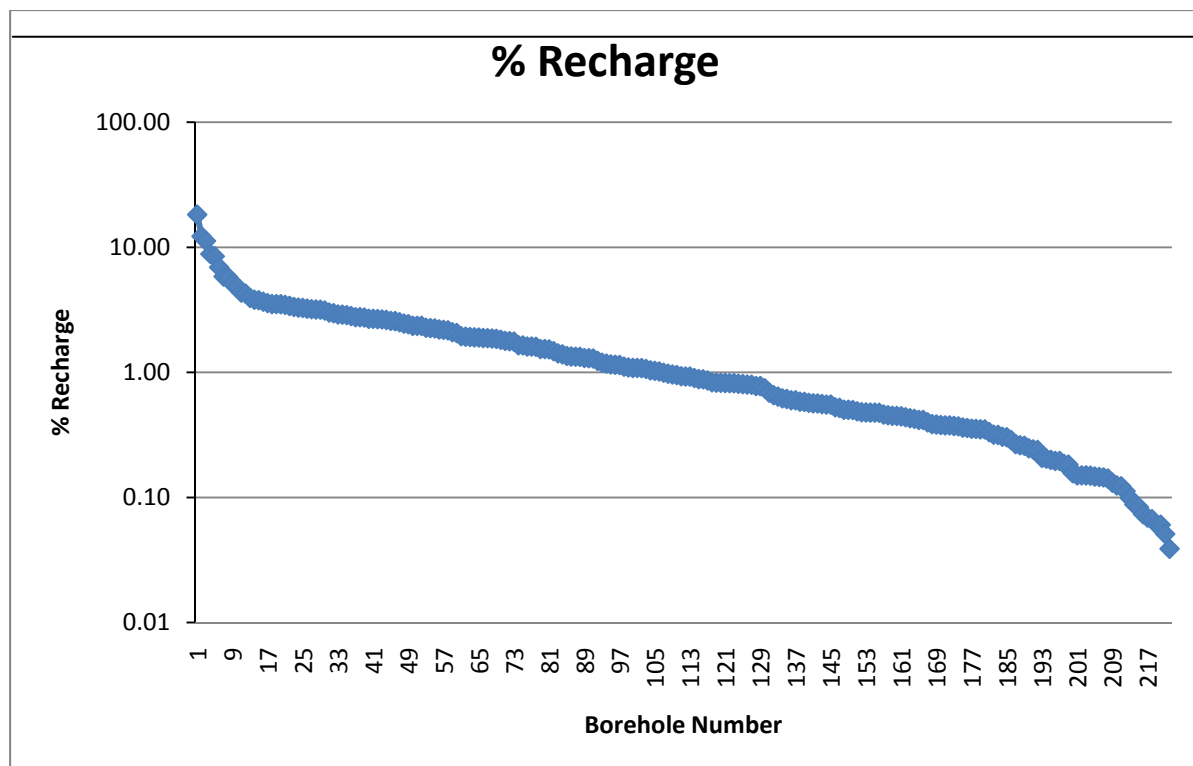


Figure 114: % Recharge for individual boreholes.

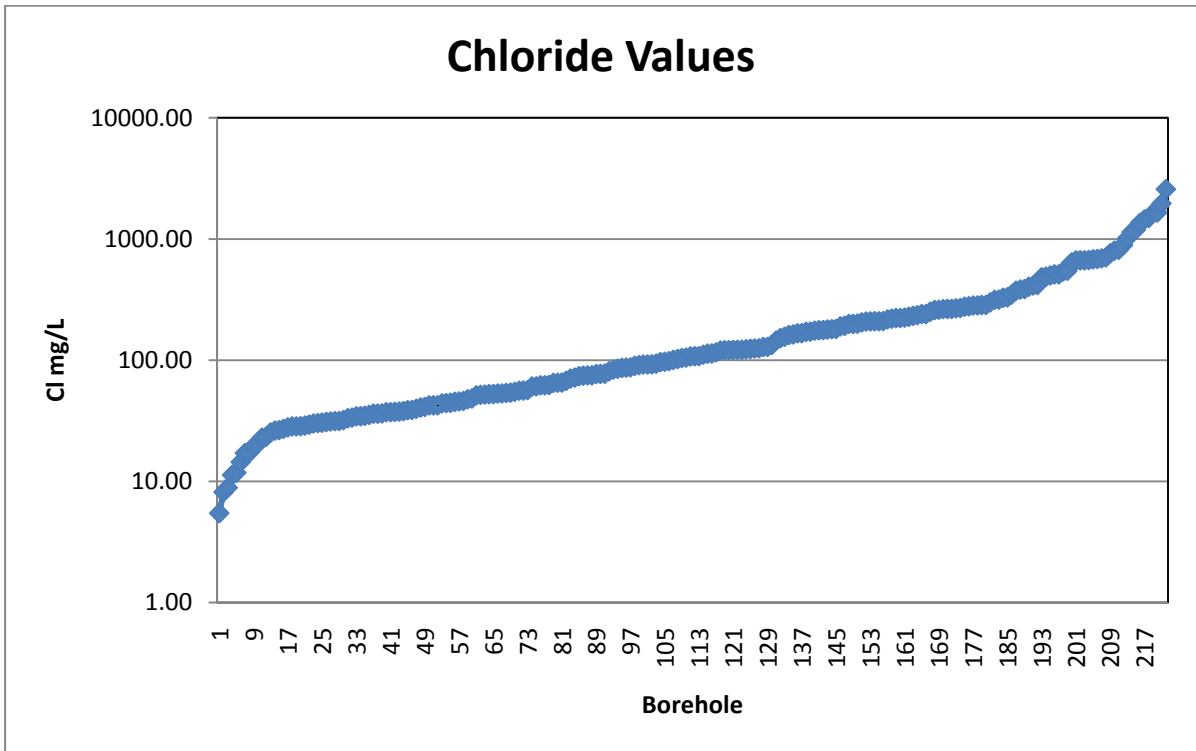


Figure 115: Cl values for each individual borehole.

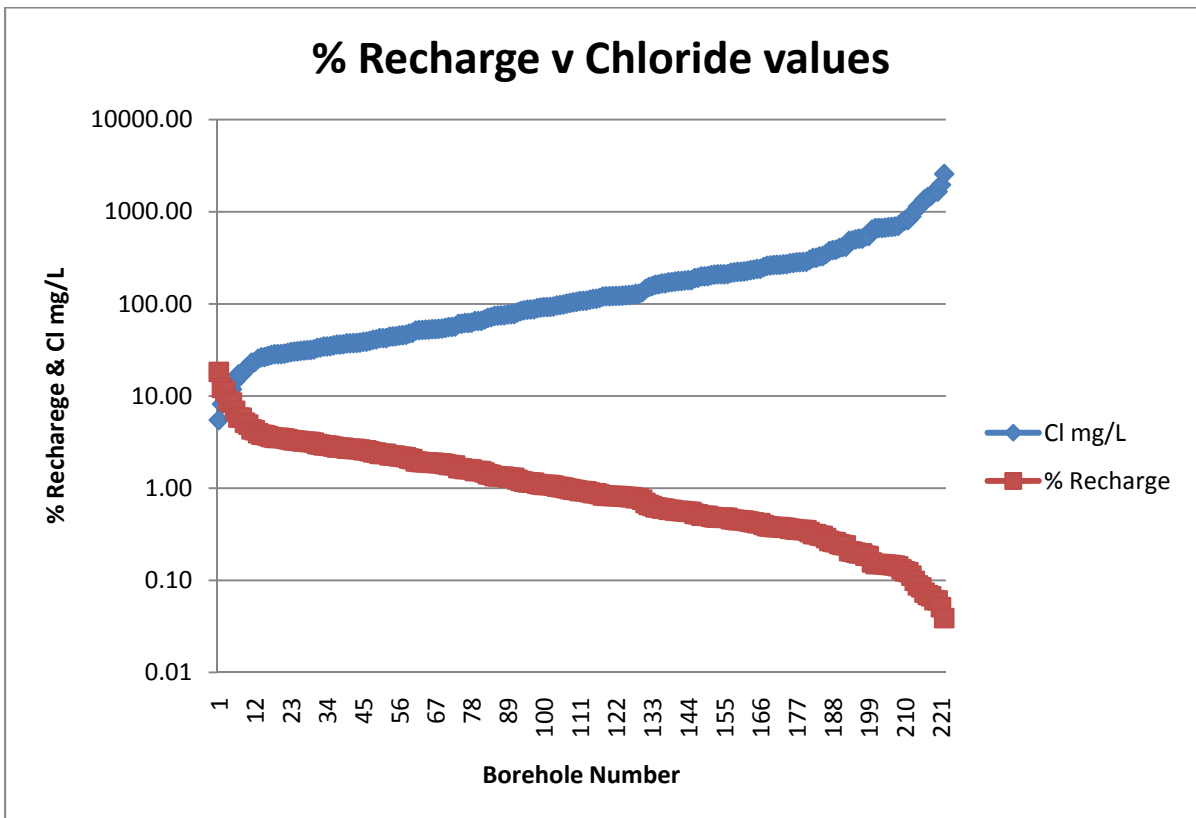


Figure 116: % Recharge v Cl in mg/l.

When the water level elevation, the percentage recharge and the Cl values are plotted against one another, the data indicates that there is no correlation between the elevation of the water level and the other two components (Figure 117).

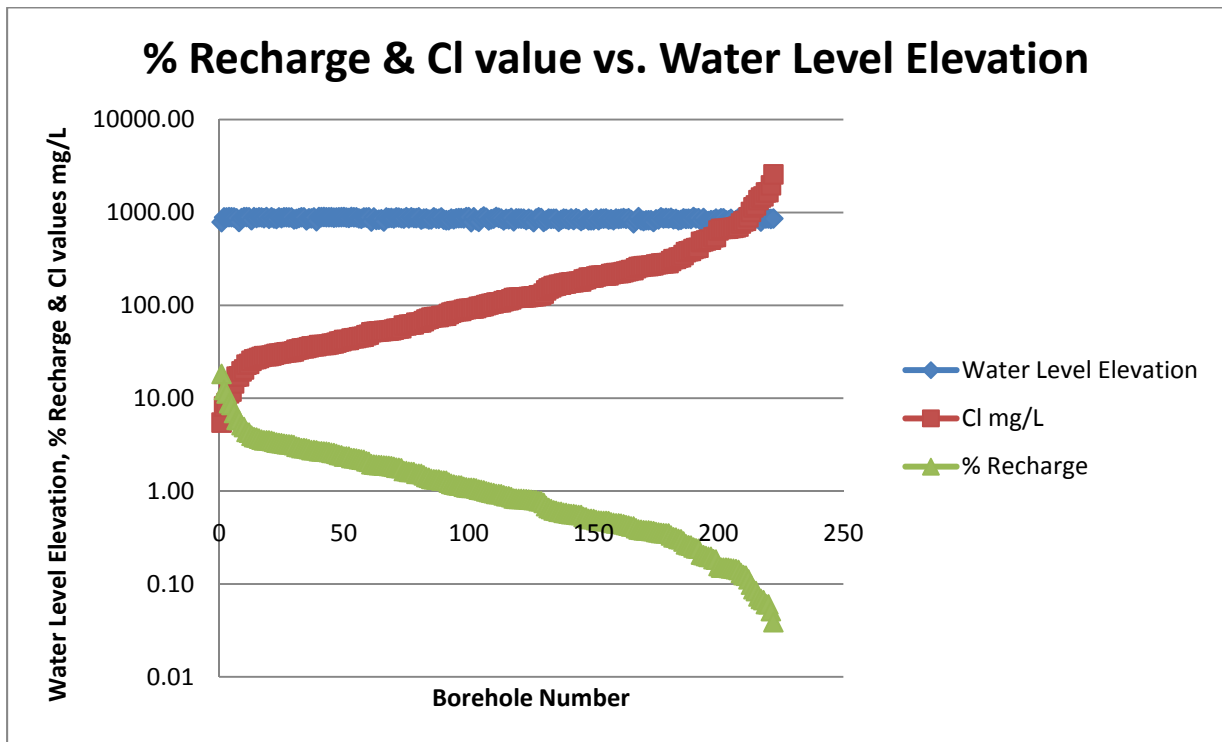


Figure 117: Water Level elevation, % Recharge and Cl plotted against one another.

The calculations from the CI method indicated that the recharge of the study area is 1.59%. This was found to be in accordance with typical Karoo aquifers and with maps produced by Vegter (1995) for the study area, which indicated a recharge of between 1.5% - 1.9%.

A contour map for the recharge in the study area was constructed (Figure 119) from the recharge values calculated for each individual borehole by means of the CI method.. This was done in order to identify areas with high and low recharge and to determine if there was any correlation between the faults and recharge. Figure 118 indicates that recharge in the study area ranges from almost zero to as high as 11% (according to the contour map). These areas of high recharge will need to be investigated as it is unlikely that recharge as high as 11% occurs within the study area.

Additionally the data indicates that the area near the centre of the study area (which shows an increase in elevation), generally also displays a higher recharge percentage than the surrounding areas. This is most clearly seen in the areas between the Daarby and Eenzaamheid faults in the south. This area towards the south which displays a higher recharge, is possibly the result of the influence of the faults in the area, with the areas between the faults displaying a generally higher recharge than that of the areas outside the faults.

The areas south of the Eenzaamheid fault indicate high levels of recharge. This is probably due to the fact that these boreholes drilled in the Waterberg Group rocks recharge along fractures and cracks. These boreholes were recently “flushed” at the time of sampling.

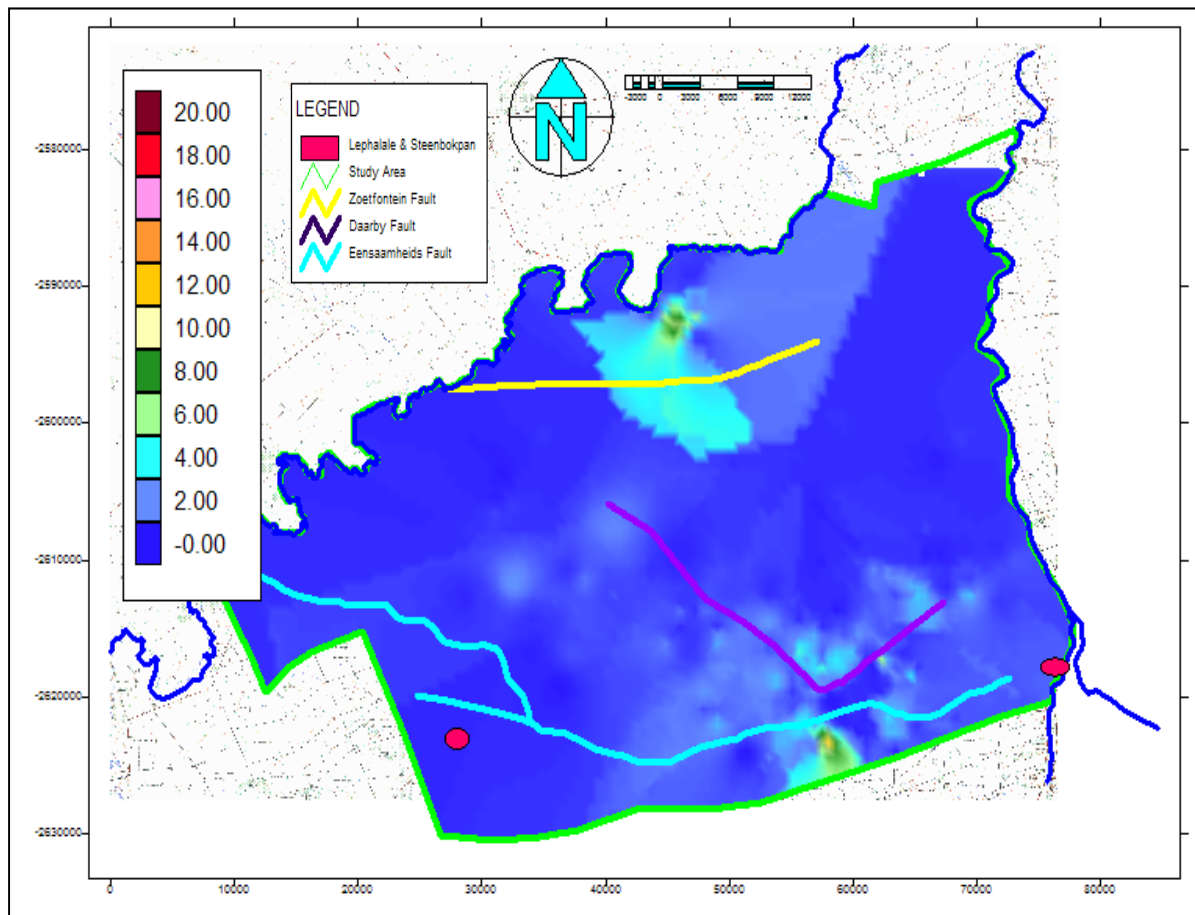


Figure 118: Recharge contour map of the study area.

Additional samples and a more detailed study, are necessary to determine the cause of these high recharge values. Additionally, there are areas towards the north that indicate areas of high recharge (Figure 119). The area outlined in red on the contour map indicates an area that has an average recharge of 4.1 %. This is much higher than the surrounding areas and the area adjacent to this area, outlined in white, also indicates higher recharge than the surrounding area (Figure 119).

It is possible that the Zoetfontein fault passing through this area is serving as a conduit for recharge. This, together with the proximity of this area to the river, is more than likely the reason for the high recharge values. The data indicated that the areas of high recharge are located near the major faults in the study area. Therefore it can be inferred that the faults do not act merely as watersheds, but also as recharge conduits for the rocks through which they run.

This was verified during dewatering and decants modelling for the new mines planned for the study area (see Chapter 10). The models showed that 50 years after mining had stopped; the flow towards the mines will be heavily influenced by the faults near the mines (Figure 156). Care should be taken when interpreting recharge for the area as the area itself is a complex system of which firsthand knowledge is necessary to form any preconceptions.

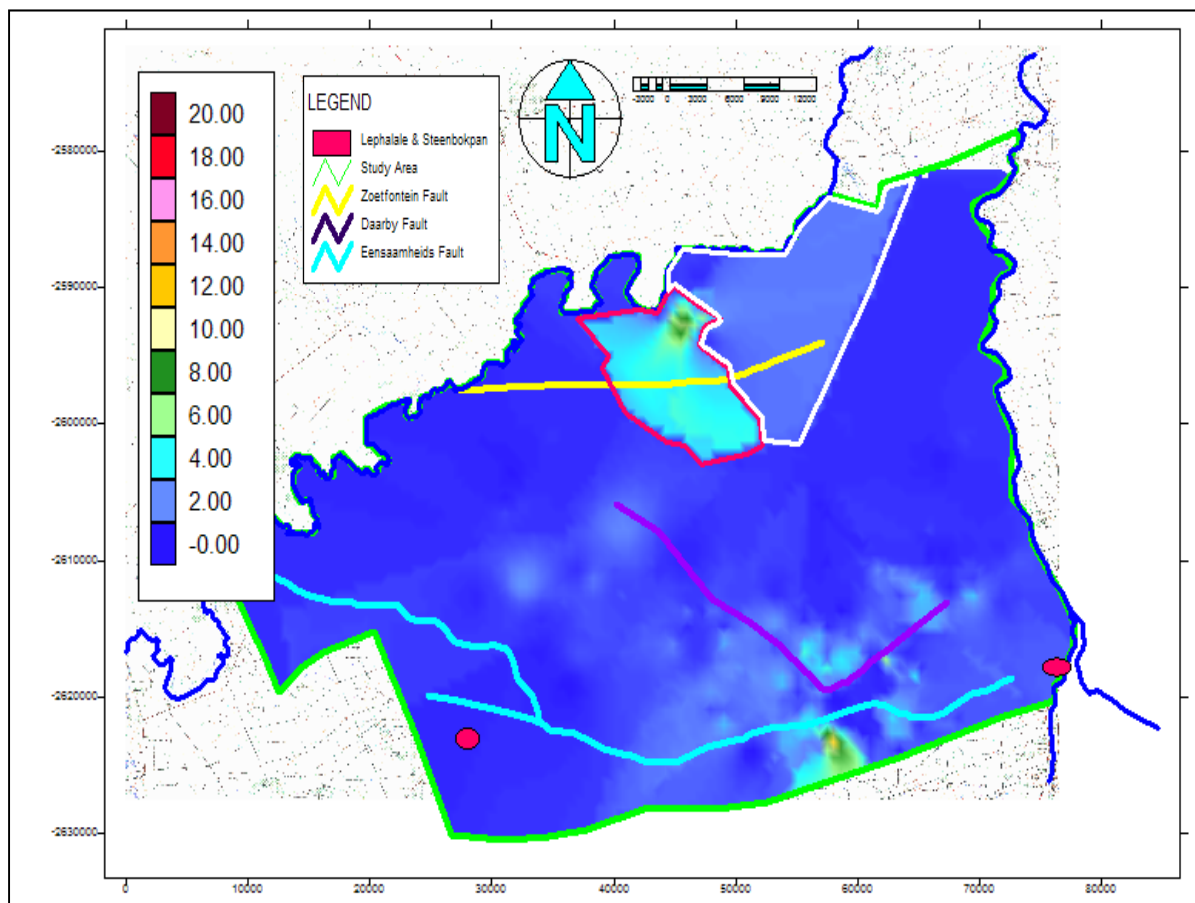


Figure 119: Recharge contour map of the study area outlining northern high recharge zones.

9.6.1.1. Discussion of the Chloride Method

From the analysed data it is clear that the central part of the study area is not only the driving force behind the movement of groundwater in the study area, but is also a driving force with regards to the recharge of the area. From other contour maps that have been generated of the study area, it has been observed that the primary flow directions of groundwater, is in directions away from this central area.

It is therefore plausible that these areas are recharged faster than the low-lying areas and that these chlorides then migrate down to the lower lying areas. Given the low transmissivity found in the aquifers of the study area, this process takes a very long time. The recharge for the study area can be considered as being low, but does vary from one location to the next. For this reason a second method for determining recharge was used.

9.6.2. The E.A.R.T.H. Method for Determining Recharge

In an effort to confirm the recharge values obtained from the Chloride method, the E.A.R.T.H. method for recharge estimation was used. Eight boreholes were used for the recharge determination and were selected due to the availability of data which spanned large periods of time.

Some of the boreholes have information dating back as far as 1973 but some of the other boreholes unfortunately have data spanning only five or eight years.

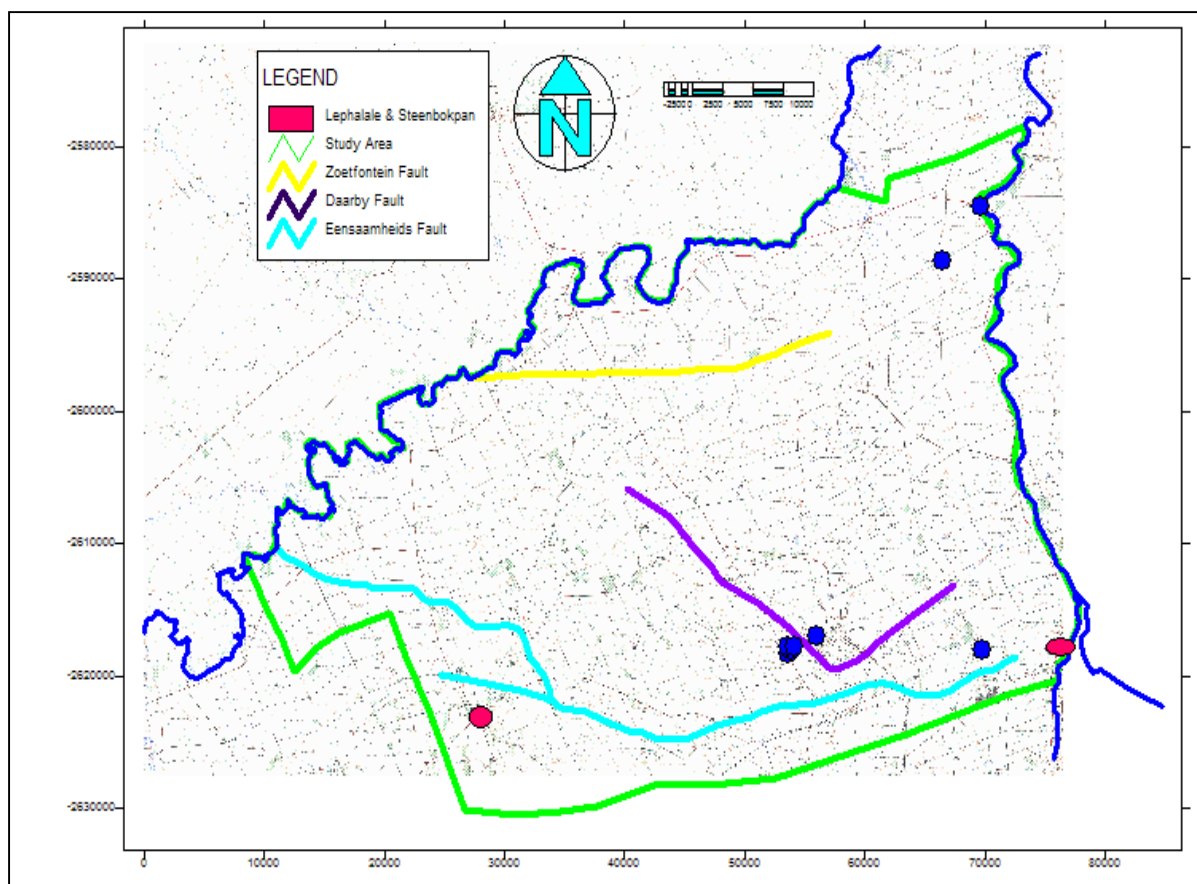


Figure 120: Distribution of the boreholes used for the E.A.R.T.H. model.

The distribution of selected boreholes unfortunately does not cover the entire study area, mainly because additional boreholes with sufficient information could not be located. The analysed boreholes will be discussed below.

9.6.2.1. Borehole 1

This borehole is located in the far north/east of the study area on the farm Windhoek. Information for this borehole spans from June 1989 to December 1991. The water levels were plotted against the rainfall for each month that data was available, and the results can be seen in Table 25 and Figure 121.

Table 25: Results for borehole 1.

EARTH MODEL for single borehole				
Lag	BH #	Resistance	%R	S
0	1	1411	1.7	0.0005

The model indicated a recharge of 1.7%. This is within the initial estimation according to Vegter's maps for recharge.

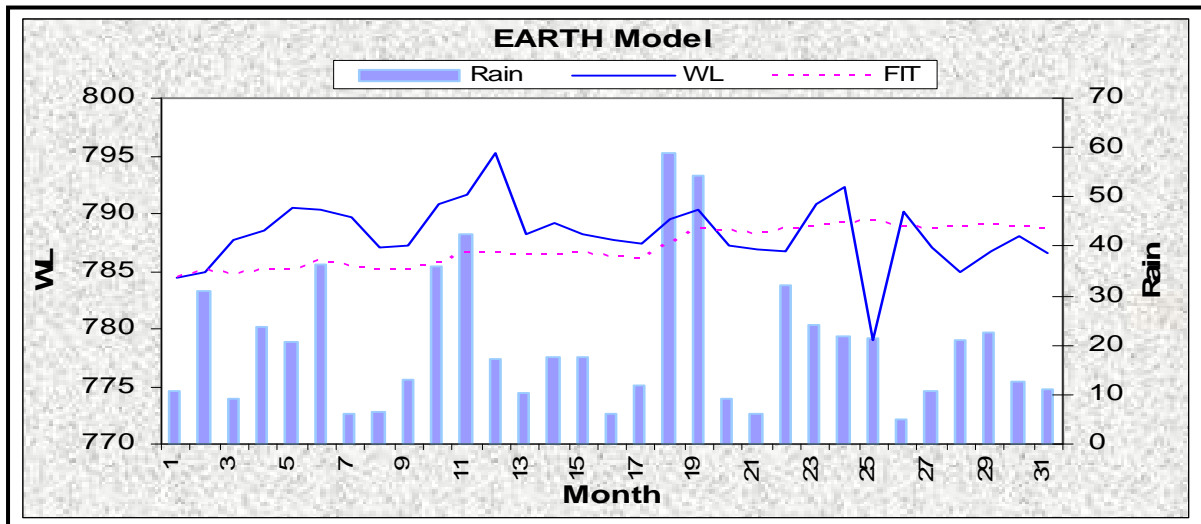


Figure 121: The E.A.R.T.H model for borehole 1.

9.6.2.2. Borehole 2

This borehole is located near the first borehole in the north/eastern part of the study area on the farm Windhoek. The same steps that were followed for the first borehole, with regards to water levels and rainfall, will be followed for all the successive boreholes. The information pertaining to this particular borehole spans from June 1989 to May 1991. The results can be seen in Table 49 and Figure 161 of Appendix D. The model indicated a recharge of 1.5%. There was, however, much more resistance and a lag of 3 months.

9.6.2.3. Borehole 3

Borehole 3 is located near the Grootegeluk Mine, east of the Daarby fault on the farm Daarby. The borehole has data spanning from June 1989 to June 1994. The results are displayed in Table 50 and Figure 162 of Appendix D. The model indicated a recharge of 1.7% with a resistance of 2631 and no lag.

9.6.2.4. Boreholes 4, 5, 6 & 7

These four boreholes are all located within close proximity to one another and will be discussed together. They are located just west of the Daarby fault on the farms Daarby and Enkelbult. The results for the boreholes are displayed in Table 51 and the fitted graphs are displayed in Figures 163 - 166 of Appendix D.

For borehole 4 the data span from June 1989 to April 1991. The model indicated a recharge of 0.9%. The same recharge was given for borehole 5. Borehole 5 however had a 3 month lag. The data for borehole 5 stretched from June 1989 to March 1994. Borehole 6 indicated a recharge of 1% with no lag, with data from June 1989 to July 1992. The final borehole in the same area was borehole 7. The model gave a recharge of 1.4% for this borehole.

9.6.2.5. Borehole 8

The final borehole-analysis involved borehole 8. This borehole is located to the south/east, east of the Daarby fault and just north of the Eenzaamheid fault. The data for this borehole spans from June 1989 to September 1999. The results for this borehole are displayed in Table 52 and the fitted graphs in Figure 167 of Appendix D. The model indicated a recharge of 3%. This is much higher than any of the other boreholes analysed so far. The reason for this high recharge is unknown.

When the average of all the boreholes is calculated, the result is a recharge of 1.51% for the area.. This is very similar to the results obtained from the Chloride method, which indicated that both methods for determining recharge can effectively be used in the study area.

9.6.2.6. Discussion of the Results for the E.A.R.T.H. Model

From the results of the E.A.R.T.H model the following conclusions can be drawn:

- There is a great degree of variation in the recharge values in the study area.
- The recharge varies between 0.9% and 3% for the E.A.R.T.H. model calculations
- The average of the measured borehole is 1.51%, which is similar to the value obtained from the Chloride method.

9.7. Conclusion

9.7.1. Aquifer Parameters

From the information gathered it is apparent that the aquifers in the study area are low yielding and that the formations have low transmissivities. These findings conform to typical Karoo aquifer parameters. Given the low transmissivities of the formations it is predicted that the new mines planned for the study area will not have problems with regards to large volumes of water flooding the mines. Furthermore, as a result of the low rainfall, the low transmissivities, the water level (averaging around 28 m) and the high evotranspiration in the study area, it is predicted that the water levels in the mines will not reach decant levels.

This was confirmed by the numerical modelling (discussed in more detail in Chapter 10), which indicated that 50 years after mining had stopped the water levels in the modelled pits rose by between two and three meters. The largest contributor to the rise in water levels in the pits is surface runoff during periods of high rainfall. The Big Hole in Kimberley can be used as an example of the above, as the area has low transmissivities, deep water levels and high levels of evapotranspiration. According to these parameters it has been predicted that the Big hole will never decant (Figure 108).

9.7.2. Recharge

The recharge determinations for the study area indicated a value of between 1.5% - 1.6% for the entire study area. This is in accordance with the maps that Vegter (1995) has drawn up of the study area, placing the recharge at between 1.5% and 1.9%. Both the E.A.R.T.H. and Chloride methods for determining recharge gave values in the same order, indicating that both of these methods may be used in the study area, and with a high degree of certainty. Furthermore, the low recharge coupled with the low transmissivities found in the study area present both positive and negative situations for both the mines and the farmers in the study area. The scenario has positive implications for mining, in the sense that there will be little inflow of water into the mines (which has been confirmed by modelling). On the negative side this poses problems, because as the boreholes in the vicinity of the mines are increasingly dewatered, they will, if ever, take very long to reach their initial levels.

For the farmers the situation is comprehensively negative. Dewatered boreholes will take long to reach their initial levels and boreholes in the vicinity of the mines are unlikely to ever recover. Therefore, precaution should be taken to minimize the impact of mining on the groundwater.

CHAPTER 10: Modelling

10.1. Introduction

Numerical modelling was done for the study area to determine the quantities of groundwater flow into mines (dewatering model) and to predict whether the mines would reach decant level (decant models). In order to achieve this, data gathered from the study area was used. This data included; borehole water levels, transmissivities from pump testing and geological data. The data from the currently active mine (Dreyer, 2009) revealed that the measured inflow from groundwater into the mine was in the order of 19000 m³/month during the initial stages of mining. This translates to 633 m³/d. At present the estimated flow into the mine is in the order of 30000 m³/month (1000 m³/d). This constitutes a very small volume of water entering the workings of the mine.

Additional information from the mine includes the following:

- The mine removes roughly 60 m of coal from the pit as mining progresses.
- The pit extends to roughly 110 m at its deepest point.
- This means that the additional 40% can be used as backfill once mining operations cease, meaning that 60% of the rock removed from the pit will not be replaced.
- The pit will therefore not be rehabilitated to surface level, but will be backfilled in a stepped manner, the highest step being at the eastern end of the mine and the lowest step towards the western parts of the mine.
- Open voids in the mines will occur, and will not be backfilled.
- Additional information that played a role in modelling was the average water levels of roughly 28 m below surface, and the low transmissivities measured in the study area by means of pumping tests.
- The very high evaporation of between 1800 mm/y - 2000 mm/y (5.6 mm per day) and low rainfall were taken into account (SA Weather Service, 2008), as surface run-off into the mine is the primary contributing factor to water in the pit.

10.2. Numerical Modelling

The Processing ModFlow for Windows (PMWin) modelling software program was used for the modelling process. It was decided not to model the entire study area, as this would decrease the accuracy of the model and increase model run times. Instead, the focus was directed to the areas west of the Daarby fault, as this is the primary area in which coal will be mined by means of surface mining methods.

10.2.1. Parameters for the Model

10.2.1.1. Regional Finite Difference Network

A grid of 40 km in length, by 30 km in breadth was chosen. This grid was divided into 200 columns and 150 rows respectively, each 200 m X 200 m in size.

Grid co-ordinates: X1 25507, Y1 -2627437

X2 65837, Y2 -2597484

A four-layer model was selected in an effort to better simulate the conditions in the study area. A thickness of 28 m per layer was taken as the average. Water depth in the study area is at 28 m below the surface and Modflow can only simulate saturated flow. The topmost layers were assigned a value of zero, with the deepest receiving a value of -110 m. Because Modflow cannot simulate unsaturated flow, water levels in the study area were valued at the zero level, and the depth of the pits at 110 m was taken into account for future mining activities (Vermeulen and Dennis, 2007). In addition, the layers were all classified as confined, given the geology of the study area (predominantly alternating layers of shale and mudstone with some sandstone and coal). Once the network was set up, all initial and boundary conditions, sources, sinks, and aquifer parameters were entered. Under normal circumstances a steady state calibration is then conducted to ensure that the flow model has the same behaviour as the actual system under investigation. This, however, could not be undertaken due to a lack of data.

10.2.1.2. Boundary Conditions

One of the first and most demanding tasks in groundwater modelling is that of identifying the model area and its boundaries. Consequently, a model boundary is the interface between the model area and the surrounding environment. Conditions on the boundaries, however, have to be specified. Boundaries occur at the edges of the model area and at locations in the model area where external influences are represented, such as rivers, wells and leaky impoundments (Vermeulen and Dennis, 2007). Criteria for selecting hydraulic boundary conditions are primarily topography, hydrology and geology. The topography, geology, or both, may yield boundaries such as impermeable strata or potentiometric surface controlled by surface water, or recharge/discharge areas such as inflow boundaries along mountain ranges. The flow system allows for the specification of boundaries in situations where natural boundaries are a great distance away. Boundary conditions must be specified for the entire boundary and may vary with time. At a given boundary section, only one type of boundary condition may be assigned. As a simple example, it is not possible to specify groundwater flux and groundwater head at an identical boundary section (Vermeulen and Dennis, 2007).

Boundaries in groundwater models may be specified as follows:

- Dirichlet (also known as constant head or constant concentration) boundary conditions
- Neuman (or specified flux) boundary conditions
- Cauchy (or a combination of Dirichlet and Neuman) boundary conditions

A box model was used, in which the northern, eastern, southern and western borders of the model were set to constant head boundaries. This was done to simplify the model. For the dewatering models, constant head boundaries were placed on the lowest levels of the layer that was to be dewatered. For the decant models, these boundaries were removed.

10.2.1.3. Initial Conditions

Initial conditions are vital for modelling flow problems. Initial conditions must be specified for the entire area. Generally, the initial water level/head distribution acts as the starting distribution for the numerical calculation (Vermeulen and Dennis, 2007). The initial water level was set to zero as the modelling program can only simulate saturated flow.

10.2.1.4. Sources and Sinks

Sources and sinks can be defined as recharge and abstraction sources in the aquifer, respectively. Sources could involve precipitation and inflow from surface water and recharging boreholes. Sinks may be constituted by abstraction boreholes, springs, evapotranspiration, mines and outflow to surface water (Vermeulen and Dennis, 2007). The groundwater recharge (R) for the area was calculated through use of the chloride method and is expressed as a percentage of the Mean Annual Precipitation (MAP). Accordingly the recharge for the study area was calculated to be 1.5% of the annual rainfall. The recharge entering into the model in general was determined at 0.023 mm/y, and at 20% of the annual rainfall in the open pits (Hodgson *et al.*, 2007), amounting to 0.31mm/y.

10.2.1.5. Aquifer Parameters

Two main parameters are used to describe the physical properties of the aquifer, namely transmissivity (T) and storage coefficient (S). Transmissivity is a measure of the ease with which groundwater flows in the subsurface. Transmissivity is related to hydraulic conductivity (K): $T = Kd$ where d is the saturated thickness of the aquifer. Storage coefficient is the volume of water an aquifer releases from or takes into storage per unit surface area of the aquifer per unit change in head (Vermeulen and Dennis, 2007).

For a confined aquifer, the storage coefficient is equal to the product of the specific storage and aquifer thickness of the saturated porous medium. For an unconfined aquifer, the storage is the ratio of the volume of water that drains by gravity to that of the total volume and is known as specific yield.

- The calculated harmonic mean of the transmissivities was $1.6 \text{ m}^2/\text{d}$.
- This was taken as the total transmissivity for the system and divided among the layers for an even distribution of $0.4 \text{ m}^2/\text{d}$ for each layer.
- Two additional transmissivities were taken to test the model (different scenarios).
- It was decided to take transmissivities of roughly $1/3$ ($0.12 \text{ m}^2/\text{d}$) and $2/3$ ($0.28 \text{ m}^2/\text{d}$)
- The reason for taking these transmissivities was to simulate different scenarios as it was suspected that the transmissivity of $0.4 \text{ m}^2/\text{d}$ was too high and did not correspond to the volumes of water entering into the pit in reality.
- An additional reason was that the model could not be calibrated due to lack of data.
- These transmissivities were used for the area as a whole, with the transmissivities in the pits set at $100 \text{ m}^2/\text{d}$ for the dewatering models, and $500 \text{ m}^2/\text{d}$ for the decant models respectively.
- The transmissivities selected for the faults was $500 \text{ m}^2/\text{d}$.

A general storage coefficient of 0.003 was selected for the model with storage coefficients of 1 and 0.25 for the dewatering and decant models in the pits themselves. Vertical hydraulic conductivity was set to 1E^{-5} for the model as a whole, and at 10 in the pits to simulate worst-case scenario situations.

10.2.1.6. Time

A time frame of 10 years was determined for the dewatering models, for the purpose of simulating the dewatering of each layer as mining progresses ever deeper into the geology. The 10 year periods were divided into lengths of 360 days (to remove leap years from the modelling calculations), with the time steps set to 12 (12 months). For the decant models, a time frame of 50 years divided into lengths of 360 days and 12 time steps was selected.

10.2.1.7. Pits

Initially only one pit was simulated with the three different transmissivity values. This was expanded to three pits for the final model; one to the north, one towards the south-east and one between the other pits. The sizes of the pits vary, with the northern pit being 1750 ha, the central pit being 2793 ha, and the south-eastern pit being 2070 ha. Large sizes for the pits were chosen to simulate the absolute worst case scenario situations.

10.2.2. Model Scenarios

Five dewatering and accompanying decant models were constructed to illustrate different scenarios that may occur during the course of mining in the study area.

10.2.2.1. Scenario 1

- Three dewatering models were constructed using all the parameters and only one pit (the northern pit).
- In the models, the faults found in the study area were not activated.
- The models were systematically dewatered, First to the second layer, then to the third layer and finally to the fourth layer to simulate the progression of the mine.
- All the models were constructed for all three transmissivities ($0.4 \text{ m}^2/\text{d}$, $0.28 \text{ m}^2/\text{d}$ and $0.12 \text{ m}^2/\text{d}$) and run for 10 years for each layer being dewatered.

10.2.2.2. Scenario 2

- The fourth dewatering model contained one activated fault that ran through the pit. This was done to simulate a scenario where a zone of higher transmissivity might be encountered during the course of mining. A transmissivity of only $0.4 \text{ m}^2/\text{d}$ was used.

10.2.2.3. Scenario 3

- The final constructed model had all three pits on the model and all the faults found in the study area were activated. All the pits were dewatered to 110 m below surface.

The results of the modelling will be discussed according the transmissivities used.

10.2.3. Dewatering for Scenario 1

10.2.3.1. Transmissivity $0.4 \text{ m}^2/\text{d}$

For the dewatering of layer 2, the constant head boundaries were placed at the bottom of the layer (56 m below surface). The model yielded a drawdown cone of 2.6 km (Figure 122) around the pit, with an inflow of $388 \text{ m}^3/\text{d}$ into the mine. For layer 3 at a transmissivity of $0.4 \text{ m}^2/\text{d}$, the model generated a drawdown cone of 2.6 km for layer 2 (Figure 123) around the mine, with an inflow of $604 \text{ m}^3/\text{d}$. For layer 3 (Figure 124), the drawdown cone was given as 2.4 km and the predicted inflow was $897 \text{ m}^3/\text{d}$. For the dewatering of layer 4 at the same transmissivity ($0.4 \text{ m}^2/\text{d}$), the model depicted a drawdown cone of 2.8 km for layer 2 (Figure 125), 2.8 km for layer 3 (Figure 126), and 2.6 km for layer 4 (Figure 127) respectively.

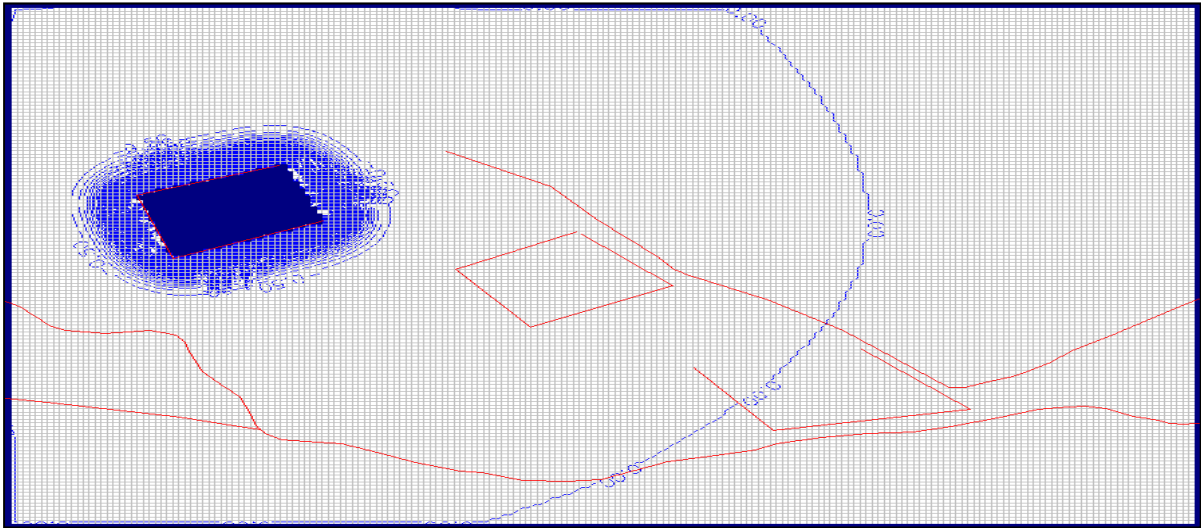


Figure 122: Dewatering of Layer 2 with a transmissivity of $0.4 \text{ m}^2/\text{d}$ showing the drawdown cone.

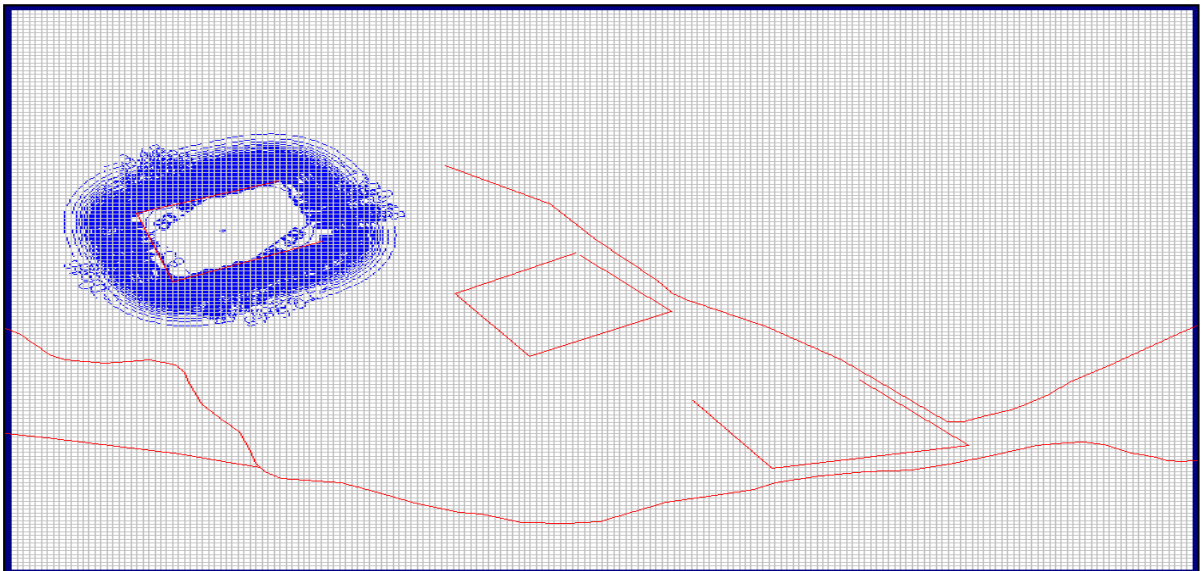


Figure 123: Layer 2 at a transmissivity of $0.4 \text{ m}^2/\text{d}$ with Layer 3 being dewatered.

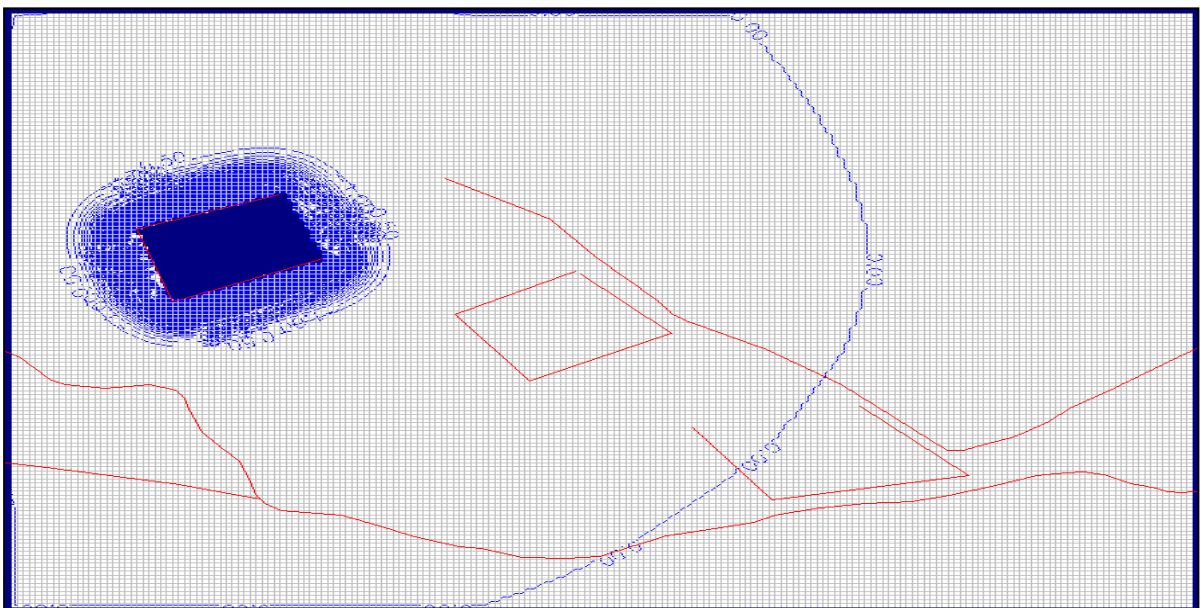


Figure 124: Layer 3 at a transmissivity of $0.4 \text{ m}^2/\text{d}$ with Layer 3 being dewatered.

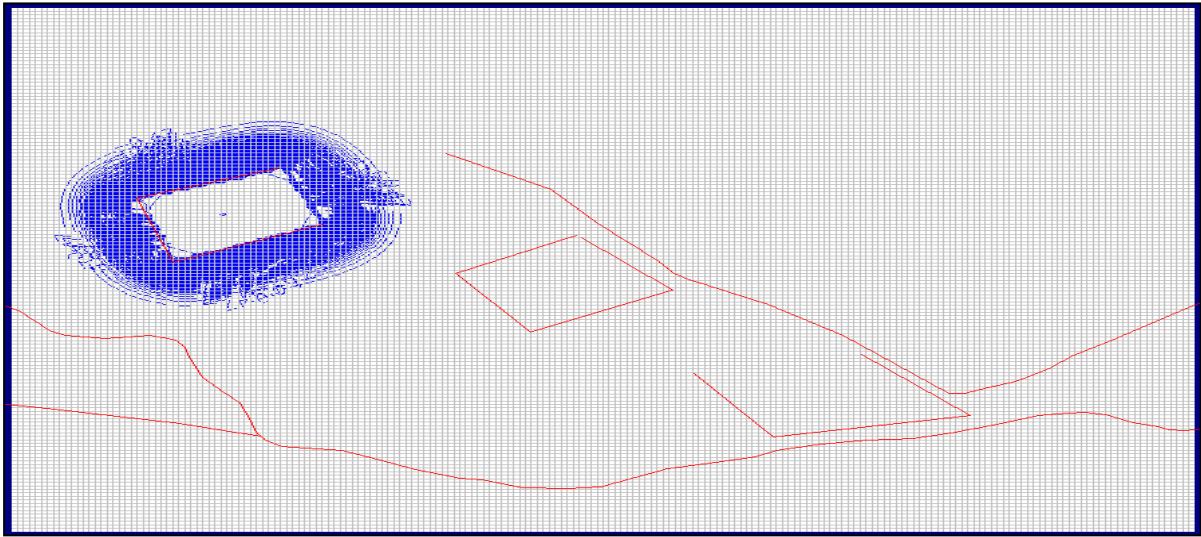


Figure 125: Dewatering of Layer 4 showing the drawdown cone for layer 2.

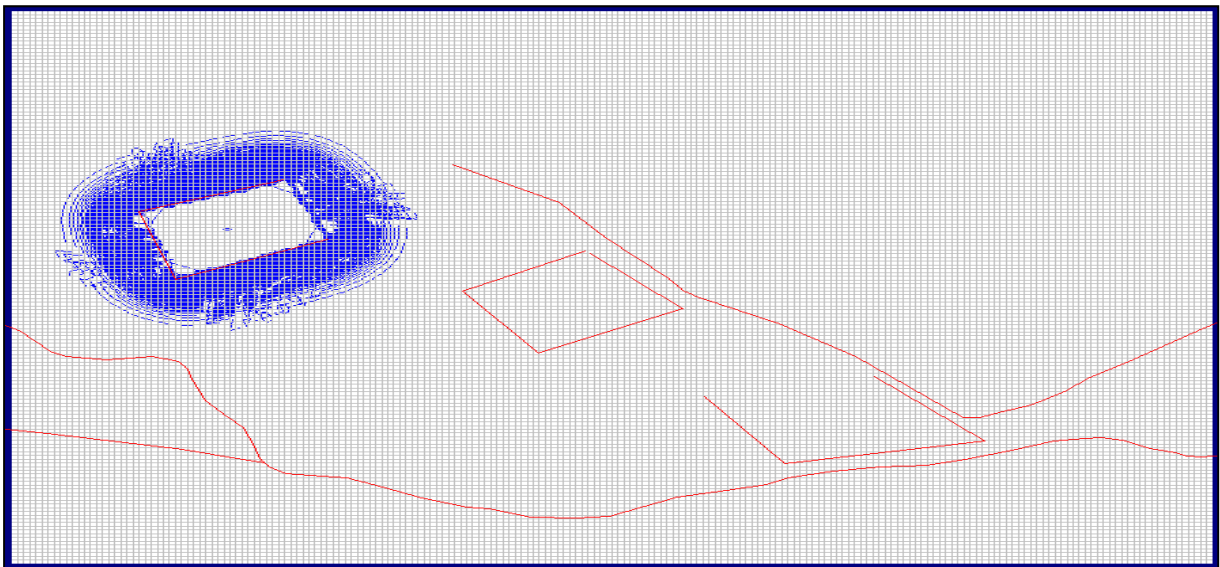


Figure 126: Dewatering of layer 4, showing layer 3's drawdown cone.

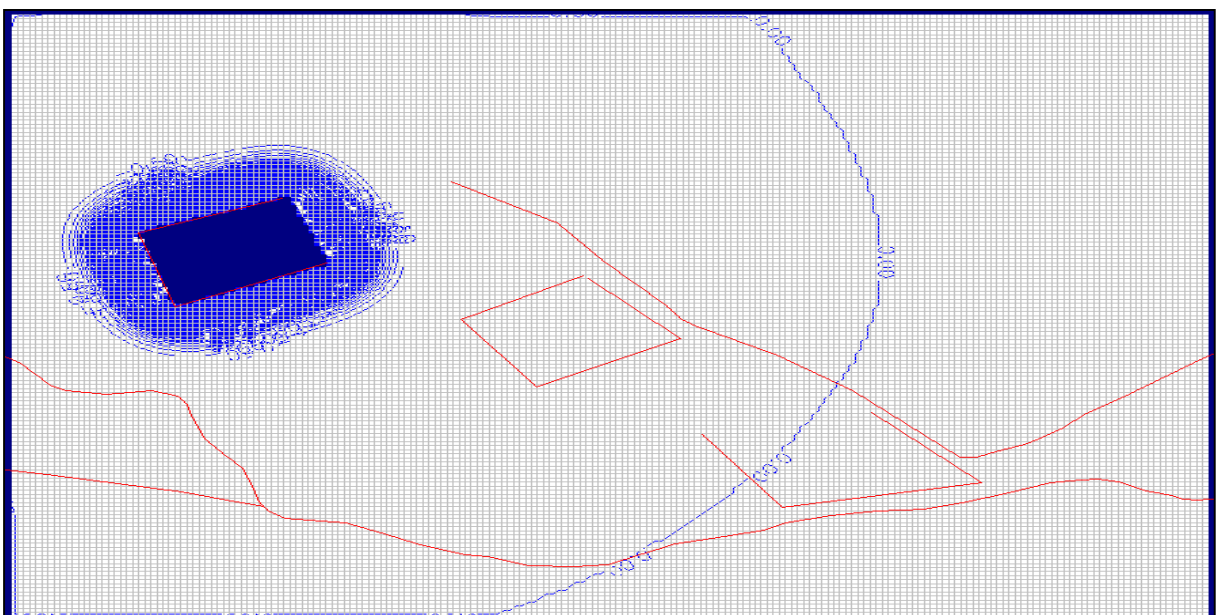


Figure 127: Showing the drawdown cone for layer 4 with layer 4 being dewatered.

The models indicated inflows of 749 m³/d, 749 m³/d, 748 m³/d and 755 m³/d for layers 1, 2, 3 and 4 respectively. As can be seen, there is very little difference in inflow between the layers, with the largest amount of water influx occurring on the layer that is being dewatered. There is also a small change in the size of the drawdown cones from the different layers, with the exception of layer 3.

10.2.3.2. Transmissivity 0.28m²/d

The same models constructed for the 0.4 m²/d transmissivity, were done for a transmissivity of 0.28 m²/d. The results are as follows: for the dewatering of layer 2, the model generated a drawdown cone of 2 km (Figure 128) and an estimated inflow of 319 m³/d. For the dewatering of layer 3, the model estimated a drawdown cone of 2.2 km for layer 2 (Figure 129) and 2 km for layer 3 (Figure 130). The estimated inflow of groundwater was 496 m³/d and 701 m³/d for layers 2 and 3 respectively.

From these values, it is clear that there is a large difference in the inflow of groundwater between layers 2 and 3. This difference is however less significant than the difference in inflow between layers 2 and 3 for a transmissivity of 0.4 m²/d. The dewatering model constructed for layer 4 showed drawdown cones of 2.2 km, 2.2 km, and 2.2 km for layers 2 (Figure 131), 3 (Figure 132) and 4 (Figure 133) respectively. The predicted inflow for the model was 614 m³/d, 613 m³/d, 618 m³/d for layers 2, 3 and 4 respectively.

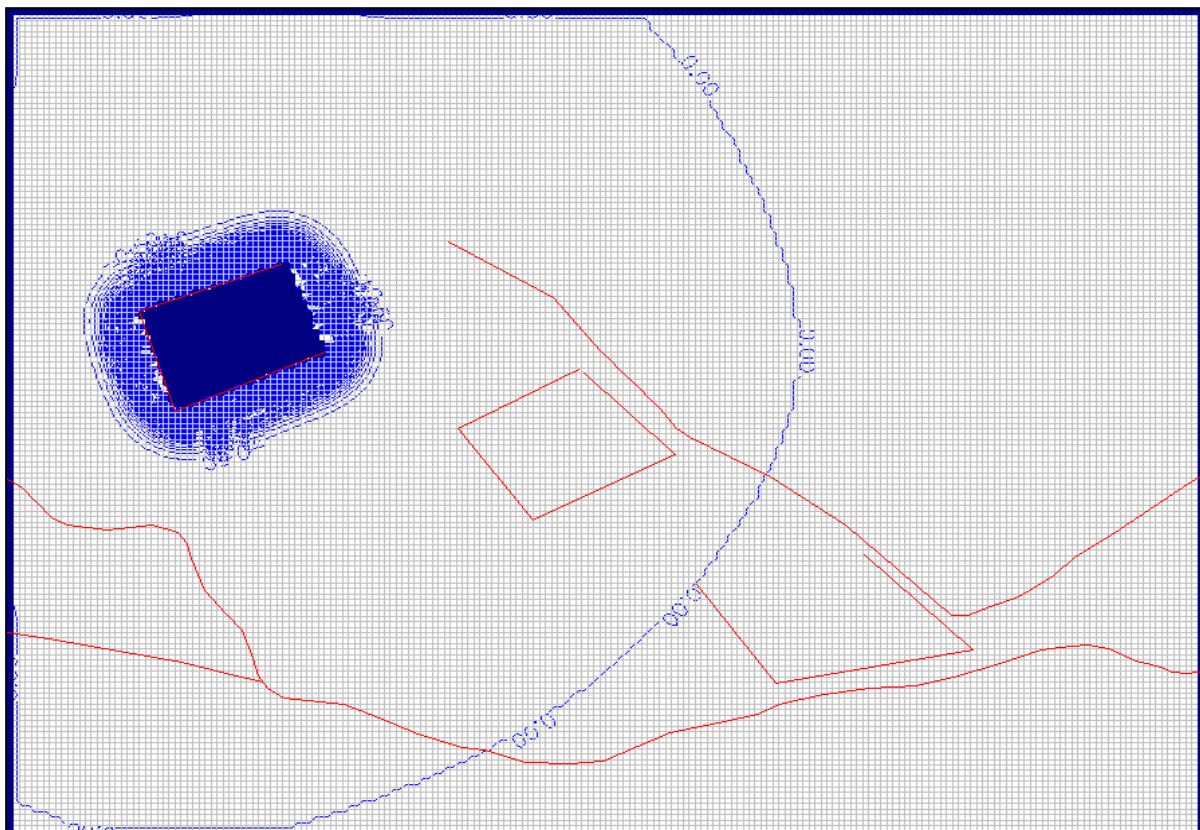


Figure 128: Showing the drawdown cone for layer 2 with layer 2 being dewatered at a transmissivity of 0.28 m²/d.

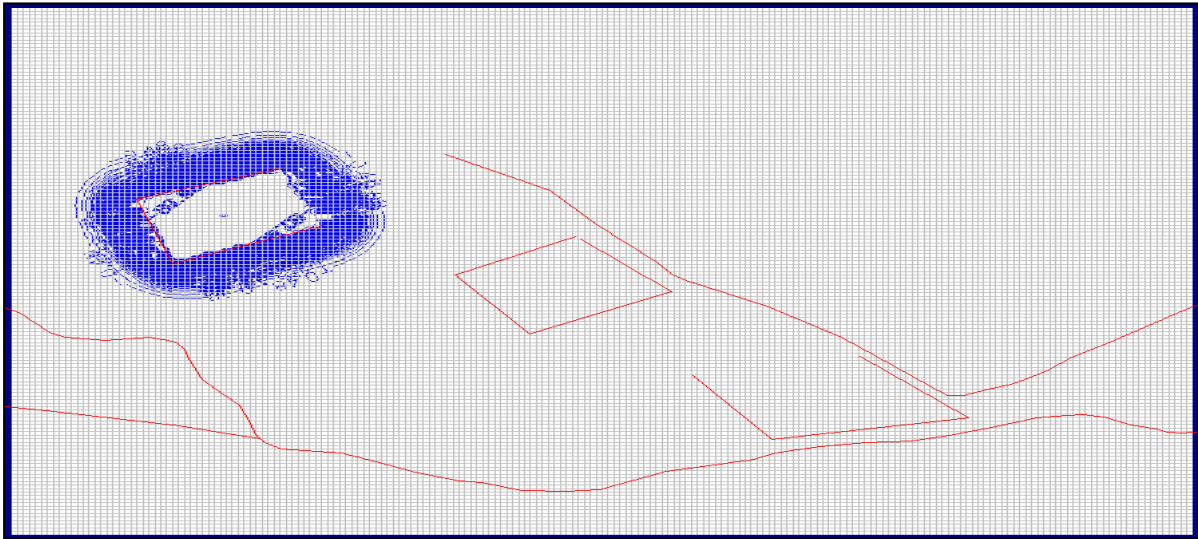


Figure 129: Drawdown cone for layer 2 with layer 3 being dewatered.

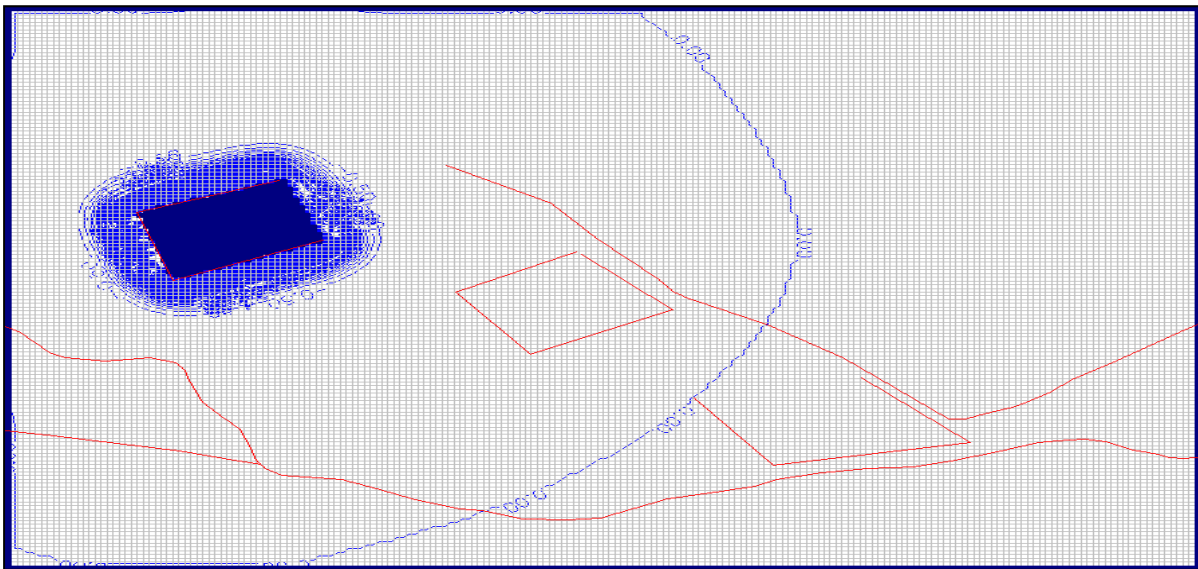


Figure 130: Drawdown cone for layer 3 with layer 3 being dewatered.

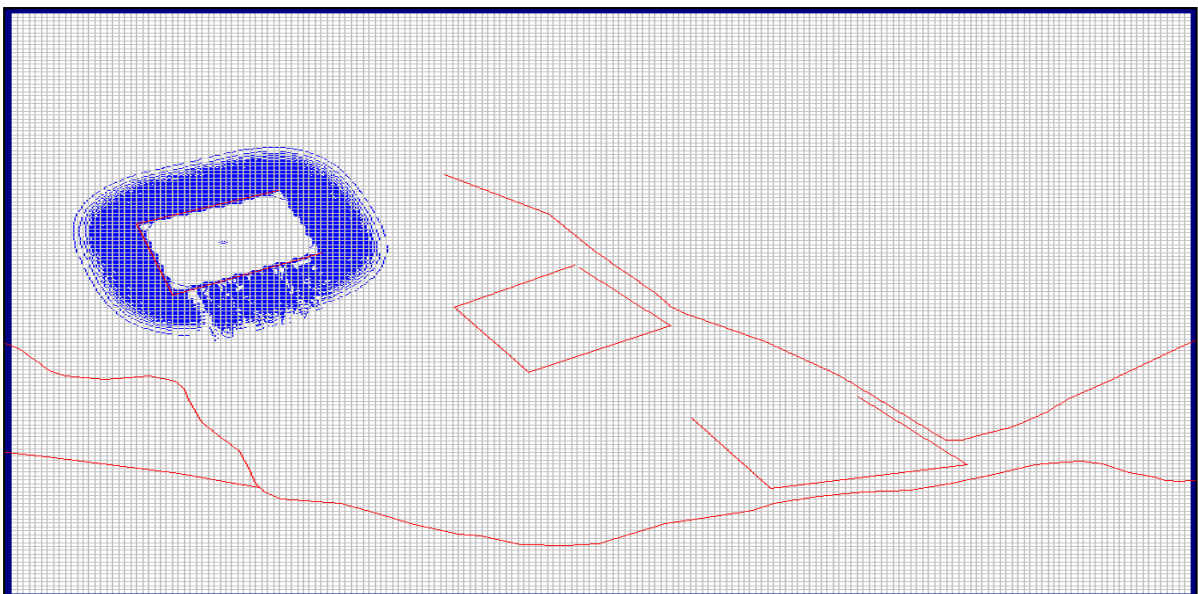


Figure 131: Drawdown cone for layer 2 with layer 4 being dewatered.

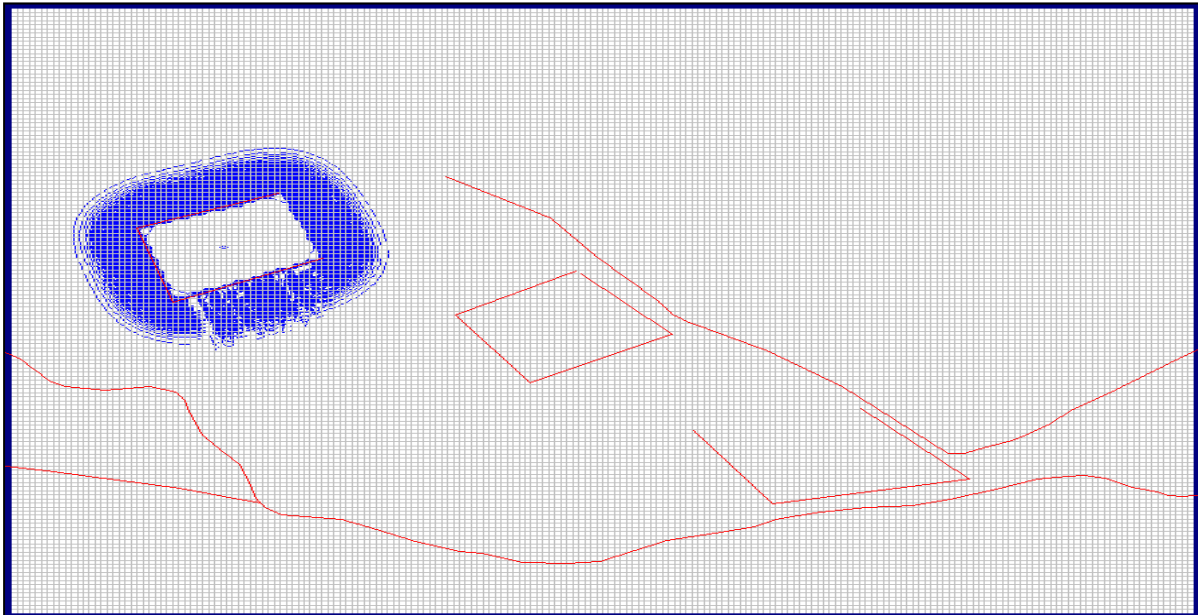


Figure 132: The drawdown cone for layer 3 with layer 4 being dewatered.

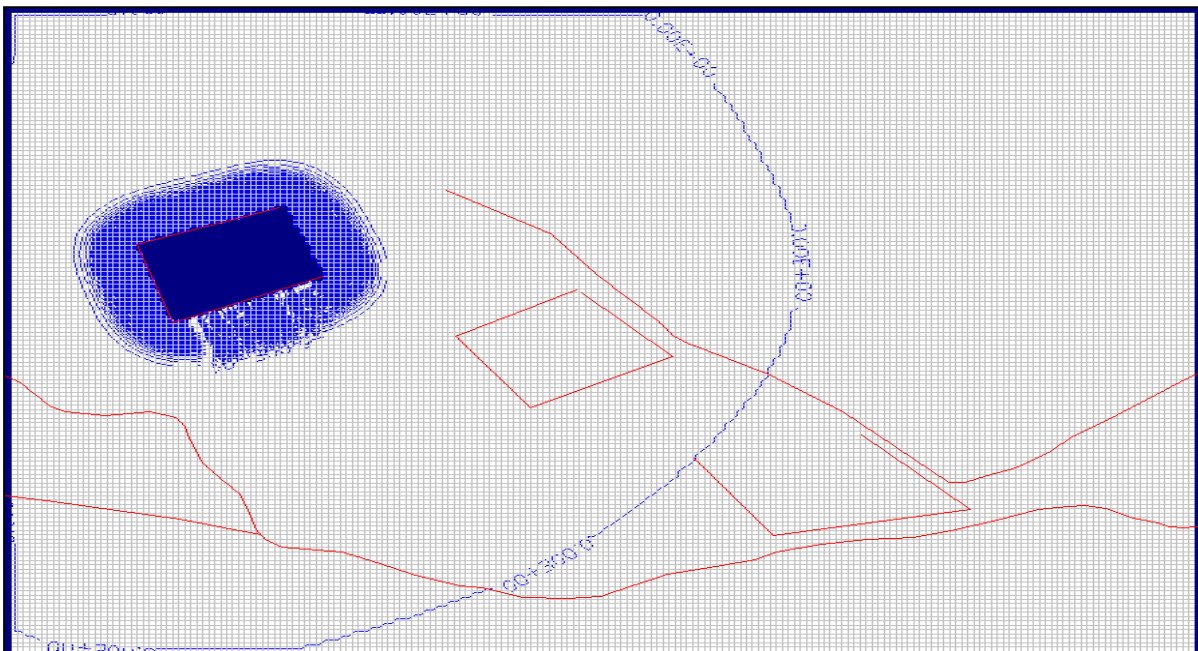


Figure 133: The dewatering of layer 4 showing the drawdown cone for layer 4.

10.2.3.3. Transmissivity 0.12 m²/d

The final set of dewatering models for this scenario was constructed using a transmissivity of 0.12 m²/d. The same parameters were used as for the previous models. For the dewatering of layer 2, a drawdown cone of 1.4 km (Figure 134) and an estimated inflow of 203 m³/d were determined. For layers 2 and 3, the model generated a drawdown cone of 1.4km (Figure 135 & Figure 136 respectively) for both layers and an inflow of 315 m³/d and 403 m³/d for layers 2 and 3 respectively. For the dewatering of layer 4, drawdown cones of 1.6 km (Figure 137, Figure 138 & Figure 139) for all three layers (2, 3 & 4) were estimated, along with inflows of 390 m³/d, 389 m³/d and 391 m³/d for layers 2, 3 and 4 respectively.

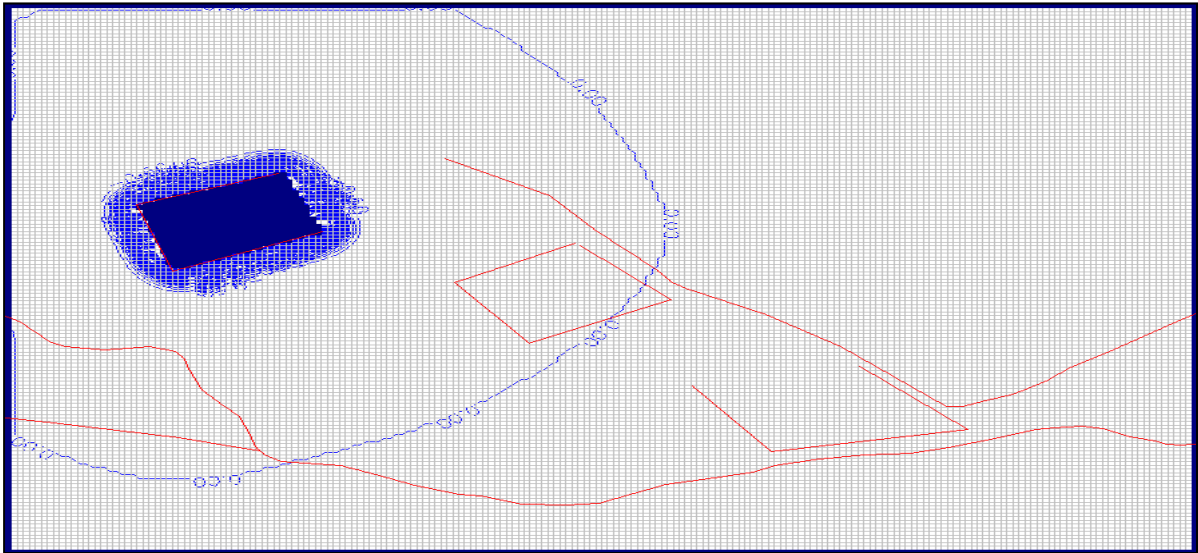


Figure 134: Dewatering of layer 2, showing drawdown cone of layer 2.

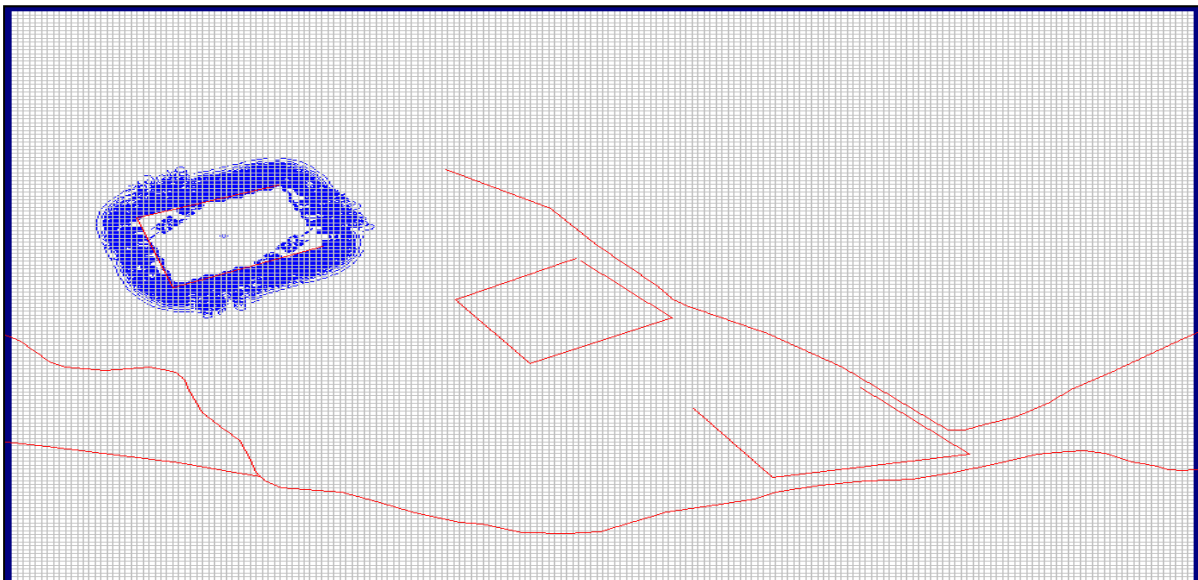


Figure 135: Drawdown cone for layer 2 with layer 3 being dewatered.

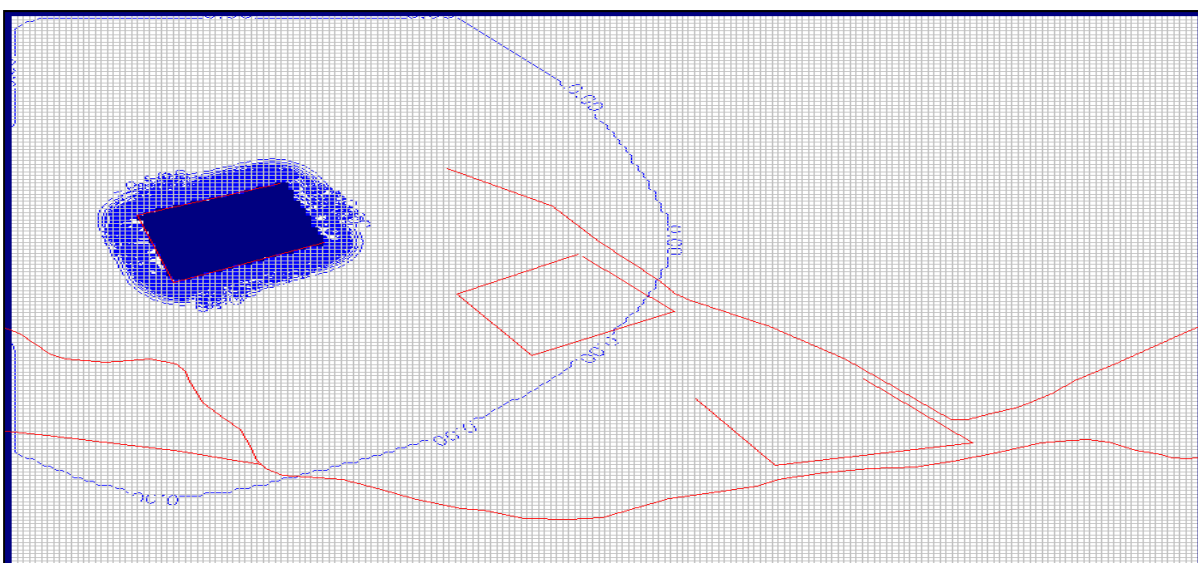


Figure 136: Drawdown cone for layer 3 with layer 3 being dewatered.

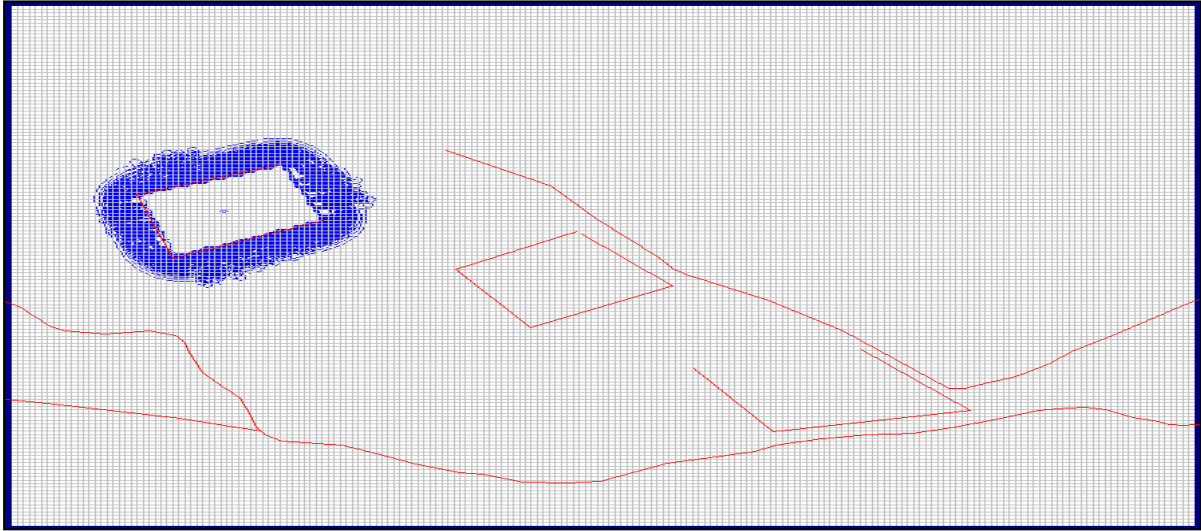


Figure 137: Showing drawdown cone for layer 2 with layer 4 being dewatered.

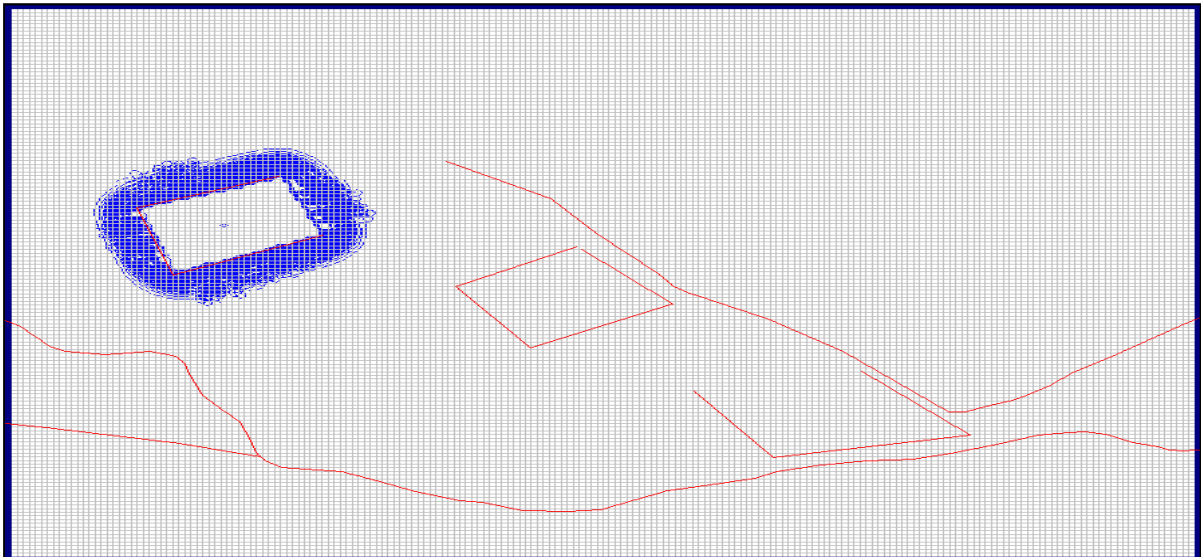


Figure 138: Drawdown cone for layer 3 with layer 4 being dewatered.

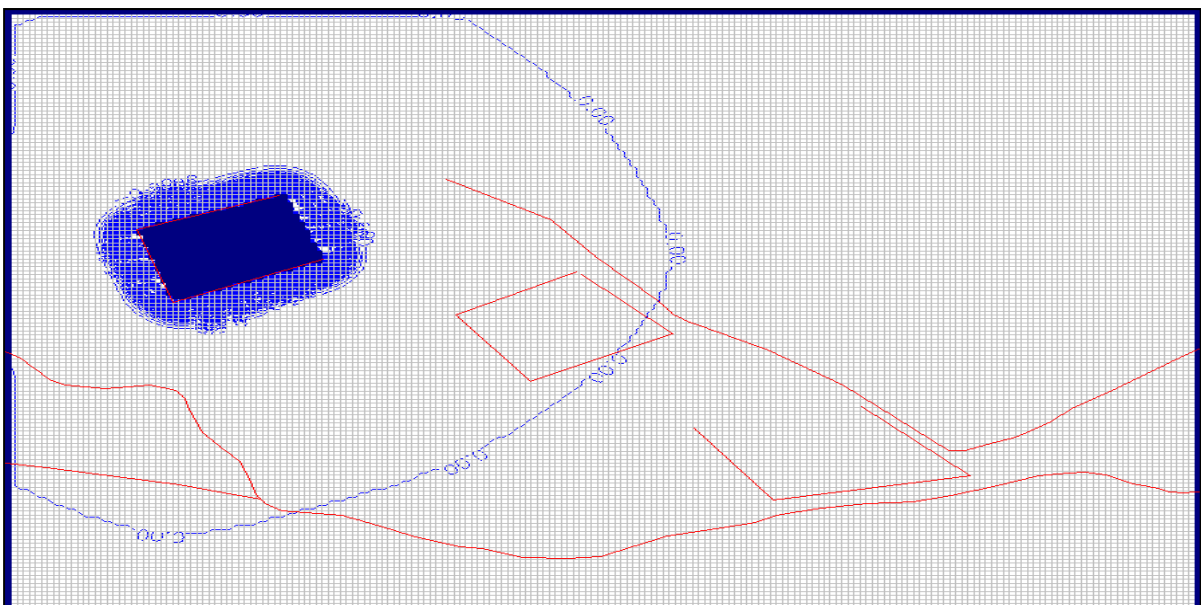


Figure 139: Showing the drawdown cone for layer 4 with layer 4 being dewatered.

10.2.3.4. Discussion of Dewatering Models for Scenario 1

From the models used to simulate dewatering for the different layers, it is clear that the different transmissivities for scenario 1 lead to different drawdown cones and different quantities of water flowing into the mine (Table 26). The models indicate that, during the initial stages of mining, there will be “large” influxes of water into the mine, the quantity of which depends on the transmissivity of the rocks and rock formations determined by the location of the mine. The largest differences in water levels with regards to pre-and post mining water levels, will be observed in the immediate vicinity of the mines and this will diminish with increased distance from the mine, reaching a maximum of 2.8 km from the mine after 10 years. According to Dreyer (pers. comm. 2009), the recorded drawdown cone generated by the Grootegeluk mine after nearly 30 years of operation is approximately 3 km. Therefore the transmissivity of 0.4 m³/d can be taken as a worst case scenario for the study area, with the transmissivity of 0.12 m³/d being closer to the actual situation, though it is likely to vary from one location in the study area to the next.

Table 26: A summary of the predicted water influxes and drawdown cones for the three different transmissivities.

Initial Dewatering Models					
Layer	Transmissivity *m ² /d	Inflow *m ³ /d	Time in Years	Drawdown Cone *km	Location of Constant Head
1	0.4	388.29	10	2.8	Layer 2
2	0.4	500.71	10	2.6	
1	0.28	318.65	10	2.2	Layer 2
2	0.28	409.72	10	2	
1	0.12	202.69	10	1.4	Layer 2
2	0.12	259.20	10	1.4	
1	0.40	574.20	10	2.6	Layer 3
2	0.40	604.68	10	2.6	
3	0.40	897.08	10	2.4	
1	0.28	470.80	10	2.2	Layer 3
2	0.28	496.27	10	2.2	
3	0.28	701.58	10	2km	
1	0.12	298.81	10	1.4	Layer 3
2	0.12	315.14	10	1.4	
3	0.12	402.57	10	1.4	
1	0.40	748.83	10	2.8	Layer 4
2	0.40	748.77	10	2.8	
3	0.40	747.78	10	2.8	
4	0.40	754.73	10	2.6	
1	0.28	613.90	10	2.2	Layer 4
2	0.28	613.87	10	2.2	
3	0.28	613.19	10	2.2	
4	0.28	617.86	10	2.2	
1	0.12	389.52	10	1.6	Layer 4
2	0.12	389.50	10	1.6	
3	0.12	389.24	10	1.6	
4	0.12	391.09	10	1.6	

10.2.4. Decant Model for Scenario 1

As the primary objective of this project is to determine what the effects of mining will be on the groundwater resources, it is prudent to determine if the mines would ever reach a level at which surface decanting would occur. Accordingly a decant model geared to the same scenarios as the dewatering models was constructed. A situation was simulated where the pit had been filled to surface level and a recharge of 20% of the annual rainfall was assigned to the pit itself. A transmissivity of $0.4 \text{ m}^2/\text{d}$ was assigned to the model to simulate worst case conditions and the transmissivity in the pit was set to $500 \text{ m}^2/\text{d}$. The model was run for 50 years. According to the model, there was a total rise in water level of 2 m in the pit after 50 years (Figure 140 & Figure 141). Given this insignificant rise in the water level after 50 years, and the high level of evaporation in the study area, it was determined, that the pits in the study area are not likely to decant.

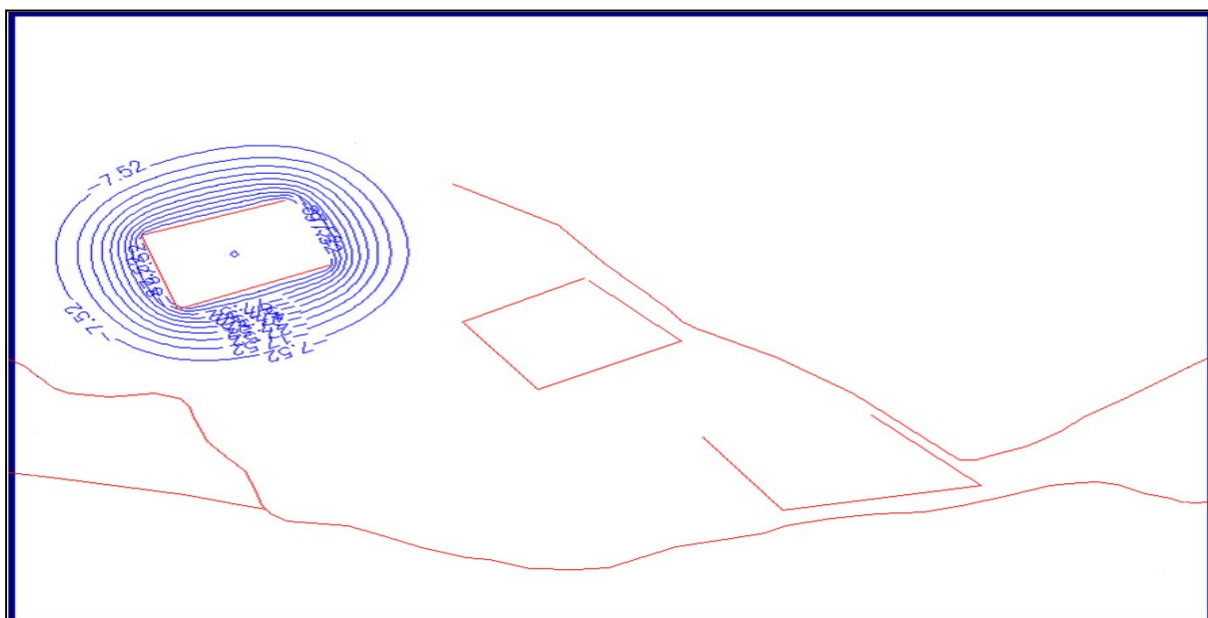


Figure 140: Showing the drawdown cone for layer 4, 50 years after mining has stopped.

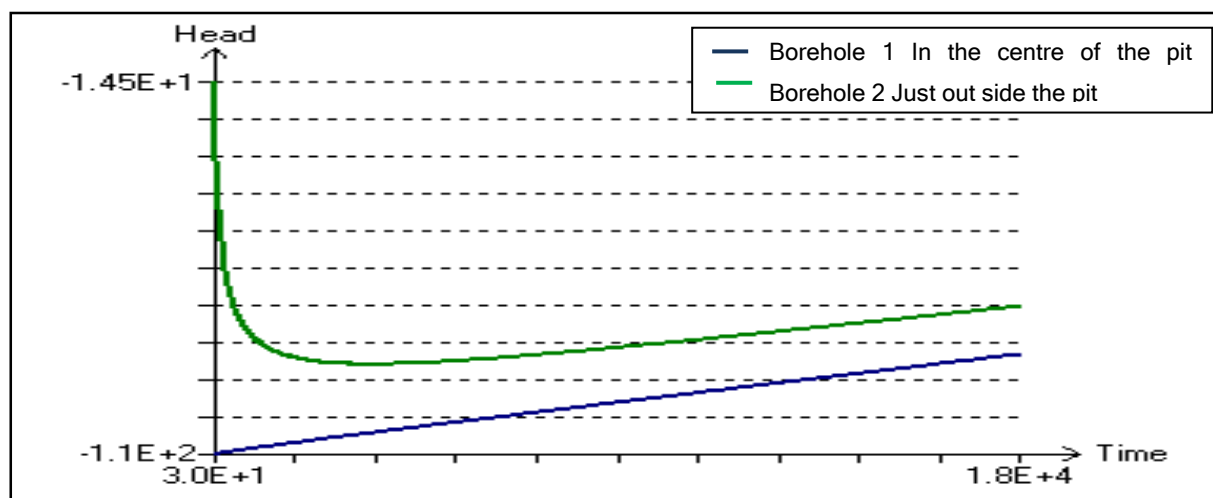


Figure 141: Head-Time graph of the first decant scenario, showing the initial fall in water level and the later rise of the water in the pit.

Two additional scenarios were modelled to improve the simulation of the situation in the study area. The first of these was to determine the conditions in the mine should the mine intersect an unknown fault running through the study area. The scenario was simulated for both dewatering and decanting. For the second scenario, all the faults in the study area were activated as zones of high transmissivity, and three pits were modelled for both dewatering and decanting scenarios.

10.2.5. Dewatering for Scenario 2: Mine Intersecting a Fault

The model was run with all the same parameters as for the models in the first scenario, with the additional parameter of one activated fault that ran through the mine from north to south. The fault was assigned a transmissivity of $500 \text{ m}^2/\text{d}$, and the pit a transmissivity of $100 \text{ m}^2/\text{d}$, while a transmissivity of $0.4 \text{ m}^2/\text{d}$ was assigned to the model in general to simulate worst case conditions. The model ran for 50 years and influx into the mine was calculated at 10 year intervals. The following figures show the differences in the drawdown cones displayed by the different layers after dewatering layer 4 for 10 and 50 years respectively.



Figure 142: Draw down cone for Layer 2, dewatering of layer 4, after 10 years.

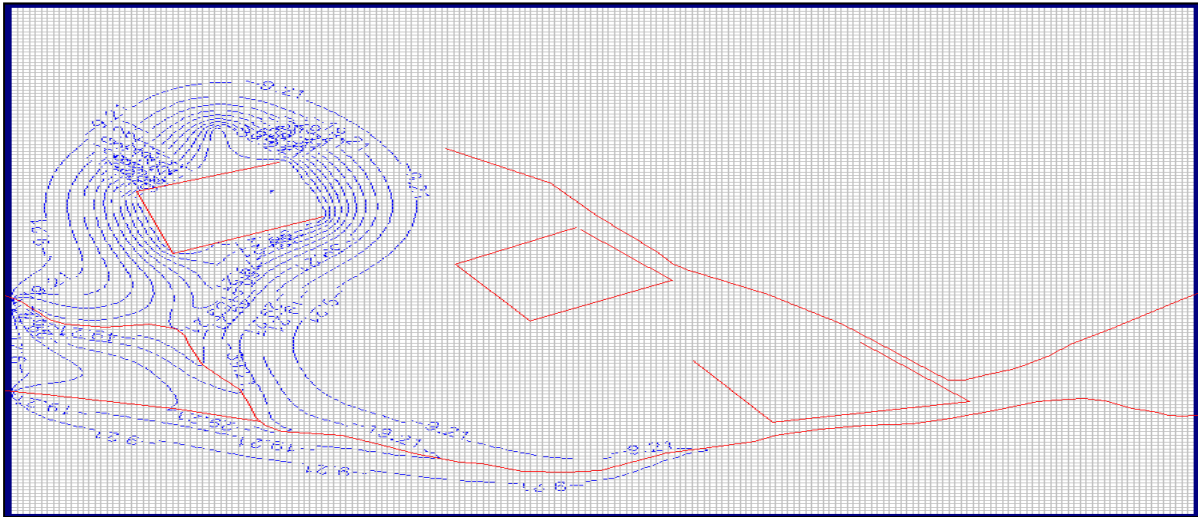


Figure 143: Drawdown cone for layer 2, dewatering layer 4, after 50 years.

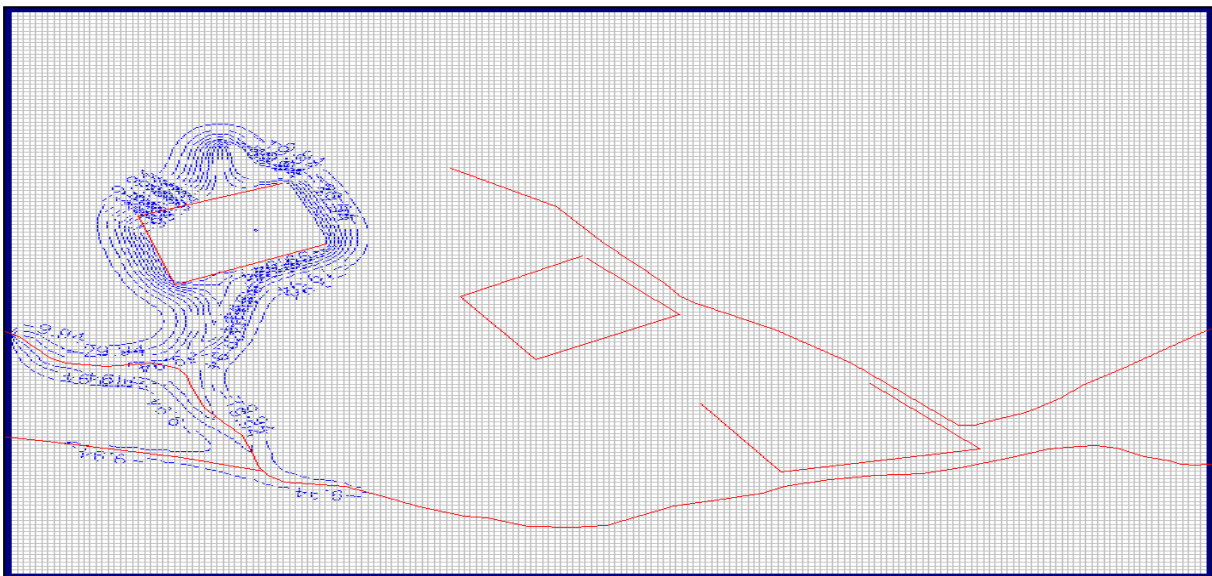


Figure 144: Drawdown cone for layer 3 after 10 years.

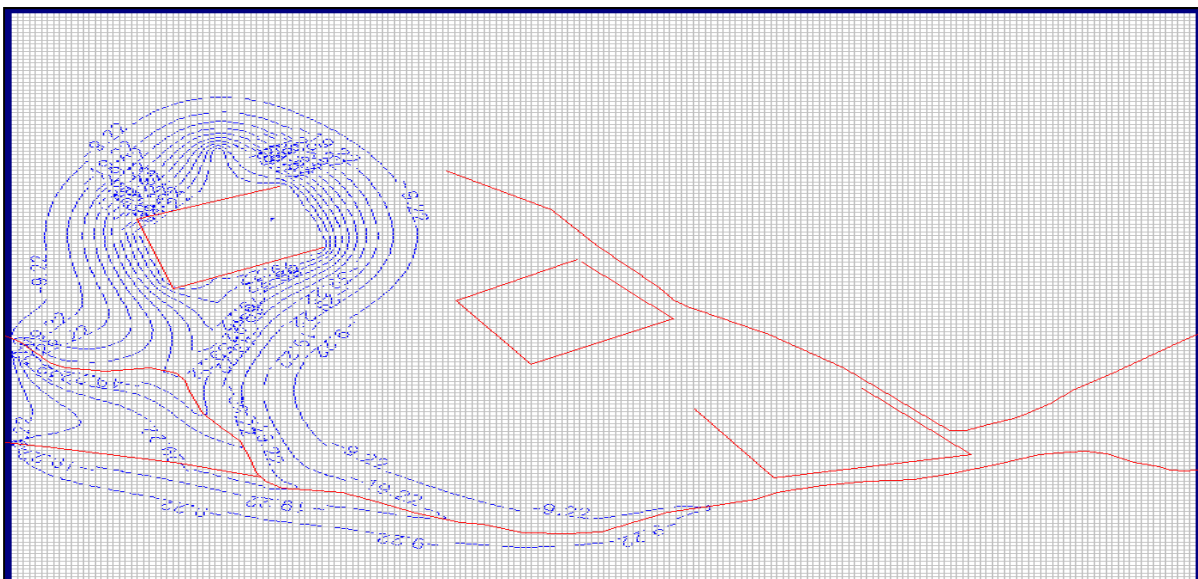


Figure 145: Drawdown cone for layer 3 after 50 years.

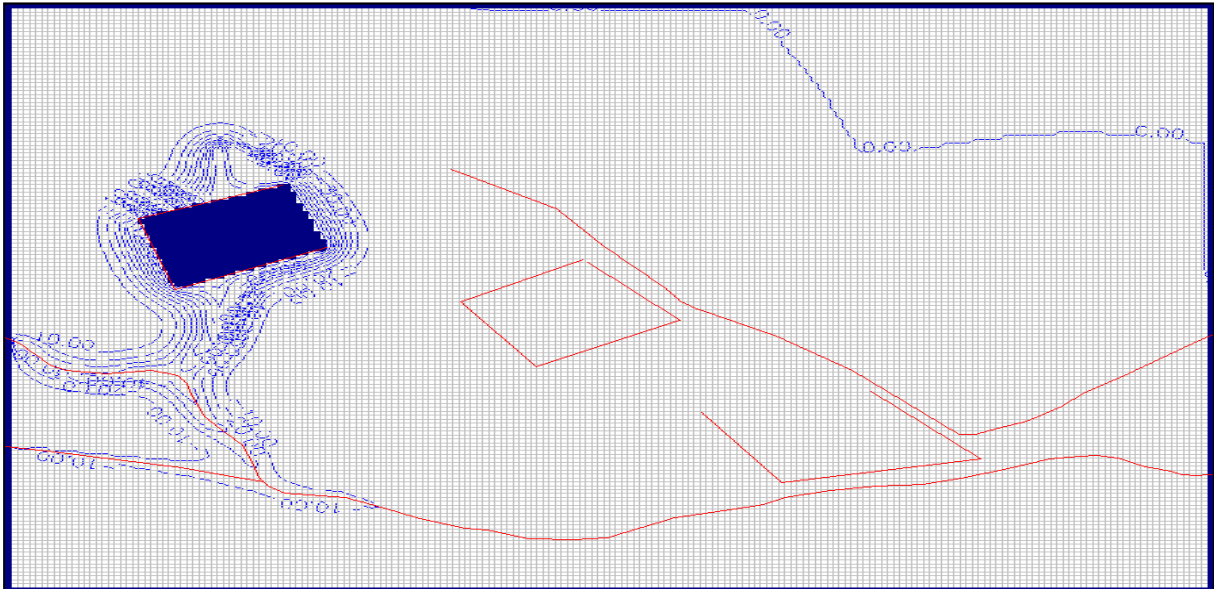


Figure 146: Drawdown cone for layer 4 after 10 years.

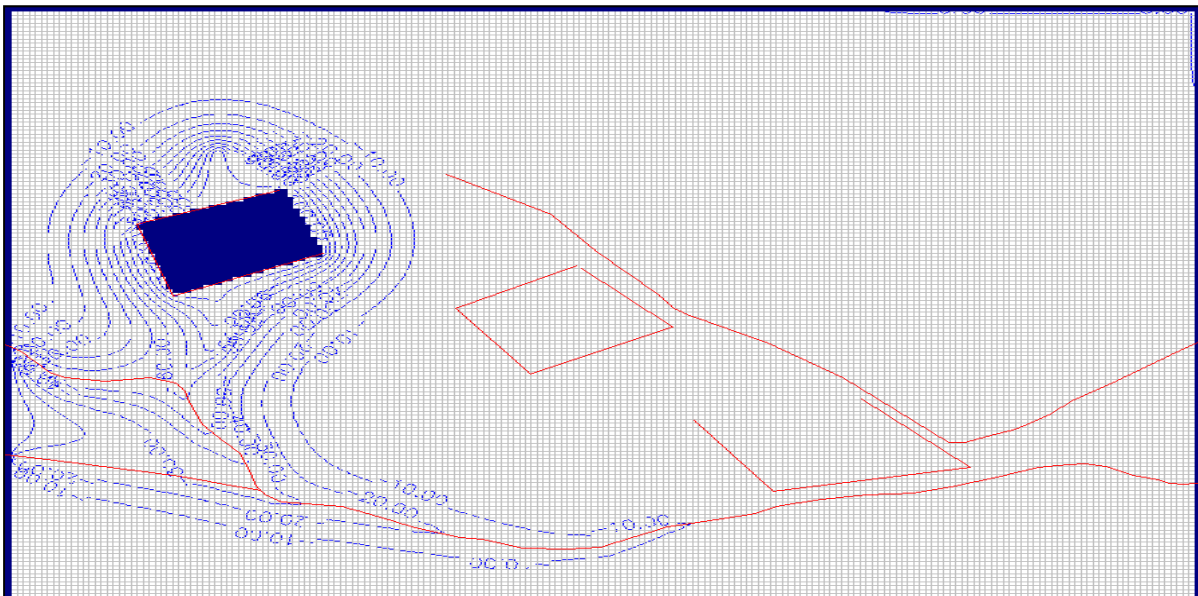


Figure 147: Drawdown cone for layer 4 after 50 years.

10.2.5.1. Discussion of Dewatering Models for Scenario 2

According to Table 27 there is a great difference in the volume of water predicted to flow into the mine should a major fault be encountered. As expected, the amount of water entering the mine decreases with time as a result of the fault being dewatered. The size of the drawdown cones increases as one move's from layer 1 down to layer 4. With layer 1 displaying a drawdown cone of 1.4 km and layer 4 a drawdown cone of 3.2 km after 50 years of dewatering. When comparing these findings to the findings for the first scenario, and using the same transmissivity there is a marked difference. The drawdown cone for layer 4 in the first scenario, after 10 years, was 2.6 km. In this scenario the drawdown cone for the same layer at the same transmissivity is far smaller (1.4 km).

However where, in the first scenario, the drawdown cone of 2.6 km was observed around the entire perimeter of the pit, the 1.4 km drawdown cone in the second scenario is only observed at the northern, eastern and western areas of the pit. Towards the south the drawdown cone follows the length of the fault, extending nearly 20 km towards the southeast, indicating that the fault acts as a preferred pathway. Therefore if the mine should intersect a fault, the impact on the water levels along the length of the fault may be severe, depending on the size, location and orientation of the fault.

It is therefore recommended that thorough surveys be conducted prior to mining in order to avoid sighting or expanding the mine through a fault. With time, the size of the drawdown cone around the pit increases as more and more of the surrounding aquifers are dewatered.

Table 27: A summary of the inflow and drawdown cones for the dewatering of scenario 2.

Mine intersecting a fault scenario:					
Layer	Transmissivity *m ² /d	Inflow *m ³ /d	Time in Years	Drawdown Cone *km	Location of Constant Head
1	0.40	1751.52	10	1.4	Layer 4
2	0.40	1750.47	10	1.4	
3	0.40	1738.45	10	1.4	
4	0.40	1870.53	10	1.4	
1	0.40	1381.22	20	2	Layer 4
2	0.40	1378.77	20	2	
3	0.40	1364.28	20	2	
4	0.40	1486.50	20	2	
1	0.40	1211.75	30		Layer 4
2	0.40	1208.06	30		
3	0.40	1192.63	30		
4	0.40	1312.49	30		
1	0.40	1107.53	40		Layer 4
2	0.40	1102.80	40		
3	0.40	1086.86	40		
4	0.40	1206.60	40		
1	0.40	1034.37	50	3.2	Layer 4
2	0.40	1028.77	50	3.2	
3	0.40	1012.45	50	3.2	
4	0.40	1133.02	50	3.2	

10.2.6. Decant Model for Scenario 2

A model was constructed to simulate the possibility for decanting, in the event of a fault being discovered. The model ran for 50 years, and the results are given in Figure 148. The model indicated a water-level rise of between 6 m and 7 m after 50 years (Figure 149).

It may therefore be concluded that, even if a fault is encountered during the course of mining, the mine will still not reach decant level. Even with a significant increase in the water level, the high degree of evaporation and the natural water level (around 28 m below the surface) will prevent the mine from reaching decant level. It is recommended that the mining houses, conduct thorough surveys of the areas where the mines are to be located, to avoid or minimise the potential for encountering faults during the course of mining operations.

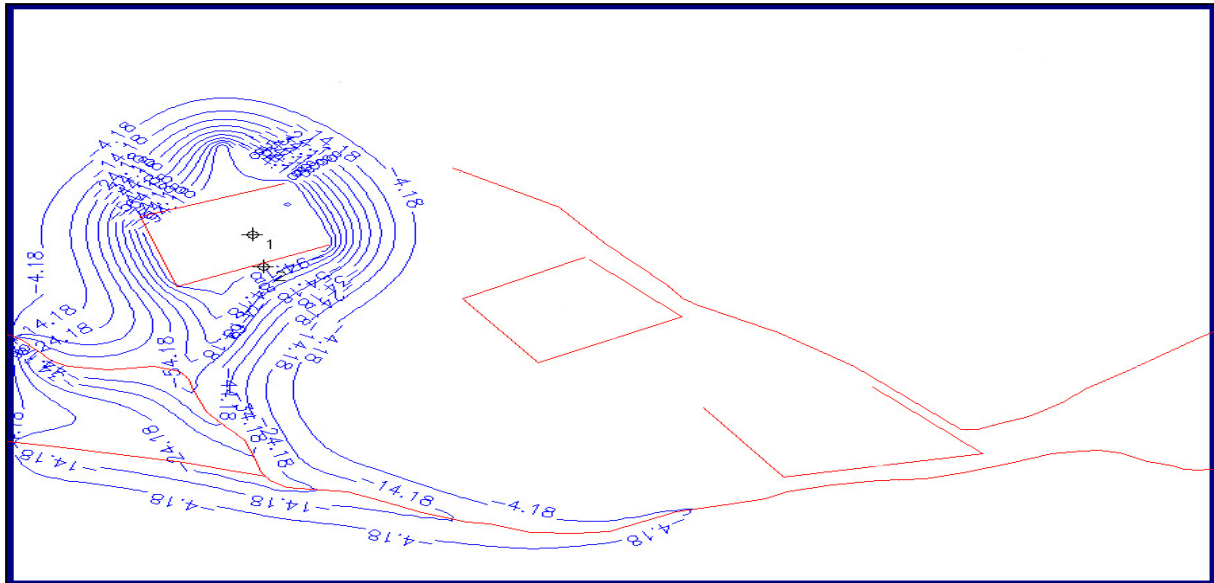


Figure 148: Decant model for Scenario 2.

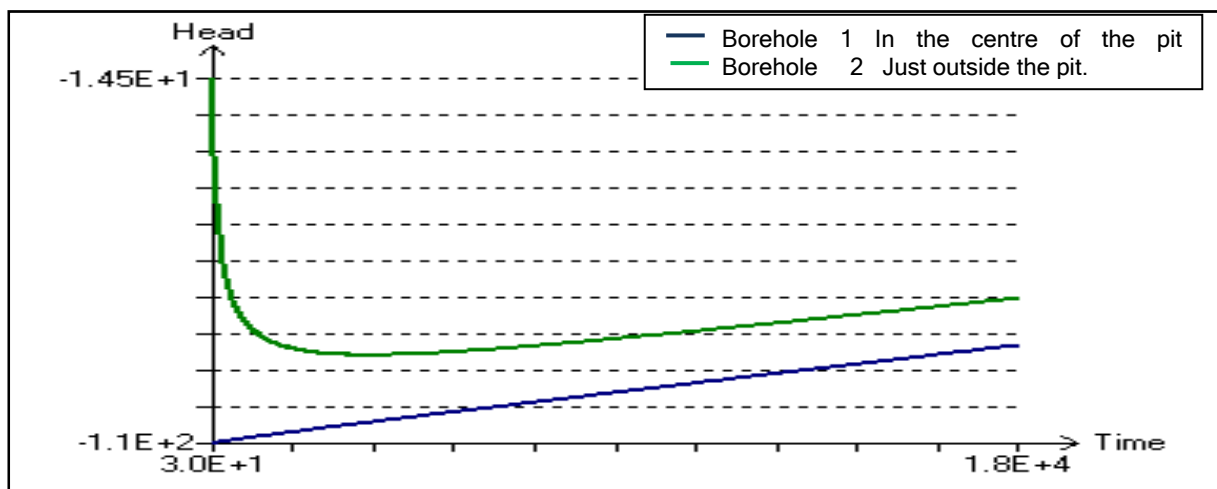


Figure 149: The Head-Time graph for the second scenario.

10.2.7. Dewatering Models for Scenario 3: Three Pits & Active Faults

The final set of constructed models were intended to demonstrate a scenario in which three pits are operational and have been mined down to a level of 110 m below surface. For this model, all the faults were activated and assigned transmissivities of 500 m²/d. The model was run for 50 years and inflow into the mine calculated for every 10 years. A transmissivity of 0.4 m²/d was used for the model.

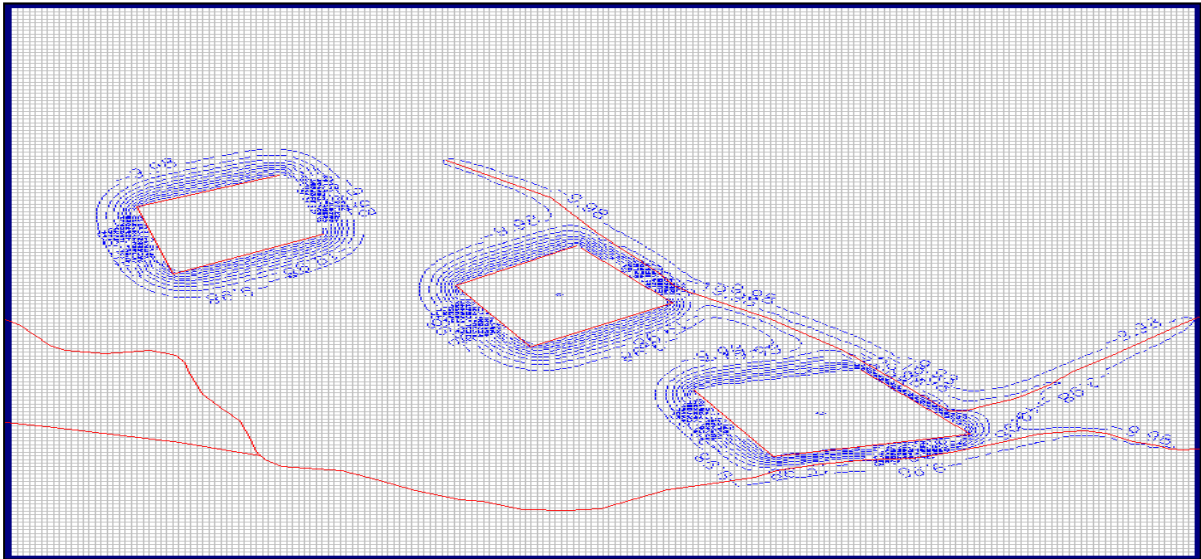


Figure 150: Drawdown cone for layer 2, 10 years after dewatering.

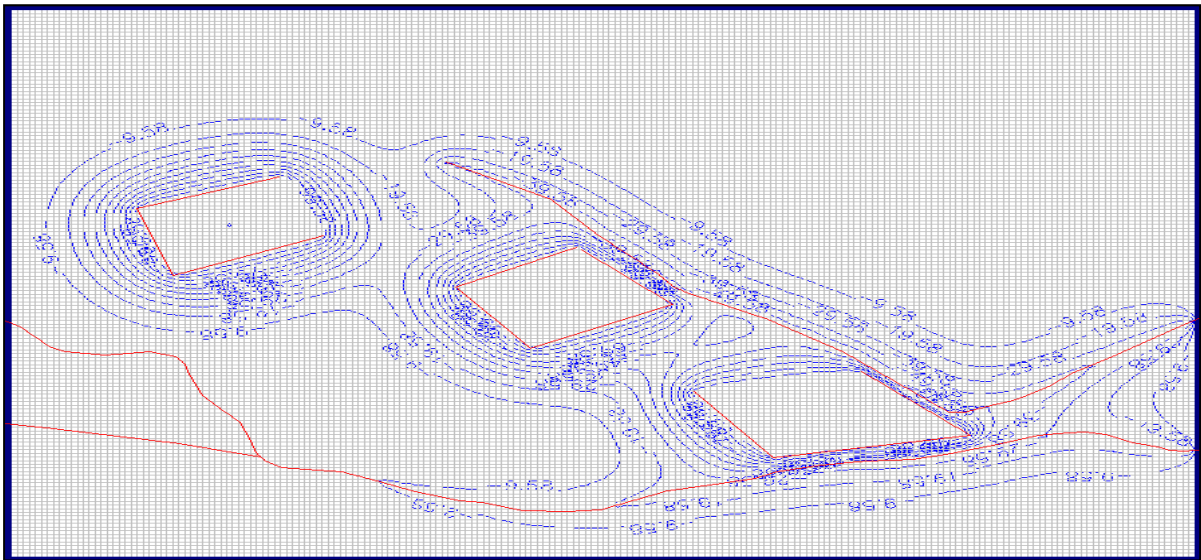


Figure 151: Drawdown cone for layer 2, 50 years after dewatering.

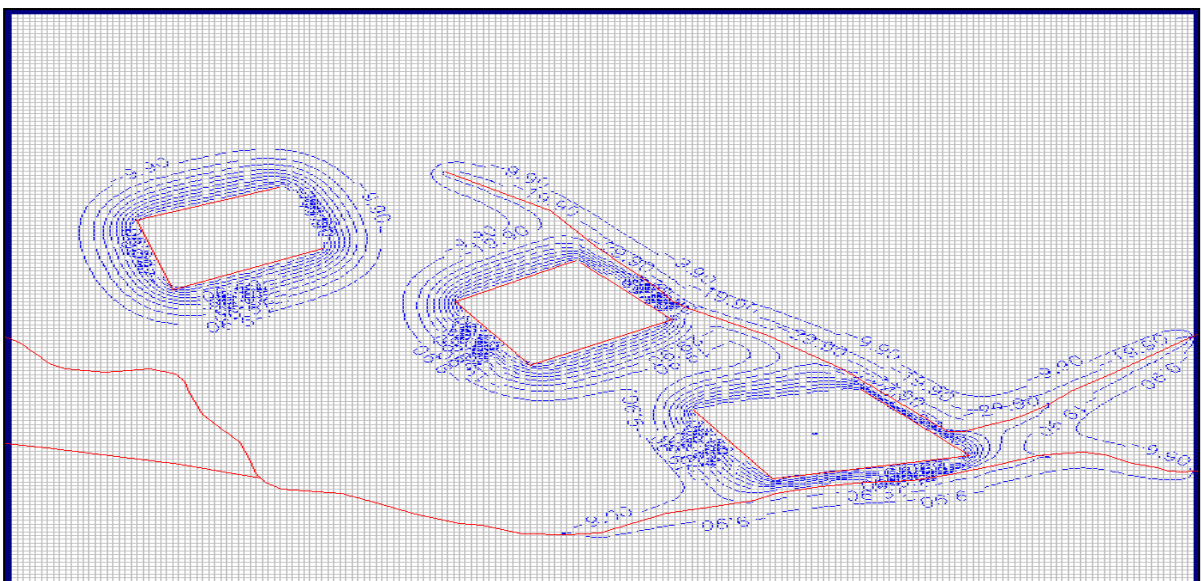


Figure 152: Drawdown cone for layer 3 after 10 years of dewatering.

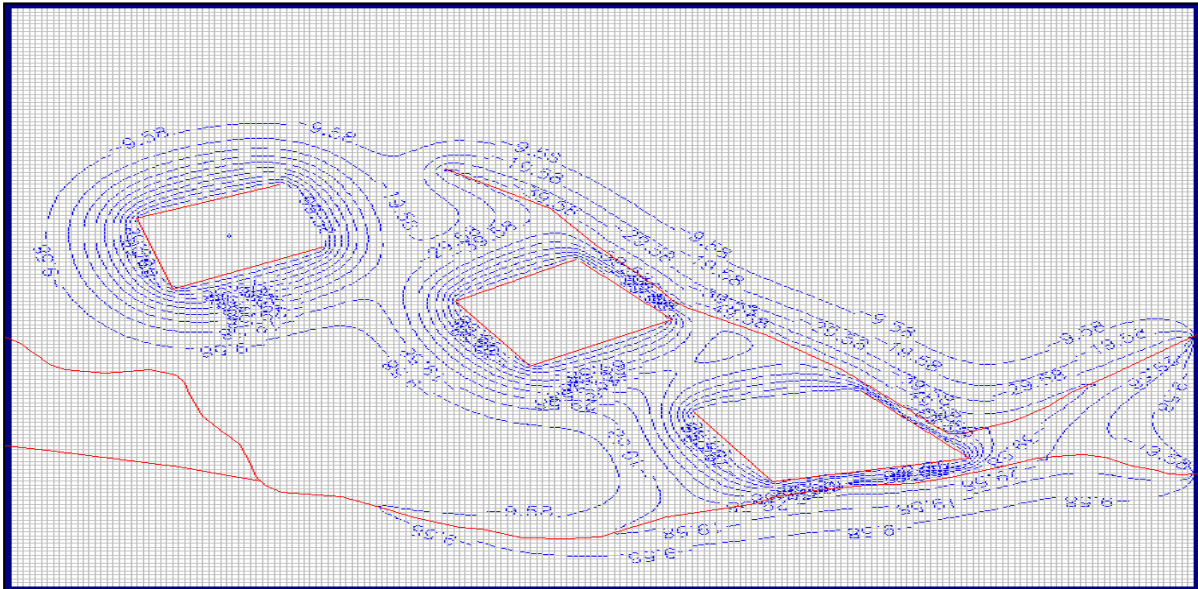


Figure 153: Drawdown cones for layer 3 after 50 years of dewatering.

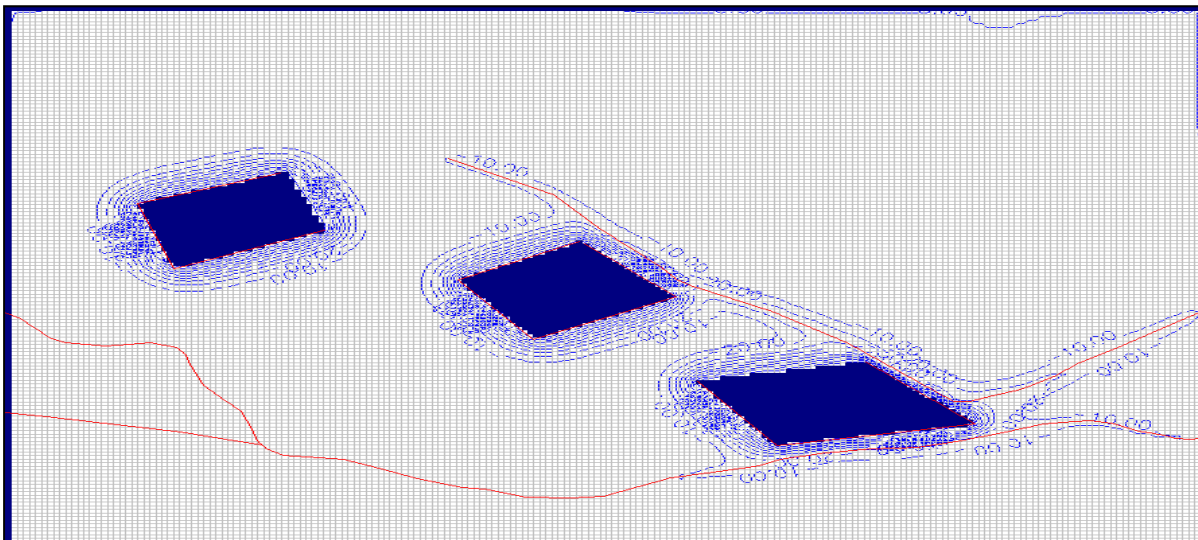


Figure 154: Drawdown cones for layer 4, 10 years after dewatering.

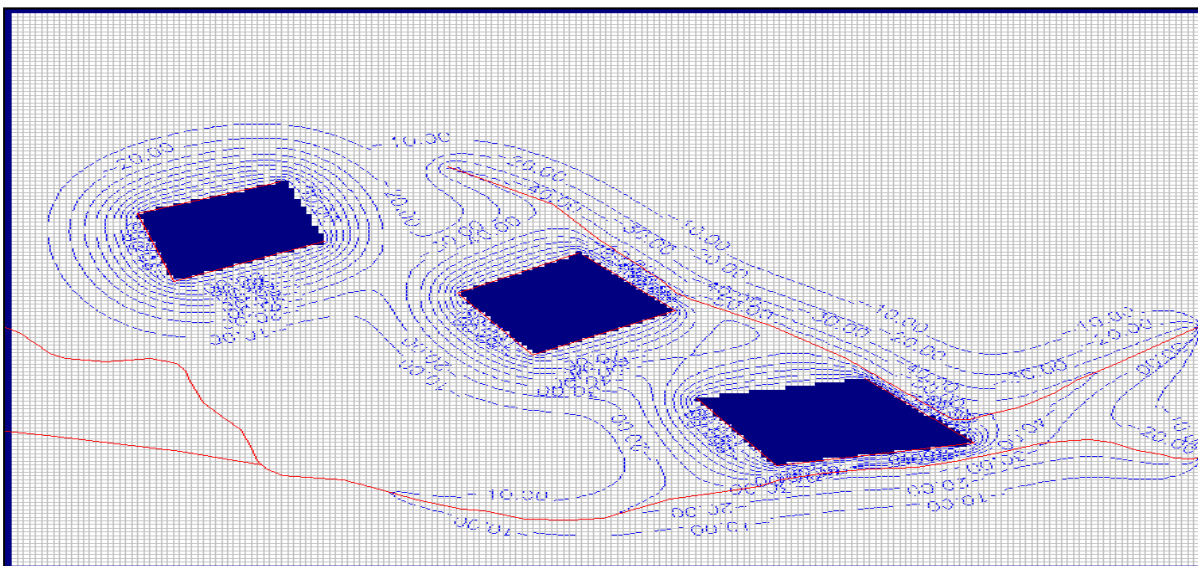


Figure 155: Drawdown cones for layer 4 after 50 years of dewatering.

10.2.7.1. Discussion of Dewatering Models for Scenario 3

The model indicates that, if the mines are located in close proximity to one another (5 km, chosen to simulate worst-case situations), dewatering from one mine will have an impact on adjacent mines. Furthermore, the faults will have an impact on both the drawdown cones of the mines and the volumes of water flowing into the mines located in the vicinity of the faults. For the northern pit, the model indicates that the amount of water entering the mine decreases with time, with an increase in the extent of the drawdown cone (Table 28).

For the central pit, a similar scenario is observed, although it is notable that the volumes of water increase due to the proximity of the pit to a fault (Table 29). Furthermore, the initial size of the drawdown cone is smaller than that for the northern pit, although it is much larger after 50 years. The volumes of water entering into the central pit decrease with time, as was the case in the northern pit. However, the volumes entering into the mine workings are higher with the addition of the much larger drawdown cones.

The initial drawdown cones for the central and northern pit are very similar, with a variation of 0.2 km after 10 years of dewatering (larger in the case of the northern pit, or smaller for the central pit). There is however, a much larger difference (1.4 km) in the final drawdown cones after 50 years of dewatering. At this stage the influence of the proximity of the mines to the faults, as well as the proximity of the mines to one another can be seen.

Again as in the case with the second scenario, the extent of the drawdown cone is amplified by the presence of the faults, with the drawdown cones “following” the faults. It is recommended that the selection of mine locations be preceded by extensive exploration to determine the location of faults. With regard to the south eastern pit, very much the same situation holds as that observed in the other two pits (Table 29). The initial drawdown cones are similar to those in the other pits, and the size of the final cone observed after 50 years is very large. The volumes of water flowing into the pit, are significantly greater than in the case of the other two pits.

This is due to the location between two faults of the south-eastern pit. The pit is thus influenced by both faults and “draws” water from both the faults. From the data displayed in the tables (Table 28, Table 29 & Table 30) we may conclude that there is a clear decrease in the volume of water flowing into the pit with the progression of time.

It must be stated that in reality the likelihood (if only initially) of the pits being in such close proximity is fairly small. It is likely that, as the models predicted, the pit proximity will play a role in determining the volumes of water flowing into the mines. This will increase in proportion to the sizes of the pits, and with the growing proximity of the pits to one another.

Table 28: A Summary of the drawdown cones and expected inflow in the northern pit for scenario 3.

Three pits active and all faults active scenario (North Pit):					
Layer	Transmissivity *m2/d	Inflow *m3/d	Time in Years	Drawdown Cone *km	Location of Constant Head
1	0.40	748.83	10	1.4	Layer 4
2	0.40	748.77	10	1.4	
3	0.40	747.78	10	1.4	
4	0.40	754.73	10	1.4	
1	0.40	558.13	20	2	Layer 4
2	0.40	558.01	20	2	
3	0.40	556.65	20	2	
4	0.40	564.00	20	2	
1	0.40	474.04	30		Layer 4
2	0.40	473.86	30		
3	0.40	472.26	30		
4	0.40	480.14	30		
1	0.40	423.52	40		Layer 4
2	0.40	423.30	40		
3	0.40	421.51	40		
4	0.40	429.95	40		
1	0.40	388.41	50	3.2	Layer 4
2	0.40	388.15	50	3.2	
3	0.40	386.20	50	3.2	
4	0.40	395.18	50	3.2	

Table 29: A summary of the expected inflow and drawdown cones for the central pit.

Three pits active and all faults active scenario (Middle pit):					
Layer	Transmissivity *m2/d	Inflow *m3/d	Time in Years	Drawdown Cone *km	Location of Constant Head
1	0.40	804.82	10	1.2	Layer 4
2	0.40	804.77	10	1.2	
3	0.40	803.77	10	1.2	
4	0.40	811.35	10	1.2	
1	0.40	624.84	20	1.8	Layer 4
2	0.40	624.72	20	1.8	
3	0.40	623.32	20	1.8	
4	0.40	631.60	20	1.8	
1	0.40	537.63	30		Layer 4
2	0.40	537.45	30		
3	0.40	535.77	30		
4	0.40	544.73	30		
1	0.40	480.36	40		Layer 4
2	0.40	480.13	40		
3	0.40	478.22	40		
4	0.40	487.80	40		
1	0.40	437.68	50	4.6	Layer 4
2	0.40	437.41	50	4.6	
3	0.40	435.31	50	4.6	
4	0.40	445.48	50	4.4	

Table 30: A Summary of the drawdown cones and the expected inflow for the south eastern pit.

Three pits active and all faults active scenario (South Eastern pit):					
Layer	Transmissivity *m ² /d	Inflow *m ³ /d	Time in Years	Drawdown Cone *km	Location of Constant Head
1	0.40	1271.40	10	1.4	Layer 4
2	0.40	1271.34	10	1.4	
3	0.40	1270.13	10	1.4	
4	0.40	1282.59	10	1.4	
1	0.40	1069.80	20	2.2	Layer 4
2	0.40	1069.66	20	2.2	
3	0.40	1067.84	20	2.2	
4	0.40	1082.77	20	2.2	
1	0.40	964.59	30		Layer 4
2	0.40	964.36	30		
3	0.40	962.08	30		
4	0.40	979.12	30		
1	0.40	893.41	40		Layer 4
2	0.40	893.09	40		
3	0.40	890.43	40		
4	0.40	909.37	40		
1	0.40	840.09	50	5.2	Layer 4
2	0.40	839.71	50	5.2	
3	0.40	836.71	50	5.2	
4	0.40	857.39	50	5	

10.2.8. Decant Model for Scenario 3

The decant model for scenario 3 indicated rises in water levels of between 2.5 m and 2.6 m for the northern pit, 2.7 m in the central pit, and between 3.4 m and 3.5 m in the south-eastern pit after 50 years (Figure 156). This is in accordance with the initial models that indicated a rise of 2 m in the northern pit. Accordingly the proximity of the adjacent pits helps to reduce the volumes of water which will flow back into the pit once mining has stopped.

According to information received from the Grootegeluk mine, the main influx of water into the pit at the mine occurs during times of intense rainfall (rainfall events measuring 25 mm or more). To account for this, the rational formula for predicting run-off ($Q = CiA$, where Q is the run-off, C is a constant, i is rainfall intensity and A is the expected run-off area (in this instance C was selected as 0.07)) was used to calculate the expected run-off into a pit with an area of 800 ha. This leads to an expected rise in water level of 0.026 m and a volume of 43200 m³/d (Q calculated to be 0.5 m³/d). This will have almost no effect on the potential for the mines to reach decant levels. The modelling results indicate that small volumes of water move into the mines. This factor, coupled with the low rainfall, deep water levels and high evapotranspiration will result in the mines not reaching the appropriate levels at which decanting can occur.

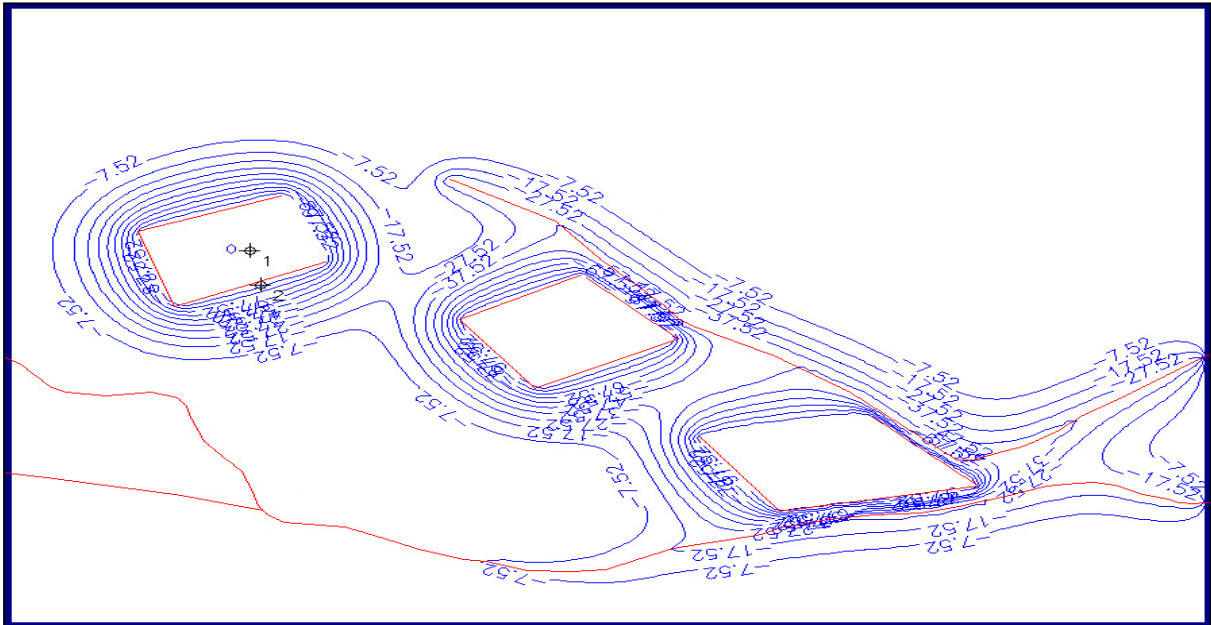


Figure 156: Decant model for the third scenario.

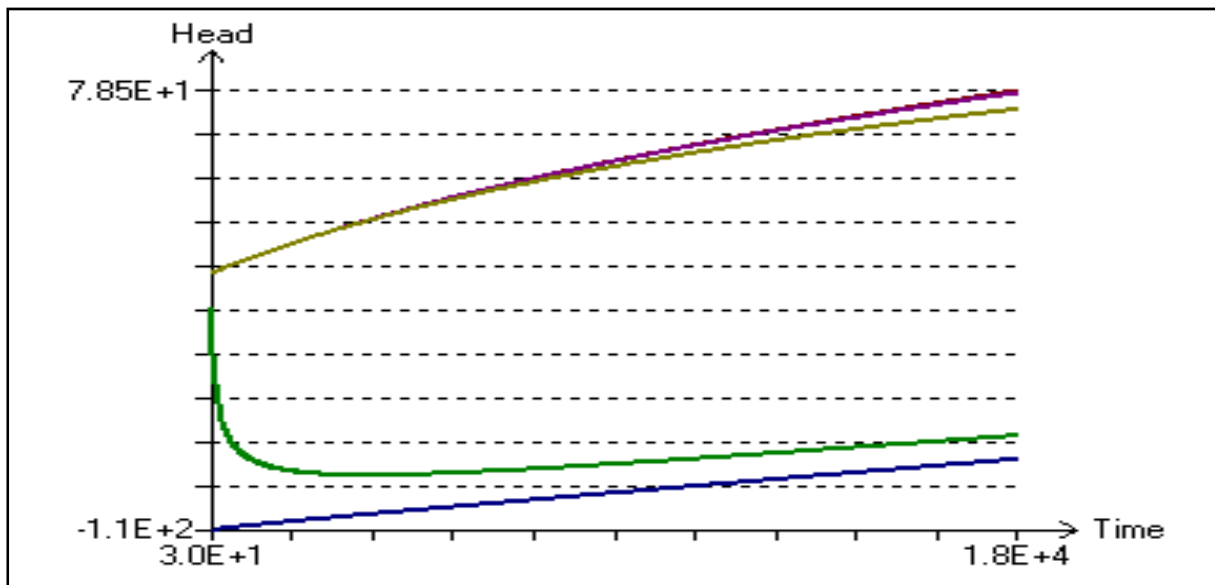


Figure 157: A graph for the decant model of the third scenario.

10.3. Discussion of Model Results

10.3.1. Inflow of Water

For all the scenarios there is very little inflow into the pits. When taking only the worst case transmissivities of $0.4 \text{ m}^2/\text{d}$, the inflow is as follows:

- **Scenario 1:** The inflow varies between $749 \text{ m}^3/\text{d}$ and $755 \text{ m}^3/\text{d}$ for layers 1 and 4 respectively. These are very small volumes, translating to $22465 \text{ m}^3/\text{month}$ and $22642 \text{ m}^3/\text{month}$.
- This is in accordance with what has been observed at the currently active mine.

- **Scenario 2:** For this scenario the inflow for the same layers over the same time period is much higher due to the influence of the fault running through the pit. The inflow is predicted to be in the order of between 1752 m³/d and 1871 m³/d for layers 1 and 4 respectively.
- This constitutes a substantial increase in the water influx and care should be taken by the mining houses to avoid mining through a fault as this will lead to a much larger radius of influence from mining activities.
- **Scenario 3:** According to the data for this scenario, the closer the pits are located to the faults and to one another, the larger the impact of the faults and the adjacent mines will be. With the increasing proximity to the faults, the volumes of water expected to move into the mines increase.
- For example for layer 4 of the northern pit located furthest away from a fault the expected influx is 755 m³/d, while the expected influx into the south-eastern pit is calculated to be 1283 m³/ in the same layer over 10 years.
- It is therefore recommended that the mines not be located too close to the faults and further, that the sizes of the mines be monitored to prevent the pits from becoming excessively large (larger than 1000 ha).

10.3.2. Drawdown Cones

- **Scenario 1:** When taking the worst case there is little variation in the drawdown cones produced in the different layers after 10 years, with all the layers displaying a drawdown cone of 2.8 km with the exception of layer 4 displaying a drawdown cone of 2.6 km.
- **Scenario 2:** Due to the fault running through the pit, the drawdown cone of the pit is dramatically increased, following the fault.
- The drawdown cone, in the immediate vicinity of the pit is not as large as in the first scenario (1.4 km for all 4 layers), but the influence of the mine dewatering can be observed for nearly the entire length of the fault.
- **Scenario 3:** In this scenario the influence of the close proximity of the pits to the faults and to one another can be clearly identified by the very large drawdown cones.
- The cones for the different pits vary with the northern and south-eastern pits displaying a drawdown cone of 1.4 km for all the layers.
- The central pit displays a drawdown cone of 1.2 km around the pit after 10 years.
- The size of the cones increases as time progresses showing the same trend as with the second scenario in that the faults amplify the impact of the dewatering caused by mining.

10.4. Conclusion

From the different scenarios simulated during modelling, several conclusions can be drawn for both decant and dewatering scenarios.

10.4.1. Dewatering

The dewatering simulations indicated that there is very little groundwater in the study area and that the water moves slowly (due to the low transmissivities of the rocks), predominantly along structures such as dykes, fractures and faults. The predominant geological structures in the study area (the three main faults) act as conduits for water movement. This was indicated by the modelling and is also observed in the field, largely through the fact that boreholes located near the structures have higher yields than boreholes located further away from the structures. Accordingly, it is predicted that should a mine intersect a fault during mining operations, the volume of water expected to flow into the mines will increase. It is therefore recommended that mines try to avoid mining through a fault.

10.4.2. Decant

From the modelling results generated by both dewatering and decanting models, there is no evidence that the pits will reach decant levels. The water volumes in existence are not large enough. Moreover, the low transmissivities and high levels of evaporation lead to the conclusion that the pits will not reach decant level.

CHAPTER 11: Groundwater Management in the Waterberg Coalfields

11.1. Introduction

From the results of the modelling it is clear that the volumes of water that will enter the mines from both groundwater sources and from surface runoff will be small. Due to the small volumes of water expected to enter the workings of the mines, it is recommended that the water be pumped out and used for run-off mine operations such as dust suppression or washing of the ore. Figure 158 & Figure 159 show sumps at the Grootegeluk mine where all the water flowing into the mine is concentrated and pumped out, to be used for the running of mine operations.



Figure 158: Surface runoff and groundwater inflow concentrated in a single location in the mine workings, courtesy of the Grootegeluk mine.

Steps should be taken to ensure or minimize the risk of encountering a fault during mining. If the mines encounter large faults and start to dewater the faults, many farmers with boreholes along the length of the fault might see significant decline in the water levels of their boreholes.



Figure 159: An obsolete sump being backfilled, courtesy of the Grootegeluk mine.

11.2. Water Quality Management

At present the main form of pit rehabilitation at the Grootegeluk mine involves the placement of rocks back into the pit in the same order as that of their removal. However, due to the large quantity of coal removed from the pit (nearly 60 m), it will never be rehabilitated to surface level. Accordingly the pit will be backfilled as a series of benches each lined and sealed, until all the backfill material has been used. This will lead to the generation of a moving void as the pit is continuously mined, while the areas that have been mined out are backfilled. Additionally to account for the volume of coal removed during mining the spoils/discard from the beneficiation process will be placed into the pit and covered with the rock removed during mining. In an effort to minimize the exposure of these rocks (and the discard from the beneficiation plants) to oxygen and water it was decided early in the study that it would be best to store the rocks with the highest acid potential near the bottom of the pit. It was hoped that the more dangerous acid generators located near the bottom of the pit would be flooded, thus diminishing the capacity for acid generation.

However, due to the low levels of rainfall in the study area, the small transmissivities, low recharge and the high evaporation, flooding of the spoils by means of natural processes will not be possible. It was proposed by Fourie (2009) that water from a pipeline that is currently under construction (for the transport of water to the study area) be used to flood the spoils.

This remains within the realms of possibility, although it is predicted that this will be too expensive an exercise, both in monetary and water-volume terms to be sustainable. Given the small volumes of water expected to flow into the mines and the porous nature of the backfilled pit, it is predicted that placing the spoil on the lowest level of the pit will inevitably lead to acid generation. It is therefore proposed that the spoil, along with other rock units that have the potential to produce acid, be placed at a higher level to keep the spoil “dry.” The spoil should only be exposed to the minimal influx of groundwater into the pit and the occasional heavy surface runoff. This will minimize the level of acid generation that will take place from the spoils. By doing so, the runoff that reaches the spoil will, unfortunately become acidic. This effluent will collect in the area of the pit that cannot be rehabilitated with waste rock. To reduce the level of generated acidity, it is recommended that the rocks with high base potential be mixed with the rocks with a high acid potential, as this will further minimize the amount of acidity that will be generated.

The generated effluent from this mixture of high acid potential and high base-potential rocks is expected to have high salt contents and will most likely turn acidic with time as the buffer potential is diminished. This effluent will become very concentrated as time passes.

The reasons for this are twofold:

- The effluent will gather in a single area in the pit.
- The effluent will be exposed to the open air and thus the high levels of evaporation in the study area.

The generation of the acidity is unavoidable, but the collection of this effluent in one location and the low volume expected to enter into the pit, does have certain advantages. The localization of the effluent can localize the treatment of said effluent, thus for example if the addition of carbonates is selected for treatment of the acidity, it will only need to be applied to one area.

Van Tonder (2009) proposed that the size of the material being used for backfill be varied. If this is done it will alter the porosity of the backfilled mine. This will lead to a very slow migration of any acid generated in the backfilled mine and will serve to delay the movement of the generated acidic effluent. Although the prevention of the generation of acid cannot be effected, time will be created for the mining houses to implement the necessary management protocols.

In addition to varying the size of the material used as backfill Van Tonder (2009) recommended that the pits be lined with a layer of Bentonite clay. This would prevent the movement of acidic or otherwise contaminated pit water from moving into the groundwater systems. This is a very solid proposal, although the major drawback is that it would be very expensive to line a pit of 700 ha or more with Bentonite.

If the mining company operating the mine has sufficient funds to finance this method, it would indeed be a very sound method for the prevention of aquifer contamination. A method of acid generation prevention proposed by Dreyer (pers. comm. 2009) involves slurring all the spoils, the discard and the effluent from slimes dams and evaporation ponds. This slurry is then to be pumped back into the pit and the entire pit is sealed. This method will be ideal for the solution of the acid generation problem and the potential movement of the contaminants into the groundwater system.

The slurry proposal along with the flooding proposal will both serve to eliminate the acid generation problem. The problem with the methods however are that they can only be employed once all the mining in the pit has stopped. Even if the method currently being used at Grootegeluk of rehabilitating in benches and sealing each bench individually is used the large volumes of contaminated water that will be present in the pit will provide an unacceptable risk to the miners. It is therefore proposed that the method currently employed at the Grootegeluk mine be used for all the new mines planned for the area. In addition it is recommended that spoils/discard be placed at levels that will minimize the exposure of these rocks to the influx of groundwater.

11.3. Potential Rehabilitation Methods for AMD

Many options for the management of water quality within opencast coal mines have been considered in the past. Unfortunately very few practical solutions have generally been available. Some of these measures will be discussed and their viability and applicability to the study area will also be discussed.

The actions in the treatment of AMD are twofold and they can be either:

11.3.1. Preventative measures

- Attempt to control the rate of acid generation
- Attempt to limit the migration of the acid generation products

11.3.2. Containment measures

- To flood as much of the spoils as possible, thus eliminating oxidation of sulphides, and/or
- To contain and evaporate the spoil water

From the above, the most viable form of treatment for AMD will be containment, as the effluent generated will gather in a single location. Although the philosophy behind containment is sound, there are several practical limitations; the final water level in any pit is regulated by it's decant level.

The decant level is the lowest topographic level where water from the pit will eventually overflow onto surface, but/ and this level will never be reached in the pits in the study area. The second reason for considering the containment of spoil water relates to evaporation as a potential management strategy. (Hodgson *et al.*, 1995). The evaporation in the study area is 2000 mm/y- a very large amount - and will decrease the water stored in the pit considerably. With the evaporation area being contained within the boundaries of the pit itself, this will cut down on costs and exposure of other areas to potential pollution. Containment whether within the spoil or in evaporation areas, will however lead to further salination of the water.

According to the chemical data of the water analysis, it becomes apparent that the groundwater found in some areas in the study area is already saline. Any further deterioration of the groundwater quality will have a detrimental effect on those who are dependent on groundwater. However, if this low quality water can be contained in the pit itself and not re-enter the groundwater system, it will have no effect on people dependant on the groundwater resource. Containment is a possible option for the management of spoil water. However, containment appears to be more applicable to new opencast mining where total containment can be planned. Containment is therefore a viable option for the newly planned collieries in the study area, but should be monitored closely.

11.3.3. Additional Options for the Treatment of Acidic Waters

11.3.3.1. Introduction of Buffering Agents

The addition of acid-consuming components increases the salt load in the environment. However, saline alkaline leachates are generally more favourable to the environment than acidic waters. Buffering agents introduced into spoils are varied (Hodgson *et al.*, 1995). The introduction of buffering agents as a means to prevent / manage acid generation, might hold problems for the study area.

From the chemical data of the groundwater analysis of the study area it has become evident that there are already areas that have high salt levels. The introduction of more salt to the system will aggravate the conditions further. This will cause the already scarce groundwater resources to become even more so.

11.3.3.2. Introduction of Lime

Where lime is added to the spoil surface, the base potential is transported into the spoil via the dissolution of the material by percolating rain water. However, there is a limit to the solubility of mineral phases within rain water. The resultant weakly buffered alkaline water may be insufficient to neutralise all the acidity of the spoil, depending on the rate of acid production (Hodgson *et al.*, 1995).

Due to the low levels of rainfall and the concentration of rainfall in the summer months, it is doubtful that this rehabilitation method will have success in the study area. Lime addition is most effective where the neutralising components are thoroughly mixed within the spoil. This places the acid-consuming materials in close proximity to the acid-generating sites, thereby inhibiting the development of acidic environments. This counteracts bacterial oxidation of the pyrite.

11.3.3.3. Introduction of Power Station Fly Ash

Power-station fly ash is considered as a commodity by the power-generating industry of South Africa. The capacity of the fly ash to neutralise acid mine drainage is only about 5% - 16% of that of lime. A further disadvantage of fly ash addition is that the material contains significant concentrations of heavy metals (Hodgson *et al.*, 1995).

If the fly ash dosage is insufficient for complete neutralisation of the system, the resultant acidity will be accompanied by the additional release of heavy metals. An excess dosage of fly ash will therefore be required to compensate for the higher risk associated with the use of this ameliorant. It may be concluded that the use of power station fly ash is only suitable for mines that are slightly acidic or alkaline in nature. It is not recommended that this material be used in very acidic mines, due to the high heavy metal content of the ash.

According to Dreyer (pers. comm. 2009) there is little to no acid generation at present taking place at the Grootegeluk mine. Due to the close proximity of the Matimba power station and the additional power station planned for the area, there will be no shortage of fly ash. If indeed the mines do not become very acidic and the acid that is generated can be neutralized in a few applications of the method, this method could be utilized with some success in the study area.

11.4. Conclusion

There are many possible water-quality control measures that can be used to either prevent groundwater contamination or to contain any possible contaminants in the study area. It is recommended that preventative measures be taken rather than focus merely on containment for the new mines planned for the area. Additionally, regarding the collected data, it is recommended that the rehabilitation methods currently employed by the Grootegeluk mine be used by the new mines as it has proven to be an effective form of rehabilitation for the local conditions in the study area.

CHAPTER 12: Conclusions

12.1. Introduction

From the various aspects of the groundwater systems of the Waterberg coalfields investigated during the course of the project, certain conclusions can be drawn. A conceptual model (Figure 160) for the Waterberg coalfield was constructed to summarize the findings of the project. The model is not to scale and focuses on the areas to the west of the Daarby fault as this area will be mined by means of opencast methods.

12.1.1. Climate

From Figure 160 one can observe that the study area has a dry climate, with low rain fall and high evapotranspiration. The model displays the primary runoff for the study area and the location of the Limpopo River

12.1.2. Geology

Figure 160 additionally displays the primary geological structures and the divisions of the coal seams in to 11 zones as found in the study area. The location of the three main geological structures (the Daarby-, Eenzaamheid- and Zoetfontein faults) and the relation of these structures to the location of the coal in the study area can also be seen. Figure 160 also displays the distribution of the primary geological formations found in the study area namely the relation of the Karoo and Waterberg group rocks to the faults. The model further shows the sub division of the study area on the basis of the weathering that had taken place. With the green areas showing the full succession of geology, the yellow areas have been eroded down to the middle Ecca and the red sections have been weathered in parts.

12.1.3. The Mine Workings

In addition to these geological parameters, the model displays the location of a single pit modeled on the Grootegeluk pit. The pit displays the method of rehabilitation currently being used at the Grootegeluk mine, in an effort to reduce the amount of acid generated, subsequent to determinations through investigation that a certain amount of acid generation is unavoidable. The current measured parameters such as the influx of water and the drawdown cone of the pit at the Grootegeluk mine are also given, showing an influx of 30000 m³/month and a drawdown cone of approximately 3 km 25 years after mining had commenced.

12.1.4. Measured Parameters and Modelling Results

Measured results such as the average water level of 28 m below surface, recharge (determined by the CI and E.A.R.T.H. methods) of 1.5% and the expected rise of 2 m in water level once mining has stopped in the area are also displayed in the model. In addition the model also shows the effect the mining infrastructure has on the groundwater in its vicinity, as is manifested by the artificial recharge witnessed at the Grootegeluk mine on the eastern side of the Daarby fault.

12.1.5. Acid-Base Results

The results of the ABA, based on the determinations of the weathering depth of the geology are summarized in Figure 160. The green areas show signs of being likely acid generators with an increased likelihood of acid generation at a depth of 50m - 80 m beneath the surface. The results for the yellow areas were inconclusive as no determinations could be made with regards to acid potential and weathering depth for these areas. In addition, the results indicated that samples taken from the red areas along with discard samples from the beneficiation plants at the Grootegeluk mine will generate acid once exposed to water and oxygen.

12.1.6. Water Quality

A summary of the observed water qualities for the different localities examined during the study, is provided in the model. Four primary localities may be distinguished, namely;

- The areas that are unaffected by activities, showing fair water qualities, with high CI contents and EC values
- The areas affected by Coal Bed Methane extraction, which display very high EC and CI values. These values are not the result of pollution but, are a natural phenomenon related to the depth of the boreholes and the age of the water.
- The areas that have been affected by mining display EC and CI values that are similar to those observed for the unaffected areas. These areas do, however, have severely elevated SO₄ levels as a result of mining activities.
- Areas affected by power generation: the focus here was on the effects of coal-fire power generation, namely the fly-ash dump found in the area, which indicated high EC values, lower pH values and elevated CI and SO₄ values.

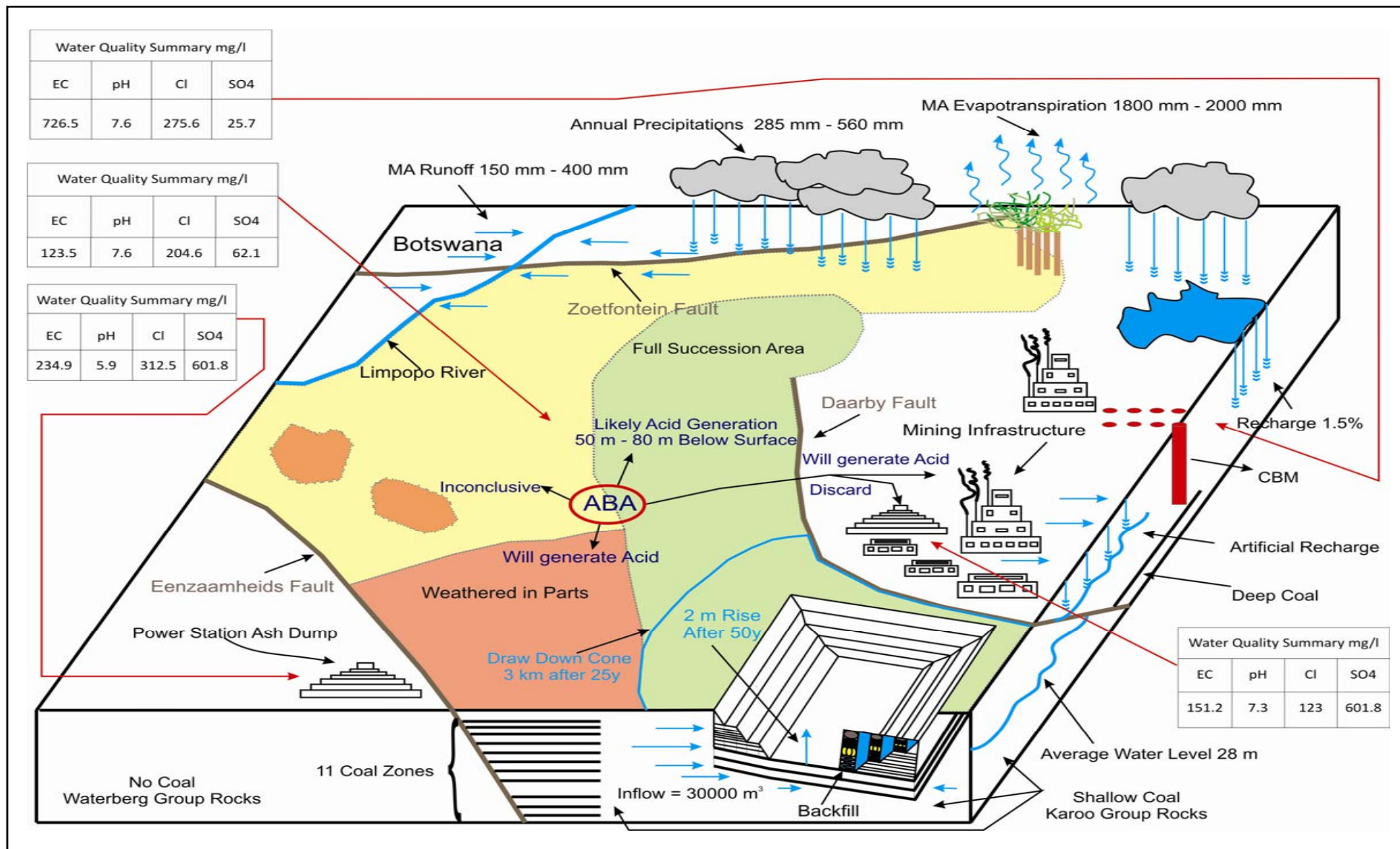


Figure 160: Conceptual model for the Waterberg coalfield, showing a single pit backfilled in the manner as is being done at the Grootegeluk mine. Additionally the model provides a summary of the water quality for the various localities of the study area along with aquifer parameters such as recharge. This model is not to scale.

This study concludes with the view that the addition of new mines to the area will have a detrimental effect on both the quality and the quantity of the groundwater in the study area. The small volumes of water that are available in the study area will be reduced by the excavation of new mines. The effects will be more visible in areas located west of the Daarby fault. The impermeable nature of the fault will prevent groundwater movement from the areas east of the fault to those west of the fault. The same applies to the areas north of the Eenzaamheid fault, as, according to Dreyer (pers. comm. 2009), this fault is also impermeable. Consequently, groundwater on the southern side of the fault will not be affected by abstraction on the northern side of the fault.

12.2. Recommendations

It is recommended that the method of mining, beneficiation, remediation and water management currently being employed by the Grootegeluk mine, be employed by the new mines. The methods being used at the Grootegeluk mine have been proven to be the best possible solutions, and are certainly the most suitable for the conditions found in the study area.

Additional Recommendations are as follows:

- The performing of additional ABA testing over a larger area and the expansion of the testing program to include kinetic tests.
- A Study to be done on the possibility of using water from the new pipeline for the purpose of flooding the spoils, and on how this will influence the rehabilitation methods for backfilling the pit.
- A study should be done on the impact of water from the new pipeline, and to determine how much of the pipeline water will enter the groundwater system.
- A study to determine the percentage of water moving into the groundwater system from the washing plants
- It is recommended that the size of the material to be replaced in the pits as backfill be varied as this will decrease the porosity of the backfilled pit and retard the movement of contaminants.
- It is recommended that the discard and spoils be slurried, pumped back into the mine and that the entire mine then be sealed by bentonite clay or other absorbent material. These measures will prevent the movement of the pollutants into the groundwater system.

CHAPTER 13: References

- Brady, K. B. C., Perry, E. F., Beam, R. L., Bisko, D. C., Gardner, M. D. and Tarantino, J. M. (1994). Evaluation of Acid-Base Accounting to predict the quality of drainage at surface coal mines in Pennsylvania, U. S. A. In: Proceedings of the International
- Bredell, J.E. (1987). South African coal resources explained and analysed. Unpubl. Rep. Geol. Surv. S.Afr., 39 pp.
- Cadle, A.B., Cairncross, B., Christie, A.D.M. and Roberts, D.L. (1993). The Karoo Basin of South Africa: type basin for the coal-bearing deposits of southern Africa. *Int. J. Coal Geol.*, 23, 117-157.
- Dreyer, C. (2008/2009) Personal Communiqué
- Fourie, F. (2009). Personal Communiqué
- Grobbelaar, R., (2001). The long-term impact of inter-mine flow from collieries in the Mpumalanga coalfields. M.Sc Thesis (Unpubl) University of the Free State, Bloemfontein
- Hunter, D. (1997a). Acid Mine Drainage Status of Research. <http://www.osmre.gov/amdres.htm>
- Hodgson, F.D.I., and Krantz, R.M. (1995). Groundwater quality deterioration in the Olifants River Catchment above the Loskop Dam with Specialised Investigations in the Witbank Dam Sub-Catchment. WRC Report No 291/1/95
- Hodgson, F.D.I., Vermeulen, P.D., Cruywagen, L.M., de Necker, E. (2007). Investigation of Water Decant from the Underground Collieries in Mpumalanga, with Special Emphasis on Predictive Tools and Long-Term Water Quality Management. WRC Report No 1263/1/07
- Johnson, M.R., van Vuuren, C.J., Visser, J.N.J., Cole, D.I., de V. Wickens, H., Christie, A.D.M., Roberts, D.I., and Brandl, G. (2006). Sedimentary Rocks of the Karoo Supergroup. In: Johnson, M.R., Anhaeusser, C.R, and Thomas, R.J. (Eds.), *The Geology of South Africa*. Geological Society of South Africa. 494 - 495 pp.
- Price, W. A., Errington, J. and Koyanagi, V. (1995). Guidelines for the prediction of Acid Rock Drainage and Metal leaching for mines in British Columbia: Part 1. General procedures and information requirements. In: Proceedings of the Fourth International Conference on Acid Rock Drainage. Vol. 1, May 31 - June 6, Vancouver, BC., pp. 1 - 14.

Scharer, J. M., Bolduc, L., Petit, C. M., Halbert, B. E. (2000). Limitation of Acid-Base Accounting for Predicting Acid Rock Drainage. In: Proceedings of the Fifth International Conference on Acid Rock Drainage. Vol. 1, Denver, Colorado.

Scharer, J. M., Petit, C. M., Kilkaldy, J. L., Bolduc, L., Halbert, B. E. and Chambers, D. B. (2000). Leaching of Metals from Sulphide Mine Waste at Neutral pH. In: Proceedings of the Fifth International Conference on Acid Rock Drainage. Vol. 1, Denver, Colorado.

Sobek, A. A., Schuller, W. A., Freeman, J. R. and Smith, R. M. (1978). Field and Laboratory methods Applicable to Overburdens and Minesoil, WVU, EPA Report No. EPA-600/2-78-054, pp. 47-50.

Steffen, Robertson and Kirsten (1989). Draft Acid Rock Drainage Technical Guide Volume 1 - Technical Guide. Steffen, Robertson and Kirsten.

Snyman, C.P. (1998) "Coal". In: Wilson, M.G.C. and Anhaeusser (Ed) The mineral resources of South Africa. Handbook 16, Council for Geosciences, 6th Edition. ISBN 1-875061-52-5

U.S. Department of the Interior. (1979). Permanent Regulatory Program Implementing Section 501(b) of the Surface Mining Control and Reclamation Act of 1977: Environmental Impact Statement. Washington, D.C.: U.S. Department of the Interior.

Usher, B.H., Cruywagen, L-M., De Necker, E. and Hodgson, F.D.I. (2002). On-site and Laboratory Investigations of Spoil in Opencast Collieries and the development of Acid-Base Accounting Procedures. Report to the Water Research Commission by the Institute for Groundwater Studies

Usher, B., Dennis, I. And Vermeulen P.D. (2005). Impact on shallow groundwater system due to irrigation, Report number: 2005/IRRI/01

Van Tonder, G. (2009) Personal Communiqué

Van Tonder G., Ingo B., Kornelius R., Van Bosch J., Dzanga P., Xu Y.(2002). Manual on Pumping test Analysis in Fractured Rock Aquifers - Part A. Practical Guide for Conducting and Analyzing Pumping Tests. Institute for Groundwater Studies, University of the Free State, Bloemfontein 9300, Report to the Water Research Commission WRC Report No: 1116/1/02.

Van Tonder G., Xu., Y (2001). A guide for the estimation of groundwater recharge in South Africa., Presented at the Workshop on Recharge At the University of Pretoria (June 2001).

Vegter, JR (1995). An Explanation of a Set of National Groundwater Maps, WRC report TT74/95, Water Research Commission, Pretoria.

Vermeulen, P.D. (2006). The impact of irrigation with coal mine water on groundwater resources. Ph.D Thesis (unpuble) University of the Free State, Bloemfontein

Vermeulen P. D., Dennis I (2007). Extension of groundwater monitoring for Matimba power station., Report number: 2007/10/PDV

Ziemkiewicz, P. F. (1997). ABA and the Sobek NP estimate.

Internet Sources

144.171.11.107/Main/Blurbs/International_Energy_Annual_2005_157820.aspx

www.bp.com/sectiongenericarticle.do?categoryId=9023784&contentId=7044480. (Accessed on August 15th 2009)

<http://www.deat.gov.za/Maps> (Accessed on June 26th 2009)

<http://www.eia.doe.gov/cneaf/electricity/epa/figes1.html> (Accessed on August 15th 2009)

<http://www.eia.doe.gov/oiaf/ieo/coal.html> (Accessed on July 22d 2009)

www.iea.org/Textbase/nppdf/free/2007/WEO_2007.pdf (Accessed on August 24th 2009)

<http://www.worldcoal.org/pages/content/index.asp?PageID=188> (Accessed on March 23d 2009)

http://www.sourcewatch.org/index.php?title=South_Africa_and_coal (Accessed on March 23d 2009)

<http://www.southafrica.info/about/geography/limpopo.htm> (Accessed on June 26th 2009)

<http://www.wheretostay.co.za/information/np/b> (Accessed on June 26th 2009)

www.weathersa.co.za SA Weather Service (2008) - Rainfall Figures (Accessed on 13th July 2008)

www.coal-is-dirty.com/category/coal-tags/mountaintop-removal?page=1. (Accessed on 27th June 2009)

www.numahammers.com/newsitems/PS-girardcoalmining.html (Accessed on 10th of November 2009)

Appendix A

Results for the Acid-Base Accounting Analyses

Table 31: Interpretation of ABA pH results.

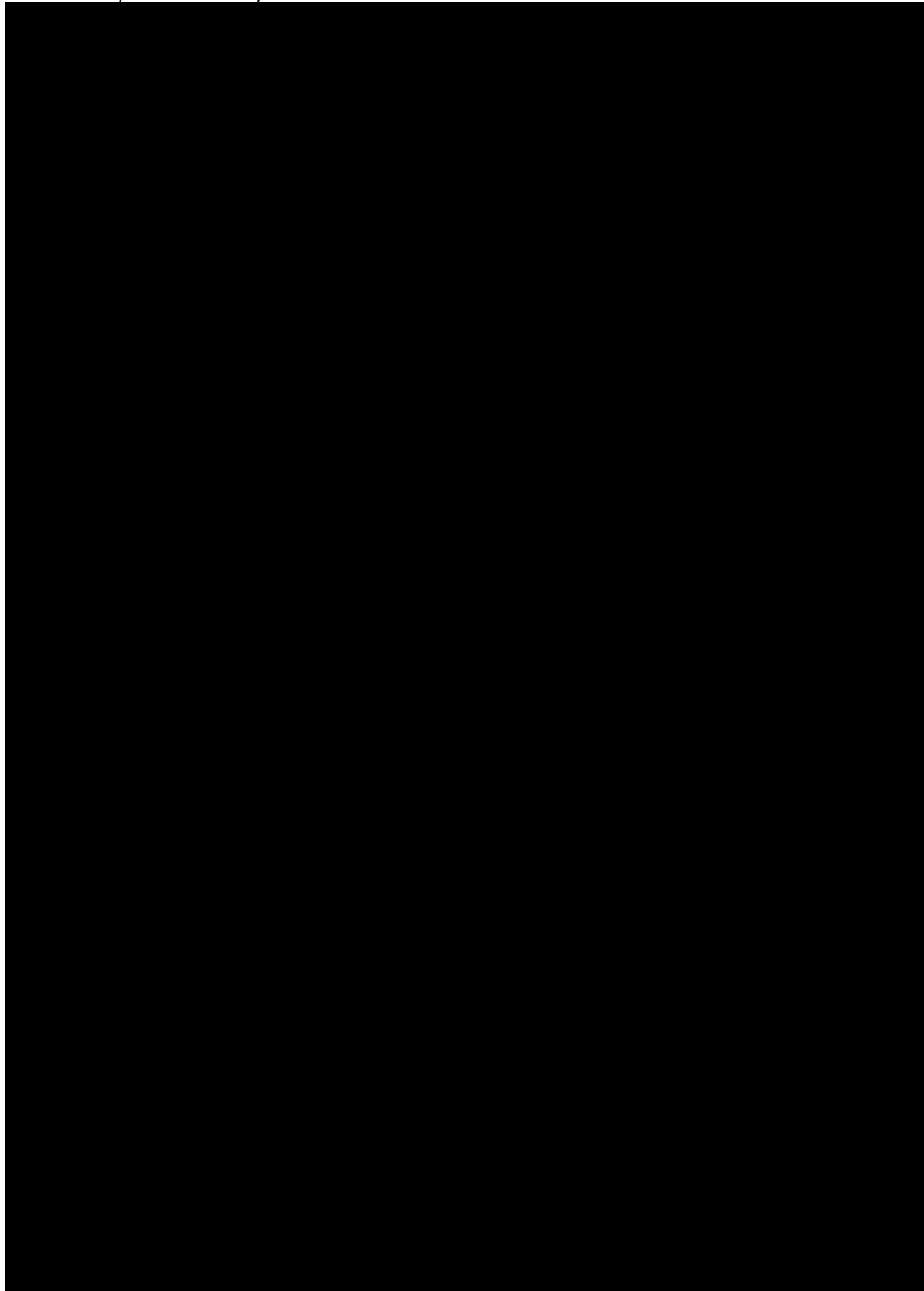


Table 32: Interpretation of ABA Net Neutralizing Potential results.

Site Name	Depth	Net Neutralising Potential (Open)	Net Neutralising Potential (Closed)	Interpretation
SS 1	5m	0.16	-0.09	Verify with other tests
SS 2	17m	1.88	1.62	Verify with other tests
SS 3	25m	3.69	3.41	Verify with other tests
SS 4	43m	-0.27	-0.55	Verify with other tests
SS 5	54m	47.02	23.68	Probably Excess Neutralising Minerals
SS 6	66m	14.16	3.49	Verify with other tests
SS 7	68m	-236.52	-488.39	Potential Acid Generator
SS 8	72m	4.80	-8.72	Verify with other tests
SS 9	75m	-6.05	-10.47	Verify with other tests
SS 10	77m	105.41	101.43	Probably Excess Neutralising Minerals
SS 11	83m	-46.23	-97.73	Potential Acid Generator
SS 12	94m	12.02	9.01	Verify with other tests
SS13	96m	-0.58	-1.02	Verify with other tests
SS 14	104m	51.02	47.16	Probably Excess Neutralising Minerals
SS 15	118m	-97.78	-209.12	Potential Acid Generator
SS16	173m	-6.84	-10.17	Verify with other tests
SS 17	187m	-2.80	-3.95	Verify with other tests
SS 18A	188m	-85.60	-187.93	Potential Acid Generator
SS 18B	188m	-0.93	-1.83	Verify with other tests
SS 19	190m	-3.04	-4.01	Verify with other tests

Table 33: Interpretation and NP/AP ratios for the north/western core samples..

Site Name	Depth	Neutralising Potential Ratio(NP/AP) for Open System	Interpretation Open System	Interpretation Closed System
SS 1	5m	1.640	Acid under certain conditions	Likely Acid Generator
SS 2	17m	8.235	No Acid Potential	No Acid Potential
SS 3	25m	14.365	No Acid Potential	No Acid Potential
SS 4	43m	0.037	Likely Acid Generator	Likely Acid Generator

SS 5	54m	3.015	Acid under certain conditions	Acid under certain conditions
SS 6	66m	2.327	Acid under certain conditions	Acid under certain conditions
SS 7	68m	0.061	Likely Acid Generator	Likely Acid Generator
SS 8	72m	1.355	Acid under certain conditions	Likely Acid Generator
SS 9	75m	0.000	Likely Acid Generator	Likely Acid Generator
SS 10	77m	27.499	No Acid Potential	No Acid Potential
SS 11	83m	0.102	Likely Acid Generator	Likely Acid Generator
SS 12	94m	4.990	No Acid Potential	Acid under certain conditions
SS13	96m	0.023	Likely Acid Generator	Likely Acid Generator
SS 14	104m	14.213	No Acid Potential	No Acid Potential
SS 15	118m	0.122	Likely Acid Generator	Likely Acid Generator
SS16	173m	0.000	Likely Acid Generator	Likely Acid Generator
SS 17	187m	0.009	Likely Acid Generator	Likely Acid Generator
SS 18A	188m	0.163	Likely Acid Generator	Likely Acid Generator
SS 18B	188m	0.011	Likely Acid Generator	Likely Acid Generator
SS 19	190m	0.010	Likely Acid Generator	Likely Acid Generator

Table 34: Initial and final pH values for south eastern samples.

Site Name	Depth	Initial pH	Final pH	Interpretation
GGs 1	33m	8.27	4.99	Medium Risk Acid Generation
GGs 2	52m	7.91	2.22	Higher Risk Acid Generation
GGs 3	150m	6.62	2.55	Higher Risk Acid Generation
GGs 4	156m	8.01	4.57	Medium Risk Acid Generation
GGs 1A	-	8.31	5.30	Medium Risk Acid Generation
GGSVZ 1	1m	5.73	3.38	Higher Risk Acid Generation
GGSVZ 2	2m	6.43	3.11	Higher Risk Acid Generation
GGSVZ 3	3m	6.63	3.85	Medium Risk Acid Generation
GGSVZ 4	4m	6.2	3.62	Medium Risk Acid Generation

Table 35: Interpretation of ABA Net Neutralizing Potential results.

Site Name	Depth	Net NP (Open)	Net NP (Closed)	Interpretation
GGs 1	33m	16.12	-2.70	Verify with other tests
GGs 2	52m	-53.97	-123.05	Potential Acid Generator
GGs 3	150m	-5.26	-7.42	Verify with other tests
GGs 4	156m	77.25	68.40	Probably Excess Neutralising

				Minerals
GGG 1A	-	11.87	11.35	Verify with other tests
GGSVZ 1	1m	-2.39	-2.56	Verify with other tests
GGSVZ 2	2m	-2.93	-3.20	Verify with other tests
GGSVZ 3	3m	-2.49	-2.64	Verify with other tests
GGSVZ 4	4m	-3.74	-4.35	Verify with other tests

Table 36: Interpretation and NP/AP ratios for Exxaro core samples.

Site Name	Depth	NP Ratio(NP/AP) for Open System	Interpretation Open System	Interpretation Closed System
GGG 1	33m	1.857	Acid under certain conditions	Likely Acid Generator
GGG 2	52m	0.219	Likely Acid Generator	Likely Acid Generator
GGG 3	150m	0.005	Likely Acid Generator	Likely Acid Generator
GGG 4	156m	9.728	No Acid Potential	No Acid Potential
GGG 1A	-	24.010	No Acid Potential	No Acid Potential
GGSVZ 1	1m	0.056	Likely Acid Generator	Likely Acid Generator
GGSVZ 2	2m	0.037	Likely Acid Generator	Likely Acid Generator
GGSVZ 3	3m	0.068	Likely Acid Generator	Likely Acid Generator
GGSVZ 4	4m	0.017	Likely Acid Generator	Likely Acid Generator

Table 37: Interpretation of ABA pH results.

Site Name	Depth	Initial pH	Final pH	Interpretation
GT1 S1	1m	6.12	4.47	Medium Risk Acid Generation
GT1 S2	2m	7.45	5.12	Medium Risk Acid Generation
GT1 S3	3m	7.17	4.92	Medium Risk Acid Generation
GT1 S4	4m	7.01	4.61	Medium Risk Acid Generation
GT1 S5	5m	6.49	4.12	Medium Risk Acid Generation
GT1 S6	6m	6.58	3.55	Medium Risk Acid Generation
GT1 S7	7m	6.43	3.38	Higher Risk Acid Generation
GT1 S8	8m	7.00	3.34	Higher Risk Acid Generation
GT1 S9	9m	6.58	3.62	Medium Risk Acid Generation
GT2 S1	1m	8.62	6.29	Lower Acid Risk
GT2 S2	2m	8.34	6.59	Lower Acid Risk
GT2 S3	3m	8.78	6.17	Lower Acid Risk
GT2 S4	4m	8.66	5.29	Medium Risk Acid Generation
GT2 S5	5m	8.48	5.99	Lower Acid Risk

GT2 S6	6m	7.31	5.90	Lower Acid Risk
GT2 S7	7m	8.50	5.64	Lower Acid Risk
GT2 S8	8m	8.43	5.19	Medium Risk Acid Generation
GT2 S9	9m	7.94	4.94	Medium Risk Acid Generation
GT3 S1	1m	6.00	3.50	Lower Acid Risk
GT3 S2	2m	6.62	5.04	Medium Risk Acid Generation
GT3 S3	3m	7.67	5.43	Medium Risk Acid Generation
GT3 S4	4m	7.30	5.26	Medium Risk Acid Generation
GT3 S5	5m	7.50	5.05	Medium Risk Acid Generation
GT3 S6	6m	7.34	4.81	Medium Risk Acid Generation
GT3 S7	7m	6.90	3.74	Medium Risk Acid Generation
GT3 S8	8m	6.82	3.40	Higher Risk Acid Generation
GT3 S9	9m	6.70	3.41	Higher Risk Acid Generation
GT3 S10	10m	6.65	3.80	Medium Risk Acid Generation
GT4 S1	1m	8.38	5.04	Medium Risk Acid Generation
GT4 S2	2m	8.10	5.02	Medium Risk Acid Generation
GT4 S3	3m	8.37	4.90	Medium Risk Acid Generation
GT4 S4	4m	8.16	4.72	Medium Risk Acid Generation
GT4 S5	5m	7.80	4.62	Medium Risk Acid Generation
GT4 S6	6m	8.07	4.62	Medium Risk Acid Generation
GT4 S7	7m	7.21	4.16	Medium Risk Acid Generation
GT4 S8	8m	6.79	3.85	Medium Risk Acid Generation
GT4 S9	9m	6.72	3.77	Medium Risk Acid Generation
GT4 S10	10m	6.77	3.73	Medium Risk Acid Generation
GT7 S1	1m	6.56	3.90	Medium Risk Acid Generation
GT7 S2	2m	7.69	4.52	Medium Risk Acid Generation
GT7 S3	3m	7.49	5.16	Medium Risk Acid Generation
GT7 S4	4m	8.10	4.39	Medium Risk Acid Generation
GT7 S5	5m	7.66	4.48	Medium Risk Acid Generation
GT7 S6	6m	7.61	4.41	Medium Risk Acid Generation
GT7 S7	7m	7.93	4.77	Medium Risk Acid Generation
GT7 S8	8m	8.16	5.75	Lower Acid Risk
GT7 S9	9m	7.43	4.86	Medium Risk Acid Generation
GT7 S10	10m	7.12	4.23	Medium Risk Acid Generation
GT7 S11	11m	6.45	3.75	Medium Risk Acid Generation
GT7 S12	12m	6.49	3.29	Higher Risk Acid Generation
GT7 S13	13m	6.46	4.03	Medium Risk Acid Generation
GT7 S14	14m	6.69	3.67	Medium Risk Acid Generation

Table 38: Interpretation of ABA Net Neutralizing Potential results.

Site Name	Depth	Net NP (Open)	Net NP (Closed)	Interpretation
GT1 S1	1m	1.317	1.082	Verify with other tests
GT1 S2	2m	6.601	6.303	Verify with other tests
GT1 S3	3m	3.781	3.492	Verify with other tests
GT1 S4	4m	1.585	1.307	Verify with other tests
GT1 S5	5m	-0.665	-1.019	Verify with other tests
GT1 S6	6m	-0.956	-1.029	Verify with other tests
GT1 S7	7m	-1.525	-1.634	Verify with other tests
GT1 S8	8m	-1.653	-2.183	Verify with other tests
GT1 S9	9m	-2.994	-4.054	Verify with other tests
GT2 S1	1m	156.529	156.001	Probably Excess Neutralising Minerals
GT2 S2	2m	665.853	665.260	Probably Excess Neutralising Minerals
GT2 S3	3m	511.680	511.352	Probably Excess Neutralising Minerals
GT2 S4	4m	395.971	395.593	Probably Excess Neutralising Minerals
GT2 S5	5m	464.427	464.115	Probably Excess Neutralising Minerals
GT2 S6	6m	220.295	220.279	Probably Excess Neutralising Minerals
GT2 S7	7m	175.360	175.046	Probably Excess Neutralising Minerals
GT2 S8	8m	210.480	210.169	Probably Excess Neutralising Minerals
GT2 S9	9m	24.734	24.388	Probably Excess Neutralising Minerals
GT3 S1	1m	-1.685	-1.988	Verify with other tests
GT3 S2	2m	-1.538	-1.867	Verify with other tests
GT3 S3	3m	4.922	4.670	Verify with other tests
GT3 S4	4m	2.984	2.968	Verify with other tests
GT3 S5	5m	3.670	3.166	Verify with other tests
GT3 S6	6m	2.661	2.701	Verify with other tests
GT3 S7	7m	-1.094	-0.875	Verify with other tests
GT3 S8	8m	-2.953	-3.110	Verify with other tests
GT3 S9	9m	-2.951	-3.244	Verify with other tests

GT3 S10	10m	-2.379	-2.515	Verify with other tests
GT4 S1	1m	140.723	140.790	Probably Excess Neutralising Minerals
GT4 S2	2m	64.082	64.127	Probably Excess Neutralising Minerals
GT4 S3	3m	36.717	36.554	Probably Excess Neutralising Minerals
GT4 S4	4m	11.003	10.828	Verify with other tests
GT4 S5	5m	5.891	5.746	Verify with other tests
GT4 S6	6m	5.474	5.361	Verify with other tests
GT4 S7	7m	-0.379	-0.515	Verify with other tests
GT4 S8	8m	-1.845	-2.102	Verify with other tests
GT4 S9	9m	-1.800	-2.081	Verify with other tests
GT4 S10	10m	-1.673	-1.895	Verify with other tests
GT7 S1	1m	-1.405	-1.533	Verify with other tests
GT7 S2	2m	0.905	0.672	Verify with other tests
GT7 S3	3m	3.822	3.644	Verify with other tests
GT7 S4	4m	1.161	1.392	Verify with other tests
GT7 S5	5m	1.771	1.610	Verify with other tests
GT7 S6	6m	3.547	3.301	Verify with other tests
GT7 S7	7m	48.483	48.651	Probably Excess Neutralising Minerals
GT7 S8	8m	337.764	337.325	Probably Excess Neutralising Minerals
GT7 S9	9m	11.988	11.799	Verify with other tests
GT7 S10	10m	7.970	7.592	Verify with other tests
GT7 S11	11m	-0.421	-0.771	Verify with other tests
GT7 S12	12m	-1.397	-1.793	Verify with other tests
GT7 S13	13m	-0.788	-1.265	Verify with other tests
GT7 S14	14m	-1.220	-1.680	Verify with other tests

Table 39: Interpretation and NP/AP ratios for northern samples.

Site Name	Depth	NP Ratio(NP/AP) for Open System	Interpretation Open System	Interpretation Closed System
GT1 S1	1m	6.608	No Acid Potential	Acid under certain conditions
GT1 S2	2m	23.148	No Acid Potential	No Acid Potential
GT1 S3	3m	14.082	No Acid Potential	No Acid Potential

GT1 S4	4m	6.715	No Acid Potential	Acid under certain conditions
GT1 S5	5m	0.028	Likely Acid Generator	Likely Acid Generator
GT1 S6	6m	0.137	Likely Acid Generator	Likely Acid Generator
GT1 S7	7m	0.092	Likely Acid Generator	Likely Acid Generator
GT1 S8	8m	0.019	Likely Acid Generator	Likely Acid Generator
GT1 S9	9m	0.009	Likely Acid Generator	Likely Acid Generator
GT2 S1	1m	297.754	No Acid Potential	No Acid Potential
GT2 S2	2m	1123.348	No Acid Potential	No Acid Potential
GT2 S3	3m	1562.742	No Acid Potential	No Acid Potential
GT2 S4	4m	1047.468	No Acid Potential	No Acid Potential
GT2 S5	5m	1489.050	No Acid Potential	No Acid Potential
GT2 S6	6m	14219.899	No Acid Potential	No Acid Potential
GT2 S7	7m	559.614	No Acid Potential	No Acid Potential
GT2 S8	8m	676.923	No Acid Potential	No Acid Potential
GT2 S9	9m	72.473	No Acid Potential	No Acid Potential
GT3 S1	1m	0.033	Likely Acid Generator	Likely Acid Generator
GT3 S2	2m	0.030	Likely Acid Generator	Likely Acid Generator
GT3 S3	3m	20.520	No Acid Potential	No Acid Potential
GT3 S4	4m	183.825	No Acid Potential	No Acid Potential
GT3 S5	5m	8.288	No Acid Potential	No Acid Potential
GT3 S6	6m	26.210	No Acid Potential	No Acid Potential
GT3 S7	7m	6.009	No Acid Potential	No Acid Potential
GT3 S8	8m	0.064	Likely Acid Generator	Likely Acid Generator
GT3 S9	9m	0.034	Likely Acid Generator	Likely Acid Generator
GT3 S10	10m	0.074	Likely Acid Generator	Likely Acid Generator
GT4 S1	1m	14.000	No Acid Potential	No Acid Potential
GT4 S2	2m	64.000	No Acid Potential	No Acid Potential
GT4 S3	3m	226.389	No Acid Potential	No Acid Potential
GT4 S4	4m	64.128	No Acid Potential	No Acid Potential
GT4 S5	5m	41.547	No Acid Potential	No Acid Potential
GT4 S6	6m	49.159	No Acid Potential	No Acid Potential
GT4 S7	7m	0.073	Likely Acid Generator	Likely Acid Generator
GT4 S8	8m	0.039	Likely Acid Generator	Likely Acid Generator
GT4 S9	9m	0.036	Likely Acid Generator	Likely Acid Generator
GT4 S10	10m	0.045	Likely Acid Generator	Likely Acid Generator
GT7 S1	1m	0.078	Likely Acid Generator	Likely Acid Generator
GT7 S2	2m	4.884	No Acid Potential	Acid under certain conditions
GT7 S3	3m	22.410	No Acid Potential	No Acid Potential

GT7 S4	4m	9.300	No Acid Potential	No Acid Potential
GT7 S5	5m	12.044	No Acid Potential	No Acid Potential
GT7 S6	6m	15.385	No Acid Potential	No Acid Potential
GT7 S7	7m	48.000	No Acid Potential	No Acid Potential
GT7 S8	8m	770.600	No Acid Potential	No Acid Potential
GT7 S9	9m	64.306	No Acid Potential	No Acid Potential
GT7 S10	10m	22.095	No Acid Potential	No Acid Potential
GT7 S11	11m	0.029	Likely Acid Generator	Likely Acid Generator
GT7 S12	12m	0.025	Likely Acid Generator	Likely Acid Generator
GT7 S13	13m	0.021	Likely Acid Generator	Likely Acid Generator
GT7 S14	14m	0.022	Likely Acid Generator	Likely Acid Generator

Table 40: Interpretation of ABA pH results.

Site Name	Initial pH	Final pH	Interpretation
GGC55	6.46	2.90	Higher Risk Acid Generation

Table 41: Interpretation of ABA Net Neutralizing Potential results.

Site Name	Net NP (Open)	Net NP (Closed)	Interpretation
GGC55	0.354	-1.291	Verify with other tests

Table 42: Interpretation and NP/AP ratios for the sandstone samples.

Site Name	NP Ratio(NP/AP) for Open System	Interpretation Open System	Interpretation Closed System
GGC55	1.215	Acid under certain conditions.	Likely Acid Generator.

Table 43: Interpretation of ABA pH results.

Site Name	Initial pH	Final pH	Interpretation
Discard GG1	7.33	1.58	Higher Risk Acid Generation
Discard GG2	7.26	1.78	Higher Risk Acid Generation

Table 44: Interpretation of ABA Net Neutralizing Potential results.

Site Name	Net NP (Open)	Net NP (Closed)	Interpretation
Discard GG1	-23.442	-60.890	Potential Acid Generator
Discard GG2	-100.973	-204.946	Potential Acid Generator

Table 45: Interpretation and NP/AP ratios for Exxaro core samples.

Site Name	NP Ratio(NP/AP) for Open System	Interpretation Open System	Interpretation Closed System
Discard GG1	0.374	Likely Acid Generator	Likely Acid Generator
Discard GG2	0.029	Likely Acid Generator	Likely Acid Generator

Appendix B

Slug Test Results

Table 46: Slug test results for Slpmt2

SLUG TEST - YIELD ESTIMATE									
Note: All the estimates are qualified guesses and could be wrong									
BH Name =	BH2 (Sasolpmt2)								
Recession time (s) for 70% recovery	28								
Yield of BH (L/s) =	2.09								
T (m ² /d) of formation in vicinity of BH =	10.45								
T (m ² /d) of formation - Average =	5.22								
<table border="1" style="width: 100%; border-collapse: collapse;"> <tr> <th colspan="2" style="background-color: #FF0000; color: white; text-align: center;">RECOMMENDATION</th> </tr> <tr> <td colspan="2" style="background-color: #FF0000; color: white; text-align: center;">Conduct a Pumptest on BH</td> </tr> <tr> <th colspan="2" style="background-color: #FF0000; color: white; text-align: center;">First estimate of sustainable yield (L/s)</th> </tr> <tr> <td style="width: 80%;"></td> <td style="background-color: #FF0000; color: white; text-align: center;">0.42</td> </tr> </table>		RECOMMENDATION		Conduct a Pumptest on BH		First estimate of sustainable yield (L/s)			0.42
RECOMMENDATION									
Conduct a Pumptest on BH									
First estimate of sustainable yield (L/s)									
	0.42								
<table border="1" style="width: 100%; border-collapse: collapse;"> <tr> <td style="width: 80%; text-align: right;">K-value of fracture (m/d) =</td> <td style="background-color: #008000; color: white;">431.12</td> </tr> <tr> <td style="text-align: right;">T-value of fracture (m²/d) =</td> <td style="background-color: #008000; color: white;">86.22</td> </tr> </table>		K-value of fracture (m/d) =	431.12	T-value of fracture (m ² /d) =	86.22				
K-value of fracture (m/d) =	431.12								
T-value of fracture (m ² /d) =	86.22								

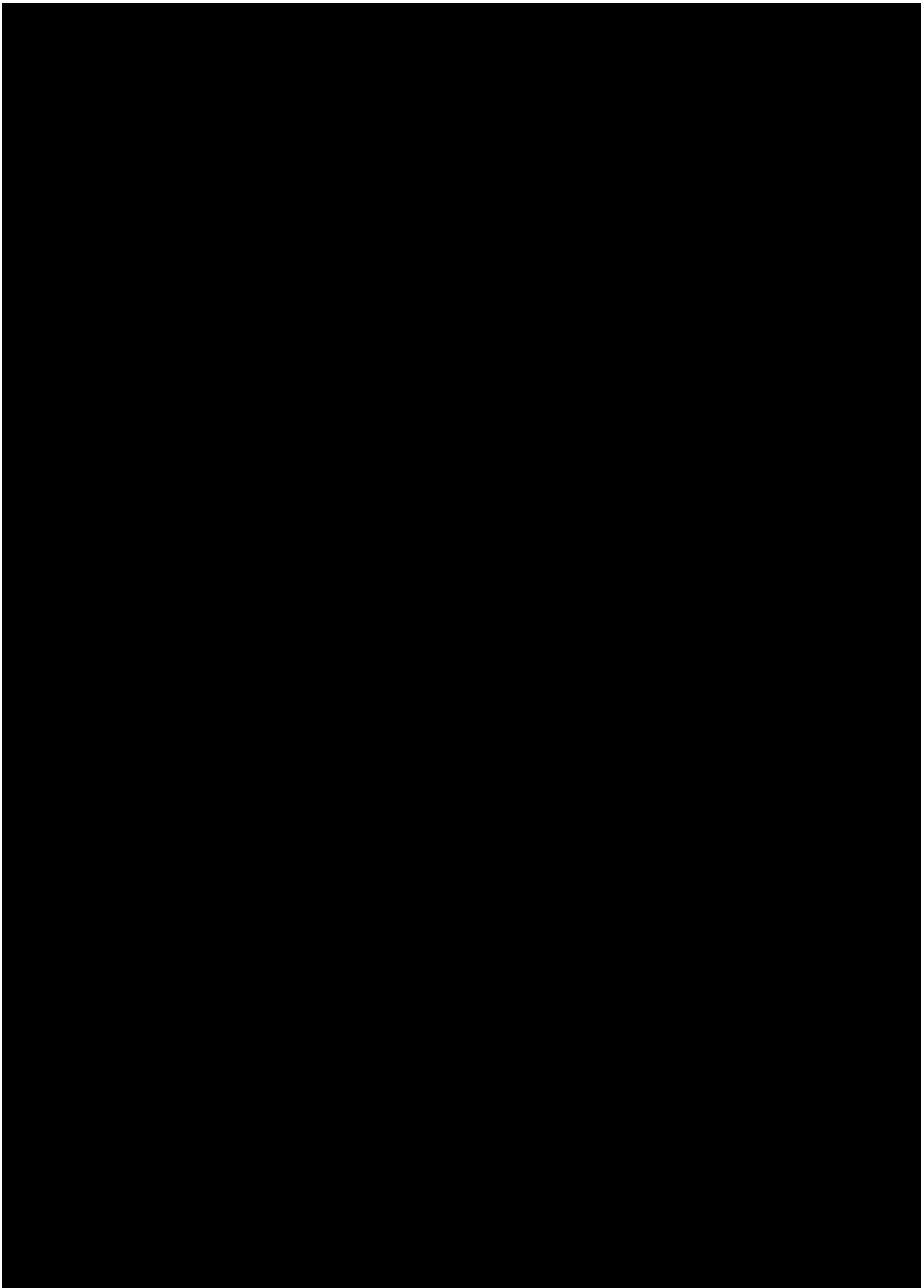
Table 47: Slug test results for Slpmt3.

SLUG TEST - YIELD ESTIMATE									
Note: All the estimates are qualified guesses and could be wrong									
BH Name =	BH3 (Sasolpmt3)								
Recession time (s) for 70% recovery	30								
Yield of BH (L/s) =	1.97								
T (m ² /d) of formation in vicinity of BH =	9.87								
T (m ² /d) of formation - Average =	4.93								
<table border="1" style="width: 100%; border-collapse: collapse;"> <tr> <th colspan="2" style="background-color: #FF0000; color: white; text-align: center;">RECOMMENDATION</th> </tr> <tr> <td colspan="2" style="background-color: #FF0000; color: white; text-align: center;">Conduct a Pumptest on BH</td> </tr> <tr> <th colspan="2" style="background-color: #FF0000; color: white; text-align: center;">First estimate of sustainable yield (L/s)</th> </tr> <tr> <td style="width: 80%;"></td> <td style="background-color: #FF0000; color: white; text-align: center;">0.39</td> </tr> </table>		RECOMMENDATION		Conduct a Pumptest on BH		First estimate of sustainable yield (L/s)			0.39
RECOMMENDATION									
Conduct a Pumptest on BH									
First estimate of sustainable yield (L/s)									
	0.39								
<table border="1" style="width: 100%; border-collapse: collapse;"> <tr> <td style="width: 80%; text-align: right;">K-value of fracture (m/d) =</td> <td style="background-color: #008000; color: white;">387.40</td> </tr> <tr> <td style="text-align: right;">T-value of fracture (m²/d) =</td> <td style="background-color: #008000; color: white;">77.48</td> </tr> </table>		K-value of fracture (m/d) =	387.40	T-value of fracture (m ² /d) =	77.48				
K-value of fracture (m/d) =	387.40								
T-value of fracture (m ² /d) =	77.48								

Table 48: Slug test results for Slpmt4

SLUG TEST - YIELD ESTIMATE									
Note: All the estimates are qualified guesses and could be wrong									
BH Name =	BH4 (Sasolpmt4)								
Recession time (s) for 70% recovery	10								
Yield of BH (L/s) =	4.88								
T (m ² /d) of formation in vicinity of BH =	24.40								
T (m ² /d) of formation - Average =	12.20								
<table border="1" style="width: 100%; border-collapse: collapse;"> <tr> <th colspan="2" style="background-color: #FF0000; color: white; text-align: center;">RECOMMENDATION</th> </tr> <tr> <td colspan="2" style="background-color: #FF0000; color: white; text-align: center;">Conduct a Pumptest on BH</td> </tr> <tr> <th colspan="2" style="background-color: #FF0000; color: white; text-align: center;">First estimate of sustainable yield (L/s)</th> </tr> <tr> <td style="width: 80%;"></td> <td style="background-color: #FF0000; color: white; text-align: center;">0.98</td> </tr> </table>		RECOMMENDATION		Conduct a Pumptest on BH		First estimate of sustainable yield (L/s)			0.98
RECOMMENDATION									
Conduct a Pumptest on BH									
First estimate of sustainable yield (L/s)									
	0.98								
<table border="1" style="width: 100%; border-collapse: collapse;"> <tr> <td style="width: 80%; text-align: right;">K-value of fracture (m/d) =</td> <td style="background-color: #008000; color: white;">2126.64</td> </tr> <tr> <td style="text-align: right;">T-value of fracture (m²/d) =</td> <td style="background-color: #008000; color: white;">425.33</td> </tr> </table>		K-value of fracture (m/d) =	2126.64	T-value of fracture (m ² /d) =	425.33				
K-value of fracture (m/d) =	2126.64								
T-value of fracture (m ² /d) =	425.33								

Appendix C
CI Values and Recharge



Appendix D

Recharge determination Results for the E.A.R.T.H. model.

Table 49: Results for borehole 2.

EARTH MODEL for single borehole				
Lag	BH #	Resistance	%R	S
3	2	2631	1.5	0.0005

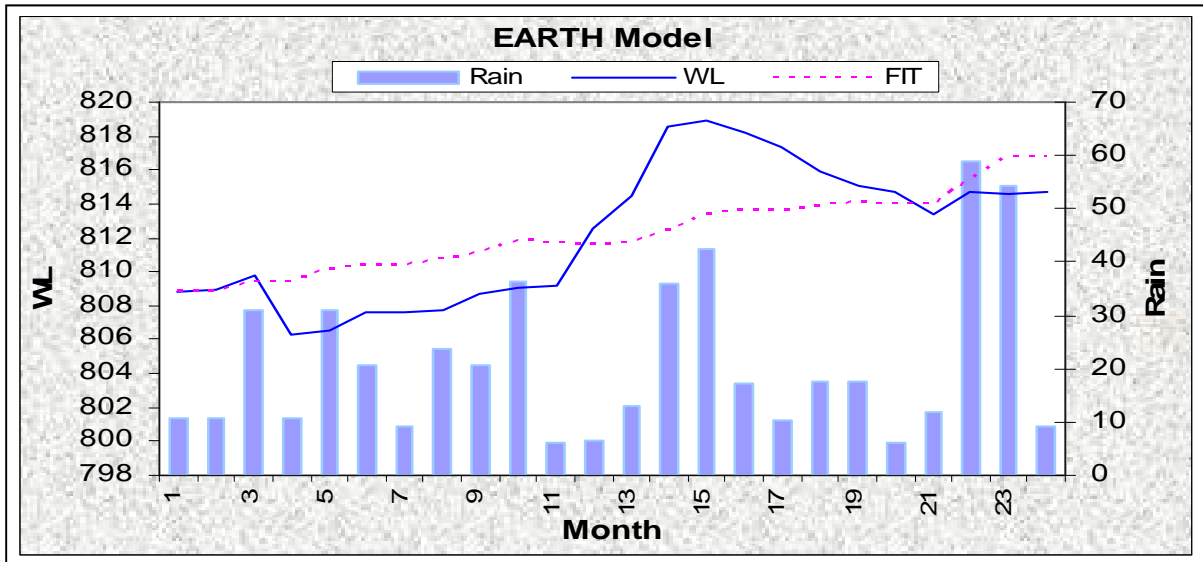


Figure 161: The fitted curve for borehole 2.

Table 50: Results for borehole 3.

EARTH MODEL for single borehole				
Lag	BH #	Resistance	%R	S
0	3	2631	1.7	0.0005

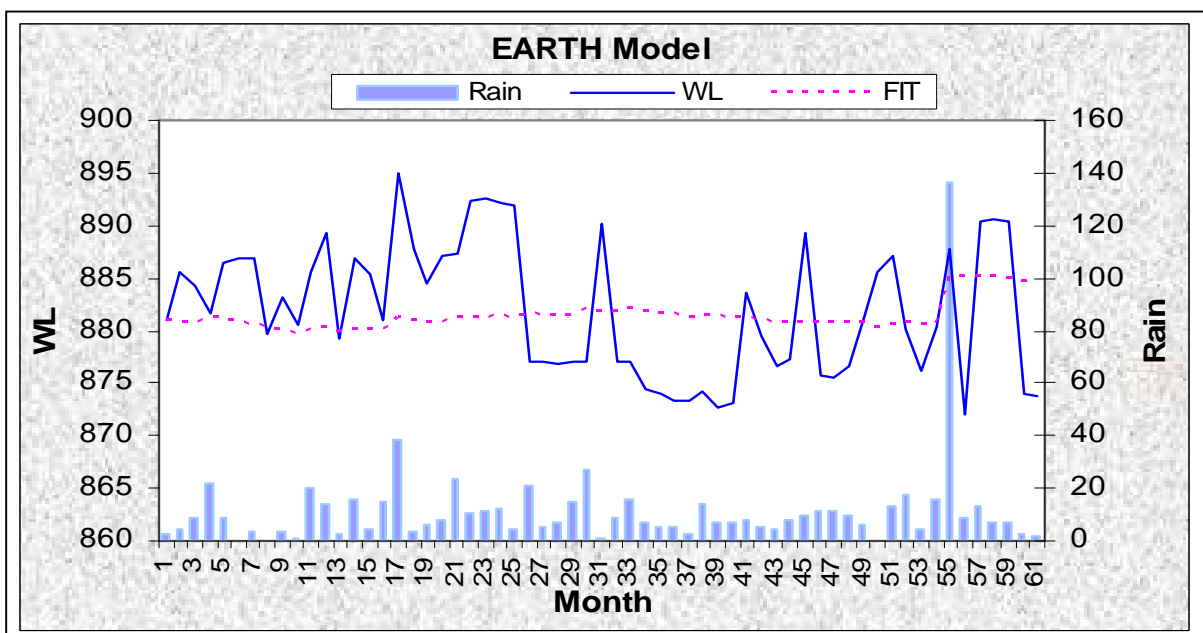


Figure 162: E.A.R.T.H model results for borehole 3.

Table 51: The results for boreholes 4, 5, 6 and 7.

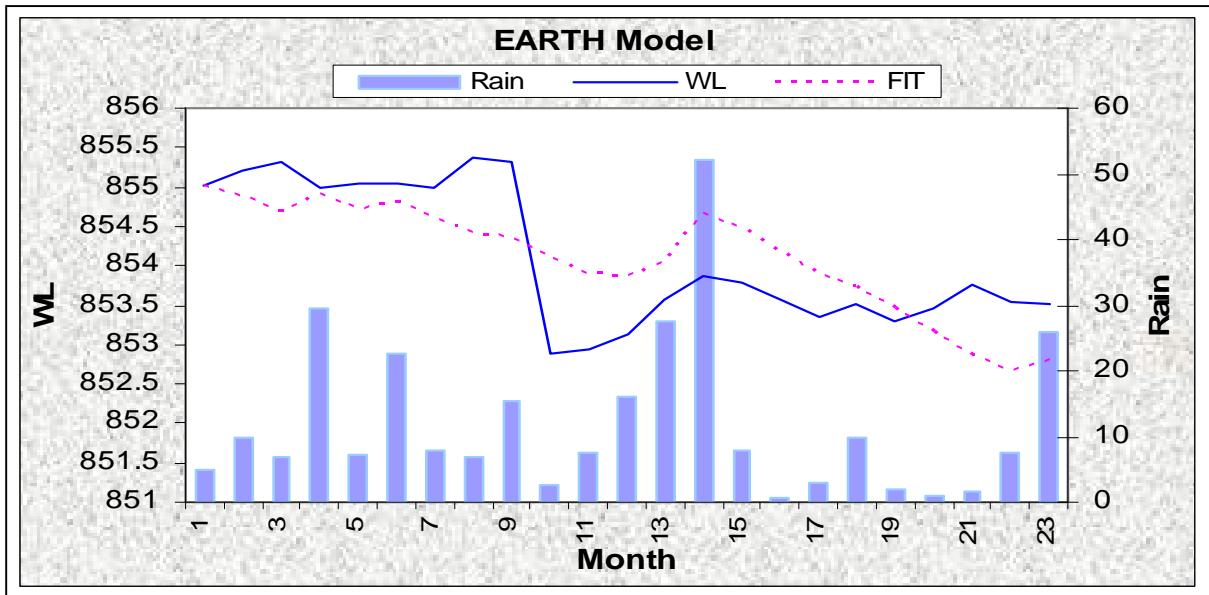


Figure 163: The fitted graph for borehole 4.

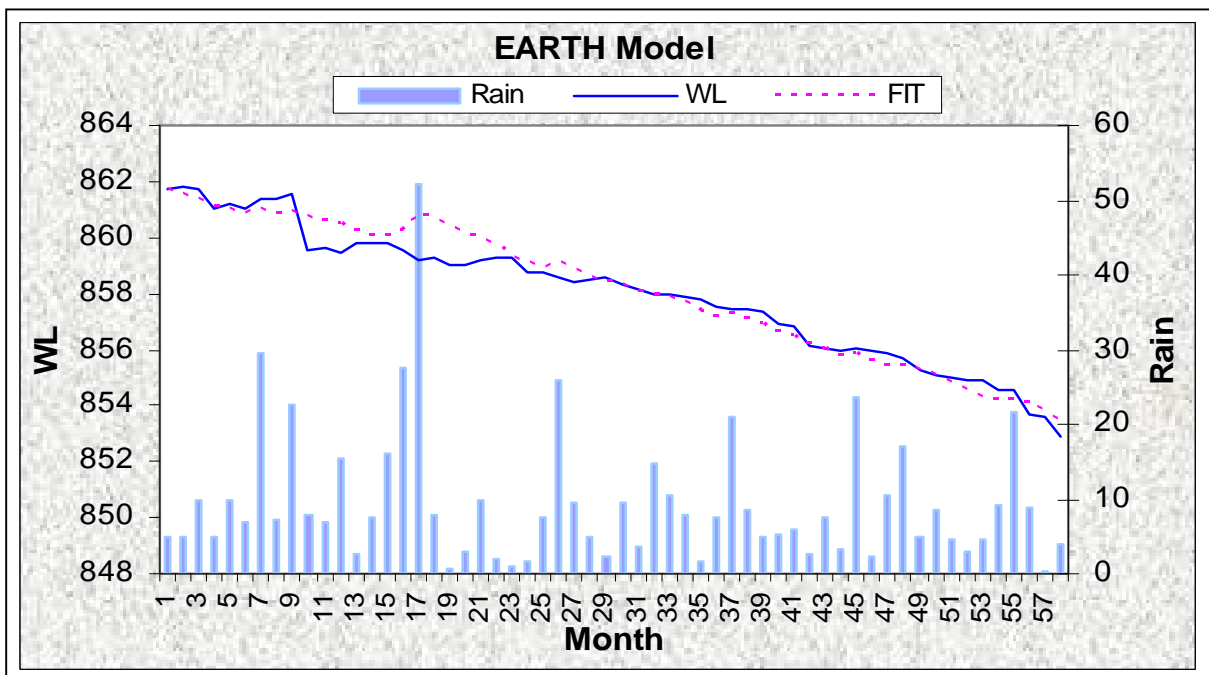


Figure 164: Results for borehole 5.

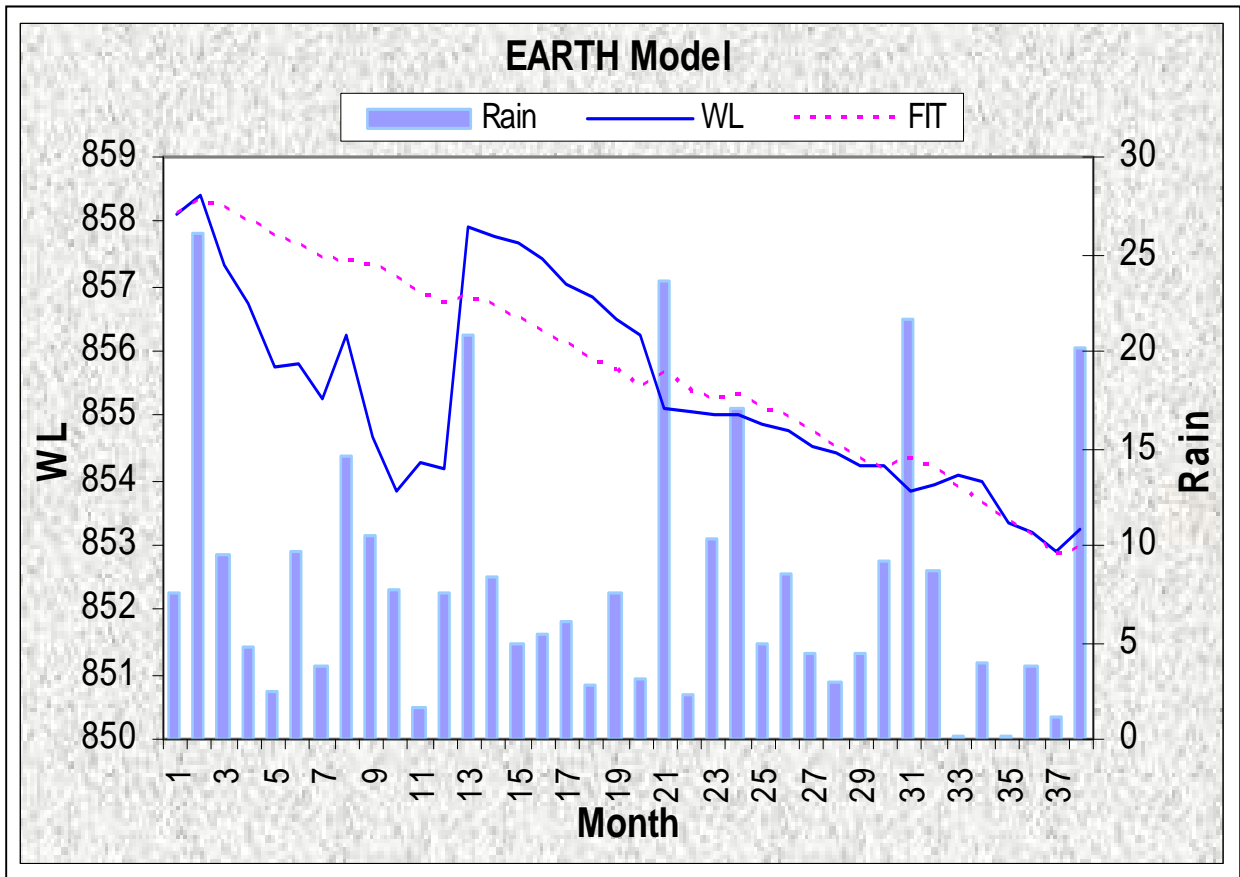


Figure 165: The graphic results for borehole 6.

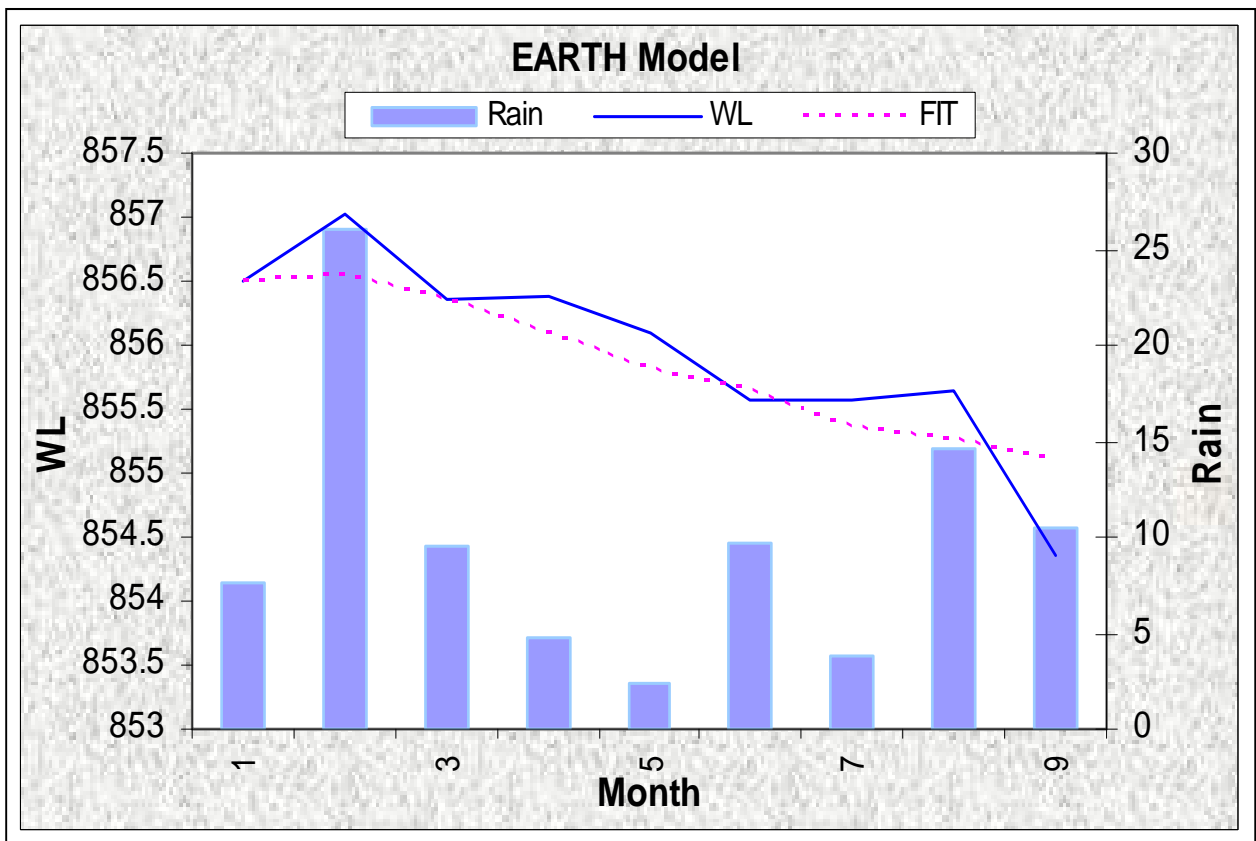


Figure 166: The E.A.R.T.H model results for borehole 7.

Table 52: Results for borehole 8.

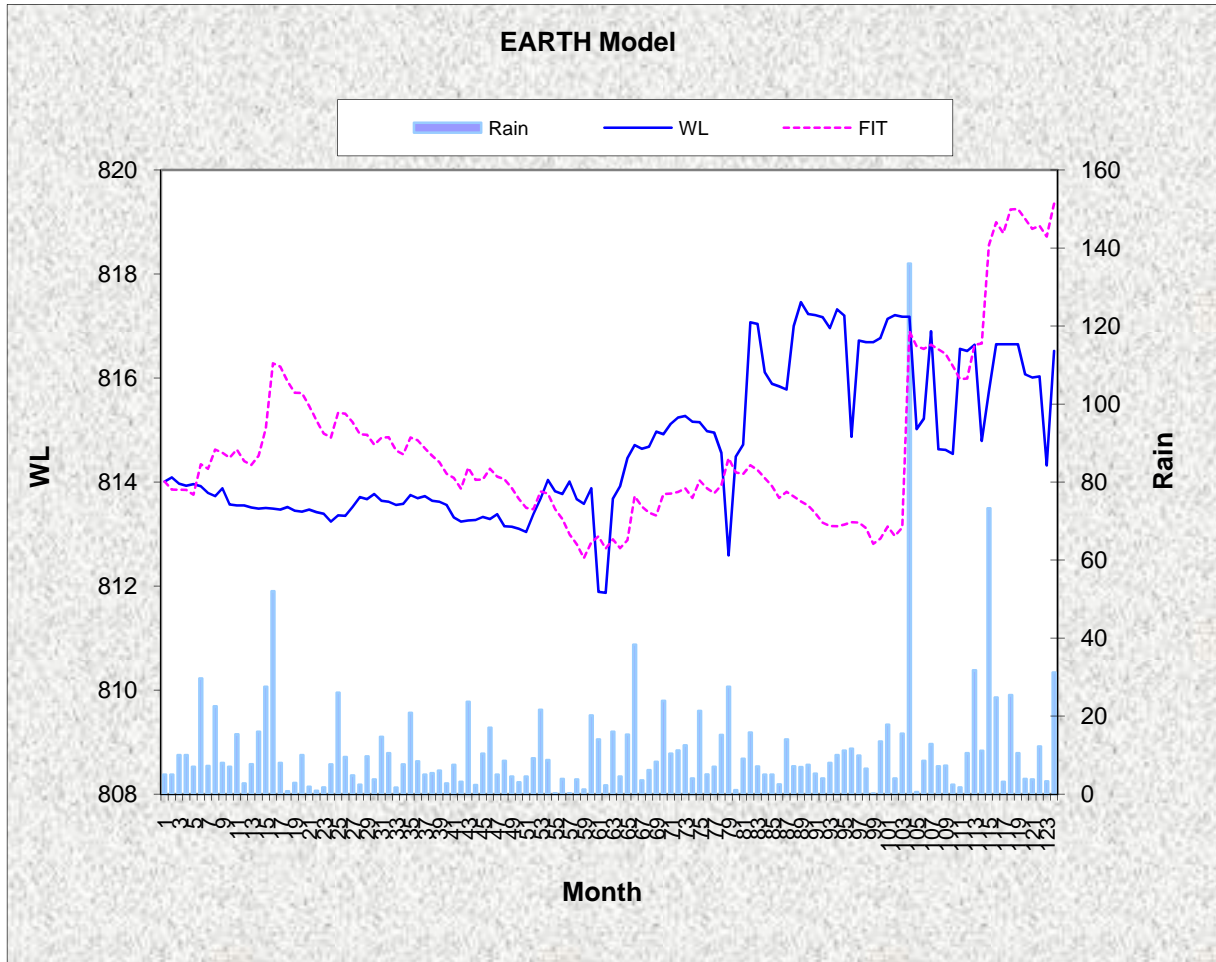


Figure 167: The fitted graph for borehole 8.

KEY TERMS

Waterberg Coalfields

Groundwater Management

Groundwater Quality

Numerical Modelling

Sampling

Aquifer Parameters

Daarby Fault

Eenzaamheid Fault

Zoetfontein Fault

Shallow Coal

Mining Methods

Summary

The Waterberg coalfields represent the last area in South Africa, which contain large quantities of coal resources. According to Dreyer (pers. comm. 2009) the Waterberg coalfields contain nearly 50% of the remaining coal resources of South Africa. Given the great demand for coal both local and abroad, primarily to be used as a fuel source for the power generation, the Waterberg coalfields have been targeted for large scale developments in order to exploit the coal. The primary method for exploiting coal is through mining. Mining, in any setting and any location has a diverse and often very serious impact on the environment.

A scoping level study was undertaken in order to determine the effect the mines will have on the groundwater resources and the pre-mining conditions of the aquifers and the quality of the groundwater. At present there is one operational colliery in the study area, the Grootegeluk mine. This mine has been in operation since the 1980's and has had a well planned and operated monitoring system in place since the beginning of mining operations. This mine was used as a model to determine the impact new mines will have on the area.

From the investigations it became apparent that the coalfield is situated in the Karoo Supergroup geology with the Mokolian Supergroup being represented in the study area by the Waterberg group quartzites. The coalfield is delineated by three major geological structures, the Daarby-, Eenzaamheid- and the Zoetfontein faults. With the Daarby- and Eenzaamheid faults being impermeable according to Dreyer (pers. comm. 2009), The Daarby fault serves to divide the study area into an area west of the fault with shallow coal and an area east of the fault with deeper coal. Only the shallow coal will be mined. According to Dreyer (pers. comm. 2009), all of the planned infrastructure for the new mines will be located on the Waterberg group rocks south of the Eenzaamheid fault or on the Karoo rocks east of the Daarby fault.

To determine the impact the mines would have on the groundwater of the study area, aquifer parameter testing (pumping test and slug tests), water quality determinations (inductively coupled spectrometry), acid-base accounting and numerical modelling were conducted. The results of the aquifer testing indicated low yielding aquifers with the harmonic mean of the transmissivities indicating a low transmissivity of $0.4 \text{ m}^2/\text{d}$. In addition the recharge for the study area was calculated by means of the CI and E.A.R.T.H. methods, resulting a value of 1.5% for the area. The average water level for the area was found to be approximately 28 m.

The water quality determinations for areas that had not been affected by mining, indicated waters that had high EC values, near neutral pH value and medium to high Cl and sulphate

values. The areas that have been affected by activities such as power generation and mining, displayed higher EC, Cl, and sulphate values than the unaffected areas.

To more accurately determine the impact the mines would have on the area, numerical modelling was done. Three scenarios were simulated using similar parameters to determine the expected inflow into the mines and whether the mines would ever decant. The results indicated that the worst possible scenario there was an influx varying between 755 m³/d and 1283 m³/d depending on the location of the pits. For the decant models, 50 years after mining had stopped there was a rise of 3 m in the pits themselves. With the pits being simulated being 110 m deep it is concluded that the mines in the area will never decant.

The results of the project indicate that the addition of new mines to the area will have an effect on the groundwater quality and quantity and steps should be taken to minimise this as much as possible.

Opsomming

Die Waterberg se steenkoolvelde verteenwoordig die laaste gebied in Suid Afrika wat oor groot steenkoolbronne beskik. Volgens Dreyer (pers. comm. 2009) bevat hierdie steenkoolvelde soveel as 50% van die oorblywende steenkool van Suid Afrika. As gevolg van die groot aanvraag na steenkool, hoofsaaklik as 'n brandstof vir kragopwekking, word die area (Waterberg se steenkoolvelde) geteiken vir grootskaalse ontwikkeling, hoofsaaklik met die oog op die eksploitering van die steenkoolbronne. Die mees ekonomiese vorm van steenkool-eksploitering is deur middel van mynbou. Daar is verskillende vorms van mynbou wat toe-gepas word om steenkool te ontgin, elkeen van hierdie metodes het sy eie afsonderlike impak op die omgewing.

'n Oorsigvlak assessering is geloods om vastestel wat die effek van die myne op die grondwater sal wees en ook wat die huidige staat van akwifere en die kwaliteit van die grondwater is. Huidiglik is een steenkoolmyn in werking in die studiegebied naamlik, Grootegeluk. Die myn is vanaf 1980 in werking en beskik oor 'n goed beplande en goed instand gehoude moniteringstelsel vir grondwater in en om die myn. Die myn is as 'n model gebruik om te bepaal wat die impak van die nuwe myne op die omgewing sal wees.

Dit het vroeg in die verloop van die ondersoek bekend geword dat die Waterbergse steenkoolvelde in die Karoo Supergroep geleë is met 'n bykomende Supergroep, die Mokolian Supergroep ook teenwoordig in die studiegebied. Die Mokolian Supergroep word in die studiearea verteenwoordig deur die Waterberggroep kwartsiete.

Die steenkoolveld word begrens deur drie groot verskuiwings, naamlik die Daarby-, die Eenzaamheid- en die Zoetfonteiverskuiwings. Volgens Dreyer (pers. comm. 2009) is die Daarby- en Eenzaamheidsverskuiwings ondeurdringbaar en verdeel die Daarbyverskuiwing die studie- gebied in twee areas, naamlik 'n area met vlak steenkool, wes van die verskuiwing en 'n area met dieper steenkool, oos van die verskuiwing.

Volgens Dreyer (pers. comm. 2009) sal al die beplande infrastruktuur vir die nuwe myne of op die Waterberggesteentes, suid van die Eenzaamheid verskuiwing, of op die Karoogesteentes, oos van die Daarbyverskuiwing, gebou word.

Om vastestel wat die impak van die nuwe myne op die grondwater sal wees, is akwifertoetse (pomptoetse), watergehalte bepalings, suur-basis bepalings (op die gesteentes) asook numeriese modellering, gedoen. Die akwifertoetse het aangedui dat die gesteentes 'n lae lewering het met 'n lae transmissiviteit van $0.4 \text{ m}^2/\text{d}$. Bykomend tot die akwifertoetse is

aanvullingberekenings gedoen met behulp van twee metodes (CI en E.A.R.T.H. metode) wat 'n aanvulling van 1.5% aangedui het. Die gemiddelde watervlak in die area is 28 m.

Die watergehalte bepalings vir areas wat nie deur aktiwiteite soos mynbiou beïnvloed is nie, het aangedui dat die water 'n hoë EC het, byna neutraal pH met medium tot hoë hoeveelhede chloor en sulfaat. Die bepalings vir areas wat wel beïnvloed is deur aktiwiteite toon hoër EC, Cl en sulfaat waardes as die areas wat nie beïnvloed is nie.

Om te bepaal wat die impak van die myne op die grondwater sal wees, is numeriese modellering gedoen. Drie moontlikhede is gemodelleer met soortgelyke parameters. Die doel was om te bepaal wat die invloed in die myne sal wees asook of die watervlakke in die myne ooit op die oppervlak sou uitloop. Die resultate het 'n invloed wat wissel tussen 755 m³/d en 1283 m³/d aangedui, afhangende van die ligging van die myn. Die opvullingsmodelle het aangedui dat die watervlakke in die myne nooit op die oppervlak sal uitloop nie. Met 'n maksimum styging van 3 m in watervlak 50 jaar nadat mynbou gestaak is.

Die bevindinge van die projek is dat die myne 'n negatiewe impak op die grondwater hoeveelhede en gehalte sal hê. Dit word aanbeveel dat die mynmaatskappye stappe neem om die impak te verminder.